UNIVERSIDADE FEDERAL DE PERNAMBUCO
CENTRO DE TECNOLOGIA E GEOCIÊNCIAS
DEPARTAMENTO DE OCEANOGRAFIA
PROGRAMA DE PÓS-GRADUAÇÃO EM OCEANOGRAFIA

ANA KAROLINE DUARTE DOS SANTOS SÁ

INTRUSÃO SALINA E SUAS IMPLICAÇÕES SOBRE A COMUNIDADE FITOPLANCTÔNICA E ESTADO TRÓFICO EM UM ESTUÁRIO DE MACROMARÉ (RIO ITAPECURU – GOLFÃO MARANHENSE)

Recife
2022

ANA KAROLINE DUARTE DOS SANTOS SÁ

INTRUSÃO SALINA E SUAS IMPLICAÇÕES SOBRE A COMUNIDADE FITOPLANCTÔNICA E ESTADO TRÓFICO EM UM ESTUÁRIO DE MACROMARÉ (RIO ITAPECURU – GOLFÃO MARANHENSE)

Tese apresentada ao Programa de Pós-Graduação em Oceanografia da Universidade Federal de Pernambuco, como requisito parcial para obtenção do título de doutor em Oceanografia.

Área de concentração: Oceanografia Biológica.

Orientador: Prof. Dr. Fernando Antonio do Nascimento Feitosa.

Coorientador: Prof. Dr. Marco Valério Jansen Cutrim.

Coorientador: Prof. Dr. Manuel de Jesus Flores-Montes.

Recife

2022

Catalogação na fonte:
Bibliotecária Sandra Maria Neri Santiago, CRB-4 / 1267

S111i Sá, Ana Karoline Duarte dos Santos.
Intrusão salina e suas implicações sobre a comunidade fitoplanctônica e estado trófico em um estuário de macromaré (Rio Itapecuru – Golfão Maranhense) / Ana Karoline Duarte dos Santos Sá. – 2022.
161 f.: il., fig., tab.

Orientador: Prof. Dr. Fernando Antonio do Nascimento Feitosa.
Coorientador: Prof. Dr. Marco Valério Jansen Cutrim.
Coorientador: Prof. Dr. Manuel de Jesus Flores-Montes.
Tese (Doutorado) – Universidade Federal de Pernambuco. CTG. Departamento de Oceanografia, Recife, 2022.
Inclui referências, apêndices e anexo.

1. Oceanografia. 2. *Polymyxus coronalis*. 3. ASSETS. 4. Modelos tróficos. 5. Bioindicadores. 6. Macromaré. 7. Gradiente de salinidade. I. Feitosa, Fernando Antonio do Nascimento (Orientador). II. Cutrim, Marco Valério Jansen (Coorientador). III. Flores-Montes, Manuel de Jesus (Coorientador). IV. Título.

UFPE

551.46 CDD (22. ed.) BCTG/2023-139

ANA KAROLINE DUARTE DOS SANTOS SÁ

INTRUSÃO SALINA E SUAS IMPLICAÇÕES SOBRE A COMUNIDADE FITOPLANCTÔNICA E ESTADO TRÓFICO EM UM ESTUÁRIO DE MACROMARÉ (RIO ITAPECURU – GOLFÃO MARANHENSE)

Tese apresentada ao Programa de Pós-Graduação em Oceanografia da Universidade Federal de Pernambuco, Centro de Tecnologia e Geociências, como requisito parcial para obtenção do título de doutor em Oceanografia. Área de concentração: Oceanografia Biológica.

Aprovada em: 14/12/2022.

BANCA EXAMINADORA

_____

Prof. Dr. Fernando Antônio do Nascimento Feitosa (Orientador)
Universidade Federal de Pernambuco

_____

Prof. Dra. Sigrid Neumann Leitão (Examinador Interno)
Universidade Federal de Pernambuco

_____

Profa. Dra. Flávia Marisa Prado Saldanha-Corrêa (Examinador Externo)
Universidade de São Paulo

_____

Prof. Dra. Andrea Christina Gomes de Azevedo Cutrim (Examinador Externo)
Universidade Estadual do Maranhão

_____

Prof. Dr. Mauro de Melo Junior (Examinador Externo)
Universidade Rural Federal de Pernambuco

Dedico essa tese de doutorado a minha querida mãe **Maria dos Prazeres Duarte** (in memorian), minha grande incentivadora, meu maior exemplo de resistência, resiliência e superação.

AGRADECIMENTOS

Com lágrimas inicio minha escrita, lágrimas de gratidão por cada estação vivenciada ao longo deste processo. Assim, quero registrar meus sinceros agradecimentos àqueles que foram fundamentais para a conclusão dessa etapa tão sonhada e importante da minha vida.

Primeiramente, agradeço à Deus pelo dom da vida, por ser fonte inesgotável de amor, fidelidade e cuidado.

À minha família que foi meu esteio durante toda essa caminhada e em especial as nossas Marias (Maria da Graça, Maria Raimunda), Talita Frizero e tio Hildac que hoje estão nos braços do Pai.

Dentre todas as Marias da minha família, quero agradecer a minha Maria dos Prazeres Duarte, mãe querida, minha maior entusiasta e orientadora de vida. Aquela que me fez acreditar que a educação me levaria a lugares inimagináveis e a realizar sonhos talvez inalcançáveis. Aquela que tanto sonhou comigo e vibrou para que esse dia chegasse. Aquela que em seus últimos momentos de vida, disse: minha filha é uma "doutora". Foram estas palavras que me fizeram prosseguir. Gratidão, minha mãe!!!

Agradeço imensamente ao meu esposo Antônio Ronnilson Dias Carneiro Sá que foi meu apoio, meu ombro amigo nos momentos difíceis, meu conselheiro, meu ajudador e que me fez acreditar que eu era forte o suficiente para enfrentar cada fase e concluí-las com sucesso. Obrigada por ser meu suporte, por confiar em mim. Você fez tudo ser mais leve, tranquilo e pacífico.

Agradeço imensamente a todas as parcerias formadas. Dentre elas, à Universidade Federal de Pernambuco e ao Programa de Pós-Graduação (PPGO), representado pelo Prof. Pedro Augusto Mendes de Castro Melo e a secretaria do PPGO, na pessoa do Nerlucyton Gomes, por todo suporte acadêmico e orientações.

Ao meu orientador Prof. Fernando Feitosa, uma tão sonhada orientação, que recebeu a missão de orientar uma leitora de seus artigos e admiradora de sua pesquisa. Obrigada por cada palavra incentivadora, por todos os ensinamentos, pela amizade, por todo carinho e respeito estimado nesse período.

Quero agradecer ao meu co-orientador Prof. Marco Valerio Jansen Cutrim, que também o considero como eterno orientador. Ele que me acompanha desde o mestrado, apresentou-me o mundo da pesquisa bem elaborada, planejada e objetiva. Sua dedicação e conhecimento aprofundado me impulsionou à leitura sistemática, a buscar uma ciência de qualidade e a ser

uma pesquisadora destemida. Ao Prof. Marco expresso nestes agradecimentos minha admiração, respeito e gratidão por acompanhar toda essa trajetória, por todos os conselhos, por ser amigo do início ao fim.

Agradeço também, ao meu co-orientador Prof. Manuel de Jesus Flores-Montes, que foi essencial nessa etapa da minha vida! Obrigada pelo incentivo, apoio, amizade e confiança.

À Fundação de Amparo à Pesquisa e ao Desenvolvimento Científico e Tecnológico do Maranhão – FAPEMA pela concessão da bolsa de doutorado.

Aos laboratórios de ficologia – LabFic e física – Lhiceai, da Universidade Federal do Maranhão, representados pelos professores Marco Cutrim e Fransciso Dias, por todo suporte técnico e científico.

Ao laboratório de oceanografia química – LoQuim, da Universidade Federal de Pernambuco, na pessoa do Prof. Manuel Flores-Montes e aos amigos Jamerson e Brenno, que nos auxiliaram prontamente nas análises químicas.

Ao Centro de Estudos e Ensaios em Risco e Modelagem Ambiental – CEERMA, em especial ao Prof. Moacyr Cunha de Araújo Filho e Marcus André Silva pela concessão dos dados que ajudaram a compor o segundo manuscrito desta pesquisa.

Aos professores do PPGO pelos ensinamentos. Especialmente à Profa. Maria da Glória Gonçalves da Silva Cunha, Prof. Pedro Augusto Mendes de Castro Melo e Prof. Manuel Flores-Montes.

Aos meus queridos membros da banca examinadora, Andrea Christina Gomes de Azevedo Cutrim, Flávia Marisa Prado Saldanha-Corrêa, Sigrid Neumann Leitão, Mauro de Melo Junior, Pedro Augusto Mendes de Castro Melo e Marcus André Silva por aceitar participar da defesa e pelas considerações assinaladas. Muito obrigada!

À prefeitura de Paço do Lumiar pelo investimento profissional e ao Instituto Federal do Maranhão – Campus Avançado Rosário. A estas instituições representadas respectivamente, por Ana Lucia Passos, Inez Gato e Marco Torreão, minha gratidão pela compreensão e apoio nesta etapa final do doutorado.

Agradeço também, aos amigos de turma, em especial a Lisana Furtado Calvacanti, pela companhia e parceira na vida e pesquisa. Às amigas de laboratório Taiza Pimentel e Quedyane Cruz por cada momento descontraído e intenso no LabFic, por construirmos juntas uma equipe sólida e que torna a pesquisa leve e agradável.

Às amigas de campo que foram muitas, mas em especial a Denise Costa e Francinara Ferreira que nos acompanharam em todas as amostragens e que foram guerreiras ao enfrentar as macromarés do Maranhão.

Além disso, quero agradecer aos amigos da caminhada, que foram muitos, incontáveis, insubstituíveis, incansáveis, mas gostaria de destacar alguns: Wendy Vasconeselos, Jeine Gomes, Erasmo Carlos, Lindalva Cardoso, Semenya Alves, Heliana Mendes, Sara Maciel e todos que estiveram comigo de forma direta ou indiretamente.

Aqui me disperso dessa fase intensa e cheia de surpresas. Olhando pelo retrovisor da vida, compreendo que “olhando para as coisas que para trás ficam, avanço para aquelas que estão diante de mim”.

Continuar sempre será preciso.

Muito obrigada a todos!!

“There is a river where goodness flows
There is a fountain that drowns sorrows
There is an ocean deeper than fear
The tide is rising, rising”

In the River - Jesus Culture

RESUMO

A intrusão da água do mar em ambientes costeiros é um fenômeno hidrológico natural que caracteriza a dinâmica estuarina. Esses sistemas são altamente sensíveis ao aos efeitos da elevação do nível do mar, constituindo uma das causas mais importantes da salinização, responsável por alterar os padrões ecológicos de distribuição e estrutura das comunidades. Este trabalho foi desenvolvido em um estuário de macromaré (rio Itapecuru), localizado na Região Hidrográfica do Atlântico Nordeste Ocidental, que está sob constante perturbação antrópica e salinização de suas águas. Assim, este estudo teve como objetivo avaliar a variabilidade espaço-temporal da comunidade fitoplanctônica e do estado geral de eutrofização em respostas as alterações ambientais promovidas pela intrusão salina. Para tanto, variáveis físicas, químicas e biológicas foram coletadas ao longo do continuum rio-estuário, e os dados foram analisados usando duas abordagens. A primeira foi baseada nos indicadores ambientais, biológicos e em seus traços funcionais. A segunda abordagem utilizou modelos de avaliação do estado trófico estuarino (ASSETS e TRIX) baseados no framework Pressão, Estado e Resposta (PSR), técnicas de modelagem e métodos não lineares. Como resultados, foram selecionados 76 indicadores de fitoplâncton, com base em suas características funcionais específicas e no valor do indicador (IndVal). *Polymyxus coronalis* foi selecionado como um bom indicador do limite de intrusão da água do mar e análises multivariadas revelaram alta dispersão de espécies entre os setores estuarinos governados por variações na salinidade, material particulado em suspensão, tamanho das células e silicato. A distribuição das espécies de água doce no setor superior foi correlacionada com baixos valores de nutrientes e salinidade. As espécies marinhas foram transportadas entre os setores médio e inferior em condições opostas. O modelo de Avaliação do Estado Trófico Estuarino (ASSETS) indicou que a eutrofização é sazonal e depende da variação climática. Os eventos de La Niña (2019–2020) contribuíram para as concentrações de clorofila *a* e ortofosfato, principalmente durante os períodos de baixa vazão do rio. Os baixos níveis de oxigênio dissolvido e altas concentrações de clorofila *a* na zona de água do mar indicam que a porção inferior do estuário foi a mais suscetível. Além disso, o modelo de floresta aleatória selecionou a salinidade, DIP e Cl-a como os principais estressores que intensificaram a eutrofização nos sistemas de macromarés. De acordo com a classificação final do ASSETS (pior-alto) para a próxima década (2021-2031), as principais estratégias planejadas devem reduzir as contribuições antrópicas e melhorar as condições tróficas na IRE. A partir desses resultados, as interações e previsões de efeitos eco-hidrológicos podem facilitar

a caracterização de riscos futuros e a gestão de sistemas estuarinos de macromarés, considerando que a intrusão salina afetou negativamente a comunidade fitoplanctônica.

Palavras-chave: *Polymyxus coronalis*; ASSETS; modelos tróficos; bioindicadores; macromaré; gradiente de salinidade.

ABSTRACT

Seawater intrusion into coastal environments is a natural hydrological phenomenon that characterizes estuarine dynamics. These systems are highly sensitive to the effects of sea level rise, constituting one of the most important causes of salinization responsible for altering ecological patterns of distribution and community structure. This work occurred in the macrotidal estuary (Itapecuru River), located in the Hydrographic Region of the western Northeast Atlantic, with constant anthropic disturbance and salinization of its waters. Thus, this study aimed to evaluate the spatiotemporal variability of the phytoplankton community and the general state of eutrophication in response to environmental changes promoted by saline intrusion. To this end, physical, chemical, and biological variables were collected along the river-estuary continuum, and the data were analyzed using two approaches. The first approach is based on environmental and biological indicators and their functional traits. The second approach used estuarine trophic state assessment models (ASSETS and TRIX) based on the Pressure, State, and Response (PSR) framework, modeling techniques, and nonlinear methods. As a result, 76 microalgae were selected as indicator species based on their specific functional characteristics and indicator value (IndVal). *Polymyxus coronalis* is a good indicator of the limit of seawater intrusion and multivariate analyses revealed high species dispersion across estuarine sectors governed by variations in salinity, suspended particulate matter, cell size, and silicate. The distribution of freshwater species in the upper sector was correlated with low values of nutrients and salinity. Marine species were transported between the middle and lower sectors under opposite conditions. The Estuarine Trophic State Assessment (ASSETS) model indicated that eutrophication is seasonal and depends on climate variation. La Niña events (2019–2020) contributed to chlorophyll- a and orthophosphate concentrations, mainly during periods of low river flow. Low levels of dissolved oxygen and high concentrations of chlorophyll-a in the seawater zone indicate that the lower portion of the estuary was the most susceptible. Furthermore, the random forest model selected salinity, DIP, and Chl-a as the main stressors that intensified eutrophication in macrotidal systems. According to the final ASSETS ranking (worst-high) for the next decade (2021-2031), the main planned strategies should be to reduce anthropogenic contributions and improve trophic conditions in the IRE. From these results, the interactions, and predictions of ecohydrological effects can facilitate the characterization of future risks and the management of macrotidal estuarine systems, considering that saline intrusion negatively affected the phytoplankton community.

Keywords: *Polymyxus coronalis*; ASSETS; bioindicators; trophic models; macrotidal; salinity gradient.

LISTA DE FIGURAS

ARTIGO 1 - PHYTOPLANKTON COMMUNITY DYNAMICS IN RESPONSE TO SEAWATER INTRUSION IN A TROPICAL MACROTIDAL RIVER-ESTUARY CONTINUUM

LISTA DE TABELAS

SUMÁRIO

1 INTRODUÇÃO

Este documento de Tese de Doutorado está estruturado no formato “artigo científicos” que avaliam a dinâmica fitoplanctônica, eventos climáticos e eutrofização estuarina em um ecossistema de macromarés. Esta pesquisa foi realizada em parceria com o laboratório de ficologia da Universidade Federal do Maranhão e com a Fundação de Amparo e Apoio a Pesquisa do Estado do Maranhão (FAPEMA). Esta seção apresenta um referencial teórico recente dos principais temas abordados nesta tese.

1.1 Intrusão da água do mar

Os estuários são regiões onde há uma interação entre a descarga de água do rio e a entrada de água oceânica forçada pelas marés (DYER, 1997; ELLIOTT e MCLUSKY, 2002; DAME, 2008; DEVLING e PAN, 2018). A definição de estuário mais utilizada é de Pritchard (1967), baseada na salinidade, em que “... Um estuário é um corpo de água costeiro semifechado que tem uma conexão livre com o mar aberto e no qual a água do mar é mensuravelmente diluída com água doce derivada da drenagem continental”. Assim, um estuário é a área na foz de um rio onde as salinidades variam de aproximadamente 0,1 a 30-35. Para Dalrymple et al. (1992), os estuários são ambientes controlados pela interação entre processos de ondas e marés, que geralmente diminuem de intensidade a montante, e processos fluviais, que diminuem de intensidade a jusante (Figura 1).

Figura 1 - Representação esquemática das definições de estuário de acordo com Pritchard (1967) e Dalrymple et al. (1992)

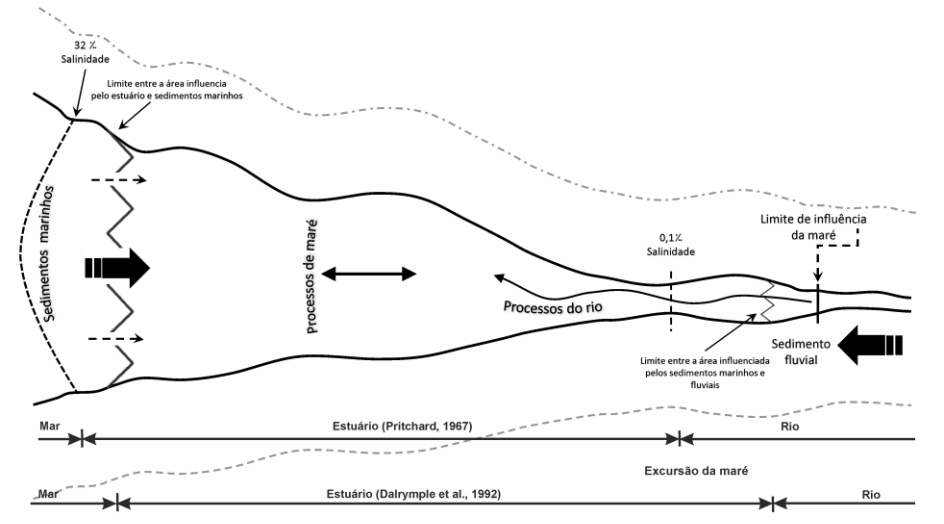

Fonte: O Autor (2022)

Outras abordagens baseadas em aspectos geomorfológicos, físicos, químicos, ecológicos e biológicos também são utilizadas para a composição da definição de estuários, tais como: Fairbridge, 1980; Lincoln et al., 1982; Perillo, 1995; Allaby e Allaby, 1999; Bricker et al., 2008; Muylaert et al., 2009; Potter et al., 2010. Lancelot e Muylaert (2011) definem estuários como sistemas abertos, rasos, fortemente influenciados por influxos, misturando-se com o oceano costeiro e promovendo trocas entre as interfaces sedimento – atmosfera – e água. Os estuários costumam estar intimamente associados a outras formas costeiras, como enseadas, deltas, florestas pantanosas e manguezais. Eles fornecem o sistema de filtragem e exemplificam a interdependência dos sistemas terrestres e marinhos (GÖLTENBOTH e SCHOPPE, 2006).

A Diretiva Europeia de Habitats define o estuário como um setor a jusante de um vale fluvial, sujeito à maré e estendendo-se desde o limite das águas salobras (DAUVIN e RUELLET, 2009). Os estuários também são definidos como águas de transição, um termo mais abrangente, que incluem estuários de planície costeira, rias, fiordes, lagos e lagoas intermitentemente fechadas e abertas (ICOLLs), que são caracterizados por um conjunto de feições que se relacionam principalmente com ecótonos e gradientes (POTTER et al., 2010).

Esses ecossistemas são responsáveis por formar uma zona de transição entre oceano e terra, construindo vários gradientes ambientais (como salinidade, temperatura e turbidez) em escalas espaciais ou temporais. Os gradientes espaciais de habitats de ecossistemas estuarinos são definidos pela extensão da intrusão de água do mar (IAM) (NEUBAUER et al. 2013; AZHIKODAN e YOKOYAMA, 2016). Em termos gerais, um estuário é onde o fluxo do rio encontra a cheia da maré, formando uma zona de transição entre os ecossistemas de água doce interior e os ecossistemas marinhos costeiros. Essa zona possui propriedades únicas, portanto, deve ser considerada como um ecossistema, em vez de apenas um ecótono (WHITFIELD e ELLIOTT, 2011).

Dentro dessa caracterização, a IAM é um fenômeno natural, de natureza muito complexa e altamente dinâmica, que depende da presença de linhas costeiras sinuosas, forma do estuário, amplitude das marés e descarga de água doce. As distribuições espaciais e temporais da salinidade podem afetar significativamente o transporte residual de sedimentos, poluentes e materiais aquáticos através de circulações gravitacionais e de marés em estuários de estratificação moderada a fraca (VEERAPAGA et al., 2019).

Recentemente, a IAM foi considerada como uma questão ambiental global, afetada por múltiplas forças externas, que pode ser intensificada pela elevação do nível do mar, redução da vazão do rio e aprofundamento da batimetria estuarina (GONG et al., 2022). Esses processos podem ser resultantes tanto de mudanças naturais quanto por intervenções humanas (WERNER et al., 2013; DHAL e SWAIN, 2022; GONG et al., 2022). Assim, a IAM torna-se uma questão mais instigante, principalmente nas regiões litorâneas que estão sujeitas as pressões produzidas por atividades antrópicas (DHAL e SWAIN, 2022).

Prevê-se que a mudança climática afetará adversamente a disponibilidade de água doce, assim como o aumento da população e a rápida industrialização (WETZ e YOSKOWITZ, 2013). Em tais circunstâncias, eventos climáticos extremos, também, podem agravar essa problemática da IAM, uma vez que, as regiões costeiras são particularmente vulneráveis a erosão e subida do nível do mar, promovido pelo aumento das temperaturas globais (RÊGO et al., 2018). De acordo com Tweedley et al. 2019, as mudanças climáticas nas próximas décadas influenciarão potencialmente a extensão da salinidade em estuários e lagoas costeiras, alterando a frequência e magnitude das chuvas e a altura do nível do mar.

Vale ressaltar que a IAM em habitats de água doce afetará a prestação de serviços ecossistêmicos no futuro, transformando drasticamente os ecossistemas costeiros, alterando a vegetação, impactando a vida aquática e as comunidades humanas que dependem desses recursos naturais (VISSCHERS et al., 2022). Portanto, prever e quantificar as mudanças na salinidade é uma das questões-chave para a gestão da água nas áreas costeiras (KRVAVICA e RUŽIĆ, 2020). Assim como, entender o mecanismo de transporte de água salgada ao longo dos estuários é de grande importância para a engenharia costeira, aquicultura, e segurança hídrica (VEERAPAGA et al., 2019), principalmente em estuários tropicais e de macromaré.

1.2 Eutrofização em estuários tropicais

Os ecossistemas estuarinos estão entre os sistemas naturais mais produtivos do planeta (MCLUSKY e ELLIOTT, 2004, GUO e KILDOW, 2015; GLASPIE et al., 2018; CHANDER et al., 2020), recebendo grandes quantidades de nutrientes e carbono orgânico da terra e dos oceanos, por meio de entradas de rios, descarga de águas subterrâneas submersas e deposição atmosférica, denominada como eutrofização natural (MEERSCHE e PINCKNEY, 2018).

Os estuários tropicais destacam-se por serem considerados “hotspots” biogeoquímicos, onde a produtividade, contida na biomassa fitoplanctônica, é responsável por suportar altas

taxas de metabolismo, sendo base de apoio da transferência trófica de energia e produção de matéria orgânica em níveis tróficos superiores (CLOERN et al. 2014; WINDER et al., 2017). De acordo com Lønborg et al., 2021, as águas tropicais tornam-se mais produtivas não apenas pela concentração de nutrientes, mas também, devido a altas temperaturas (20 e 32°C) e maior incidência solar permanente, quando comparadas às regiões temperadas.

Esses ecossistemas, provavelmente experimentarão nas próximas décadas, o aumento mais intenso de nutrientes, delimitando zonas de eutrofização que resultam da intensificação agrícola e urbanização (FORTUNE et al., 2020). A eutrofização costeira passa a ser considerada como artificial ou cultural, constituindo-se como uma ameaça ambiental futura aos ecossistemas costeiros em todo o mundo (LE MOAL et al., 2019). Portanto, assim como a IAM, a eutrofização costeira, o enriquecimento excessivo da água com nutrientes, tornou-se um problema ecológico global (ZHANG et al., 2022).

Conforme Paerl, (1998) e Paerl et al. (2014), o enriquecimento antropogênico de nutrientes e outros poluentes das águas costeiras está causando mudanças sem precedentes na estrutura e função da comunidade microbiana. Em estuários tropicais urbanizados, os estágios de eutrofização são avançados, conduzindo a profundas alterações no metabolismo do ecossistema e na ciclagem biogeoquímica, deteriorando a saúde ecológica e a qualidade da água (PAERL e JUSTIC, 2011).

Além disso, os estuários têm sido considerados como importantes fontes de emissão global de gases do efeito estufa (GEE - CO_2 e CH_4), responsáveis por mais de 80% do aumento real da temperatura atmosférica média global (COTOVICZ-JUNIOR et al., 2021; NGUYEN et al., 2022), promovendo uma relação direta entre mudanças climáticas, eutrofização e intrusão salina.

Então, os problemas enfrentados por metade da população global que vive perto das áreas costeiras são desafios mundiais, tornando fundamental a compreensão das restrições biofísicas, especialmente ao longo do continuum do ecossistema bacia-rio-estuário para poder enfrentar esses desafios. O gerenciamento dessas áreas garante a manutenção da estrutura e o funcionamento ecológico, e ao mesmo tempo permite que esses sistemas forneçam serviços que produzam bens e benefícios sociais, agora e no futuro (ELLIOTT et al., 2019).

A eutrofização antropogênica de ecossistemas aquáticos continua sendo um dos maiores problemas ambientais no Brasil (COTOVICZ-JUNIOR et al., 2012). Assim, indicadores de

avaliação de eutrofização e distribuição de frequências têm sido aplicados para desenvolver escalas que definem o estado trófico dos ambientes aquáticos. O reconhecimento da eutrofização como um processo, em vez de um estado, que é impulsionado pelo aumento da carga antropogênica de nutrientes foi um passo fundamental na evolução da compreensão dessa questão global cada vez mais acelerada (LEMLEY e ADAMS, 2019).

Por outro lado, muita ênfase tem sido colocada na resposta dos estuários aos estressores antropogênicos por meio do uso de programas de monitoramento. A chave para o sucesso desses programas pode ser a utilização de indicadores, pois eles transformam dados em informações úteis (LEMLEY et al., 2015). Vários critérios de classificação foram desenvolvidos para avaliar a condição trófica dos ecossistemas costeiros por meio de índices uni e multimétricos baseados em combinações aritméticas desses fatores ambientais (CARLSON, 1977; VOLLENWEIDER et al., 1998; KARYDIS, 2009).

Os índices unimétricos consideram variáveis utilizadas no monitoramento da qualidade da água por meio de algoritmos ou com referência a um nível trófico estabelecido. Já os índices multimétricos, consideram o enriquecimento por nutrientes, a produção de biomassa e as concentrações de oxigênio como variáveis que refletem as principais causas e efeitos da eutrofização (BRUGNOLI et al., 2019).

O número de variáveis necessárias para essa avaliação da eutrofização é bastante limitado, incluem: azoto inorgânico (nitrato, nitrito e íon amônio), fósforo inorgânico (ortofosfatos) e produção de matéria orgânica (clorofila *a*, densidade fitoplanctônica e biomassa de macrófitas). Estas têm sido as variáveis mais adequadas na avaliação da eutrofização (KITSIOU e KARYDIS, 2011).

Dentre as inúmeras ferramentas utilizadas para avaliar o "status" de eutrofização de ecossistemas costeiros, destaca-se o índice trófico (TRIX) de Vollenweider et al. (1998) e Giovanardi e Vollenweider (2004). Esse índice multimétrico foi originalmente testado para avaliar áreas costeiras do mar Adriático, e é uma combinação linear de indicadores químicos (Nitrogênio e Fósforo) e biológicos (Clorofila *a* e Oxigênio Dissolvido) que expressam a produção primária. No Brasil, foi adaptado às águas costeiras do Complexo Estuarino-Lagunar Mundaú-Manguaba por Cotovicz-Junior et al. (2013).

Um outro exemplo, é o modelo multiparamétrico de avaliação do estado trófico estuarino (ASSETS) desenvolvido pela NEEA (US National Estuarine Eutrophication

Assessment), utilizado para classificar o estado geral de eutrofização de estuários e áreas costeiras, e para abordar opções de gestão ambiental. O modelo utiliza componentes semiquantitativos e quantitativos para geração de indicadores de pressão, estado e resposta (PER) (BRICKER et al., 2003) (Figura 2).

Figura 2 - Fluxograma da metodologia do modelo ASSETS, adaptado de Bricker et al. (2003). Onde: OD – oxigênio dissolvido e NTB – Bloom de Algas Nocivas e Tóxicas

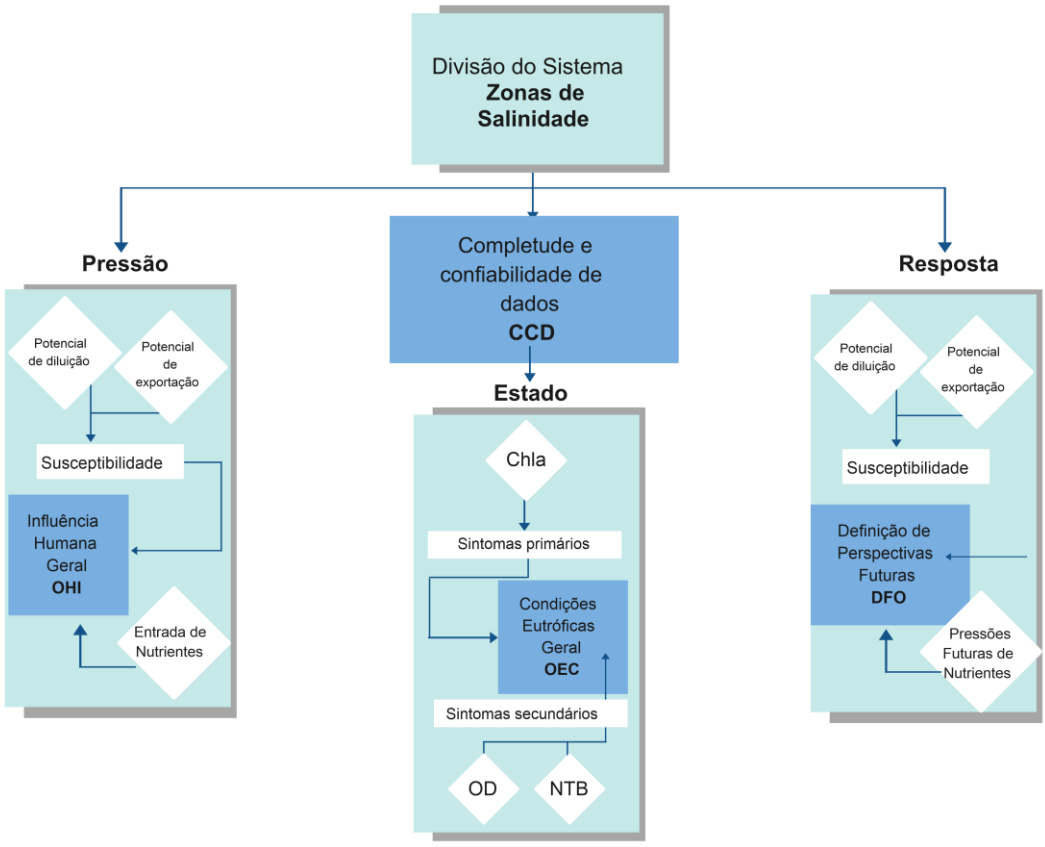

Fonte: O Autor (2022).

Esta ferramenta diagnóstica tem sido comumente utilizada para regular novas pressões ou minimizar as pressões atuais, além de aprimorar a política de gerenciamento dos ecossistemas aquáticos (SOUSA-FÉLIX et al., 2017). A PER foi desenvolvida pela Organização de Cooperação e Desenvolvimento Econômico (Organization of Economic Cooperation and Development - OECD, 1993) e pela Agência Europeia do Meio Ambiente (European Environment Agency - EEA, 1995) para a gestão adaptativa de Sistemas Socioecológicos (SESs), que são sistemas ecológicos intimamente ligados e afetados por um ou mais sistemas sociais. A metodologia do ASSETS se baseia em três ferramentas de

diagnóstico: um índice heurístico de pressão (Influência Humana Geral - OHI), uma avaliação de estado baseada em sintomas (Condições Eutróficas Gerais - OEC) e um indicador de resposta de gerenciamento (Definição de Perspectivas Futuras-DFO) que inclui métricas de suscetibilidade (FERREIRA et al., 2007; NEEA/ASSETS, 2021).

No Brasil, existe uma lacuna de conhecimento na compreensão de como as pressões antrópicas influenciam o processo de eutrofização dos ecossistemas aquáticos. A avaliação do estado trófico utilizando índices multimétricos ainda é incipiente, poucos estudos avaliaram o processo de eutrofização da zona costeira norte-nordeste brasileira (Tabela 1). A falta de medições in situ sistemáticas de cargas, vazões e concentrações de nutrientes constituem como o principal problema nessas áreas altamente sensíveis a impactos ambientais relacionados às atividades humanas (PAULA-FILHO et al., 2015).

Tabela 1 - Aplicação de índice de estado trófico (TRIX) e modelo ASSETS nos últimos 10 anos em estuários tropicais (norte e nordeste do Brasil)

Índices	**Ano**	**Autores**	**Local**	**Estado Trófico**
TRIX/ASSETS	2012	Cotovicz-Junior et al.	Complexo estuarino – AL	Mesotrófico
TRIX/ASSETS	2013	Alves et al.	Estuário do Complexo Portuário de Suape – PE	Mesotrófico
TRIX	2014	Batista e Flores-Montes	Estuários dos rios Ipojucae Merepe - PE	Hipereutrófico
TRIX	2014	Tavares et al.	Estuário do rio Potengi - RN	Mesotrófico-eutrófico
TRIX	2015	Guenther et al.	Porto do Recife - PE	Hipereutrófico
TRIX	2019	Noriega et al.	Rio Pirapama, Jaboatão, Tejipió, Capibaribe, Beberibe e Timbó - PE	Eutrófico
TRIX	2019	Cutrim et al.	Lagoa costeira da Jansen – MA	Hipereutrófico
TRIX	2020	Paula-Filho et al.	Delta do rio Parnaíba – PI	Mesotrófico-eutrófico
TRIX	2020	Mourão et al.	Estuário do Curuça - PA	Eutrófico-hipereutrófico
TRIX	2021	Sá et al.	Estuário do rio Bacanga – MA	Hipereutrófico
TRIX	2022	Cavalcanti et al.	Estuário do rio Paciência – MA	Mesotrófico-eutrófico
TRIX	2022	Silva et al.	Lagoa recifal - AL	Mesotrófico-oligotrófico

Fonte: O Autor (2022).

1.3 Fitoplâncton como indicador da intrusão salina

O fitoplâncton é um indicador de mudança ecológica muito eficiente e facilmente detectável (TAS et al., 2009). Ele representa um amplo conjunto de microrganismos foto-autotróficos que são componentes essenciais para manter o equilíbrio e a integridade do ecossistema como produtores primários, servindo como bons indicadores do estado trófico e

tensões ambientais (ROSHITH et al., 2018). A biodiversidade dessa comunidade tem sido amplamente utilizada para compreender o funcionamento dos ecossistemas aquáticos, bem como, os impactos das atividades humanas nesses ecossistemas (LERUSTE et al., 2018).

A comunidade fitoplanctônica responde eficazmente a gradientes de salinidade espacial, pois espécies e grupos variam consideravelmente em sua tolerância à salinidade (OLOFSSON et al., 2020). O gradiente de salinidade, por sua vez, é um aspecto hidrológico único dos estuários, responsável por impulsionar o desenvolvimento e dominância de espécies do fitoplâncton a partir de uma interação complexa entre os processos que ocorrem nas bacias oceânicas regionais e dentro das bacias hidrográficas. Sob condições intermediárias de salinidade, espécies marinhas e de água doce podem desaparecer devido ao estresse osmótico, ou ao fato dessa região funcionar como um ambiente de transição de uma comunidade de água doce para marinha ao longo do gradiente de salinidade (LANCELOT e MUYLAERT, 2011).

Mudanças nesse padrão de salinidade, como o avanço da IAM, podem afetar a dinâmica das comunidades aquáticas, aumentando o estresse ou a mortalidade de organismos, além de modificar os padrões de dispersão e a seleção de características das espécies-chave menos tolerantes. Assim, a IAM pode impactar severamente as comunidades aquáticas dos sistemas oligohalinos naturais, levando a uma perda de diversidade e/ou funcionalidade desses ambientes, bem como, dos serviços e benefícios para as sociedades locais (CUNILLERA-MONTCUSÍ et al., 2022).

Além disso, variações temporais desse gradiente de salinidade devem ser consideradas, uma vez que, a maior extensão da IAM pode ser observada em estuários tropicais durante o período de menor descarga dos rios, devido à redução das chuvas. Durante esse período, a mistura das marés é responsável por mudanças significativas na salinidade, turbidez e composição de nutrientes, que atuam como fatores-chave para regular a comunidade fitoplanctônica em escalas espaço-temporais (AZHIKODAN e YOKOYAMA, 2016; BHARATHI et al., 2022; NWE et al., 2022). Compreender essas interações bióticas ou associações entre diferentes espécies de fitoplâncton são cruciais para avaliar o efeito de mudanças nas condições ambientais nas funções do ecossistema (TARAFDAR et al., 2022). Recentemente, muitos pesquisadores investigaram a influência das variações hidrológicas do gradiente de salinidade sob a composição, abundância e biomassa fitoplanctônica em estuários tropicais (KASAI et al, 2010; NCHE-FAMBO et al., 2015; AZHIKODAN e YOKOYAMA, 2016; OLLI et al., 2019; BHARATHI et al., 2022; NIVEDITHA et al., 2022).

No Brasil, poucos estudos utilizam essa abordagem para avaliar os efeitos da intrusão salina (LELES et al., 2014; SILVA et al., 2017; CONCEIÇÃO et al., 2021; SILVA et al., 2021), com destaque para Santos et al. (2017), Cavalcanti et al., (2020) e Costa e Cutrim (2021), como trabalhos pioneiros para o estado do Maranhão (Tabela 2).

Tabela 2 - Sumário de publicações sobre espécies indicadoras do fitoplanctôn na costa norte e nordeste do Brasil (2010-2022)

Região	Estuários	Ano	Gradiente de Salinidade	Espécies-chave	Referência
NORDESTE	Rio Capibaribe – PE Bacia do Pina – PE	2005	21-36	*Helicotheca tamesis*, *Coscinodiscus centralis*, *Coscinodiscus* sp., *Aulacoseira granulata*	Santiago et al. (2010)
	Rio Ilha Grande – PE	2012	25,98-31,8	*Leptocylindrus minimus, Leptocylindrus danicus, Dactyliosolen fragilissimus, Skeletonema costatum*	Leles et al. (2014)
	Rio Paraguaçu – BA	2018-2019	0,2-31,9	*Cyclotella meneghiniana, Scrippsiella acuminata, Planktothrix isothrix*	Conceição et al. (2021)
	Rio Jaboatão – PE	1999-2011	0,04-27,54	*Microcystis aeruginosa*	Silva et al. (2017)
	Rio Beberibe – PE Rio Capibaribe – PE Porto do Recife – PE	2011	12,4-28,4	*Cylindrotheca closterium, Nitzschia longissima, Planktothrix isothrix*	Borges et al. (2020)
	Rio Beberibe – PE Rio Capibaribe – PE	2015	10,73-31,77	*Thalassiosira* sp., *Melosira* sp. *Chroococcus* sp.	Silva et al. (2021)
	Rio Bacanga – MA	2012-2013	7,16-25,78	*Skeletonema costatum, Euglena gracilis, Chlamydomonas* sp.	Santos et al. (2017)
	Rio Curuça – PA	2011	8,47-30,55	*Diploneis bombus, Coscinodiscus concinnus*	Ribeiro et al. (2019)
	Rio Caruperé-PA	2015	0-40	*Cylindrotheca closterium, Yonedaella* sp., *Navicula gregaria*	Reis et al., 2019
NORTE	Rio Arienga - PA	2009	-----	***Polymyxus coronalis*** *Coscinodiscus* sp.	Sena et al. (2015)
	Rio Paciência – MA	2017	8,91-35,2	*Trieres sinensis, Nitzschia reversa, Protoperidinium* sp., *Thalassiosira subitilis*	Cavalcanti et al. (2020)
	Rio Bom Gosto – MA	2018-2019	0,11-33,78	*Cyclotella meneghiniana*	Costa e Cutrim (2021)
	Rio Mocajuba - PA Rio Tijoca - PA Rio Pará - PA	2019	0-18	Aulacoseira granulata, Coscinodiscus rothii, ***Polymyxus coronalis***	Vilhena et al. (2021)
	Rio Taperaçu - PA	2013-2014	6,44-38,55	*Hobaniella longicruris, Odontella aurita, Zygoceros rhombus* e *espécies* de *Trieres*	Oliveira et al. (2022)

Fonte: O Autor (2022).

2 DESCRIÇÃO DA ÁREA

Nesta seção, foi fornecida a descrição da área abordando uma visão geral da Zona Costeira Amazônica Brasileira, Golfão Maranhense e do Estuário do Rio Itapecuru, onde os dados amostrais foram coletados e analisados.

2.1 Zona Costeira Amazônica Brasileira

O Brasil ocupa 47% da área da América do Sul apresentando uma linha de costa de, 9.200 km de extensão, com diversos ecossistemas tropicais e subtropicais (LARA, 2003; Gomes et al., 2009). A região costeira do norte do Brasil está delimitada entre o Cabo Orange (Amapá) e o Rio Parnaíba (Piauí), entre as latitudes 4ºN e 3ºS. A largura da plataforma continental (área = 285.000 km^2) varia entre 80 e 320 km e a quebra da plataforma ocorre na isóbata de 100 m. Essa região está sobre influência da Corrente Norte do Brasil (CNB) e apresenta fluxo hidrológico de 7,8 milhões de km^2 da bacia de drenagem, com descarga média de 200.00 $m^3 . s^{-1}$ (NICOLODI et al., 2009).

A Zona Costeira Amazônica Brasileira (ZCAB) inclui os estados do Amapá (57.858 km^2, 40% da área total do estado), Pará (43.659 km^2, 3,5% da área total do Pará) e Maranhão (66.790 km^2, 20% da área total do estado) (SZLAFSZTEIN, 2012). Essa região abriga 85% dos manguezais brasileiros (área=10.713 km^2), ocorrendo ao longo de 1.800 km do Litoral Norte do Brasil (SCHAEFFER-NOVELLI et al., 1990; VANNUCCI, 1999; KJERFVE et al., 2002; VISSCHERS et al., 2022). O setor entre Belém (Pará) e São Luís (Maranhão) representam 83% da área total de manguezais desses três estados amazônicos e é considerada como uma das mais extensas áreas contínuas de manguezal do mundo (área=8.900 km^2) (KJERFVE e LACERDA, 1993).

A ZCAB representa, cerca de 35% dessa faixa costeira do Brasil (~2.500 km de extensão), compreendida entre o Rio Oiapoque no Amapá (5°N, 51°W) e nela está inserida a Baía de São Marcos no Maranhão (2°S, 44°W), local, onde estão diversos ambientes, por exemplo, praias, planícies de marés, pântanos salinos e doces, estuários, manguezais, floresta de várzea, florestas tropicais, lagoas, lagunas, ilhas, rias, deltas, dunas, etc. (PEREIRA et al., 2009) (Figura 3).

Figura 3 - Zona Costeira da Amazônia Brasileira com ênfase nos estados do Maranhão, Pará e Amapá indicando municípios legalmente definidos

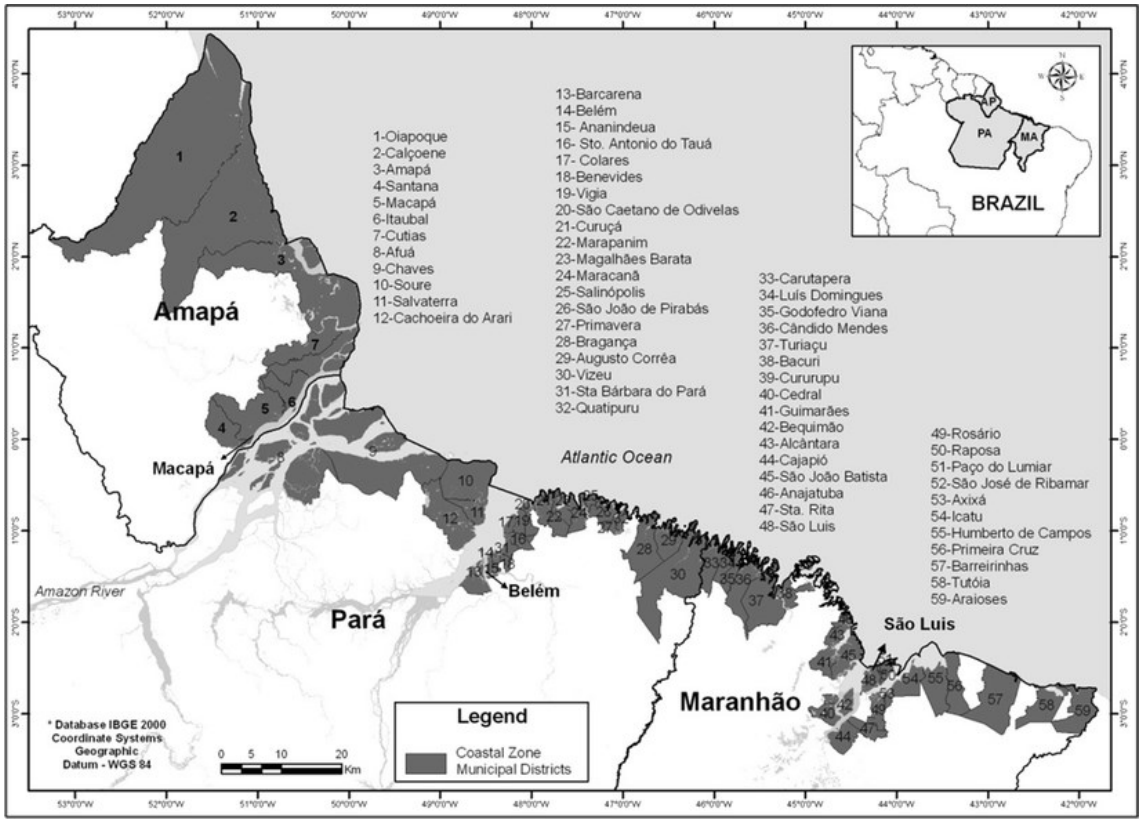

Fonte: Szlafsztein (2012).

A ZCAB está inserida no contexto das regiões tropicais úmidas (sítios Ramsar), situadas entre 4ºN e 4ºS, formando uma das áreas litorâneas mais extensas e bem preservadas do mundo (Souza-Filho et al., 2005; Pereira et al., 2018). Nesta faixa territorial encontram-se ainda as regiões metropolitanas de Macapá-Santana (AP), Belém (PA) e São Luís (MA). Nos três grandes centros urbanos estão concentrados, aproximadamente, 2,8 milhões de habitantes e a economia está baseada, principalmente, nas atividades industriais, portuárias, metalúrgicas, imobiliárias, pesqueiras, turísticas, comerciais, extrativistas e pecuaristas (Figura 3) (Pereira et al., 2009).

Os processos costeiros na ZCAB resultam de uma combinação de macromarés locais (faixa de maré de 4 a 12 m durante as marés vivas), ondas de energia moderada (Hs até 2 m), fortes correntes de maré (normalmente acima de 1,0 $m.s^{-1}$), e altos níveis de precipitação (~ 2000–3000 mm) (Pereira et al., 2018). Ao longo da costa de manguezais do nordeste do Pará e noroeste do Maranhão desemboca uma série de estuários que promovem o aumento da turbidez, associada também a processos frontais de maré e a variações sazonais (Souza-Filho

et al., 2005). Nesse contexto encontra-se a Zona Costeira Maranhense (ZCM), que cobre 640 km de linha de costa, dividida em litoral ocidental (reentrâncias maranhenses), oriental (baías, praias e lenções maranhenses), e entre eles, o golfão maranhense (AZEVEDO et al., 2008).

2.2 Golfão Maranhense

O golfão maranhense é considerado como um recorte da ZCAB que inclui inúmeros ecossistemas (estuários, estreitos, muitas ilhas) e uma grande floresta de mangue que margeiam os canais estuarinos, ocupando uma área de 1.622,91 km^2 (SOUZA-FILHO, 2005). A Ilha do Maranhão, onde está localizada a cidade de São Luís (capital do Maranhão), ocupa a parte central desse sistema estuarino. A Ilha é separada do continente pelo Estreito dos Mosquitos que junto com o Estreito dos Coqueiros ligam as massas d'água da Baía Arraial/ São José com as da Baía de São Marcos (SEREJO et al., 2020) (Figura 4).

Figura 4 - Localiação do Golfão Maranhense indicando a Baía de Cumã, Baía de São Marcos (SMEC) e Baía do Arraial/São José

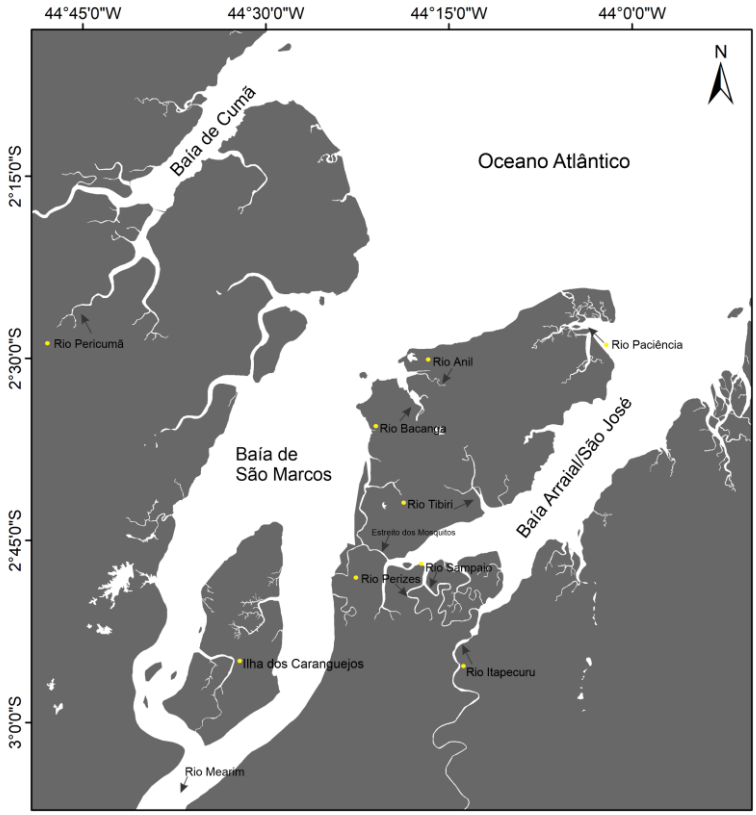

Fonte: O Autor (2022).

O golfão maranhense apresenta um litoral irregular, com entrada de 115 km de largura e comprimento máximo de 173 km no Complexo Estuarino de São Marcos, o maior canal do golfão (Figura 4). Esta área recebe descargas de água doce de três rios principais: Rio Pericumã na Baía de Cumã, Rio Mearim no Complexo Estuarino São Marcos e Rio Itapecuru na Baía de Arraial/São José (CZIZEWESKI et al., 2020).

A Baía de São Marcos é uma vasta zona estuarina ativa (2.250 km^2 de extensão), com largura de ~55 km e canal central bem definido (~15 km; 97 m de profundidade) dominado por correntes de vazante. Esse canal serve de hidrovia para as principais instalações portuárias do Maranhão: Porto de São Luís, Porto do Itaqui, terminal Ponta da Madeira e terminal da Alumar, considerado o canal mais profundo, largo e longo do Brasil (LIMA et al., 2021). Essa região conta com usinas siderúrgicas e de alumínio, e a exportação de minério de ferro é a maior força motriz da região (235 milhões de toneladas anuais) (GONZÁLEZ-GORBEÑA et al., 2015).

A Baía do Arraial/São José apresenta extensão de 665 km^2 (18 m de profundidade), sendo formada principalmente pelos aportes fluviais dos rios Itapecuru e Munim, não apresentado um canal de maré desenvolvido como a Baía de São Marcos (MACEDO, 1989). A Baía do Arraial/São José é uma continuação do estuário do rio Itapecuru, que atravessa regiões geológicas, as quais refletem tanto na morfologia como na distribuição das faceis sedimentares (COUTINHO e MORAIS, 1976).

As amplitudes de maré (>6 m) e fortes correntes (>3 $m.s^{-1}$) classificam o golfão maranhense como um sistema de macromaré a hipermaré semidiurnas. O prisma de maré varia entre $3{,}194 \times 10^{10}$ m^3 para a sizígia e $1{,}517 \times 10^{10}$ m^3 para a quadratura (CZIZEWESKI et al., 2020). O clima dessa região é tropical úmido do tipo Am, segundo o sistema de classificação climática de Köppen, com regime de ventos predominante de NE e velocidade média anual de 3,5 $m.s^{-1}$. Os períodos sazonais são bem definidos (estiagem - julho a dezembro; chuvoso - janeiro a junho) (TEIXEIRA e SOUZA-FILHO, 2009) e a precipitação pluviométrica é superior a 2.000 mm anuais e temperaturas médias superiores a 25ºC (LEFÈVRE et al., 2017; SANTOS et al., 2020).

Esse regime de chuvas e de ventos é influenciado pelo posicionamento da Zona de Convergência Intertropical (ZCIT) e linhas de instabilidade, que varia sua posição ao longo do ano, penetrando no Sul do continente americano durante o verão e outono, e movendo-se para

o norte, afastando-se da costa, durante o inverno e a primavera austral. Maior precipitação e velocidades de vento reduzidas estão associadas à ZCIT (DOMINGUEZ, 2009).

2.3 Estuário do Rio Itapecuru

O estuário do rio Itapecuru (ERI) está inserido na Região Hidrográfica do Atlântico Nordeste Ocidental, delimitando a ZCAB e a região semiárida do Maranhão. Essa região possui área de 274.000 km^2 que compreende 3,2% da região hidrográfica do Brasil e aproximadamente 90% das suas sub-bacias hidrográficas estão concentradas no Maranhão (ABREU et al., 2020). O ERI está localizado dentro do domínio da Margem Equatorial Brasileira e sobre influência da Corrente Norte do Brasil, responsável por transportar águas quentes e salinas em direção noroeste (STRAMMA et al., 2003).

Situado ao leste da ilha de São Luís, o ERI representa a segunda maior bacia hidrográfica do estado do Maranhão com área de 53.216,84 km^2 e extensão de 1.050 km desde a montante até a foz do rio. O ERI deságua no Complexo Estuarino de São José (CESJ), sendo o seu principal contribuinte de água doce e sedimentos, que em conjunto com o Complexo Estuarino São Marcos (CESM) formam o golfão maranhense (FEITOSA, 1983; ALCÂNTARA, 2004). Esse vasto sistema estuarino é conectado por um canal estreito (Estreito dos Mosquitos) responsável por fazer a troca de água entre as duas baías (COUTINHO e MORAIS, 1976; EL-ROBRINI et al., 1992) (Figura 5).

A bacia hidrográfica do rio Itapecuru (BHI) envolve 56 municípios do Maranhão, entre esses 39 possuem a sede localizada na bacia e 11 destas são localizadas as margens do rio, destacando: Mirador, Colinas, Caxias, Codó, Timbiras, Coroatá, Pirapemas, Cantanhede, Itapecuru-Mirim, Santa Rita e Rosário. Nessa bacia, contabiliza-se mais de 1,2 milhões de habitantes, o que representa 17,5% da população do estado. Através do sistema de abastecimento ITALUÍS, aproximadamente 2,00 $m^3 . s^{-1}$ da água da BHI é captada para o fornecimento de mais de 1,6 milhões de pessoas da região metropolitana da grande São Luís (MASULLO et al., 2019).

Figura 5 - Localiação do estuário do Rio Itapecuru e rios adjascentes, Golfão Maranhense, Brasil

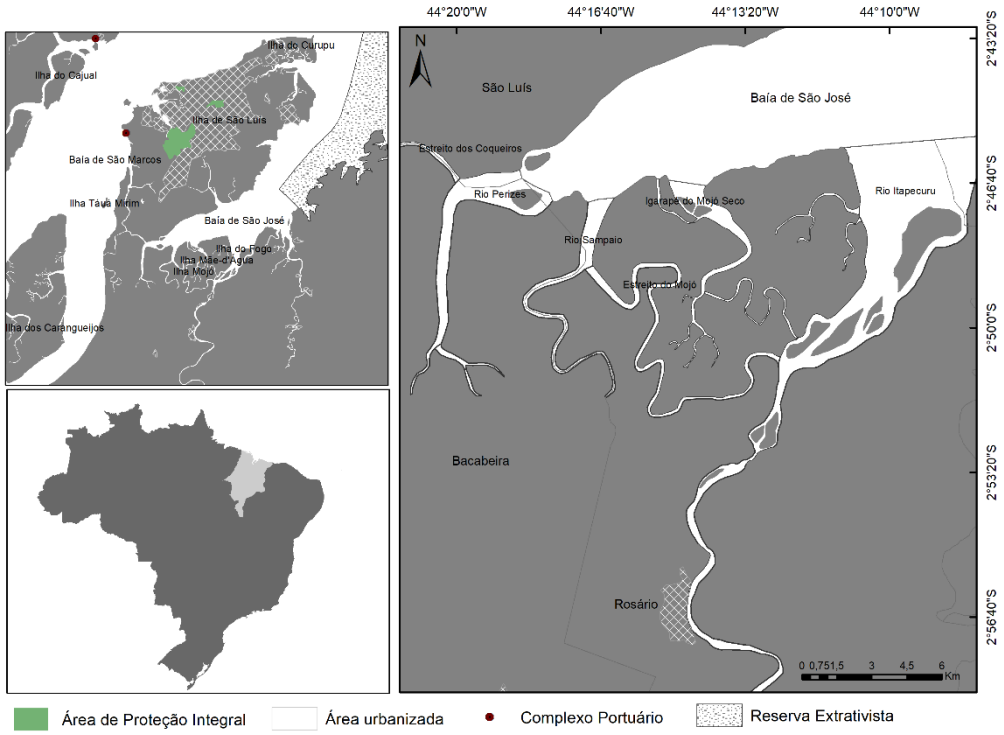

Fonte: O Autor (2022).

No estuário do rio Itapecuru existe pouca variação da intensidade das correntes na coluna d'água. A circulação horizontal apresenta um comportamento semelhante ao observado na superfície e no fundo, com defasagem significativa na inversão do sentido da corrente e na elevação do nível da maré. Os perfis durante o estágio de maré enchente registram fluxo de correntes característico de maré vazante e sentido Montante → Jusante.

A distribuição vertical na coluna d'água é praticamente homogênea com pequenas variações de salinidade, temperatura e densidade, limitadas apenas ao primeiro metro de profundidade. Esse perfil enquadra o estuário como do tipo bem misturado na vertical, resultante principalmente da difusão de turbulência gerada na camada-limite de fundo do rio. A distribuição de salinidade obtida a partir dos levantamentos verticais e longitudinais no estuário do rio Itapecuru estão descritos na Figura 6.

Figura 6 - Distribuições verticais e longitudinais de salinidade do estuário do Rio Itapecuru durante maré de enchente

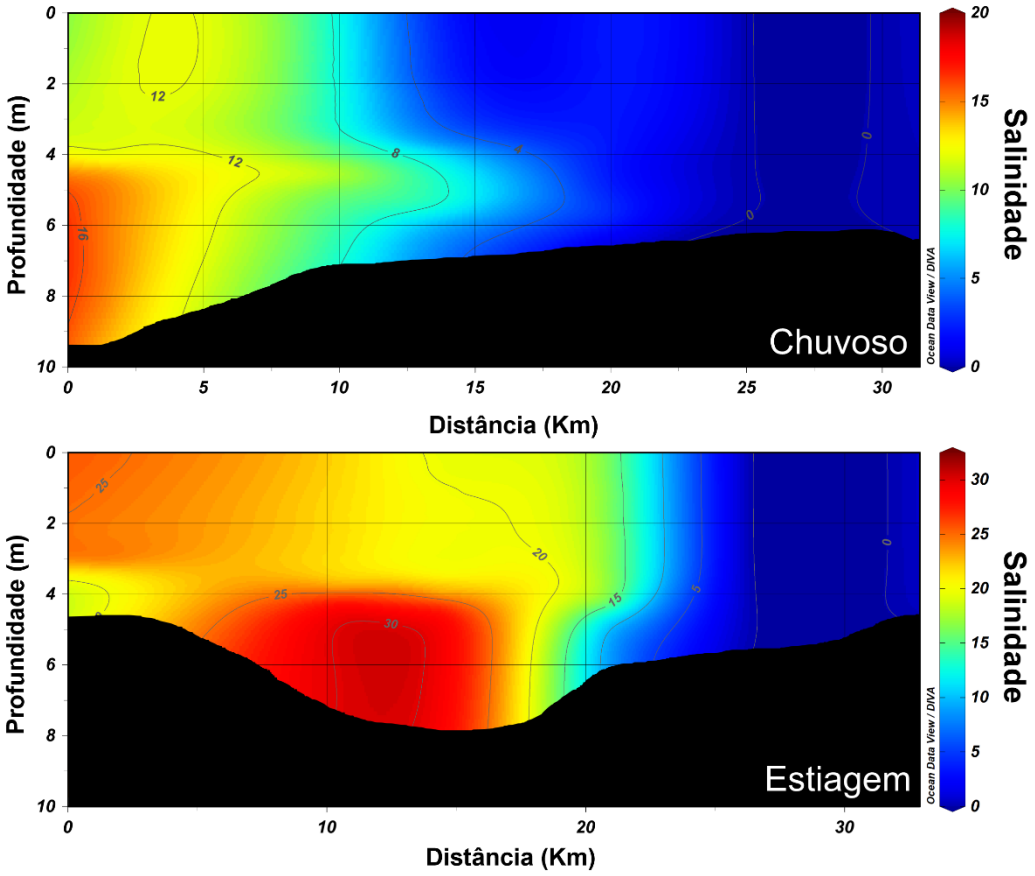

Fonte: O Autor (2022).

A partir dos perfis verticais, os valores mensurados in situ pela CTD durante o estudo, apontaram para um estuário bem misturado. Sazonalmente, observou-se um gradiente longitudinal de salinidade, com maior intrusão salina com alcance de 25 km durante a estiagem. No período chuvoso, o alcance da maré é limitado a aproximadamente 16 km.

Dados pretéritos indicam que a forçante astronômica (maré dinâmica) se propaga cerca de 16 km a montante do município de Rosário e a inversão de sentido de correntes alcança esta posição durante o estágio de enchente. A variação do nível d'água indica a existência de defasagens significativas entre o estofo de maré (PM e BM), em relação as previsões para o Porto de São Luís (01h40) e para o Terminal da Alumar (01h10). A curva de maré a partir do município de Rosário possui período de vazante maior que o período de enchente, com 08h50 vazando e 03h50 enchendo, totalizando 12:40h para completar um ciclo de maré semidiurna.

Assim, o estuário do rio Itapecuru é considerado como um grande exportador de sedimentos para a zona costeira maranhense.

Estudos pretéritos e de monitoramento da qualidade da água, realizado pelo CEERMA, indicam que a variabilidade astronômica (marés de sizígia ou quadratura) não exerce influência significativa sobre a distribuição longitudinal dos dados ambientais no trecho estuarino do Itapecuru. Essa caracterização foi baseada nos dados não oficiais do Relatório Técnico do Centro de Estudos e Ensaios em Risco e Modelagem Ambiental da Universidade Federal de Pernambuco – CEERMA.

A Formação Itapecuru, representa o Cretáceo mais jovem da Bacia do Parnaíba e é composta por sedimentos clásticos depositados em planícies aluviais costeiras (MENEZES et al., 2019). Constituída por arenitos e lutitos (siltitos, argilas e folhelhos), conglomerados e por calcário, a bacia do Itapecuru está dividida em três membros (inferior, médio e superior) com base em seções sísmicas e perfis de poços (FERREIRA et al., 2016; BATISTA et al., 2020; FERREIRA et al., 2020).

Os paleoambientes deposicionais são: estuarino-lagunar, leques aluvial-deltaicos, fluviais e costeiros, fluvial-lacustre e marinho restrito, frente delta, frente delta retrabalhada de onda, barras distais e ambientes de baixa energia, possivelmente relacionados ao prodelta e plataforma restrita (FERREIRA et al., 2021). A Formação Itapecuru preserva um importante registro fóssil, composto principalmente por restos vegetais (angiospermas), bivalves de água doce, fragmentos de ossos de dinossauros, escamas de peixes e conchostracans (MENEZES et al., 2019).

3 OBJETIVOS

Os objetivos gerais e objetivos específicos serão apresentados na próxima seção, compreendendo os objetivos aplicados em cada capítulo publicado.

3.1 Objetivo Geral

Avaliar a variabilidade espaço-temporal da comunidade fitoplanctônica e do estado geral de eutrofização em resposta às alterações ambientais promovidas pela intrusão salina e pelas mudanças climáticas (El Niño/ La Niña) no estuário do Rio Itapecuru (ERI).

3.2 Objetivos Específicos

- Determinar as implicações ecológicas da intrusão salina nos principais indicadores de fitoplâncton e selecionar os fatores hidrológicos que melhor explicam a variabilidade na comunidade fitoplanctônica;

- Quantificar a magnitude das múltiplas pressões antrópicas no ERI e o efeito de múltiplos estressores sobre o estado trófico;

- Classificar as variáveis que atuam direta e indiretamente na explicação de interações tróficas no ERI.

4 HIPÓTESES

- A intrusão salina ao alterar os gradientes ambientais espaço-temporal promove mudanças abruptas ou graduais na estrutura e dinâmica da comunidade fitoplanctônica do estuário do Rio Itapecuru.

- As pressões antrópicas e múltiplos estressores quando associados ao fenômeno da intrusão salina em um estuário de macromarés aumentam o estado geral de eutrofização e comprometem a qualidade de suas águas.

5 ESTRUTURA DA TESE

De acordo com os objetivos e resultados obtidos ao longo da realização do presente estudo, os resultados da tese estão organizados em dois capítulos. Os capítulos 3 e 4 correspondem aos artigos científicos (Original Articles e/ou Research Papers) publicados nas revistas Hydrobiologia (artigo 1) e Journal of Sea Research (artigo 2), respectivamente.

ARTIGO 1 - Phytoplankton community dynamics in response to seawater intrusion in a tropical macrotidal river-estuary continuum. Dinâmica da comunidade fitoplanctônica em resposta a intrusão de água do mar em um continuo rio-estuário tropical de macromarés. Este estudo gerou importantes informações sobre os efeitos da intrusão da água do mar na variação espaço-temporal da comunidade fitoplanctônica e forneceu uma ferramenta para o manejo sustentável de estuários tropicais baseada nos indicadores ambientais, biológicos e seus traços funcionais (Figura 7).

Figura 7 - Diagrama de fluxo do procedimento de pesquisa de coleta e análise de dados referentes ao capítulo 3

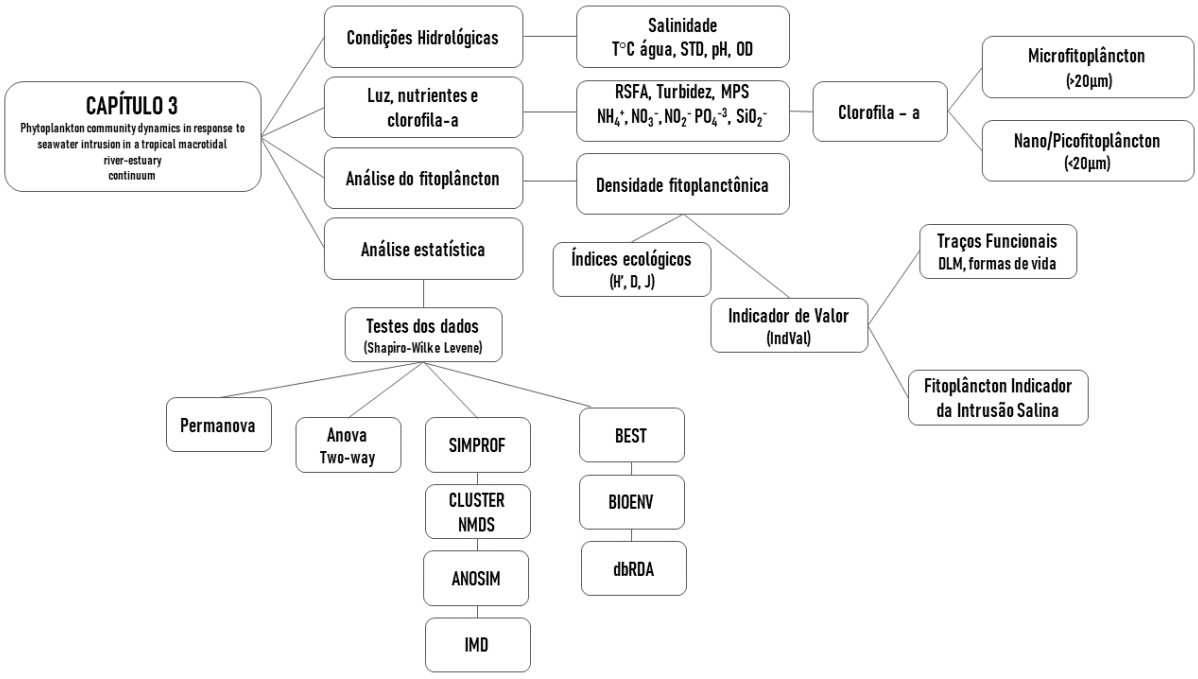

Fonte: O Autor (2022).

ARTIGO 2 - Multiple stressors influencing the general eutrophication status of transitional waters of the Brazilian tropical coast: An approach utilizing the pressure, state, and response (PSR) framework. Múltiplos estressores influenciando o estado geral de eutrofização das águas transicionais da costa tropical brasileira: uma abordagem utilizando o framework Pressão, Estado e Resposta (PSR). Este estudo utilizou modelos de avaliação do estado trófico estuarino (ASSETS e TRIX) aplicando a abordagem Pressão, Estado e Resposta (PER) a fim de indicar o grau de eutrofização do estuário do Rio Itapecuru, associando às mudanças climáticas globais. O cenário futuro do IRE foi construído para a próxima década (2021–2031) baseado na suscetibilidade natural do sistema à eutrofização e mudanças previsíveis no uso da terra e tratamento de efluentes (Figura 8).

Figura 8 - Diagrama de fluxo do procedimento de pesquisa de coleta e análise de dados referentes ao capítulo 4

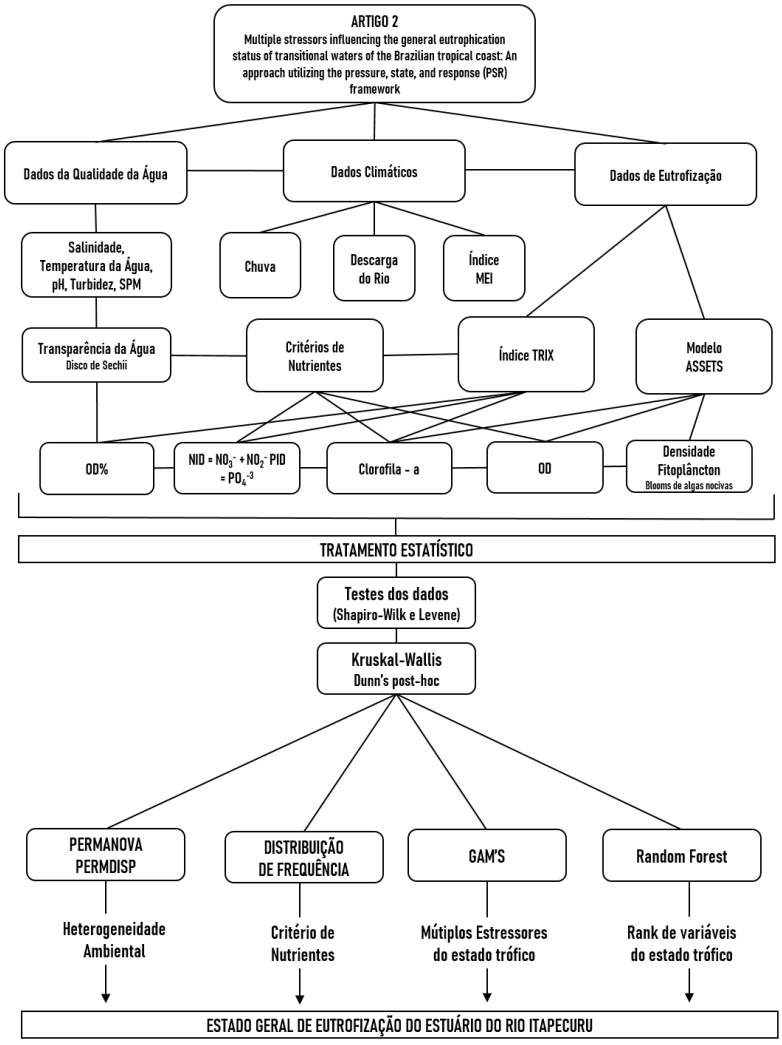

Fonte: O Autor (2022).

6 ARTIGO 1 - PHYTOPLANKTON COMMUNITY DYNAMICS IN RESPONSE TO SEAWATER INTRUSION IN A TROPICAL MACROTIDAL RIVER-ESTUARY CONTINUUM

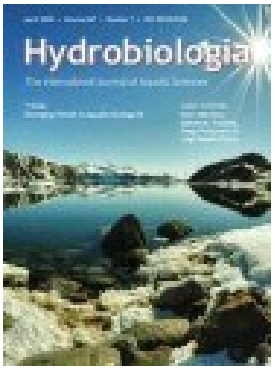

Manuscript published in Hydrobiologia
Published: 05 May 2022
Special Issues: Effects of changes in salinity
https://doi.org/10.1007/s10750-022-04851-7

Abstract

Coastal environments are at the frontline of sea-level rise effects, and seawater intrusion constitutes one of the most important causes of salinization, changing the ecological patterns. Hence, we hypothesized that seawater intrusion would alter environmental gradients, causing either abrupt or gradual changes in the phytoplankton of Itapecuru River estuary. Physical and chemical and biological variables were collected bimonthly at six sites between 2019 and 2020. Seventy-six phytoplankton indicators were selected based on their specific functional traits and indicator value. *Polymyxus coronalis* was a good indicator of the limit of seawater intrusion. Multivariate analyses revealed high species dispersion among the estuarine sectors governed by variations in salinity, suspended particulate matter, cell size, and silicate. The distribution of freshwater species in the upper sector was correlated with low nutrient values and salinity. The marine species were transported between the middle and lower sectors under the opposite conditions. The seawater intrusion negatively affected the community, primarily in the dry season when the displacement of the turbidity maximum zone estuarine altered the structure, reducing its density, diversity, and biomass. The present study generated important information about seawater intrusion effects on the spatiotemporal variation in the phytoplankton community and provided a tool for the sustainable management of tropical estuaries.

Keywords: Diatoms · Macrotides · Bioindicators · Seasonal changes · Salinity gradient · *Polymyxus coronalis*

Introduction

Seawater intrusion (SWI) into coastal environments is a natural, hydrological phenomenon characterizing estuarine dynamics, which determines the transport of sediments, nutrients, and contaminants as driven by the interactions of tides, river flows, and coastal

currents (Lu & Gan, 2015; Wang et al., 2019; Onalube et al., 2020). Climate change, deepening river beds, and sediment resuspension are the primary mechanisms altering salt transport and are thus responsible for controlling the baroclinic circulation, the longitudinal and transverse density gradient of the estuary, sediment dynamics, and water quality (Liu et al., 2019a, b).

Coastal environments represent the frontline of sea-level rise vulnerability (Chang et al., 2011; Werner et al., 2013), and as 80% of the world's population lives along the coast and uses local aquifers for water supply (Long et al., 2013). Advances in SWI constitute one of the most important causes of surface and groundwater salinization (Wang et al., 2019; Gomes et al., 2019; Prusty & Farooq, 2020), and they have the potential to change the ecological distribution patterns, as well as the structure of faunal and floral communities (Rice et al., 2012; Tian, 2019; Da Silva et al., 2020).

Phytoplankton communities act as indicators of this impact and play a key role in quickly responding to any ecological changes affecting coastal ecosystems, reflecting environmental health and water quality conditions (Srichandan et al., 2015; Lemley et al., 2019). Thus, understanding the interactions regulating community growth, as well as the distribution patterns associated with river discharge and longitudinal salinity gradients is of particular importance in affected tropical estuaries (Kasai et al., 2010; Watanabe et al., 2014; Azhikodan & Yokoyama, 2016; Krvavica & Ružić, 2020).

Most research on SWI in Brazil (De Miranda et al., 2005, 2012; Sanders et al., 2012; Melo et al., 2014; Cary et al., 2015; Gomes et al., 2019; da Silva et al., 2020) has assessed SWI and mixing processes in subtropical and tropical estuaries using hydrodynamic models, isotopic approaches, and characterization of physical processes. In contrast, analyses of the distribution and structure of the phytoplankton communities in tropical macrotidal estuaries in Brazil remain scarce and restricted to the subtropical estuaries (Abreu et al., 1995; Fujita & Odebrech, 2007; Da Silva et al., 2017). To narrow this knowledge gap, and considering that SWI modifications are a global issue, this study was conducted in the Itapecuru River Estuary.

The IRE is a coastal system of the Brazilian Equatorial Margin, with a seasonal pattern controlled by the latitudinal displacement of the Intertropical Convergence Zone (ITCZ; Souza-Júnior et al., 2013). This macrotidal estuary maintains a tidal excursion of ~ 40 km upstream from the river mouth and has a water supply system 27 km from the penetration limit of the

saltwedge. The Itapecuru River is also the principal water source for ~ 1.6 million people on the Island of São Luís, in addition to numerous riverside municipalities (Masullo et al., 2019).

The Itapecuru basin is an area of constant anthropogenic disturbance (e.g., urbanization and domestic sewage input; Santos et al., 2019). Some of these disturbances stem from activities such as the provision of water supply for human use, agricultural activity, and an industrial sector in the Metropolitan Area of the São Luís Island. These activities add to other anthropogenic pressures from the growth of urban centers, deforestation, the rapid growth of agricultural activities, pollution from the release of fresh domestic sewage, and products resulting from industrial expansion (e.g., metallurgical complexes, mining, and port operations). These impacts in the lower course of the Itapecuru River are more severe due to the salinity increase, siltation of the bed, and destruction of riparian forests (Porto et al., 2017).

Accordingly, we hypothesized that SWI would alter environmental gradients spatiotemporally, causing either abrupt or gradual changes in the IRE phytoplankton community. This study thus attempted to (1) identify the spatial and temporal variability of environmental variables, (2) define the concentrations of chlorophyll-a in the river-estuary continuum, (3) determine the ecological implications of SWI on the principal phytoplankton indicators, and (4) select the hydrological factors that best explain the observed variability in the phytoplankton community. The biological interactions and environmental variables observed in this macrotidal estuary can provide an ecologically predictive dataset for use in managing environmental quality.

Materials and methods

Study area

The IRE (02°51–6°56S and 43°02–43°58 W) is located in the western Northeast Atlantic Hydrographic Region (area, 274,000 km^2), east of the island of São Luís, and comprises the second largest hydrographic basin in Maranhão (area, 53,216.84 km^2). The estuary is strongly influenced by the tidal ranges of the western Atlantic Ocean, as well as the freshwater flow of the Itapecuru River, the longest river in Maranhão (length, 1050 km; Stramma et al., 2003; Abreu et al., 2020). Extensive industrial and urban areas are located around and at the mouth of the Itapecuru River, primarily associated with the urban centers of

São Luís and Rosário (Fig. 1).

Fig. 1 Geographical locations of the sampling and study area in Itapecuru River Estuary (IRE), Maranhão—Brazil

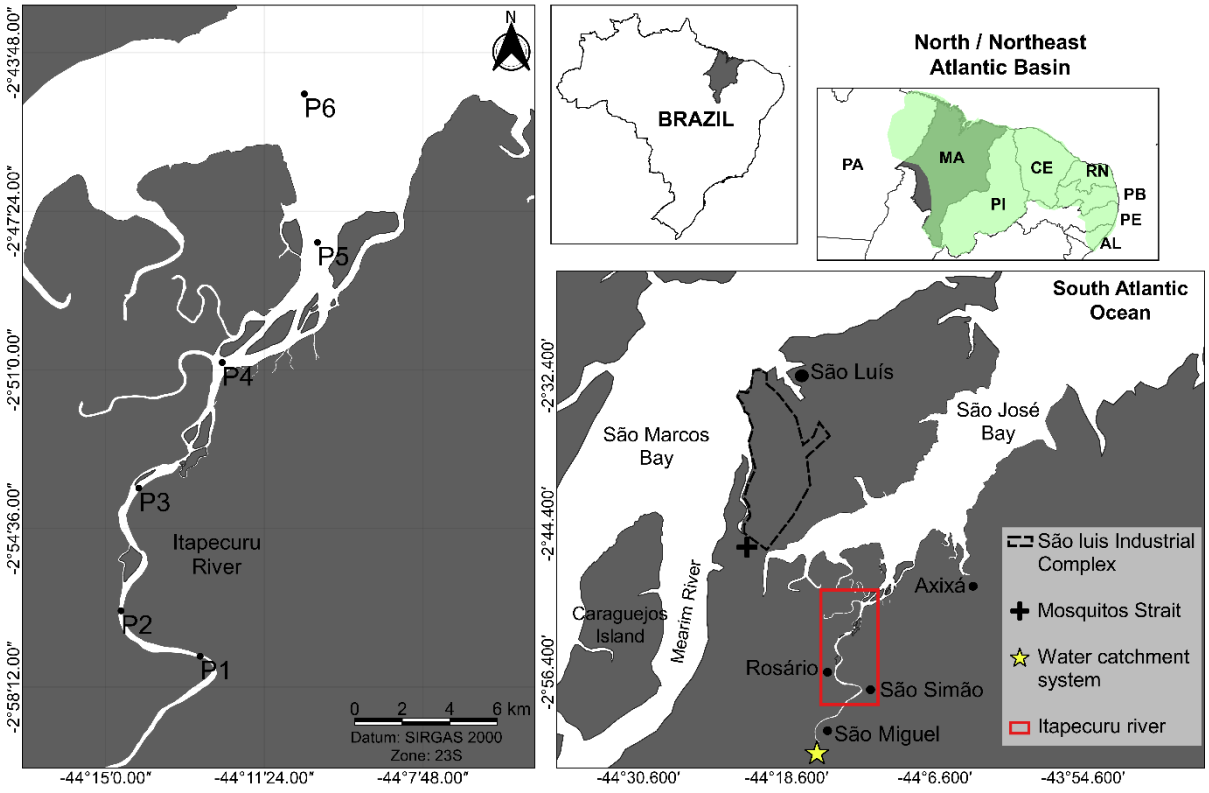

Source: The author (2022).

Notably, the IRE flows into the Arraial-São José Estuarine Complex (ASJEC), contributing to a discharge of river water and sediment. The ASJEC and the São Marcos Estuarine Complex (SMEC) form the Maranhense Gulf, an estuarine-wide system into which the tributaries of the Mearim and Munim rivers also flow (Santos et al., 2020). The SMEC has a well-developed central channel dominated by ebb currents, and sandy banks extend its mouth to the interior. By contrast, the ASJEC does not have a well-developed tidal channel due to constant sediment migration. In addition, there are asymmetrical banks at its mouth, which move from ENE to WSW, oblique to the coast, and are separated by narrow channels that change position seasonally (Coutinho & Morais, 1976).

According to the Köppen-Geiger classification, the local climate is tropical humid (Am) with predominantly northeasterly winds averaging 3.5 m s^{-1} (Alvares et al., 2013). The fluvial regime is controlled by the position of the ITCZ, the primary controlling mechanism of seasonal

patterns, with substantial rainy (January–June) and dry seasons (July–December). Rainfall is > 2,000 mm year^{-1}, and the average temperature is > 25 ºC (Lefèvre et al., 2017). The Itapecuru River is an estuary of a coastal plain with a Cretaceous formation and eastern Amazon coast attributes (Coutinho & Morais, 1976), alternating between extensive floodplains and lakes. This region also has sandbanks and thin mangrove fringes. *Rhizophora mangle* Linnaeus is the dominant species, and together with *R. harrisonii* Leechm, *R. racemosa* G. Mey, *Avicennia germinans* (L.) Linnaeus., A. schaueriana Stapf & Leechm, *Laguncularia racemosa* C. F. Gaertn, and *Conocarpus erectus* Linnaeus. constitute the Upaon-Açu Environmental Protection Area as per Decree 12,428 (Masullo et al., 2019).

Sampling design

An ~ 28 km length of the study area was demarcated and divided into three sectors based on their salinity range. A total of six sampling points, two sampling points in each sector, placed longitudinally, were selected for the study (McLusky, 1993; Fig. 1; Table 1). Samples were collected bimonthly for seasonal monitoring of physical and chemical (e.g., salinity, light, nutrients) and biological (chlorophyll-a, phytoplankton density) variables comprising an annual cycle, collected in the rainy (May 2019, March, June 2020) and dry (August, October, December 2019) periods. In addition, the sampling considered the astronomical cycle (spring tide) and daily tidal cycle (flood tide). Water quality samples were collected using a Van Dorn bottle (5 l) in the subsurface layer (c. 0.3 m; average estuary depth, 5.37 m), totaling 36 samples.

Tab. 1 Description of sampling sites in the Itapecuru River Estuary

Sectors	Station	Geographical cordinates		Salinity	Depth (m)	Venice system
		Latitude	Longitude			
Upper	P1	2°56'28,14"	44°14'38,992"	0.03-0.05	5.70	Limnetic
	P2	2°56'28,14"	44°14'38,992"	0.03-0.54	6.11	Oligohaline
Middle	P3	2°53'41,12"	44°14'14,76"	6.51-24.44	6.50	Mesohaline
	P4	2°50'50,04"	44°12'21,17"	12.20-29.31	7.72	Polyhaline
Lower	P5	2°48'40,93"	44°12'15,25"	16.48-30.54	7.28	Euhaline
	P6	2°44'44,25"	44°10'29,32"	17.67-30.43	9.28	Euhaline

Source: The author (2022).

The total precipitation in 2019 and 2020 was well above the historical average (2,730.65 mm) of the last 40 years. The peak of precipitation was recorded in March of 2019 and 2020 with 818.2 mm and 658.8 mm, respectively (National Institute of Meteorology—INMET, portal.inmet.gov.br). The minimum and maximum daily precipitation values recorded during

field observation were 2.1 mm in the dry season and 226.70 mm in the rainy season. The resulting average discharge of the IRE was 130.78 $m^3 s^{-1}$ in 2019 and 145.55 $m^3 s^{-1}$ in 2020, with 76.32% of this total annual discharge occurring during the rainy season (average, 121.98 $m^3 s^{-1}$; National Water Agency—ANA, ana.gov.br). Over the sampling period, the wind velocities ranged from 0.78– 2.68 m s^{-1} in 2019 to 0.76–2.63 m s^{-1} in 2020, with higher values recorded in September and October (Fig. 2).

Fig. 2 a Historical average rainfall and **b** river discharge (based on the 40 years) showing records for 2019 and 2020 and **c** wind speed for the sampling months

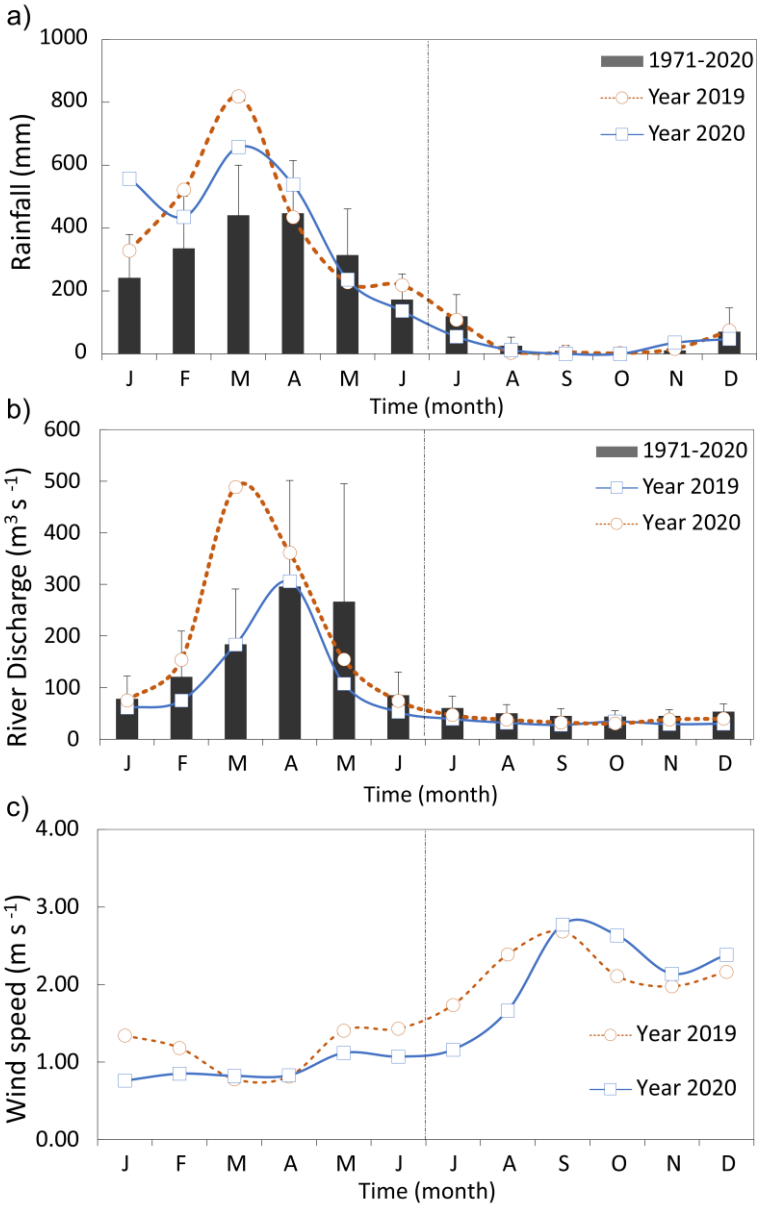

Source: The author (2022).

The local circulation pattern is generally well-mixed, and the regional tides are semidiurnal. The sea reaches up to 7 m, with water-current speeds of 2.5 m s^{-1}, influencing up to 150 km off the coast of Maranhão. The IRE presents a significant difference between the durations of flood and ebb (3:50–8:50), although current flows between tidal scenarios were similar, with reduced vertical variations in intensity and direction. The average interval is $0.02 \leq |\bar{v}| \leq 0.75$ m s^{-1} (average, 0.42 m s^{-1}). The influence of the dynamic tide occurs 16 km upstream, and that of the saline tide 4 km downstream of the larger of the two urban centers in the estuary, the municipality of Rosário. The tidal height during the study period ranged from 5.7 m (December 2019) to 6.7 m (March 2020), with an amplitude of 2.54 m (Brazilian Navy's Directorate of Hydrography and Navigation—DHN, marinha.mil.br).

Hydrological conditions in surface waters

Salinity (resolution = 0.01; accuracy = ± 0.1), temperature (resolution = 0.01; accuracy = ± 0.05 °C), and pressure (resolution = 0.01 m; accuracy = ±0.25% scale) were measured in situ in the middle channel of the estuary with a CTD probe ([Conductivity, Temperature, and Depth] - Castway, Sontek Instrument Company, USA), maintaining a data acquisition frequency of 5 Hz, with a descending speed of 1 m s^{-1}. Total dissolved solids (TDS) and pH data were obtained using a multiparameter probe (HANNA-9878, Italy). Dissolved oxygen (DO) was determined using the chemical method of Winkler, as modified by Golterman et al. (1978).

Light, nutrients, and chlorophyll-a conditions

Atmospheric and sub-aquatic photosynthetically active solar radiation (PAR; superficial and 1 m depth) were recorded with the aid of LI-COR Quanta Meter (LI-1500-USA) connected to a spherical sensor (Li-193). Turbidity was measured using a turbidimeter (Lamotte 2020, USA), and suspended particulate matter (SPM) was assessed using the gravimetric analysis described by Strickland and Parsons (1972). From the weighed SPM samples, particulate inorganic matter (PIM) and particulate organic matter (POM) levels were determined by heating the filters at 450 °C for 4 h. The determination of ammonium ions followed the methodology described by Koroleff (1983). The nitrite and nitrate concentrations were based on Strickland and Parsons (1972), whereas orthophosphate and silicate measurements were derived according to Grasshoff et al. (1983). The detection limits were 0.1, 0.01, 0.05, 0.006 and 0.1 μg l^{-1}, respectively.

To determine the chlorophyll-a concentrations, samples were vacuumed (0.05–0.50 l) through fiberglass filters (Whatman GF/F, UK; pore diameter = 0.7 μm). Photosynthetic pigments were extracted with 90% acetone after 24 h in the dark at –18 °C. Chlorophyll concentrations were determined using the spectrophotometric method (UNESCO, 1966) through a Spectronic 200 spectrophotometer (Thermo Fisher Scientific, USA; Strickland & Parsons, 1972). The fractionation of samples by a 20 μm mesh allowed for the evaluation of microphytoplankton (> 20 μm) and nano-(2–20 μm) and picophytoplankton (0.2–2 μm) fractional contributions in the phytoplankton biomass.

Phytoplankton analysis

Samples for phytoplankton analysis were fixed with Lugol's acid solution (1%) and deposited in sedimentation chambers (2.5–25 ml) for 24 h in the laboratory for further phytoplankton cell counts (20–200 μm cell size). A systematic analysis was carried out in illuminated fields following the Utermöhl technique (Utermöhl, 1958) using an inverted microscope (Zeiss Axiovert 100, Germany) at 400 × magnification to count nano-(10– 20 μm) and microphytoplankton (20–200 μm). Phytoplankton density was calculated according to Villafañe and Reid (1995), expressed in cells l^{-1}. The synonyms and ecology of the taxa were updated via the international database AlgaeBase (www.algaebase.org). The ecological conditions of the phytoplankton were evaluated using the following indices: Shannon diversity (H'; 1948), Margalef richness (D; 1958), and Pielou evenness (J; 1966). The equations of the diversity indexes are defined as follows:

$$\text{Shannon index: } H' = -\sum_{i=1}^{s} Pi \log_2 \times Pi \qquad Pi = \frac{Ni}{N} \quad (1)$$

$$\text{Margalef richness index: } D = \frac{(s-1)}{\ln \times N} \quad (2)$$

$$\text{Pielou evenness index: } J = \frac{H'}{\log 2\ S} \quad (3)$$

where Ni is the number of individuals of one particular species found, N is the total number of individuals found, and S is the total number of species at any sampling point.

Indicator phytoplankton and functional traits

The indicator value method (IndVal) was used to select the indicator species, combining phytoplankton density with the relative frequency of occurrence, as expressed by the product of the fidelity and specificity of each taxon with the spatial factor (sectors). The IndVal of species i for class j was obtained according to Eq. (4):

$$\mathrm{IndVal} = A_{ij} \times B_{ij} \times 100$$

where A_{ij} corresponds to specificity, and B_{ij} to fidelity (Dufrêne & Legendre, 1997). Species with IndVal > 30% and $P < 0.05$ according to a randomized distribution Monte Carlo test were considered the top indicators of the phytoplankton community. The functional traits of the indicator phytoplankton community were determined from the maximum linear dimensions (MLD; Lewis, 1976) and classification in terms of life form (Kruk et al., 2010).

Statistical analysis

To choose between the parametric and non-parametric techniques, the normality and homoscedasticity of the variances were verified by the Shapiro–Wilk and Levene tests, respectively (IBM SPSS Statistics v.24). Multivariate data analyses were performed using the PRIMER—6 extensions + PERMANOVA package (Clarke et al., 2014). All non-normally distributed environmental data were transformed to log scale (x + 1) and biological data to square roots. For the multivariate permutational analysis of variance (PERMANOVA; permutations, n = 9999), a Euclidean distance similarity matrix was considered together with fixed spatiotemporal factors to determine environmental variable heterogeneity ($P < 0.05$), followed by a two-way ANOVA.

Similarity profiles (SIMPROF) were compared in the cluster analysis to assess the grouping significance of the functional indicator communities, and the connectivity of these phytoplankton groups (Bray-Curtis similarity) was represented using non-metric multidimensional scaling (NMDS) with a stress of 0.2. Analysis of similarity (ANOSIM) was used to examine the significance of spatial and temporal similarities, and the index of multivariate dispersion (IMD) tested the variability of the phytoplankton community as a function of SWI. The RELATE routine in PRIMER - 6 extensions + PERMANOVA package identified significant correlations between environmental and biological variables, followed by the best correspondence analysis (BEST) in the Biota and/or Environment matching (BIO-ENV) submodule. The distance-based multiple linear regression model (DistLM), with

selection criterion R^2, identified the combinations of predictor variables that best explained the observed structure of phytoplankton communities, whereas the Draftsman plot from the Spearman correlation was used for evaluating variable collinearity ($R^2 > 0.7$). The complementary analysis of distance-based redundancy (dbRDA) assessed the representation of the revealed relationships, with overlapping vectors of environmental and biological variables ($R^2 = 0.4$).

Results

The PERMANOVA analysis revealed that the water quality and photosynthetic data had a significant spatio-temporal heterogeneity (P<0.001). There was also a significant interaction between spatial and temporal factors (P < 0.001). The differences between the estuarine sectors were evident from the pairwise test. Regarding spatiotemporal variations as a function of time, both the middle and lower sectors expressed significant variability. However, spatially, the upper and middle sectors were similar during the rainy season, and the middle and lower sectors were similar during the dry season (Table 2).

Tab. 2 PERMANOVA analysis results from the environmental data matrix and pairwise test of the spatial term vs. temporal for the pairs of "temporal" and "spatial" factor levels. Significant results (P = * < 0.05; ** < 0.01; *** < 0.001)

Source	**df**	**SS**	**MS**	**Pseudo-F**	**P (perm)**
Spatial	2	180.52	90.262	13.137	0.001***
Temporal	1	115.43	115.43	16.801	0.001***
Spatial *vs.* Temporal	2	50.193	25.096	3.6528	0.001***
Res	30	206.12	6.8705		
Total	35	552.27			
Level		**Groups**		**t**	**P (perm)**
Upper				0.8666	0.621
Middle		Rainy vs. Dry		3.3344	0.005**
Lower				2.7208	0.006**
Level		**Groups**		**t**	**P (perm)**
Rainy		Upper *vs.*Middle		0.866	0.621
		Upper *vs.* Lower		3.334	0.005**
		Middle *vs*. Lower		2.720	0.006**
Dry		Upper *vs.* Middle		3.978	0.004**
		Upper *vs.* Lower		3.962	0.005**
		Middle *vs*. Lower		1.168	0.235

Source: The author (2022).

Environmental gradients

The environmental gradients of the IRE were expressed in terms of the hydrological variation, which resulted from the marked spatial variability of salinity, TDS, and SPM.

Salinity, water temperature, TDS, and pH also varied temporally. When spatiotemporal factors interacted, only salinity, TDS, and pH were significantly altered. Salinity and TDS were the main variables characterizing SWI in the estuary, with adjusted R^2 values of 0.72 and 0.86 (Bonferroni correction), respectively (Fig. 3). The hydrological characteristics and photosynthetic properties of the IRE are summarized in Table 3.

Fig. 3 Temporal and spatial changes of salinity (**a, b**); total dissolved solids (**c, d**); pH (**e, f**); and dissolved oxygen (**g, h**) in Itapecuru River Estuary (IRE)

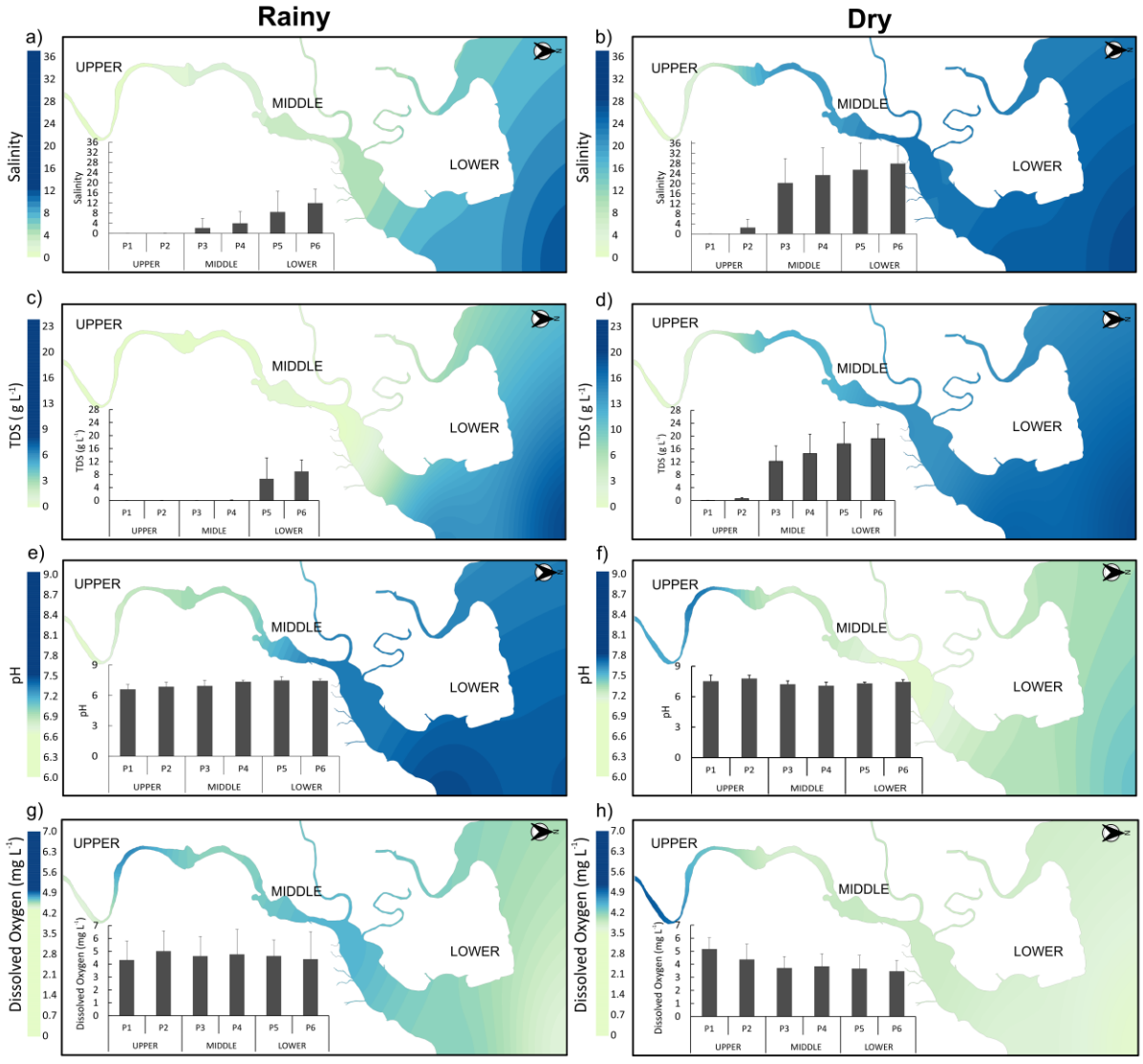

Source: The author (2022).

Tab. 3 Mean values and standard deviation (Average + SD) of environmental variables in surface waters in the upper, middle, and lower sectors. Repeated measure ANOVA two-way. Significant values (P = * < 0.05; ** < 0.01; *** < 0.001)

Environmental Variables	Unity	Upper		Middle		Lower		p ≤ 0.05		
		Rainy	Dry	Rainy	Dry	Rainy	Dry	Temporal	Spatial	Interaction
Salinity	-	0.04 ± 0.02	1.25 ± 2.50	3.08 ± 3.90	21.82 ± 9.36	10.22 ± 6.51	26.71 ± 8.25	0.001***	0.001***	0.002**
Temperature	°C	29.16 ± 3.24	32.01 ± 1.13	29.20 ± 3.32	31.24 ± 0.93	29.57 ± 3.29	31.12 ± 0.94	0.01**	0.93	0.80
TDS	g L^{-1}	0.04 ± 0.01	0.33 ± 0.36	0.06 ± 0.06	13.38 ± 5.03	7.81 ± 4.82	18.42 ± 5.10	0.001***	0.001***	0.001***
DO	mg L^{-1}	4.66 ± 1.42	4.77 ± 1.02	4.69 ± 1.56	3.77 ± 0.83	4.51 ± 1.57	3.57 ± 0.84	0.16	0.40	0.51
DO	%	58.28 ± 13.91	65.74 ± 14.93	59.95 ± 13.93	56.65 ± 13.26	59.04 ± 19.24	55.35 ± 12.36	0.97	0.70	0.58
pH	-	6.73 ± 0.44	7.65 ± 0.46	7.14 ± 0.43	7.15 ± 0.31	7.46 ± 0.26	7.38 ± 0.18	0.02*	0.15	0.003**
Turbidity	NTU	38.53 ± 22.95	70.33 ± 39.24	75.58 ± 87.35	100.02 ± 77.63	35.78 ± 23.55	68.83 ± 27.32	0.04*	0.20	0.57
SPM	mg L^{-1}	50.05 ± 12.75	77.53 ± 46.07	116.95 ± 118.93	140.84 ± 92.13	144.45 ± 68.65	167.84 ± 43.35	0.31	0.01**	0.99
PAR	µmol m^2 s^{-1}	926.74 ± 832.56	540.70 ± 327.39	592.71 ± 813.63	915.44 ± 426.11	1312.98 ± 1342.25	1211.51 ± 906.15	0.84	0.23	0.59
Nitrate	µmol L^{-1}	4.25 ± 1.90	1.79 ± 0.98	3.95 ± 2.15	5.48 ± 2.11	3.99 ± 2.95	5.13 ± 1.78	0.91	0.10	0.04**
Nitrite	µmol L^{-1}	0.05 ± 0.02	0.05 ± 0.01	0.06 ± 0.05	0.10 ± 0.05	0.09 ± 0.03	0.09 ± 0.03	0.27	0.05*	0.53
Ammonium ion	µmol L^{-1}	0.56 ± 0.25	0.27 ± 0.13	0.58 ± 0.19	0.36± 0.21	0.44 ± 0.14	0.85 ± 1.22	0.86	0.55	0.21
Orthophosphate	µmol L^{-1}	0.38 ± 0.14	0.78 ± 0.27	0.40 ± 0.22	1.46 ± 0.58	0.56 ± 0.28	1.27 ± 0.11	0.001***	0.01**	0.04*
Silicate	µmol L^{-1}	27.7 ± 16.96	39.31 ± 21.17	40.90 ± 26.31	55.66 ± 18.27	34.22 ± 21.50	44.54 ± 11.28	0.07	0.20	0.96
Biological Variables	**Unity**	**Rainy**	**Dry**	**Rainy**	**Dry**	**Rainy**	**Dry**	**Temporal**	**Spatial**	**Interaction**
Chl-a Total	µg L^{-1}	9.86 ± 12.48	41.64 ± 33.87	9.06 ± 5.94	17.67 ± 12.28	14.03 ± 4.36	50.46 ± 48.23	0.01**	0.31	0.26
Chl-a (<20)	µg L^{-1}	3.21 ± 2.17	11.09 ± 5.53	4. 84 ± 3.85	9.57 ± 6.13	8.89 ± 5.29	23.19 ± 20.74	0.005**	0.03**	0.52
Chl-a (>20)	µg L^{-1}	6.66 ± 10.42	30.55 ± 32.92	4.22 ± 3.09	8.10 ± 8.16	5.14 ± 5.47	27.27 ± 31.29	0.04**	0.51	0.23
Density	10^4 cells L^{-1}	27.17 ± 31.47	37.68 ± 36.18	25.98 ± 44.00	13.08 ± 5.73	41.85 ± 27.21	17.33 ± 14.44	0.36	0.53	0.34
Diversity Index	bits $cells^{-1}$	1.81 ± 0.66	2.30 ±0.18	2.22 ± 0.86	2.35 ± 0.33	2.14 ± 0.52	2.36 ± 0.36	0.12	0.54	0.69
Richness Index	-	4.11 ± 1.87	4.91 ± 0.79	4.53 ± 3.00	4.36 ± 0.86	5.16 ± 1.75	4.36 ± 1.06	0.92	0.89	0.52
Eveness Index	-	0.68 ± 0.25	0.72 ± 0.08	0.80 ± 0.11	0.83 ± 0.08	0.67 ± 0.14	0.82 ± 0.11	0.92	0.89	0.53

Source: The author (2022).

The pairwise test comparisons (temporal *vs.* spatial) revealed that only significant variations in pH and TDS were recorded in the upper sector (e.g., P1 and P2) of the estuary. In this sector, higher variability of pH was found in the rainy season (Fig. 3e–f), while TDS displayed a wide seasonal variation, with a notable ionic increase during the dry season (Fig. 3c–d). The middle (e.g., P3 and P4) and lower (e.g., P5 and P6) sectors were marked by temporal variations in TDS and salinity, with higher values recorded during the dry period (Fig. 3d, f).

Pairwise (spatial *vs.* temporal) comparisons of salinity and TDS showed significant variations between the upper and lower sectors and similarities between the upper and middle sectors during the rainy season. The similarity interactions were evident between the middle and lower sectors in the dry season. Indeed, TDS values exhibited strongly heterogeneous distributions, clearly defining the three sectors of the estuary in each season. Indeed, TDS was the hydrological tracer of the estuarine regions (Fig. 3c–d). Dissolved oxygen (DO) concentrations did not vary significantly in time or space; however, states of hypoxia were observed during the dry period (2.27 mg l^{-1}; Fig. 3g–h).

Light conditions, nutrients, and chlorophyll-a

The light conditions characterized the IRE as a turbid system, where the average PAR presented a homogeneous profile, the maximum recorded in the lower sectors during the dry season and the minimum in the upper sectors during the rainy season (Fig. 4a, b). Vertically, the average incident light absorption was 34.41 ± 26.63%, delimiting the euphotic zone (Z_{eu}) to 1 m depth. The water turbidity presented significant seasonal variability, doubling the values in the dry season (Fig. 4c–d). The middle sector was identified as the most turbid (100.02 ± 77.63 NTU), characterizing this region as the turbidity maximum zone estuarine (TMZE), peaking in both seasons. SPM values an increased longitudinally toward the river mouth, with higher values recorded in the lower sector (156.15 ± 56.09 mg l^{-1}; Fig. 4e–f). Of all the SPM transported by the estuarine waters, POM represented 81.67 ± 16.34% and PIM, 18.33 ± 16.34%.

The nutrient analysis did not indicate significant spatiotemporal variations, except for NO_3^- and PO_4^{3-} with higher values in the middle and lower sectors, revealing a flow toward the river mouth following the salinity gradient (Table 3; Fig. 4g–h; k–l). In the IRE, the interactions between the spatiotemporal factors were responsible for the maximum levels of

NO_3^- (Fig. 4i–j) and (in particular) PO_4^{3-}, contributing to the enrichment of the middle sector during the dry period (Fig. 4k–1). The low DIN:DIP ratios at ~ 91% of the sites indicated that the IRE was nitrogen-limited, and NO_3^- was the predominant form of DIN at 84.4% of the sampling sites.

Total chlorophyll-a concentrations showed significant temporal variability, with a maximum mean value observed in the dry season upper sector five times greater than the overall mean (10.13 ± 10.99 μg l^{-1}; Fig. 5a–b), and the minimum recorded in the rainy season TMZE (Fig. 5a). For fractionation, microphytoplankton (> 20 μm) varied seasonally, with higher values recorded in the dry season upper sector (Fig. 5d). Nano/picophytoplankton (< 20 μm) showed significant spatial and temporal variations, the maximum values observed in the lower sector during the dry season, and the minimum observed in the upper sector during the rainy season (Fig. 5e–f). Microphytoplankton were predominant in the upper sector (56.2%) and nano/picophytoplankton in the lower sector (56.1%). The microphytoplankton community was the most sensitive to the hydrological conditions established in TMZE, accounting for 46.2% of total biomass.

Phytoplankton community structure

A total of 187 taxa were identified: 154 during the rainy season and 113 in the dry season. Diatoms (Bacillariophyta) dominated the phytoplankton community (49.7% of the total density), followed by chlorophytes (Chlorophyta, 18.1%), cyanobacteria (Cyanophyta, 15.5%), phytoflagellates (Euglenophyta, 10.7%; Myozoa, 5.3%), and ochrophytes (Ochrophyta, 0.5%). Diatoms dominated the lower sector (85.5%) and were also dominant during the period of higher SWI (58.4%).

Chlorophytes were abundant in the upper sector (33.3%) and rainy seasons (20.1%). Cyanobacteria peaked during the dry season (19.4%) and were restricted to the upper (26.3%) and middle sectors (10.7%). The ochrophytes were less diverse, represented only by *Mallomonas acaroides* Perty, a taxon exclusive to the rainy season upper and middle sectors.

Fig. 4 Temporal and spatial changes of photosynthetically active radiation (PAR) (**a, b**); turbidity (**c, d**); suspended particulate matter (**e, f**); nitrite (**g, h**); nitrate (**i, j**); and orthophosphate (**k, l**) in Itapecuru River Estuary (IRE)

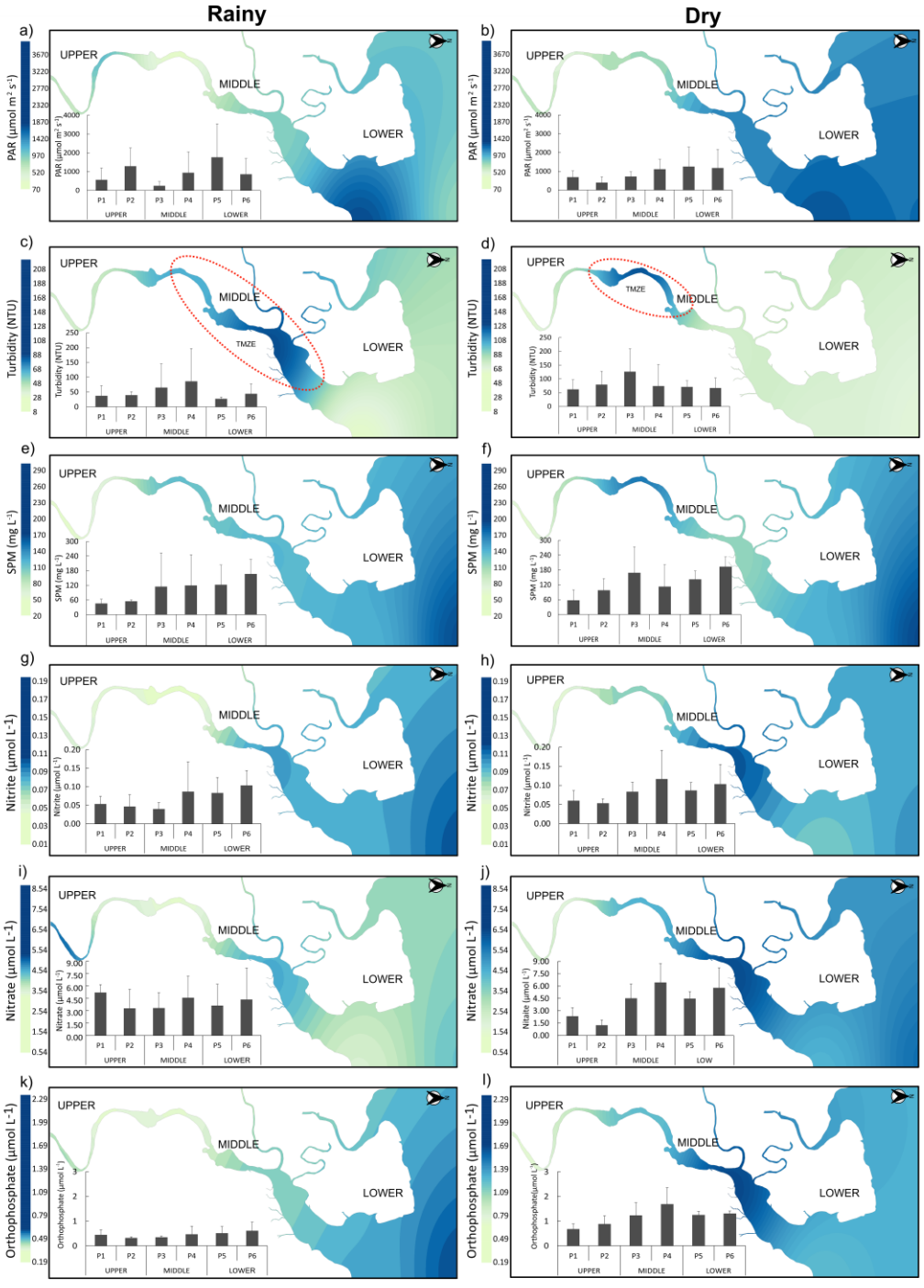

Source: The author (2022).

Total phytoplankton density presented mean values ranging from $2.22 \pm 1.56 \times 10^4$ to $2.89 \pm 4.05 \times 10^4$ cells l^{-1} in the dry and rainy seasons, respectively (Fig. 5g–h). This slight dry

season density reduction was likely in response to SWI, which trapped freshwater diatoms in the upper sector, thus increasing their density in Aug 2019 (1.24×10^4 cells l^{-1}). The driest months of this period (Oct 2019 [L02]; Dec 2019 [L03]) showed a decrease in overlapping phytoplankton groups in the lower sector (Fig. 6).

Fig. 5 Temporal and spatial changes of chlorophyll-a (**a, b**); microphytoplankton (**c, d**); nano/picophytoplankton (**e, f**); phytoplankton density (**g, h**); Shannon diversity (H' index) (**i, j**); and Margalef richness (D Index) (**k, l**) in Itapecuru River Estuary (IRE)

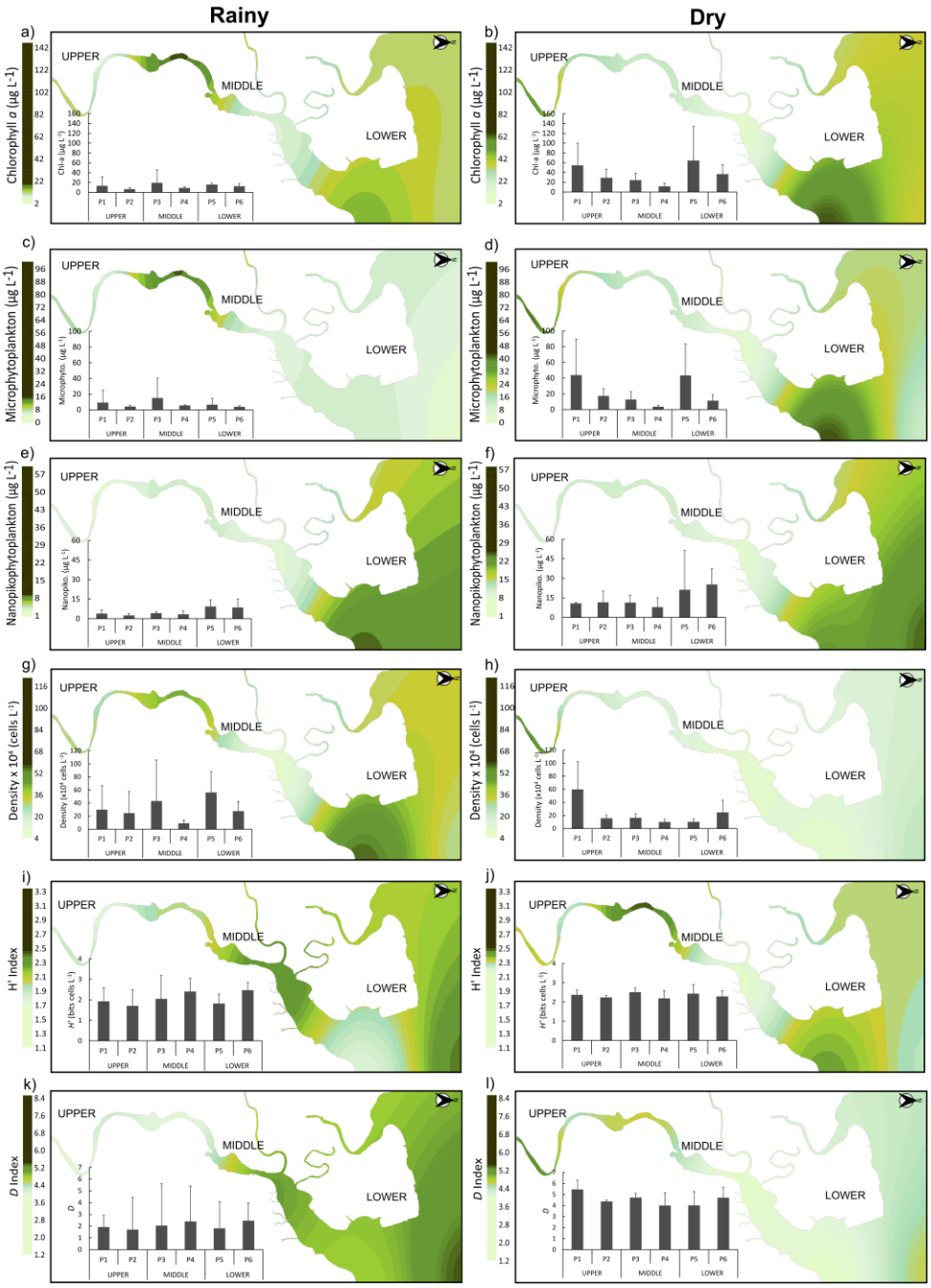

Source: The author (2022).

Conversely, there was a substantial overlap between groups recorded during the rainy season. In the upper sector (May 2019 [U01]), euglenophytes, chlorophytes, and cyanobacteria competed for similar hydrological conditions. In the middle sector (Jun 2020 [M03]), this overlap occurred between euglenophytes, chlorophytes, and dinoflagellates, with a predominance of the diatom *Nitzschia palea* (Kützing) W.Smith (11.55×10^4 cells l^{-1}) in TMZE. Finally, in the lower sector, overlapping occurred between euglenophytes and chlorophytes (May 2019 [L01]), chlorophytes and cyanobacteria (Mar 2020 [L02]), and dinoflagellates, cyanobacteria, and euglenophytes (Jun 2020 [L03]; Fig. 6).

The ecological status of the IRE, defined by the application of diversity indices, was defined by low diversity (H'), with significant temporal variance. In the rainy season, the abundance of species diversity and richness (D) occurred in the lower sector (Fig. 5i–j, k–l), whereas during the dry season, a transition area with reduced diversity and richness was observed between the middle and lower sectors (Fig. 5j, l). Regarding the species distribution in the IRE, the phytoplankton community was relatively homogeneous, with a reduced balance between species in the upper sector during the rainy season. This result was probably due to the dominance of *Polymyxus coronalis* L.W.Bailey (18.38×10^4 cells l^{-1}) and *Aulacoseira granulata* var. *angustissima* (O.Müller) Simonsen (93.66×10^4 cells l^{-1}).

Other dominant species must also to be mentioned. These include *Aphanocapsa delicatissima* West & G.S.West (9.46×10^4 cells l^{-1}), *Microcystis aeruginosa* (Kützing) Kützing (11.71×10^4 cells l^{-1}), *Craticula ambigua* (Ehrenberg) D.G.Mann (55.74×10^4 cells l^{-1}), *P. coronalis* (60.76×10^4 cells l^{-1}), and *A. granulata* var. *angustissima* (99.85×10^4 cells l^{-1}) dominated the upper sector. The lower sector was dominated by chain-forming marine diatoms, such as *Skeletonema costatum* (Greville) Cleve (89.36×10^4 cells l^{-1}) and *Thalassiosira gravida* Cleve (51.63×10^4 cells l^{-1}), while *N. palea* (18.26×10^4 cells l^{-1}) was predominant in the TMZE (Table 4).

Fig. 6 Temporal and spatial distribution of total phytoplankton density (bar) and taxonomic groups (circles) in logarithmic scale for each sampled period (U-upper; M-middle; L-lower)

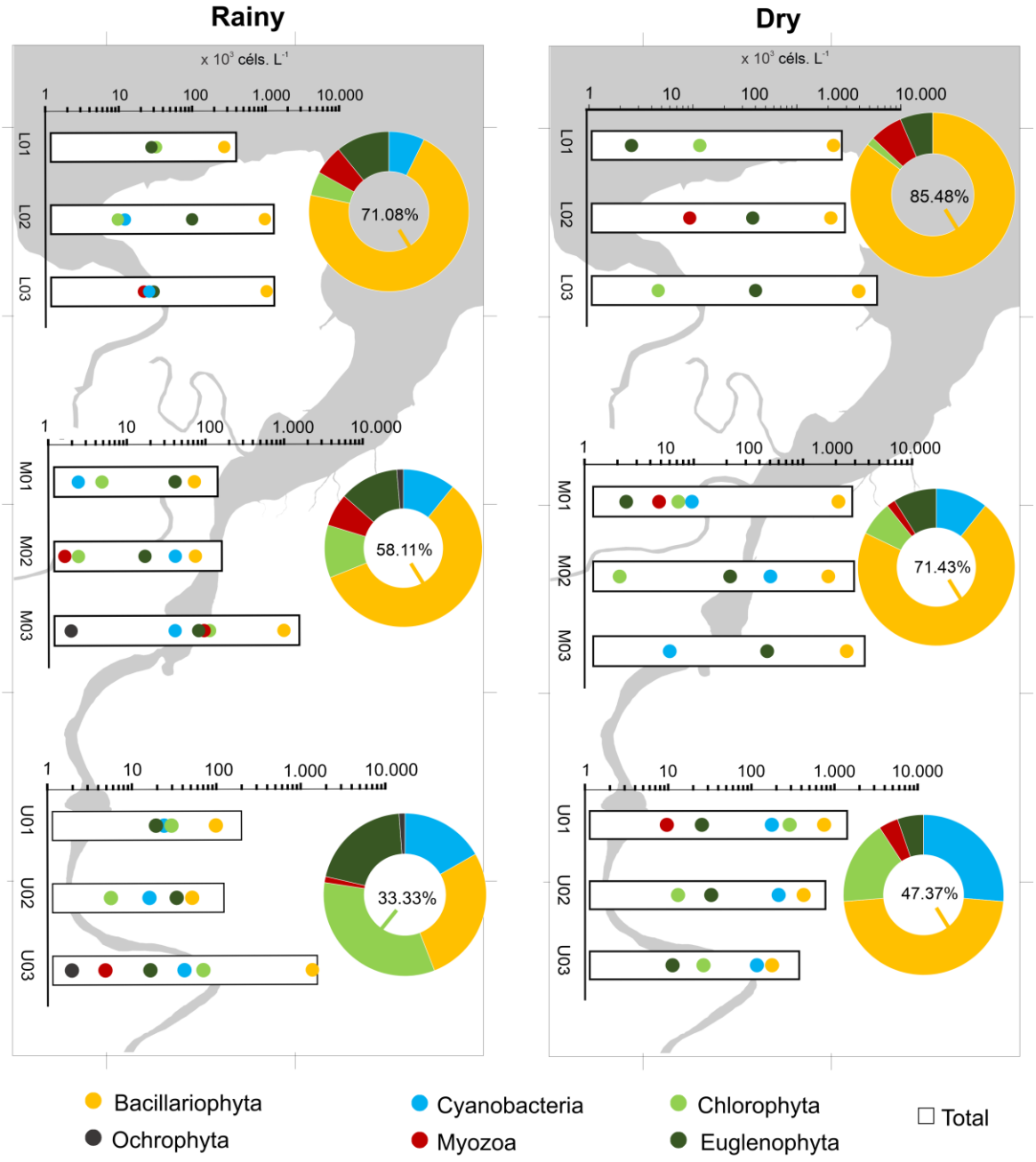

Source: The author (2022).

Tab. 4 Value Indicator (IndVal), total density, and functional traits of phytoplankton in the upper, middle and lower sectors of the Itapecuru River Estuary (IRE)

GROUP/PHYTOPLANKTON INDICATOR	Code	Indicator Value Index						IndVal %	P (MC)	Density 10^4x céls L^{-1}	Life Form	MLD µm	Ecology
		Upper			Middle	Lower							
Cyanobacteria		**U01**	**U02**	**M03**	**M04**	**L05**	**L06**						
Aphanocapsa incerta (Lemmermann) G.Cronberg & Komárek, 1994	*Aphinc*	57	3.4	3.579	2.99	0	0	67	0.0002	**12.86**	colonial	1.93	freshwater
Chroococcus minutus(Kützing) Nägel, 1849	*Chrmin*	24	0	0	0	0	9.25	33	0.0052	0.87	colonial	5.00	freshwater
Geitlerinema sp.	*Geisp*	0	19.05	14.29	0	0	0	33	0.0035	0.56	Filamentous	91.75	others
Leptolyngbya sp.	*Lepsp*	26	6.87	0	0	0	0	33	0.0019	4.24	Filamentous	59.00	others
Lynbya sp.	*Lynsp*	26	7.24	0	0	0	0	33	0.0019	0.92	Filamentous	110.24	others
Merismopedia tenuissima Lemmerman, 1898	*Mertenu*	24	22.22	0	3.70	0	0	50	0.0141	1.30	colonial	2.50	estuarine
Microcystis aeruginosa (Kützing) Kützing, 1846	*Micaerug*	38	5.32	0	0	0	7.05	50	0.0028	**13.64**	colonial	5.73	estuarine
Microcystis wesenbergii (Komárek) Komárek ex Komárek in Joosen, 2006	*Micwes*	29	1.02	20.43	0	0	0	50	0.0075	4.71	colonial	5.18	freshwater
Oscillatoria sp.	*Oscsp*	17	0	16.67	0	0	0	33	0.0014	0.48	Filamentous	-	others
Planktolyngbya limnetica (Lemmermann) Komárková-Legnerová & Cronberg, 1992	*Plalim*	29	0	0	4.67	0	0	33	0.0003	1.37	Filamentous	4.22	freshwater
Planktothrix agardhii (Gomont) Anagnostidis & Komárek, 1988	*Plaaga*	47	23.16	6.57	3.67	2.62	0	83	0.0471	**7.63**	Filamentous	74.80	freshwater
Pseudanabaena acicularis (Nygaard) Anagnostidis & Komárek, 1988	*Psesp*	8.3	25	0	0	0	0	33	0.0029	0.88	Filamentous	309.97	freshwater
Spirulina sp.	*Spisp*	33	10.4	0	0	0	6.60	50	0.022	1.82	Filamentous	42.33	others
Synecocystis aquatilis Sauvageau, 1892	*Synaquatilis*	0	0	26.62	0	6.71	0	33	0.0026	4.78	colonial	3.75	freshwater
Chlorophyta													
Actinotaenium globosum (Bulnheim) Kurt Förster ex Compère, 1976	*Actglo*	25	8.33	0	0	0	0	33	0.0031	0.39	solitary	27.83	freshwater
Ankistrodesmus falcatus (Corda) Ralfs, 1848	*Ankfalcatus*	29	3.92	0	0	0	0	33	0.0004	0.82	colonial	57.20	freshwater
Closterium setaceum Ehrenberg ex Ralfs, 1848	*Closet*	61	0.81	4.99	0.25	0	0	67	0.0001	**25.68**	solitary	38.00	freshwater
Cosmarium speciosum P.Lundell, 1871	*Cosspe*	36	6.75	7.43	0	0	0	50	0.0056	1.62	solitary	13.41	freshwater
Desmodesmus flavescens (Chodat) E.Hegewald, 2000	*Desflav*	7.1	2.04	40.82	0	0	0	50	0.0009	2.36	coenobium	13.33	freshwater
Desmodesmus lunatus (West & G.S.West) E.Hegewald, 2000	*Deslun*	22	11.11	0	0	0	0	33	0.0065	0.29	coenobium	18.67	freshwater
Desmodesmus serratus (Corda) S.S.An, Friedl & E.Hegewald, 1999	*Desserr*	13	20.83	0	0	0	0	33	0.0061	0.26	coenobium	3.75	freshwater
Monoraphidium griffithii (Berkeley) Komárková-Legnerová, 1969	*Mongriffithii*	0	9.52	0	23.81	0	0	33	0.0041	0.34	solitary	38.00	freshwater
Mucidosphaerium pulchellum (H.C.Wood) C.Bock, Proschold & Krienitz, 2011	*Mucpulc*	35	4.40	24.77	2.20	0	0	67	0.0378	**5.83**	colonial	4.09	freshwater
Scenedesmus obtusus Meyen, 1829	*Scenobtu*	11	22.22	0	0	0	0	33	0.0062	0.29	coenobium	9.17	freshwater
Scenedesmus quadricauda (Turpin) Brébisson, 1835	*Scenquad*	26	19.25	0	4.27	0	0	50	0.033	2.82	coenobium	14.14	freshwater
Staurastrum elongatum J.Barker, 1869	*Staelon*	24	9.52	0	0	0	0	33	0.005	0.34	solitary	29.08	freshwater
Bacillariophyta													
Aulacoseira granulata (Ehrenberg) Simonsen, 1979	*Aulgran*	13	43.61	0	8.73	0	1.21	67	0.0264	**7.35**	chain-forming	95.77	freshwater
Aulacoseira granulata var. angustissima (O.Müller) Simonsen 1979	*Aulangu*	41	37.66	3.03	1.478	0.19	0	83	0.0066	**105.83**	chain-forming	78.73	freshwater
Caloneis permagna (Bailey) Cleve, 1894	*Calperm*	0	0	18.75	0	18.75	12.5	50	0.0409	0.64	solitary	-	tychoplankton
Chaetoceros lorenzianus Grunow, 1863	*Chalor*	0	0	0	4.54	36.36	9.09	50	0.0065	2.65	chain-forming	34.00	marine oceanic
Chaetoceros sp.	*Chasp*	0	5.28	0	5.81	52.33	3.23	67	0.0008	2.76	chain-forming	-	others
Chaetoceros subtilis var. *abnormis* Proscкina-Lavrenko, 1961	*Chaabnormis*	0	0	0	22.22	20.83	6.94	50	0.0401	3.47	chain-forming	90.00	marine neritic
Cocconeis placentula Ehrenberg, 1838	*Cocpla*	0	0	0	18.18	15.15	0	33	0.004	0.53	solitary	15.83	freshwater
Cocconeis sp.	*Cocsp*	0	0	32.52	0.81	0	0	33	0.0001	3.95	solitary	15.33	others
Coscinodiscus radiatus Ehrenberg, 1840	*Cosrad*	0	0	0	0	30	3.33	33	0.0002	1.60	solitary	43.00	marine neritic
Craticula ambigua (Ehrenberg) D.G.Mann in Round, R.M.Crawford & D.G.Mann,1990	*Cratamb*	51	14.69	10.46	2.98	11.77	8.72	100	0.0065	**91.99**	solitary	36.242125	freshwater
Cyclotella stylorum Brightwell, 1860	*Cycstyl*	0	7.80	68.66	1.14	2.86	2.86	83	0.0003	**7.01**	solitary	18.38	tychoplankton
Cymbela sp.	*Cymsp*	41	6.48	6.66	8.55	10.7	26.94	100	0.0448	**6.75**	solitary	29.61	others
Diploneis ovalis (Hilse) Cleve, 1891	*Dipova*	0	24.57	0	0	4.76	20.66	50	0.0278	2.52	solitary	11.88	freshwater
Discostella stelligera (Cleve & Grunow) Houk & Klee, 2004	*Cycste*	0	1.39	6.99	0	3.49	54.78	67	0.0007	**4.59**	solitary	15.88	freshwater
Ditylum brightwellii (T.West) Grunow, 1885	*Ditbrig*	0	0	15.5	0	0	17.83	33	0.0034	0.90	solitary	86.50	marine neritic

Continue...

GROUP/PHYTOPLANKTON INDICATOR	Code	Indicator Value Index						IndVal %	P (MC)	Density 10^4x céls L^{-1}	Life Form	MLD µm	Ecology
		Upper		Middle		Lower							
Bacillariophyta		**U01**	**U02**	**M03**	**M04**	**L05**	**L06**						
Frustulia interposita (Lewis) De Toni, 1891	*Fruint*	0	0	31.75	1.58	0	0	33	0.0001	2.02	solitary	63.17	freshwater
Guinardia flaccida (Castracane) H.Peragallo, 1892	*Guiflac*	0	0	0	9.57	9.57	30.85	50	0.0315	1.26	chain-forming	112.33	marine neritic
Leptocylindrus danicus Cleve, 1889	*Lepdan*	0	0	0	0	26.47	6.86	33	0.0012	1.82	chain-forming	77.25	marine neritic
Lithodesmium undulatum Ehrenberg, 1839	*Litund*	0	0	0	5.55	27.78	0	33	0.0003	0.58	chain-forming	27.00	marine neritic
Melosira nummuloides C.Agardh, 1824	*Melnum*	0	0	36.04	0	3.39	10.57	50	0.006	3.54	chain-forming	30.25	marine
Navicula sp.	*Navsp*	20	16.72	0	14.45	16.05	16.05	83	0.0104	**5.00**	solitary	21.90	others
Nitzschia palea (Kützing) W.Smith,1856	*Nitpal*	9	2.30	56.92	9.03	18.25	4.53	100	0.0136	**27.70**	solitary	42.49	tychoplankton
Nitzschia sp.	*Nitsp*	0	0	34.62	3.84	11.54	0	50	0.0124	8.34	solitary	36.13	others
Odontella regia (M.Schultze) Simonsen, 1974	*Odoreg*	0	0	4.96	4.57	28.56	28.56	67	0.0237	2.81	solitary	98.33	marine neritic
Opephora marina (W.Gregory) Petit, 1888	*Opemar*	0	0	0	20.51	12.82	0	33	0.0067	0.63	solitary	18.00	marine
Opephora pacifica (Grunow) Petit, 1888	*Opepac*	10	0	0	0	10	30	50	0.0416	1.20	solitary	-	tychoplankton
Pleurosigma sp1	*Plesp1*	3.1	6.28	65.71	5.92	4.80	14.14	100	0.001	**10.02**	solitary	115.01	others
Pleurosigma sp2	*Plesp2*	0	9.52	0	0	0	23.81	33	0.0046	0.34	solitary	134.00	others
Polymyxus coronalis L.W.Bailey, 1862	*Polcoronalis*	77	12.86	4.09	2.13	3.85	0.51	100	0.001	**62.36**	solitary	72.38	marine
Rhizosolenia setigera Brightwell,1858	*Rhiseti*	0	0	0	0	3.48	29.84	33	0.0001	2.30	solitary	134.00	marine neritic
Skeletonema costatum (Greville) Cleve, 1873	*Skecost*	0	0	0.58	3.61	42.56	19.91	67	0.0212	**95.37**	chain-forming	161.95	marine neritic
Thalassiosira eccentrica (Ehrenberg) Cleve, 1904	*Thaecc*	0	4.06	43.23	0	0	2.70	50	0.0002	2.47	solitary	27.63	marine oceanic
Thalassiosira gravida Cleve, 1896	*Thagrav*	0	0.92	7.82	1.91	54.53	18.14	83	0.0192	**59.22**	chain-forming	49.29	marine
Thalassiosira leptopus (Grunow) Hasle & G.Fryxell, 1977	*Thalep*	4.7	0	0	0	4.68	40.63	50	0.0004	2.57	solitary	25.50	marine oceanic
Thalassiosira nanolineata (A.Mann) Fryxell & Hasle, 1977	*Thanan*	0	3.14	30.19	0	0	0	33	0.0001	2.13	solitary	15.00	marine oceanic
Thalassiosira subtilis (Ostenfeld) Gran, 1900	*Thasubt*	0	0	6.94	2.77	40.28	0	50	0.0013	8.66	colonial	22.75	marine oceanic
Triceratium favus Ehrenberg, 1839	*Trifavus*	0	0	32	0	0	1.33	33	0.0001	4.01	solitary	43.00	tychoplankton
Trybliоptychus cocconeiformis (Grunow) Hendey, 1958	*Trycocc*	0	2.34	67.64	1.12	2.81	9.39	83	0.0005	**7.12**	solitary	18.08	marine
Ulnaria ulna (Nitzsch) Compère, 2001	*Ulnuln*	36	8.82	0	0	5.11	0	50	0.0074	4.71	solitary	170.12	freshwater
Dinophyta													
Dinophysis caudata W.S.Kent, 1881	*Dincaud*	0	0	0	9.524	23.81	0	33	0.0051	0.34	solitary	36.50	marine oceanic
Heterocapsa rotundata (Lohmann) Gert Hansen, 1995	*Hetrotu*	11	24.57	0	0	22.22	0	33	0.007	0.72	solitary	6.25	marine oceanic
Prorocentrum micans Ehrenberg, 1834	*Promic*	0	0	26.67	0	6.66	0	33	0.0013	4.81	solitary	20.50	marine oceanic
Scrippsiella trochoidea (F.Stein) A.R.Loeblich III, 1976	*Scrtroch*	17	16.67	0	0	16.67	0	50	0.0047	1.44	solitary	12.50	marine oceanic
Eugleophyta													
Euglena acus (O.F.Müller) Ehrenberg, 1830	*Eugacus*	5.8	5.76	40.38	0	0	14.74	67	0.0375	2.78	solitary	42.00	freshwater
Euglena sp.	*Eugsp*	0	7.01	26.32	0	0	0	33	0.0015	0.76	solitary	11.25	others
Phacus longicauda (Ehrenberg) Dujardin, 1841	*Phalong*	0	13.33	20	0	0	0	33	0.0071	0.40	solitary	29.00	freshwater
Strombomonas verrucosa (E.Daday) Deflandre, 1930	*Strver*	0	0	27.16	0	6.17	0	33	0.002	6.50	solitary	11.67	freshwater
Trachelomonas armata (Ehrenberg) F.Stein, 1878	*Traarm*	38	12.6	22.81	8.74	9.36	8.32	100	0.0475	**10.28**	solitary	19.31	freshwater
Trachelomonas hispida (Perty) F.Stein, 1878	*Trahisp*	0	6.52	64.18	2.44	6.12	4.07	83	0.0001	**3.28**	solitary	22.33	freshwater
Ochrophyta													
Mallomonas acaroides Perty, 1852	*Malaca*	0	16.67	0	16.67	0	0	33	0.0016	0.39	solitary	-	freshwater

Conclusion

Source: The author (2022).

Phytoplankton indicators as a function of salinity

Based on the IndVal of the 187 species identified: 76 taxa were selected as key indicators. The best phytoplankton indicators (IndVal = 100%, $P < 0.05$) were *C. ambigua* (91.99×10^4 cells l^{-1}), *N. palea* (27.69×10^4 cells l^{-1}), *P. coronalis* (62.35×10^4 cells l^{-1}), and *Trachelomonas armata* (Ehrenberg) F.Stein (10.27×10^4 cells l^{-1}; Fig. 7). The phytoplankton community of the upper sector contained species that preferred limnetic conditions—*Aphanocapsa incerta* (Lemmermann) G.Cronberg & Komárek, *Planktothrix agardhii* (Gomont) Anagnostidis & Komárek, *Closterium scetaceum* Ehrenberg ex Ralfs, *A. granulata* (Ehrenberg) Simonsen, *C. ambigua*, and *T. armata*— occurred during the rainy season with a salinity range of 0.05–6.33. Whereas *Mucidosphaerium pulchellum* (H.C.Wood) C.Bock, Proschold & Krienitz, *A. granulata* var. *angustissim*a, and *P. coronalis* preferred salinities of 0.03–0.09 in the dry season. Most of the middle sector indicators existed under salinity conditions ranging from 0.03 to 9.12 during the rainy period—*Desmodesmus flavescens* (Chodat) E. Hegewald, *Cyclotella stylorum* Brightwell, *Trybliоptychus cocconeiformis* (Grunow) Hendey, *N. palea*, and *Trachelomonas hispida* (Perty) F.Stein. Only *Euglena acus* (O.F.Müller) Ehrenberg, found in the salinity ranges of 9.15–30.13 during the dry season, was selected as an indicator of mesohaline/polyhaline waters.

The lower sector was characterized by diatoms, where *Discostella stelligera* (Cleve & Grunow) Houk & Klee and *Opephora pacifica* (Grunow) Petit were restricted to mesohaline conditions (0.09–17.62) in the rainy season. On the other hand, *Guinardia flaccida* (Castracane) H.Peragallo, *S. costatum*, and *T. gravida* were specific to mesohaline/euryhaline conditions (13.20–33.43) in the dry season. Based on ecological preferences, 76.31% of the indicators comprised planktonic freshwater (43.42%) and marine (30.26%) species, whereas the remainder consisted of tychoplankton (6.57%) and estuarine (2.63%) species. Most diatoms were marine neritic (25.00%) and oceanic (27.77%) species (Table 4).

Functional traits of indicator phytoplankton

Regarding the maximum linear dimension (MLD) functional trait of indicator phytoplankton, 46.06% showed MLD > 20 µm, with diatoms comprising the largest percentage of this class (23.68%; 18 taxa). The size class < 20 µm comprised 26% (20 taxa) of the indicator taxa, of which 9.21% were cyanobacteria, 7.89% chlorophytes, and 3.94% diatoms. During the dry season, 21 taxa of the indicator phytoplankton increased in size, primarily diatoms such as

C. ambigua, *N. palea*, *P. coronalis*, and *S. costatum*.

Based on the morphology of the 39 indicator diatoms, 74.36% were centric, and 25.64% were penates, while 69.23% were primarily solitary, and 30.77% formed chains. Filamentous indicator cyanobacteria (57.14%) were more abundant than mucilaginous (42.86%). Within the cyanobacteria, 85.71% were classified as CyanoHab, potentially harmful and bloom-forming species. Chlorophytes constituted 58.33% of the colonial species, of which 41.67% formed coenobium. Phytoflagellates (dinoflagellates, euglenophytes, and ochrophytes) are solitary, with no distinction in the percent representation of cell size.

Figure 8 shows the similarity in the indicator group composition. The dendrogram is divided into three groups (cut: 26.48%; Pi = 2.07, P = 0.02): Cluster I (upper sector), Cluster II (middle sector), and Cluster III (lower sector), with similarities of 36.02%, 50.35%, and 44.30%, respectively. This functional phytoplankton community grouping, as confirmed by NMDS (stress 0.2), reflected solitary diatoms (> 20 μm) as the cosmopolitan indicators with dominant species in each sector. Filamentous cyanobacteria and coenobial chlorophytes (< 20 μm) were restricted to a group of rare species from the upper sector. The middle sector was characterized by solitary and occasional euglenophytes (< 20 μm), together with solitary and dominant diatoms (> 20 μm). The euglenoid phytoflagellates moved toward the middle and upper sectors during the rainy season, while the dinoflagellates moved between the middle and lower sectors during the dry season.

Effects of environmental variables on the phytoplankton indicator

ANOSIM revealed significant spatial differences (Global R = 0.208; P = 0.001), indicating heterogeneity of the indicator phytoplankton between the upper and middle sectors (R = 0.190, P = 0.014), as well as the upper and lower sectors (R = 0.432, P = 0.001). The average IMD value was 1, showing a high dispersion of species among the estuarine sectors. The highest community variability occurred in the middle sector (IMD = 1.178), whereas high stability occurred between the upper and middle sectors (IMD = -0.250). These dispersion patterns were evident during both the rainy (IMD = 1.111) and dry seasons (IMD = 0.889) (Table 5).

Fig. 7 Plot of the main phytoplankton indicator (cells l^{-1}) of seawater intrusion in Itapecuru River Estuary (IRE). Taxa were selected according to IndVal = 100%, P < 0.05

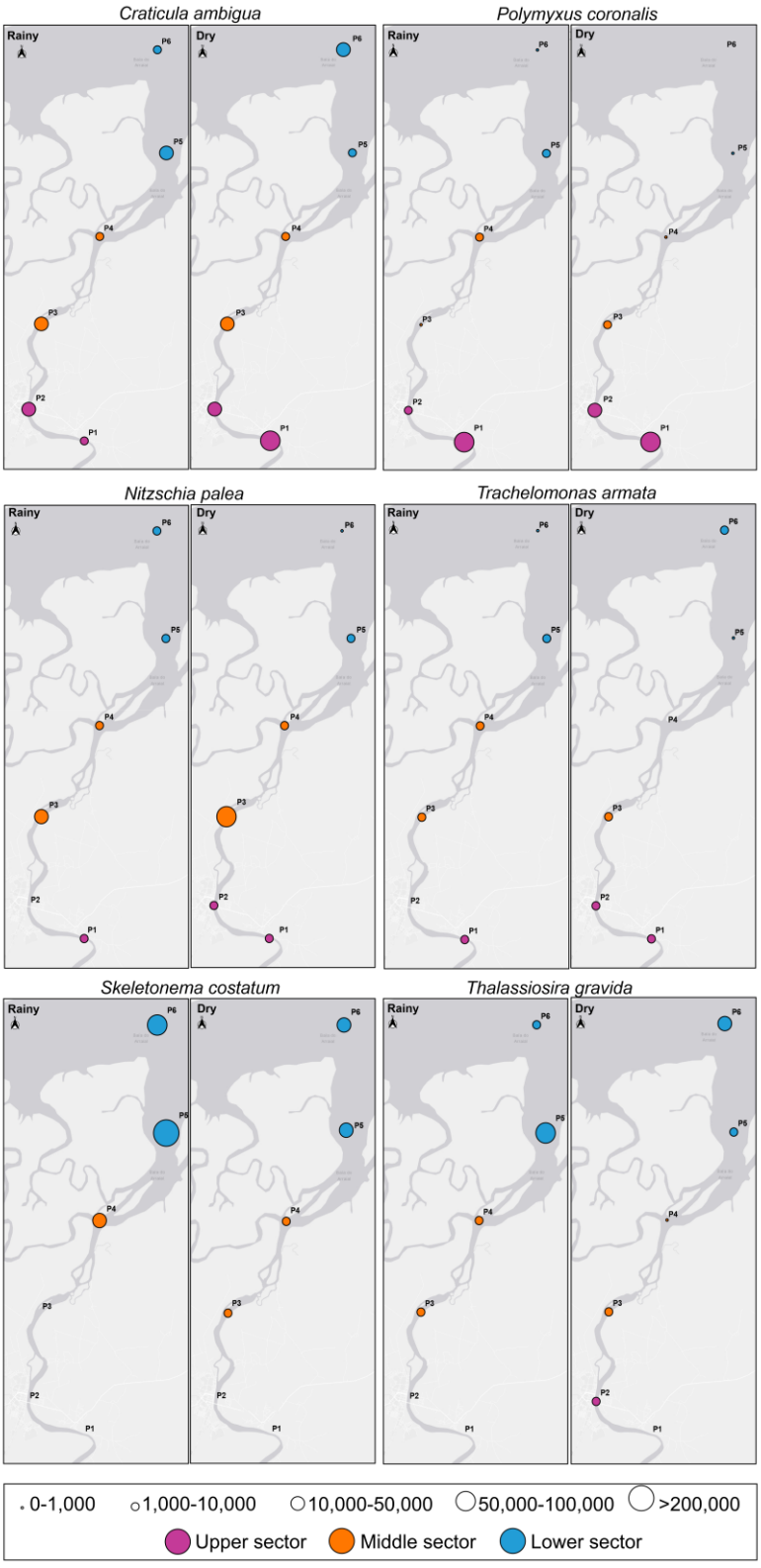

Source: The author (2022).

Tab. 5 Biota-environmental (BIO-ENV) analysis registering 10 best combinations of environmental variables with spatial variations in phytoplankton indicator in Itapecuru River Estuary (IRE). Significant values (P = * < 0.05; ** < 0.01; *** < 0.001).

Rank	Environmental variables	R value	P value
1	Sal, SPM, <20µm, >20µm, Silicate	0.331	0.01
2	Sal, Turbidity, SPM, >20µm, Silicate	0.330	0.01
3	Sal, DO, SPM, >20µm, Silicate	0.329	0.01
4	Sal, SPM, >20µm, Orthophosphate, Silicate	0.328	0.01
5	Sal, pH, SPM, >20µm, Silicate	0.327	0.01
6	Sal, SPM, >20µm, Nitrite, Silicate	0.327	0.01
7	Sal, SPM, >20µm, Silicate	0.327	0.01
8	Sal, Temp., SPM, >20µm, Silicate	0.327	0.01
9	Sal, SPM, Chla, >20µm, Silicate	0.326	0.01
10	Sal, SPM, PAR, >20µm, Silicate	0.325	0.01

Source: The author (2022).

According to the BIO-ENV analysis, this dispersion heterogeneity of the phytoplankton community was driven by variations in salinity, SPM, cell size (nano/picophytoplankton and microphytoplankton), and silicate, collectively equating to a maximum Spearman correlation value (R = 0.331); however, the lowest correlation coefficient (R = 0.325) also included PAR. DistLM (stepwise selection) revealed a significant correlation (P < 0.001) between phytoplankton and salinity, SPM, nano/picophytoplankton, nitrite, and orthophosphates according to the marginal tests. The sequential results indicate that salinity and SPM parameters play a central role in the phytoplankton community structure, creating deterministic distributions of phytoplankton indicators (Table 6).

The model explained 74.35% of the adjusted variation in the first three axes, and the dbRDA was represented by axes 1 (40.80%) and 2 (18.60%). Salinity, SPM, nitrite, and nano/picophytoplankton concentrations showed direct relationships in the lower and middle sectors, with higher values corresponding to periods of higher wind intensity, lower river discharge, and lower precipitation. In contrast, the concentrations of orthophosphate and microphytoplankton were most strongly correlated with the upper sector and decreased during periods of lower wind intensity, higher river discharge, and higher precipitation (Fig. 9a).

Tab. 6 Marginal and sequential tests according to the distance-based linear model (DistLM) of environmental variables and phytoplankton indicators from the Itapecuru River Estuary (IRE) indicators. Significant values (P = * < 0.05; ** < 0.01; *** < 0.001)

MARGINAL TESTS			
Variables	**Sum of Squares**	**Pseudo-F**	**p**
Salinity	11214	3.6628	0.001***
SPM	7170.1	2.2543	0.001***
Chl-a (<20)	5262.7	1.6259	0.043**
Chl-a(>20)	4013.2	1.226	0.205
Nitrite	7885.1	2.4956	0.001***
Orthophosphate	6539.8	2.0442	0.008**
Temperature	3690.3	1.1241	0.311
TDS	10110	3.2675	0.001***
DO	4745	1.4591	0.074
pH	3677.5	1.12	0.313
Turbidity	3674.6	1.1191	0.317
PAR	3712.4	1.131	0.317
Chla Total	4520.9	1.3874	0.121
Ammonium	3370.1	1.0236	0.467
Nitrate	4001.4	1.2222	0.217
Silicate	4151.4	1.2697	0.206
SEQUENTIAL TESTS			
Variables	**Sum of Squares**	**Pseudo-F**	**p**
Salinity	11214	3.6628	0.001***
SPM	7170.1	2.2543	0.001***

Source: The author (2022).

These relationships ultimately led to a clear spatial separation of indicator species ($R \geq 0.4$; Fig. 9b). Freshwater species (chlorophytes, cyanobacteria, and pennate diatoms) were distributed in the upper sector under nutrient-poor (NO_2^- and PO_4^{3-}) conditions, low salinity, and low SPM. Marine and estuarine species (e.g., dinoflagellates, centric diatoms, and chain-forming species) were transported between the middle and lower sectors under the opposite conditions. In addition, from the linear regression analysis between the indicator phytoplankton and the selected variables in the dbRDA, only the chain-forming diatoms *Ditylum brightwellii* (T.West) Grunow, *Chaetoceros subtilis* var. *abnormis* Prosckina-Lavrenko, and *Rhizosolenia setigera* Brightwel were correlated directly with salinity, with an increasing trend toward the estuarine mouth. In contrast, *P. coronalis* showed a reduction in cell density as a function of salinity and increasing SPM, which can be considered an indicator of SWI in this study ($R > 0.40$, $P < 0.05$).

Fig. 8 Hierarchical cluster analysis (SIMPROF test) and two-dimensional non-metric multidimensional scaling (NMDS) of taxonomic groups of phytoplankton indicator, functional traits and phytoplankton density in Itapecuru River Estuary (IRE)

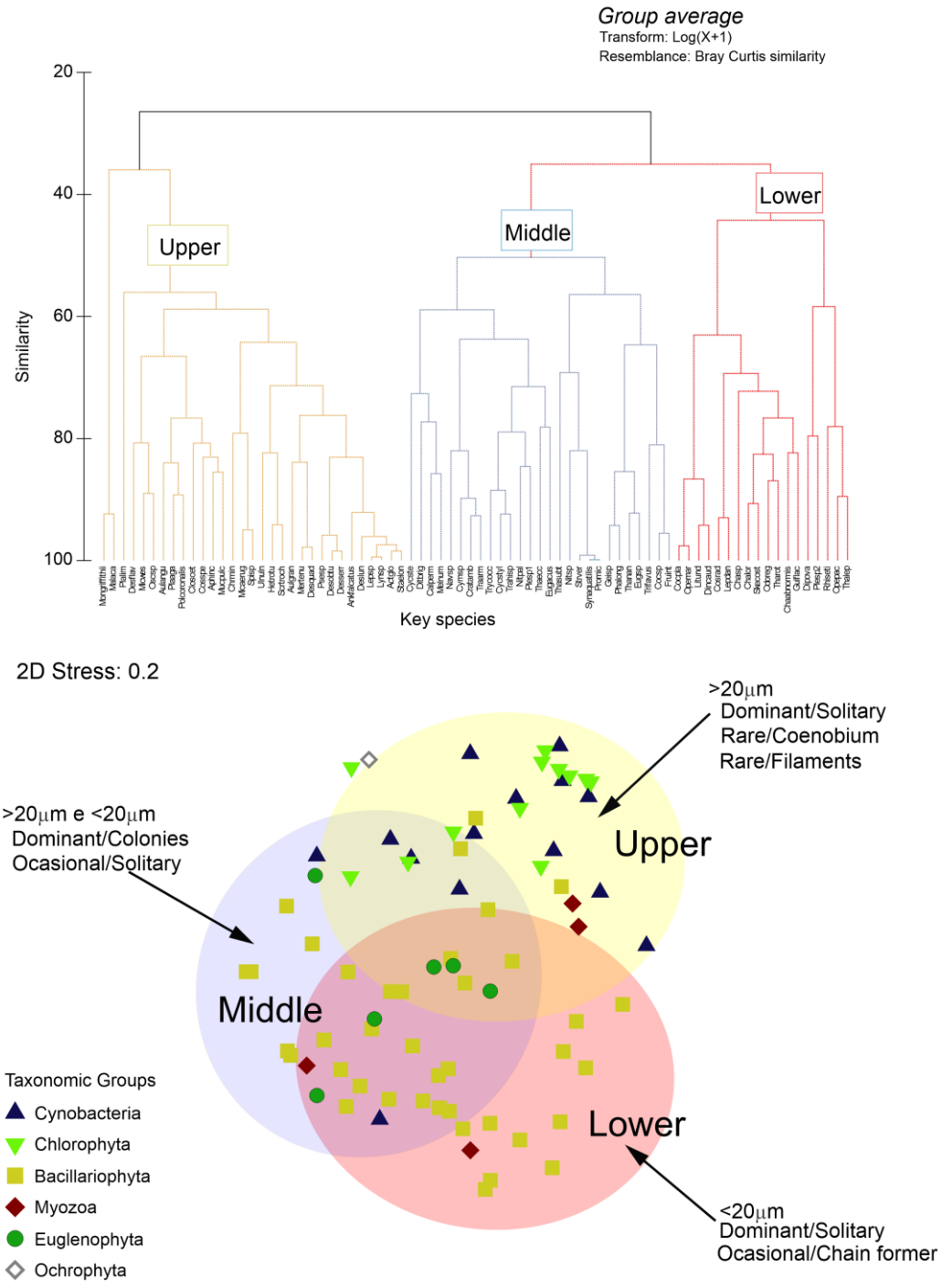

Source: The author (2022).

Furthermore, the sudden increase in nutrient load (nitrite) in the lower sector favored an increase in cell density of *C. subtilis* var. *abnormis* ($R = 0.35$, $P = 0.03$). In contrast, the

upper sector, with a lower concentration of this nutrient, promoted an increasing abundance of *Scenedesmus quadricauda* (Turpin) Brébisson (R = 0.38, P = 0.02). For the phytoplankton fractions, *P. coronalis* (R = 0.40, P = 0.01), *Cosmarium speciosum* P. Lundell (R = 0.48, P = 0.002), *Ankistrodesmus falcatus* (Corda) Ralfs (R = 0.63, P < 0.001) were the main species which represented the microphytoplankton (> 20 µm).

Fig. 9 Distance-based on Redundancy Analysis (dbRDA) of the variables that best describe the indicator phytoplankton community of the Itapecuru River Estuary (IRE). **a** Vectors representing the environmental variables selected in DistLM and **b** vectors representing the indicator phytoplankton community

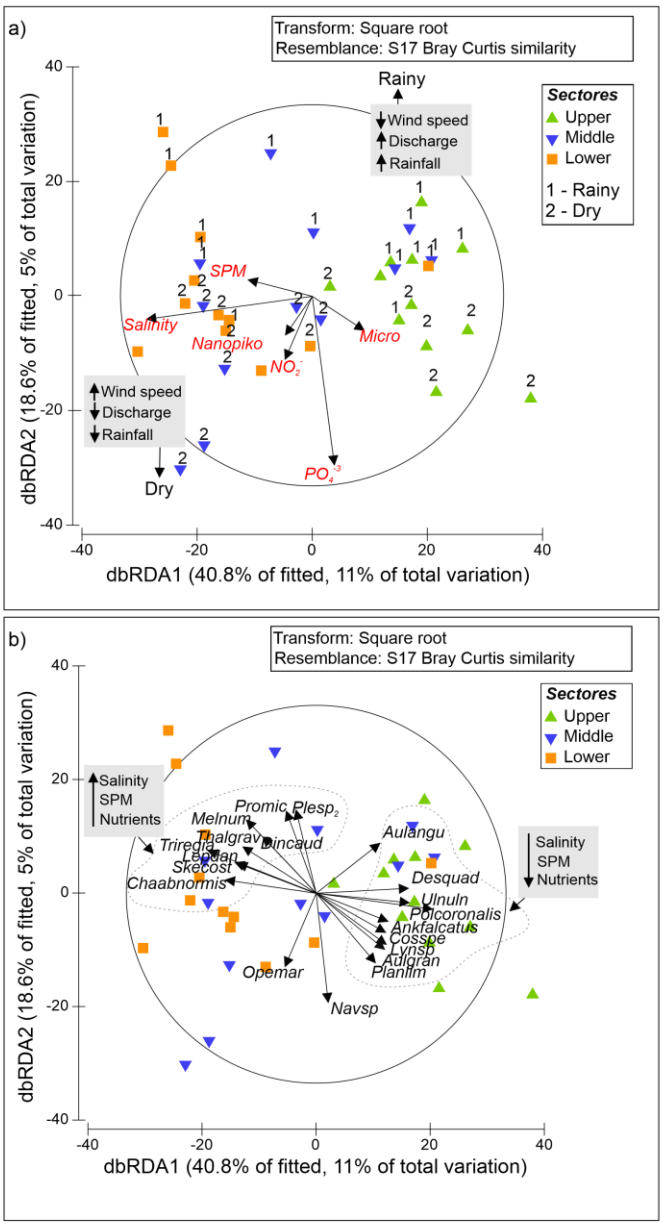

Source: The author (2022).

Discussion

Weather patterns and salinity gradients

The IRE is a tropical system governed by the climatic variations associated with the ITCZ and macrotidal dynamics (> 7 m); therefore, these two conditions act synergistically upon the distribution and abundance of local biological communities (Barros et al., 2011; Porto et al., 2017; Santos et al., 2019). The climatological and river discharge data obtained over the research period (2019–2020) were atypical in relation to the historical average. The rainy seasons during these years were more intense, and the increase in the estuary river discharge probably limited the advance of SWI during this period. This scenario differs from other recent research on regional estuaries (Cavalcanti et al., 2020; Santos et al., 2020; Sá et al., 2021).

Unimodal rainfall patterns can define the heterogeneity of environmental gradients in the IRE, particularly the variations in salinity, TDS, and SPM. These variables indicated SWI to the upper sector, with greater penetration during the dry season (up to ~ 20 km of excursion). This greater tidal penetration and wind migration to the northeast strengthened the SWI and shifted the saltwater to the upper sector, as noted by Liu et al. (2019a, b) in the Pearl River estuary, the second largest estuary in China by freshwater discharge. Thus, even during periods of heavy river discharge, the IRE showed changes in salinity between the middle and lower sectors. Accordingly, the middle estuary revealed itself as a floating sector, while the upper sector was stable to the hydrological tracers of SWI. Similar results have been observed in other northern Brazilian estuaries (Costa et al., 2013; Pamplona et al., 2013; Monteiro et al., 2016; Vilhena et al., 2016). These authors attributed the period of lower precipitation, decreased dilution of urban effluents, and lower Amazon flow as favorable for the increase in salinity and extension of the SWI into the upper sectors.

Notably, during the transition period (July–August), there is an intensification of the North Current of Brazil (i.e., western border current), which renews the waters of the Maranhense Gulf, due to the presence of stronger trade winds that blow toward the ITCZ and push a greater volume of seawater toward coastal areas (Lefèvre et al., 2017; Santos et al. 2020). Therefore, the ITCZ migration and wind patterns were consistent with variations in salinity (Magalhães et al., 2011; Guenther et al., 2015; Araújo et al., 2017), and rainfall was the primary factor controlling the dynamics and structure of estuarine phytoplankton communities in

Maranhão, including the IRE (Azevedo et al., 2008; Duarte-dos-Santos et al., 2017; Cavalcanti et al., 2020; Costa and Cutrim, 2021).

Chlorophyll-a concentrations as a function of light and nutrient conditions

Seawater intrusion and rainfall are key drivers of the photosynthetic patterns and productivity of tropical estuaries (Magalhães et al., 2011; Karthik et al., 2020; Navas-Parejo et al., 2020; Niu et al., 2020). In the IRE, light conditions were homogeneous, with limited incident light in the water column, resulting in a dark and turbid water environment (Morais and Coutinho, 1976; Teixeira et al., 1988). The greatest light penetration occurred in the lower sector, absorbing < 50% of PAR in the underwater layer (~ 1 m depth) and coinciding with the lowest tidal height (5.7 m) during data sampling.

Like the IRE, most estuaries dominated by macrotides are subject to a constant resuspension of sediments from the bottom, ultimately transported to the continent (Lancelot and Muylaert, 2011). However, when extreme rainfall regimes dominate these systems, the input SPM is directed toward the sea, promoting an increase in the lower sector turbidity of estuarine waters (Mitchell, 2013; Shi et al., 2017; Onabule et al., 2020). This form of suspended solid export directly affects phytoplankton productivity due to nutrient dynamics and pollutant transport into the coastal ocean (Doxaran et al., 2009).

This accounts for the SPM and turbidity we recorded in the IRE, with high values throughout the year, increasingly so downstream, implying that the freshwater flow had minimal influence on the SPM input; notably different results from those of Bharathi and Sarma (2019). These authors observed that the highest SPM values occurred during the period of higher river discharge, explaining the reduction in light penetration, abundance, and biomass of phytoplankton. According to Santos et al. (2020), resuspension of sediments on the north coast of Brazil reached estuaries regardless of river volume, suggesting the formation of a hydraulic barrier from the inversion of the baroclinic pressure gradient, thus resulting in the retention of water, particulate matter, and nutrients inside the IRE.

As a response to this process, the turbidity of the water in Itapecuru was proportional to the SWI in the estuary, clearly delimiting the medium sector as the TMZE. The macrotidal estuaries of the Amazon coast, commonly present in the middle estuarine sector, have a greater convergence of sediments during the dry season, with an increase in turbidity proportional to

the decrease in river flow (Asp et al., 2018). The heavy fluvial discharge during the rainy season drives the nutrient-rich river plume to the sea, providing a more stable and transparent upper sector water column, as has been seen in other tropical estuaries around the world (Gong et al., 2014; Lu and Gan, 2015; Bharathi and Sarma, 2019; Onabule et al., 2020).

Based on this, the phytoplankton response followed PAR, with an increase in the chlorophyll-a concentrations during the dry period, as corroborated by Pamplona et al. (2013), Machado et al. (2017), and Da Silva et al. (2019). Light heterogeneity was marked by lower values of chlorophyll-a in the TMZE (Azevedo et al., 2008; Jyothibabu et al., 2018; Cutrim et al., 2019), as well as a reduction in the euphotic zone and the rapid attenuation of light energy, thereby reducing light absorption by phytoplankton (Teixeira et al., 1988; Azhikodan and Yokoyama, 2016; Costa and Cutrim, 2021).

Nutrient distribution patterns (NO_2^-, NO_3^-, and PO_4^{3-}) followed the saline intrusion gradient, and nitrogen limitations were responsible for controlling phytoplankton variability, indicative of a heavy marine influence in the estuary and a low fluvial input during the dry season. The SWI causes sediment resuspension and nutrient release into the water, which can be absorbed by phytoplankton or adsorbed onto sediment particles, where higher salinities reflect strong tidal dynamics and vertical mixing (Niu et al., 2020). Further, nitrogen is an essential component of photosynthetic pigments, and its limitation directly affects phytoplankton growth and productivity (Yang and Tan, 2019; Tao et al., 2020).

In the present study, it was observed that saline intrusion promoted nutrient retention in the middle and lower sectors of the estuary. The joint action of external factors—tides, wind, and (to a lesser extent) river discharge, and precipitation—created the fundamental conditions for nutrient availability within the water column. Thus, these conditions controlled the dispersion of marine phytoplankton and were responsible for structuring the corresponding communities of the IRE.

Accordingly, phytoplankton, predominantly nano-(2–20 μm) and pico-(0.2– 2 μm) phytoplankton biomass, increased in the upper sector. Microphytoplankton were associated with the marine influx and ultimately increased chlorophyll-a concentrations in the upper sector. Similar findings were made by Zhou et al. (2016) and Carrasco Navas-Parrejo et al. (2020). Therefore, it was observed that phytoplankton fractions were sensitive to the established TMZE conditions, favoring less turbid and saline waters. Similar spatial variability

of chlorophyll-a concentrations is common in severely disturbed estuaries, where phytoplankton biomass levels can exhibit a wide range (±1–>100 μg l^{-1}; Tao et al., 2020). Nano/picophytoplankton are typically more efficient than microphytoplankton at exploiting lower light intensities and nutrient concentrations (Madhu et al., 2009).

This photosynthetic efficiency is maximized in coastal waters, and microphytoplankton are limited to limnetic and transparent waters (Watanabe et al., 2014; Zhou et al., 2016), as observed in the IRE. Increased water column turbidity, low residence time, and high freshwater inflow may also be significant environmental factors that drive phytoplankton size classes, such as microphytoplankton growth (Paul et al., 2021). This set of hydrological characteristics act directly on the distribution of the phytoplankton community and may favor the growth of some taxonomic groups. Diatoms, for example, are dominant in tropical estuaries and cyanobacteria in brackish and stagnant waters, which can be a strong indicator of SWI (Bharathi and Sarma, 2019).

Phytoplankton indicators and environmental dispersion gradients

The IRE's phytoplankton community was typical of tropical estuaries (Paiva et al., 2006; Ribeiro et al., 2010; Lancelot and Muylaert, 2011; Oseji et al., 2018; Affe et al., 2019; Riberio et al. 2019; Karthik et al., 2020). Diatoms were predominant in the lower sector, under the significant influence of environmental gradients governed by SWI and rainfall, varying spatiotemporally, ultimately affecting physiology and biomass (Azhikodan and Yokoyama, 2016; Chai et al., 2016; da Silva et al., 2017).

The lower levels of rainy season SWI (~ 10 km) led to increased cell density and diversity of taxonomic groups in the upper and lower sectors, with overlapping and enhanced interspecific competition for light. This scenario was reversed during the dry period, with increased density restricted to the upper sector only, revealing a stronger balance between the other estuarine sectors. Previously, phytoplankton density and diversity have been shown to increase under heterogeneous drivers in response to greater levels of competition and ecological adaptation (Silva et al., 2009; Santiago et al., 2010; Nunes et al., 2018). Increased SWI excursion has also resulted in eco-environmental effects that generate osmotic stress on phytoplankton, ultimately altering the corresponding community in favor of diatoms with greater ecological plasticity (Kasai et al., 2010; Long et al., 2013; Li et al., 2019).

The densities of marine diatoms and cyanobacteria were positively correlated with SWI, whereas all other groups were selected against, corroborating the findings of Bharathi et al. (2018) and Lemley et al. (2019). The intense fluvial flow induced the coexistence of freshwater diatoms (> 20 μm) with chlorophytes, cyanobacteria, and phytoflagellates (< 20 μm); therefore, salinity promoted community reorganization, changing the physiological structure of the phytoplankton, and preventing the proliferation of freshwater diatoms. Furthermore, low precipitation enables adapted species to grow in the absence of competition. In addition, waters enriched with SPM are an ideal medium for phytoplankton succession (Guenter et al., 2015; Nche-Fambo & Tirok, 2015; Saifullah et al., 2016; Oseji et al., 2018; Dursun and Tas, 2019).

Given this variability, the best phytoplankton indicators—*C. ambigua*, *N. palea*, *P. coronalis*, and *T. armata*—recorded well-defined temporal dispersion and ecological preferences and were reliable under low salinity and SPM conditions in the upper sector. An exception was *N. palea*, which preferred mesohaline and more turbid conditions. Diatoms commonly constitute maximum populations comprised of species with different optimal salinity concentrations and restricted tolerances, as has also been observed by Muylaert et al. (2009).

Among these indicators, *P. coronalis* density increased under low salinity, turbidity, and water temperature, constituting the first citation for Maranhão. This centric and planktonic diatom is abundant in the brackish waters of South America and is often regarded as an indicator of Amazonian estuaries (Navarro and Peribonio, 1993; Paiva et al., 2006; Ribeiro et al., 2008; Ribeiro et al., 2010; Sena et al., 2015). It is also intolerant of salinity levels > 30. In the present study, the identification of *P. coronalis* as a good indicator of the seawater intrusion limit in the IRE was an important finding.

The gradual changes promoted by SWI during the dry period were the primary causes of trapped salinity, SPM, and nutrients inside the estuary, ultimately contributing to the dominance of *N. palea* in the TMZE. This effect created a barrier to the dispersion of marine phytoplankton, reducing the growth of planktonic species and modifying the succession patterns of non-adapted organisms (Lancelot and Muylaert, 2011; Nche-Fambo and Tirok, 2015). Thus, it was evident that the community composition changed due to the spatial heterogeneity promoted by the tracers of the SWI: salinity, SPM, and nitrogen limitation (Costa et al., 2013; Srichandan et al., 2015; Affe et al., 2019; Karthik et al. 2020). Diatoms—*C. ambigua*, *N. palea*, *P. coronalis*, and *S. costatum*—expressed the strongest levels of

ecological plasticity, with the ability to change cell size to > 20 μm as SWI intensified (Muylaert et al., 2009; Barroso et al., 2016; Santana et al., 2018).

This ability to change cell size can be considered an adaptation to SWI. Large phytoplankton tend to grow in nutrient-rich coastal waters and mostly include larger (> 20 μm) diatoms and dinoflagellates (Madhu et al., 2021). Diatoms, for example, have a higher sedimentation rate than other phytoplanktonic groups. This feature is advantageous in reducing grazing pressure and improving buoyancy in marine waters (Santana et al., 2018). In addition, the cell-size change provides greater tolerance to the limiting light conditions caused by SWI (Kruk et al., 2010).

Such an adaptive ability enables the phytoplankton to tolerate stressors affecting successional patterns and promotes competitive advantage, ultimately increasing species dispersion and community diversity. Thus, the dispersal system of the diatoms functionally adapted to the IRE's heterogeneity was revealed and was particularly evident in the rainy season due to the unique functional traits.

Accordingly, a clear separation of populations among the estuarine sectors was observed. Marine, centric, and chain-forming diatoms are favored in the dynamic regions, while limnetic, pennate, and solitary diatoms dominate under more stable conditions. Therefore, changes in the estuary's climatic and circulation patterns can impact sediment transport and the water quality of the IRE, resulting in substantial changes to the structure and distribution of phytoplankton communities and ultimately affecting the ecological balance. A representation of the effects of saltwater intrusion on the phytoplankton community is given in Fig. 10.

Fig. 10 Conceptual model representing the seawater intrusion and the phytoplankton community with environmental factors of the Itapecuru River Estuary (IRE)

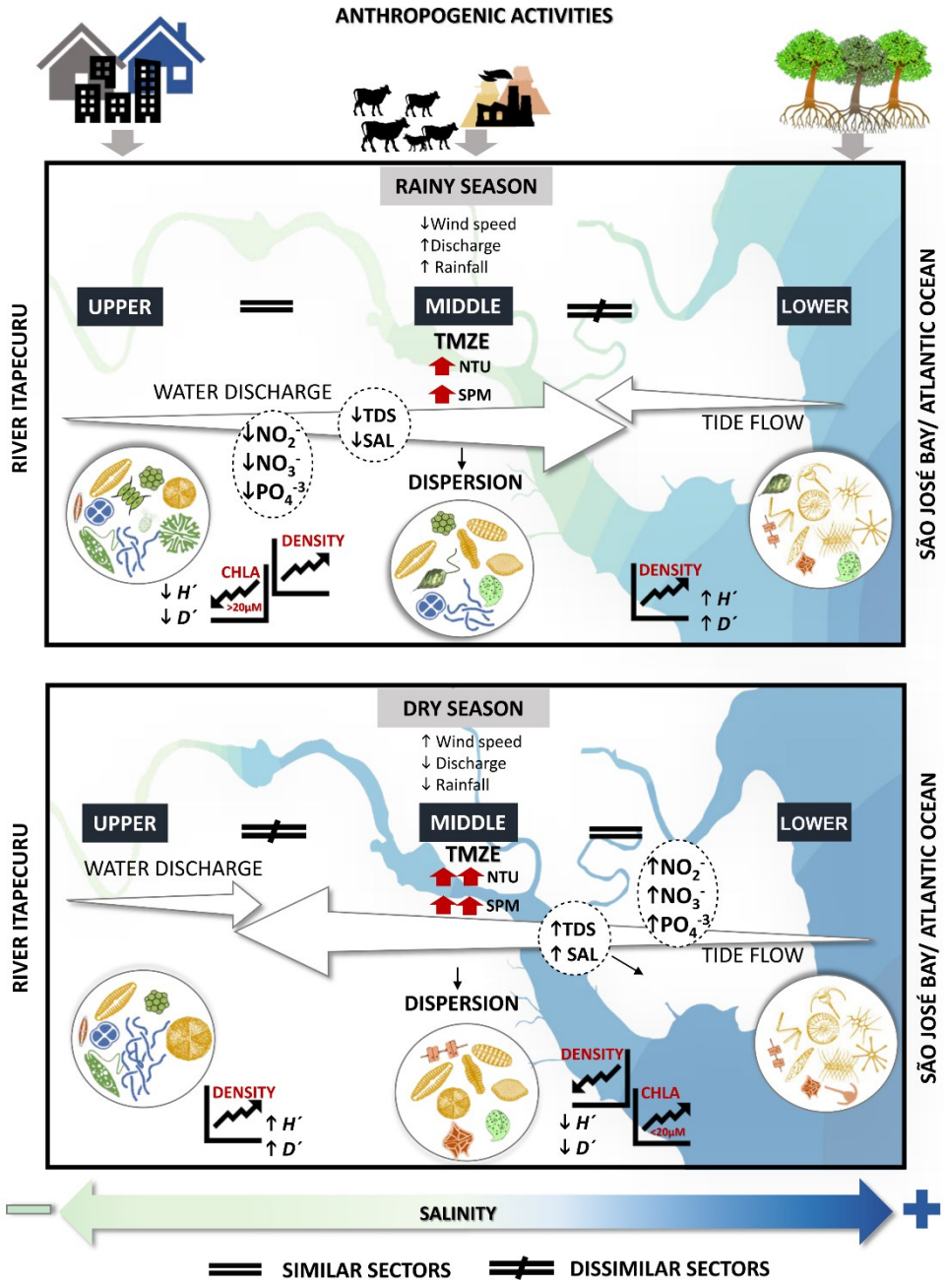

Source: The author (2022).

These changes in environmental variables affecting the phytoplankton community can extend to the entire trophic web, leading to a succession of dominant species and the occurrence of potentially harmful algal blooms that inhibit the growth and diversity of zooplankton. On the other hand, there is the tropical ascending cascade effect, in which herbivorous zooplankton favored by SWI reduce phytoplankton diversity (Xiang et al., 2021). In addition, algal blooms also reduce water quality which can affect organisms at higher

trophic levels (e.g., fish). These potential changes are expected under different global change scenarios (warming, increased nutrient load, and sea-level rise). Moreover, possible toxic cyanobacteria proliferation should be considered, given that the seasonal conditions of the IRE favor such occurrences. From this, it is clear that time-series observations are essential for understanding possible modifications related to SWI in the IRE in the future.

Conclusion

The SWI revealed spatiotemporal heterogeneity in salinity, TDS, and SPM, variables that clearly define the three estuarine sectors of the IRE. The magnitude of SWI was greater during the dry season, increasing the similarity between the middle and lower sectors, where SWI contributes to an increase in nutrient concentration and marine species dispersion. As a result, the freshwater species became confined to the upper sector. Variations in salinity, SPM, cell size, and silicate influenced this dispersion. SWI is responsible for the displacement of the TMZE during the dry season, constituting a turbid and unfavorable environment for the development of phytoplankton, as demonstrated by the lower density, diversity, and biomass. The upper sector registered increased chlorophyll-a concentrations, with higher hydrological stability. Microphytoplankton comprised the fractional majority in this sector, while nano/picophytoplankton were dominant in the lower sector. Centric diatoms and species > 20 µm— *C. ambigua*, *N. palea*, *P. coronalis*, and *S. costatum*—constitute the most expressive indicator group, all of which increase their cell density with SWI. Thus, the advance of SWI during the dry period reduces phytoplankton diversity and increases the cyanobacteria fraction, favoring the predominance of CyanoHab, a potentially harmful and bloom-forming species in the IRE. During the rainy season, an opposite pattern of community structure was observed with species overlap. In this sense, SPM and salinity are considered to be hydrological tracers of SWI and deterministic parameters of the indicator phytoplankton species distribution in the IRE. In conclusion, the study findings proved that the phytoplankton community was affected by SWI.

Lack of environmental management will result in biodiversity loss. The control of land-based emissions and sewage disposal, a major form of coastal pollution, is critical for maintaining water quality in this coastal ecosystem. The current scenario results from a set of anthropogenic actions and climate changes that may be taking place in this estuary. Thus, well-structured environmental management is needed, with monitoring of the effects of the advance of saline intrusion, including phytoplankton community changes and possible toxic

cyanobacterial blooms. We also suggest using the *Polymyxus coronalis* indicator as a tool to assess the SWI advance in tropical estuaries of South Atlantic macrotides.

Acknowledgements This research was supported by a grant from the Foundation for the Support of Scientific and Technological Research and Development of Maranhão – Brazil (FAPEMA) through the granting/concession (BD-01850/19) of a doctoral scholarship to the first author. The authors acknowledge the Federal University of Maranhão State and the Federal University of Pernambuco State for the technical and structural support. We would like to thank Editage (www.editage. com) for English language editing and the anonymous reviewers for the positive and insightful comments/suggestions in the manuscript.

References

ABREU, J. M. S., A. C. S. SARAIVA, J. S. ALBERT & N. M. PIORSKI, 2020. Paleogeographic influences on freshwater fish distributions in northeastern Brazil. Journal of South American Earth Sciences 102: 102692.

ABREU, P. C., C. HARTMANN & C. ODEBRECHT, 1995. Nutrient-rich saltwater and its influence on the phytoplankton of the Patos Lagoon estuary, Southern Brazil. Estuarine, Coastal and Shelf Science 40: 219–229.

AFFE, H. M., F. R. PIEDRAS, L. M. SANTANA, G. A. O. MOSER, M. MENEZES & J. M. NUNES, 2019. Phytoplankton functional groups: Short-term variation in a tropical tidal-forced estuarine system. Marine Ecology 40: e12555.

ALVARES, C. A., J. L. STAPE, P. C. SENTELHAS, J. L. DE MORAES GONÇALVES & G. SPAROVEK, 2013. Köppen's climate classification map for Brazil. Meteorologische Zeitschrift 22: 711–728.

ARAÚJO, M., C. NORIEGA, G. A. HOUNSOU-GBO, D. VELEDA, J. ARAUJO, L. BRUTO, F. FEITOSA, M. FLORES-MONTES, N. LEFÈVRE, P. MELO, A. OTSUKA, K. TRAVASSOS, R. SCHWAMBORN & S. NEUMANN-LEITÃO, 2017. A synoptic assessment of the amazon river-ocean continuum during boreal autumn: from physics to plankton communities and carbon flux. Frontiers in Microbiology 8: 1358.

ASP, N. E., V. J. C. GOMES, C. A. F. SCHETTINI, P. W. M. SOUZA- FILHO, E. SIEGLE, A. S. OGSTON, C. A. NITTROUER, J. N. S. SILVA, W. R. NASCIMENTO, S. R. SOUZA, L. C. C. PEREIRA & M. C. QUEIROZ, 2018. Sediment dynamics of a tropical tide-dominated estuary: turbidity maximum, mangroves and the role of the Amazon River sediment load. Estuarine, Coastal and Shelf Science 214: 10–24.

AZHIKODAN, G. & K. YOKOYAMA, 2016. Spatio-temporal variability of phytoplankton (Chlorophyll-a) in relation to salinity, suspended sediment concentration, and light intensity in a macrotidal estuary. Continental Shelf Research 126: 15–26.

BARROS, M., E. FRAGA & J. BIRINDELLI, 2011. Fishes from the Itapecuru River basin, State of Maranhão, northeast Brazil. Brazilian Journal of Biology 71: 375–380.

BHARATHI, M. D. & V. V. S. S. SARMA, 2019. Impact of monsoon-induced discharge on phytoplankton community structure in the tropical Indian estuaries. Regional Studies in Marine Science 31: 100795.

BHARATHI, M. D., V. V. S. S. SARMA & K. Ramaneswari, 2018. Intra-annual variations in phytoplankton biomass and its composition in the tropical estuary: Influence of river discharge. Marine Pollution Bulletin 129: 14–25.

CARRASCO NAVAS-PAREJO, J. C., A. CORZO & S. PAPASPYROU, 2020. Seasonal cycles of phytoplankton biomass and primary production in a tropical temporarily open-closed estuarine lagoon — the effect of an extreme climatic event. Science of the Total Environment 723: 138014.

CARY, L., E. PETELET-GIRAUD, G. BERTRAND, W. KLOPPMANN, L. AQUILINA, V. MARTINS & D. PIERRE, 2015. Origins and processes of groundwater salinization in the urban coastal aquifers of Recife (Pernambuco, Brazil): a multi-isotope approach. Science of the Total Environment 530–531: 411–429.

CAVALCANTI, L. F., M. V. J. CUTRIM, C. B. LOURENÇO, A. K. D. S. SÁ, A. L. L. OLIVEIRA & A. C. G. DE AZEVEDO-CUTRIM, 2020. Patterns of phytoplankton structure in response to environmental gradients in a macrotidal estuary of the Equatorial Margin (Atlantic coast, Brazil). Estuarine, Coastal and Shelf Science 245: 106969.

CHAI, C., T. JIANG, J. CEN, W. GE & S. LU, 2016. Phytoplankton pigments and functional community structure in relation to environmental factors in the Pearl River Estuary. Oceanologia 58: 201–211.

CHANG, S. W., T. P. CLEMENT, M. J. SIMPSON & K. K. LEE, 2011. Does sea-level rise have an impact on saltwater intrusion? Advances in Water Resources 34: 1283–1291.

CLARKE, K.R., R.N. GORLEY, P.J. SOMERFIELD & R.M. WARWICK, 2014. Change in marine communities: an approach to statistical analysis and interpretation. PRIMER-E, Plymouth.

COUTINHO, P. N. & J. O. DE MORAIS, 1976. Distribuição de sedimentos na Baía de São José, no Estado do Maranhão (Brasil). Arquivos De Ciências Do Mar. 16: 123–127.

CUTRIM, M. V. J., F. S. FERREIRA, A. K. DUARTE DOS SANTOS, L. F. CAVALCANTI, B. DE OLIVEIRA ARAÚJO, A. C. G. DE AZEVEDO- CUTRIM, & A. L. L. OLIVEIRA, 2019. Trophic state of an urban coastal lagoon (northern Brazil), seasonal variation of the phytoplankton community and environmental variables. Estuarine, Coastal and Shelf Science 216: 98–109.

DA COSTA, K. G., T. R. BEZERRA, M. C. MONTEIRO, M. VALLINOTO, J. F. BERRÊDO, L. C. C. PEREIRA & R. M. DA COSTA, 2013. Tidal-induced changes in the zooplankton community of an Amazon estuary. Journal of Coastal Research 289: 756–765.

DA COSTA, R. M., J. B. MATOS, K. S. T. PINTO & L. C. C. PEREIRA, 2013. Phytoplankton of a dynamic Amazon sandy beach. Journal of Coastal Research 65: 1751–1756.

DA SILVA, A. S. X., C. NORIEGA, M. L. KOENING, M. F. MONTES & M. ARAUJO, 2017. Distribution of nutrients and changes in phytoplankton composition in a tropical Mesotidal Estuary, Northeastern Brazil. Open Journal of Ecology 7: 460–494.

DA SILVA, F. P., J. R. S. MARTINS & F. F. NOGUEIRA, 2020. Impacts of sea level rise on seawater intrusion in Cubatão River, Brazil. Environmental Modeling & Assessment 25: 831–884.

DA SILVA, L. M., F. A. DO N. FEITOSA, M. DE J. FLORES-MONTES, A. Y. OTSUKA, F. SALDANHA-CORRÊA & C. NORIEGA, 2019. Phytoplankton productivity and hydrology in an impacted estuarine complex in Northeastern Brazil. Open Journal of Ecology 09: 458–477.

DA SILVA, M. H., M. DA G. G. DA SILVA-CUNHA, J. Z. DE O. PASSAVANTE, C. K. DA S. GREGO & K. MUNIZ, 2009. Estrutura sazonal e espacial do microfitoplâncton no estuário tropical do rio Formoso, PE, Brasil. Acta Botanica Brasilica 23: 355–368.

DE AZEVEDO, A. C. G., F. A. N. FEITOSA & M. L. KOENING, 2008. Distribuição espacial e temporal da biomassa fitoplanctônica e variáveis ambientais no Golfão Maranhense, Brasil. Acta Botanica Brasilica 22: 870–877.

DE BARROSO, H. S., H. BECKER & V.M.M. MELO, 2016. Influence of river discharge on phytoplankton structure and nutrient concentrations in four tropical semiarid estuaries. Brazilian Journal of Oceanography 64: 37–48.

DE MELO, G. V., J. A. B. NETO, S. B. VINZÓN, A. S. DE OLIVEIRA, M. A. F. VICENTE, O. MALM & C. G. SILVA, 2014. Salinity intrusion in the Guapimirim estuary, Rio de Janeiro state, Brazil. Revista Brasileira De Geofísica 32: 161–176.

DE MIRANDA, L. B., A. L. BÉRGAMO & B. M. DE CASTRO, 2005. Interactions of river discharge and tidal modulation in a tropical estuary, NE Brazil. Ocean Dynamics 55: 430–440.

DE MIRANDA, L. B., E. D. OLLE, A. L. BÉRGAMO, L. DOS S. SILVA & F. P. ANDUTTA, 2012. Circulation and salt intrusion in the Piaçaguera Channel, Santos (SP). Brazilian Journal of Oceanography 60: 11–23.

DE RIBEIRO, D. C., G. D. A. PALHETA, F. C. PAMPLONA, I. G. HAMOY, M. L. S. DE SANTOS & N. F. A. C. MELO, 2019. Effects of environmental factors on succession of microphytoplankton community in a marine shrimp pond and adjacent Amazon estuary. Boletim Do Instituto De Pesca 45: e508–e509.

DE SOUZA-JÚNIOR, A. N., A. MAGALHÃES & L. C. C. PEREIRA, 2013. Zooplankton dynamics in a tropical Amazon estuary. Journal of Coastal Research 165: 1230–1235.

DOS COSTA, D. & S. M. V. J. CUTRIM, 2021. Spatial and seasonal variation in physicochemical characteristics and phytoplankton in an estuary of a tropical delta system. Regional Studies in Marine Science 44: 101746.

DOS SANTOS, A. K. D., A. L. L. OLIVEIRA, J. A. FURTADO, F. S. FERREIRA, B. DE O. ARAÚJO, J. J. M. CORRÊA, & M. V. J. CUTRIM, 2017. Spatial and seasonal variation of microphytoplankton community and the correlation with environmental parameters in a hypereutrophic tropical estuary - Maranhão - Brazil. Brazilian Journal of Oceanography 65: 356–372.

DOS SANTOS, G. S., J. AGUIAR-SANTOS, A. C. L. DE CASTRO & N. M. PIORSKI, 2019. Length-weight relationships of seven fish species from Amazonian Equatorial coast, Brazil. Journal of Applied Ichthyology 35: 1169–1171.

DOS SANTOS, V., H. M., F. J. DA SILVA DIAS, A. R. TORRES, R. A. SOARES, L. C. TERTO, A. C. L. DE CASTRO, R. L. SANTOS, M. V. J. CUTRIM, 2020. Hydrodynamics and suspended particulate matter retention in macrotidal estuaries located in Amazonia-semiarid interface (Northeastern-Brazil). International Journal of Sediment Research 35: 417–429.

DOXARAN, D., J.-M. FROIDEFOND, P. CASTAING & M. BABIN, 2009. Dynamics of the turbidity maximum zone in a macrotidal estuary (the Gironde, France): observations from field and MODIS satellite data. Estuarine, Coastal and Shelf Science 81: 321–332.

DUARTE-DOS-SANTOS, A. K., A. L. L. OLIVEIRA, J. A. FURTADO, F.S. FERREIRA, B. DE O. ARAÚJO, J. J. M. CORRÊA, L.F. CAVALCANTI, A.C.G. AZEVEDO-CUTRIM, & M. V. J. CUTRIM, 2017. Spatial and seasonal variation of microphytoplankton community and the correlation with environmental parameters in a hypereutrophic tropical estuary - Maranhão - Brazil. Brazilian Journal of Oceanography 65: 356–372.

DUFRENE, M. & P. LEGENDRE, 1997. Species assemblages and indicator species: the need for a flexible asymmetrical approach. Ecological Monographs 67: 345–366.

FUJITA, C. & C. ODEBRECHT, 2007. Short term variability of chlorophyll a and phytoplankton composition in a shallow area of the Patos Lagoon estuary (southern Brazil). Atlantica 29: 93–16.

GOLTERMAN, H. L., R. S. CLYMO & M. A. M. OHNSTAD, 1978. Methods for physical and chemical analysis of freshwater, Blackwell, Oxford:

GOMES, O. V. O., E. D. MARQUES, V. T. KÜTTER, J. R. AIRES, Y. TRAVI & E. V. SILVA-FILHO, 2019. Origin of salinity and hydrogeochemical features of porous aquifers from northeastern Guanabara Bay, Rio de Janeiro, SE - Brazil. Journal of Hydrology: Regional Studies 22: 100601.

GONG, W., J.P.-Y. MAA, B. HONG & J. SHEN, 2014. Salt transport during a dry season in the Modaomen Estuary, Pearl River Delta, China. Ocean & Coastal Management 100: 139–150.

GRASSHOFF, K., M. EHRHARDT & K. KREMLING, 1983. Methods of seawater analysis. Verlag Chemie, New York 16: 581–614.

GUENTHER, M., M. ARAÚJO, M. FLORES-MONTES, E. GONZALEZ- RODRIGUEZ & S. NEUMANN-LEITÃO, 2015. Eutrophication effects on phytoplankton size-fractioned biomass and production at a tropical estuary. Marine Pollution Bulletin 91: 537–547.

JYOTHIBABU, R., N. ARUNPANDI, L. JAGADEESAN, C. KARNAN, K. R. LALLU & P. N. VINAYACHANDRAN, 2018. Response of phytoplankton to heavy cloud cover and turbidity in the northern Bay of Bengal. Scientific Reports 8: 11282.

KARTHIK, R., R. S. ROBIN, I. ANANDAVELU, R. PURVAJA, G. SINGH, M. MUGILARASAN, T. JAYALAKSHMI, V. DEEPAK SAMUEL & R. RAMESH, 2020. Diatom bloom in the Amba River, west coast of India: a nutrient-enriched tropical riverfed estuary. Regional Studies in Marine Science 35: 101244.

KASAI, A., Y. KURIKAWA, M. UENO, D. ROBERT & Y. YAMASHITA, 2010. Salt-wedge intrusion of seawater and its implication for phytoplankton dynamics in the Yura Estuary, Japan. Estuarine, Coastal and Shelf Science 86: 408–414.

KRUK, C., V. L. M. HUSZAR, E. T. H. M. PEETERS, S. BONILLA, L. COSTA, M. LÜRLING & M. SCHEFFER, 2010. A morphological classification capturing functional variation in phytoplankton. Freshwater Biology 55: 614–627.

KRVAVICA, N. & I. RUŽIĆ, 2020. Assessment of sea-level rise impacts on salt-wedge intrusion in idealized and Neretva River Estuary. Estuarine, Coastal and Shelf Science 234: 106638.

LANCELOT, C. & K. MUYLAERT, 2011. Trends in estuarine phytoplankton ecology. Treatise on Estuarine and Coastal Science. https://doi.org/10.1016/b978-0-12-374711-2. 00703-8.

LEFÈVRE, N., F. J. DA SILVA DIAS, A. R. DE TORRES, C. NORIEGA, M. ARAUJO, A. C. L. DE CASTRO, C. ROCHA, S. JIANG & J. S. P. IBÁNHEZ, 2017. A source of CO_2 to the atmosphere throughout the year in the Maranhense continental shelf (2°30'S, Brazil). Continental Shelf Research 141: 38–50.

LEMLEY, D. A., J. B. ADAMS & G. C. BATE, 2016. A review of microalgae as indicators in South African estuaries. South African Journal of Botany 107: 12–20.

LEMLEY, D. A., J. B. ADAMS, G. M. RISHWORTH & C. BOULAND, 2019. Phytoplankton responses to adaptive management interventions in eutrophic urban estuaries. Science of the Total Environment 693: 133601.

LEMLEY, D. A., J. B. ADAMS, S. TALJAARD & N. A. STRYDOM, 2015. Towards the classification of eutrophic condition in estuaries. Estuarine, Coastal and Shelf Science 164: 221–232.

LESSA, G. C., F. M. SANTOS, P. W. SOUZA-FILHO & L. C. CORRÊA- GOMES, 2018. Brazilian Estuaries: A Geomorphologic and Oceanographic Perspective. In Lana, P. & A. Bernardino (eds), Brazilian Estuaries, Brazilian Marine Biodiversity. Springer, Cham.

LEWIS, W. M., 1976. Surface/volume ratio: implications for phytoplankton morphology. Science 192: 885–887.

LIU, B., S. PENG, Y. LIAO & H. WANG, 2019A. The characteristics and causes of increasingly severe saltwater intrusion in Pearl River Estuary. Estuarine, Coastal and Shelf Science 220: 54–63.

LIU, C., M. YU, L. JIA, H. CAI & X. CHEN, 2019B. Impacts of physical alterations on salt transport during the dry season in the Modaomen Estuary, Pearl River Delta, China. Estuarine, Coastal and Shelf Science 227: 106345.

LONG, A., L. SUN, R. SHI, W. ZHOU & A. DANG, 2013. Salt- water intrusion induced by a complete neap tide and its effect on nutrients variation in the estuary of Pearl River, China. Journal of Coastal Research 29: 1158–1168.

LU, Z. & J. GAN, 2015. Controls of seasonal variability of phytoplankton blooms in the Pearl River Estuary. Deep Sea Research Part II: Topical Studies in Oceanography 117: 86–96.

MACHADO, R. C. A., F. A. N. FEITOSA, M. L. KOENING & M. J. FLORES MONTES, 2017. Spatial and seasonal variation of the phytoplankton community structure in a reef ecosystem in North-eastern Brazil. Journal of the Marine Biological Association of the United Kingdom 98: 557–566.

MADHU, N. V., R. JYOTHIBABU & K. K. BALACHANDRAN, 2009. Monsoon-induced changes in the size-fractionated phytoplankton biomass and production rate in the estuarine and coastal waters of southwest coast of India. Environmental Monitoring and Assessment 166: 521–528.

MAGALHÃES, A., D.S.B. NOBRE, R.S.C. BESSA, L.C.C. PEREIRA & R.M. DA COSTA, 2011. Seasonal and short-term variations in the copepod community of a shallow Amazon estuary (Taperaçu Estuary, Northern Brazil). Journal of Coastal Research SI 64 (Proceedings of the 11th International Coastal Symposium), pp. 1520–1524.

MARGALEF, R., 1958. Temporal sucession and spatial heterogeneity in phytoplankton. In Buzzati-Traverso, A. A. (ed), Perspectives in Marine Biology Universidade California Press, Berkeley: 323–349.

MASULLO, Y. A. G., L. S. SOARES, C. E. DE CASTRO & E. A. L. PINHEIRO, 2019. Dinâmica da paisagem da bacia hidrográfica do rio Itapecuru - MA. Revista Brasileira De Geografia Física 12: 1054.

MCLUSKY, D. S., 1993. Marine and estuarine gradients — an overview. Netherlands Journal of Aquatic Ecology 27: 489–493.

MITCHELL, S. B., 2013. Turbidity maxima in four macrotidal estuaries. Ocean & Coastal Management 79: 62–69.

MONTEIRO, M. C., J. A. JIMÉNEZ & L. C. C. PEREIRA, 2016. Natural and human controls of water quality of an Amazon estuary (Caeté-PA, Brazil). Ocean & Coastal Management 124: 42–52.

MUYLAERT, K., K. SABBE & W. VYVERMAN, 2009. Changes in phytoplankton diversity and community composition along the salinity gradient of the Schelde estuary (Belgium/The Netherlands). Estuarine, Coastal and Shelf Science 82: 335–340.

NAVARRO, J. N. & R. G. DE PERIBONIO, 1993. A light and scanning electron microscope study of the centric diatom Polymyxus coronalis (Bacillariophyta). European Journal of Phycology 28: 167–172.

NAVAS-PAREJO, J. C., A. CORZO & S. PAPASPYROU, 2020. Seasonal cycles of phytoplankton biomass and primary production in a tropical temporarily open-closed estuarine lagoon — the effect of an extreme climatic event. Science of the Total Environment 723: 138014.

NCHE-FAMBO, F. A., U. M. SCHARLER & K. TIROK, 2015. Resilience of estuarine phytoplankton and their temporal variability along salinity gradients during drought and hypersalinity. Estuarine, Coastal and Shelf Science 158: 40–52.

NIU, L., X. LUO, S. HU, F. LIU, H. CAI, L. REN, S. OU, D. ZENG & Q. YANG, 2020. Impact of anthropogenic forcing on the environmental controls of phytoplankton dynamics between 1974 and 2017 in the Pearl River estuary, China. Ecological Indicators 116: 106484.

NUNES, M., J. B. ADAMS & G. M. RISHWORTH, 2018. Shifts in phytoplankton community structure in response to hydrological changes in the shallow St Lucia Estuary. Marine Pollution Bulletin 128: 275–286.

ONABULE, O. A., S. B. MITCHELL & F. COUCEIRO, 2020. The effects of freshwater flow and salinity on turbidity and dissolved oxygen in a shallow Macrotidal estuary: a case study of Portsmouth Harbour. Ocean & Coastal Management 191: 105179.

OSEJI, O. F., P. CHIGBU, E. OGHENEKARO, Y. WAGUESPACK & N. CHEN, 2018. Spatiotemporal patterns of phytoplankton composition and abundance in the Maryland Coastal Bays: the influence of freshwater discharge and anthropogenic activities. Estuarine, Coastal and Shelf Science 207: 119–131.

PAIVA, R. S., E. ESKINAZI-LEÇA, J. Z. O. PASSAVANTE, M. G. G. SILVA-CUNHA & N. F. A. C. MELO, 2006. Considerações ecológicas sobre o fitoplâncton da baía do Guajará e foz do rio Guamá (Pará-Brasil). Boletim Do Museu Paraense Emílio Goeldi Ciências Naturais 1: 133–146.

PAMPLONA, F. C., E. T. PAES & A. NEPOMUCENO, 2013. Nutrient fluctuations in the Quatipuru river: a macrotidal estuarine mangrove system in the Brazilian Amazonian basin. Estuarine, Coastal and Shelf Science 133: 273–284.

PAUL, M., M. NIKATHITHARA VELAPPAN, U. NANAPPAN, V. GOPINATH, R. THEKKENDAVIDA VELLOTH, A. RAJENDRAN, N. MAHESWARI & A. PEARIYA, 2021. Characterization of phytoplankton size-structure based productivity, pigment complexes (HPLC/CHEMTAX) and species composition in the Cochin estuary (southwest coast of India): special emphasis on diatoms. Oceanologia 43:643

PIELOU, E. C., 1966. Species diversity and pattern-diversity in the study of ecological succession. Journal of Theoretical Biology 10: 370–383.

PORTO, H. L. R., A. C. L. DE CASTRO, J. W. DE JESUS AZEVEDO, L. SILVA SOARES, C. F. CHAGAS FERREIRA M & H., LOPES SILVA & H. R. SILVA FERREIRA, 2017. Mineral content in fishes in the lower course of the Itapecuru river in the state of Maranhão, Brazil. Korean Journal of Chemical Engineering 34: 1985–1991.

PRUSTY, P. & S. H. FAROOQ, 2020. Seawater intrusion in the coastal aquifers of India - a review. HydroResearch 3: 61–74.

RIBEIRO, F. C. P. & C. DO S. F. DE SENNA & L. C. TORGAN, 2008. Diatomáceas em sedimentos superficiais na planície de maré da Praia de Itupanema, estado do Pará, Amazônia. Rodriguésia 59: 309–324.

RIBEIRO, F., C. SENNA & L. TORGAN, 2010. The use of diatoms for paleohydrological and paleoenvironmental reconstructions of Itupanema Beach, Pará State, Amazon Region, during the last millennium. Revista Brasileira De Paleontologia 13: 21–32.

RICE, K. C., B. HONG & J. SHEN, 2012. Assessment of salinity intrusion in the James and Chickahominy Rivers as a result of simulated sea-level rise in Chesapeake Bay, East Coast, USA. Journal of Environmental Management 111: 61–69.

SÁ, A. K. D. S., M. V. J. CUTRIM, D. S. COSTA, L. F. CAVALCANTI, F. S. FERREIRA, A. L. L. OLIVEIRA & J. H. F. SEREJO, 2021. Algal blooms and trophic state in a tropical estuary blocked by a dam (Northeastern Brazil). Ocean and Coastal Research 69: e21009.

SAIFULLAH, A. S. M., A. H. M. KAMAL, M. H. IDRIS, A. H. RAJAEE & M. K. A. BHUIYAN, 2015. Phytoplankton in tropical man- grove estuaries: role and interdependency. Forest Science and Technology 12: 104–113.

SANDERS, C. J., I. R. SANTOS, R. BARCELLOS & E. V. SILVA FILHO, 2012. Elevated concentrations of dissolved Ba, Fe and Mn in a mangrove subterranean estuary: consequence of sea level rise? Continental Shelf Research 43: 86–94.

SANTANA, R. M. C., M. DOLBETH, J. E. L. BARBOSA & J. PATRÍCIO, 2018. Narrowing the gap: phytoplankton functional diversity in two disturbed tropical estuaries. Ecological Indicator 86: 81–93.

SANTIAGO, M. F. & M. DA G. G. DA SILVA-CUNHA, S. NEUMANN-LEITÃO, K. M. P. DA COSTA, G. C. B. PALMEIRA, F. DE F. PORTO NETO & F. S. NUNES, 2010. Phytoplankton dynamics in a highly eutrophic estuary in tropical Brazil. Brazilian Journal of Oceanography 58: 189–205.

SENA, B. A., V. B. COSTA, L. NAKAYAMA & R. M. ROCHA, 2015. Composition of microphytoplankton of an estuarine Amazon River, Pará, Brazil. Biota Amazônia 5: 1–9.

SHANNON, C. E., 1948. A mathematical theory of communication. The Bell System Technical Journal 27: 379–423.

SRICHANDAN, S., J. Y. KIM, P. BHADURY, S. K. BARIK, P. R. MUDULI, R. N. SAMAL & G. RASTOGI, 2015. Spatiotemporal distribution and composition of phytoplankton assemblages in a coastal tropical lagoon: Chilika, India. Environmental Monitoring and Assessment 187: 47.

STRAMMA, L., J. FISCHER, P. BRANDT & F. SCHOTT, 2003. Circulation, variability and near-equatorial meridional flow in the central tropical Atlantic. Elsevier Oceanography Series 68: 1–22.

STRICKLAND, J. D. H. & T. R. PARSONS, 1972. A practical handbook of seawater analysis. Bulletin Fisheries Research Board of Canada, Ottawa 167: 1–205.

TAO, W., L. NIU, F. LIU, H. CAI, S. OU, D. ZENG & Q. YANG, 2020. Influence of river-tide dynamics on phytoplankton variability and their ecological implications in two Chinese tropical estuaries. Ecological Indicators 115: 106458.

TEIXEIRA, C., F. J. ARANHA, R. BARBIERI & O. T. MELO, 1988. Produção primária e clorofila *a* do fitoplâncton e parâmetros físicos e químicos do estreito dos Coqueiros - Maranhão - Brasil. Revista Brasileira De Biologia 48: 29–39.

TIAN, R., 2019. Factors controlling saltwater intrusion across multi-time scales in estuaries, Chester River, Chesapeake Bay. Estuarine, Coastal and Shelf Science 223: 61–73.

UNITED NATIONS EDUCATIONAL, SCIENTIFIC AND CULTURAL ORGANIZATION – UNESCO, 1966. Determination of photosynthetic pigments in sea-water. (Monographs on Oceanographic Meth- odology), Paris.

UTERMÖHL, H., 1958. Zur vervollkommung der quantitativen phytoplankton - methodik. Mitteilungen Internationale Vereinigung Fuer Theoretische Und Angewandte Limnologie 9: 1–38.

VILAFAÑE, V. E. & F. H. M. REID, 1995. Métodos de microscopia para la cuantificación del fitoplancton. In Alvear, K., M. E. Ferrario, E. C. Oliveira Filho & E. Sars (eds), Manual de métodos ficológicos Universidad de Concepción, Chile: 169–185.

VILHENA, M. P. S. P., M. L. COSTA, J. F. BERRÊDO, R. S. PAIVA & C. C. S. SOUZA, 2016. Chemical elements in pearl oysters (Paxyodon ponderosus), phytoplankton and estuarine sediments from eastern Amazon (Northern Brazil): Bioaccumulation factors and trophic transfer factors. Journal of South American Earth Sciences 67: 1–10.

WANG, J., L. LI, Z. HE, N. A. KALHORO & D. XU, 2019. Numerical modelling study of seawater intrusion in Indus River Estuary, Pakistan. Ocean Engineering 184: 74–84.

WARWICK, R. M. & K. R. CLARKE, 1993. Comparing the severity of disturbance: a meta-analysis of marine macrobenthic community data. Marine Ecology Progress Series, Oldendorf 92(221): 231.

WATANABE, K., A. KASAI, E. S. ANTONIO, K. SUZUKI, M. UENO & Y. YAMASHITA, 2014. Influence of salt-wedge intrusion on ecological processes at lower trophic levels in the Yura Estuary, Japan. Estuarine, Coastal and Shelf Science 139: 67–77.

WERNER, A. D., M. BAKKER, V. E. A. POST, A. VANDENBOHEDE, C. LU, B. ATAIE-ASHTIANI & D. A. BARRY, 2013. Seawater intrusion processes, investigation and management: recent advances and future challenges. Advances in Water Resources 51: 3–26.

WOLANSKI, E. & M. ELLIOTT, 2016. Estuarine water circulation. In Wolanski, E. & M. Elliott (eds), Estuarine Ecohydrology Elsevier, Amsterdam: 35–76.

XIANG, C., Z. KE, K. LI, J. LIU, L. ZHOU, X. LIAN & Y. TAN, 2021. Effects of terrestrial inputs and seawater intrusion on zooplankton community structure in Daya Bay. South China Sea. Marine Pollution Bulletin 167: 112331.

YANG, H., X. ZHANG, H. CAI, Q. HU, F. LIU & Q. YANG, 2020. Seasonal changes in river-tide dynamics in a highly human-modified estuary: Modaomen Estuary case study. Marine Geology 427: 106273.

ZHOU, W., J. GAO, J. LIAO, R. SHI, T. LI, Y. GUO & A. LONG, 2016. Characteristics of phytoplankton biomass, primary production and community structure in the modaomen channel, Pearl River estuary, with special reference to the influence of saltwater intrusion during neap and spring tides. PLOS ONE 11: e0167630.

7 ARTIGO 2 - MULTIPLE STRESSORS INFLUENCING THE GENERAL EUTROPHICATION STATUS OF TRANSITIONAL WATERS OF THE BRAZILIAN TROPICAL COAST: AN APPROACH UTILIZING THE PRESSURE, STATE, AND RESPONSE (PSR) FRAMEWORK

Manuscript published in Journal of Sea Research
Volume 189, November 2022, 102282
https://doi.org/10.1016/j.seares.2022.102282

ABSTRACT

Modeling approaches are useful tools for assessing the general state of eutrophication and understanding the effects of multiple stressors on coastal ecosystems. Thus, we hypothesized that anthropogenic pressures and multiple stressors would increase the trophic state of macrotidal estuaries. Datasets from long-term (2012-2020) environmental and biological monitoring in the Itapecuru River estuary (IRE) were analyzed using the pressure- state-response (PSR) approach and nonlinear methods. Our results indicated a low dilution of nutrients and a moderate flushing potential of urban effluent (2150.94 ton year^{-1}) in the estuary. The estuary was consequently classified as being in a high trophic state, being susceptible to and suffering high estuarine pressure to develop eutrophic symptoms. The Assessment of estuarine trophic status (ASSETS) model indicates that eutrophication is seasonal and depends on climatic variation. La Niña events (2019–2020) contributed to chlorophyll-a (>40 μg L^{-1}) and orthophosphate (0.04 mg L^{-1}) concentrations, principally during periods of low river discharge. Ac- cording to the GAM's model, brackish waters (salinity>10) with high temperatures (> 30 ◦C) and high dissolved oxygen (>4 mg L^{-1}) have more intense trophic conditions, especially in the mixing zone. The low dissolved oxygen (DO) levels (DO<3 mg L^{-1}) and high concentrations of chlorophyll-a in the seawater zone indicate that the lower portion of the estuary was the most susceptible. In addition, the random forest model selected salinity, DIP and Chl-a as the principal stressors that intensified eutrophication in the macrotidal systems. According to the ASSETS final ranking (worsen-high) for the next decade (2021-2031), the primary planned strategies should be to reduce anthropogenic contributions and improve trophic conditions in the IRE. From these results, the interactions and predictions of ecohydrological effects could facilitate the characterization of future risks and the management of macrotidal estuarine systems.

Keywords: Model trophic, Macrotidal, ENSO, Nutrients input, Brazilian estuary, Random forest

1. Introduction

Globally, estuaries are subject to intense environmental stress resulting from anthropogenic pressures (dredging, sewage, mining runoff, loss of habitat, and fishing) that affect the ecosystem structure and functioning (Xiao et al., 2007; Wu et al., 2016). These factors lead to eutrophication in transitional environments through the excessive enrichment of water with nutrients. This has become a global ecological problem in recent decades (Liu et al., 2018; Xie et al., 2021). In addition, climate change and seasonal periodicity of rainfall have contrasting effects on tropical estuarine communities (Andrades et al., 2021).

Consequently, the eutrophication of a watershed is influenced by multiple stressors that incorporate a wide variety of factors including land management, population growth, and climatic effects (Hutchins and Hitt, 2019). These multiple effects associated with anthropogenic pressures cause the loss of biodiversity and ecosystem integrity, forcing new challenges in its management and restoration. Nutrient criteria are recommended to provide reference conditions for the environment (Liu et al., 2018; Yang et al., 2019). Evidence of changing trophic states and the creation of these nutrient criteria are considered essential for controlling coastal eutrophication (Xie et al., 2021). Likewise, understanding the effects of multiple stressors is necessary for managing coastal waters and related ecosystems (Feld et al., 2016).

Numerous well-known eutrophication assessment methodologies have been developed worldwide (e.g., Assessment of estuarine trophic status [ASSETS], United Kingdom Water Framework Directive [UK- WFD], French Research Institute for the Exploitation of the Sea [IFREMER], HELCOM Eutrophication Assessment Tool [HEAT], Transitional Water Quality Index [TWQI], etc.) to analyze water quality in the context of multiple stressors. Among them, ASSETS is a sophisticated and integrated method considered a promising tool to classify the general eutrophication status of estuaries and coastal areas and to address environmental management options. It has been applied successfully in systems from different ecoregions representing all sizes in the U.S. and Europe to monitor estuarine ecosystems (see http://www.eutro.org/sys list.aspx) (Ferreira et al., 2007; Xiao et al., 2007; Borja et al., 2008;

Nobre et al., 2011; Garmendia et al., 2012; Wang et al., 2012; Wu et al., 2016; Kong et al., 2017).

ASSETS combines essential components of pressure (overall human influence [OHI]), state (overall eutrophic conditions [OEC]), and response (Definition of Future Outlook [DFO]), including susceptibility metrics (Ferreira et al., 2007), estuary-specific characteristics and spatiotemporal variability. These quantitative and semiquantitative components comprise a set of eutrophication indicators that support the precise characterization of trophic conditions, which can be performed and compared among highly varied systems (Bricker et al., 2003).

In addition, the ASSETS approach is based on pressure-state-response (PSR) indicators that address the assessment of coastal waters by tracking sustainable relationships and the direct effect of drivers. ASSETS and the slightly more elaborate PSR method provide multifaceted, nationally, or regionally consistent classifications of coastal ecosystem health (Hagy et al., 2022). In PSR, a stressor is a measurable environmental variable resulting from pressure that can affect the biological and ecological integrity of an ecosystem. The approach of multiple stressors is fundamental for the interpretation of anthropogenic effects on estuarine biotic communities. This is because the analysis combines adequate pressure and stressor variables (Feld et al., 2016).

The use of tools to evaluate eutrophication processes provides a simplified method to assess nutrient-related water quality conditions, linking sources that may cause degradation to future situations, serving as a means of prevention and information for the development of successful management measures (Bricker et al., 2014). The water quality and ecological integrity of estuaries reflect human activities upstream of the basin. The use of monitoring programs emphasizes human stressors, and indicators ensure success in the assessment of estuaries, transforming data into useful information (Lemley et al., 2015; Lemley et al., 2017).

Recently, several sets of legislation in different countries (Oceans Act in the USA, Australia, and Canada; Water Framework Directive or Marine Strategy in Europe, National Water Act in South Africa, etc.) have addressed the quality and ecological integrity of estuarine and coastal systems (Borja et al., 2008). In Brazil, although there is a resolution for defining water quality, CONAMA 357/2005 (Resolution National Environment Council), there remains a void in the integrated approach regarding trophic conditions and the construction of eutrophication scenarios. These tools are essential for monitoring these ecosystems and

establishing watershed management plans. CONAMA Resolution 357/ 2005 only provides classification and environmental guidelines for the framework of surface water bodies, establishing conditions and standards for discharging effluents in an unrelated manner. This scenario contributes to the lack of implemented systems that assess and monitor the ecological status of Brazilian transitional aquatic ecosystems, especially tropical and macrotidal ecosystems.

However, there is a lack of robust analytical frameworks and guidance to analyze these data in the context of multiple stressors (Feld et al., 2016). Multivariate trophic indices provide an efficient way to assess and classify the eutrophication level and ecological status of a given water body, but the use of only traditional methods that are based on a nutrient index has led to overestimated results and ambiguous interpretations (Xiao et al., 2007; Béjaoui et al., 2018). Machine learning (ML) has recently contributed to defining the nonlinear and complex relationships between input and output data and has recently been recognized as a powerful model in predicted complicated nonlinear systems (Latif et al., 2022). In this context, there is a need to use an advanced modeling approach that could tackle all of these features. Here, we aim to bridge this gap and present an approach to analyze multiple stressor effects based on modeling techniques nonlinear (GAM's model) and machine learning (ML) modeling.

The random forest model (RF) is a ML efficient technique that has been applied in many studies (Béjaoui et al., 2016; Béjaoui et al., 2018; Hadid et al., 2021; Hagy et al., 2022). RF is well suited for biological statistical models because they can be trained even on small datasets. The predictions are also highly reliable and do not assume any probability distribution for variables. It can also manage many predictors, choosing among them the most useful within the given scope (Béjaoui et al., 2018).

Hence, this study is the first to apply numerical tools to assist coastal management in protecting the environmental quality of transitional waters and estuarine environments on the Brazilian tropical Amazon coast. Due to the importance and dynamic nature of Brazilian estuarine ecosystems, we understand the urgent need to use sensitive and widely applicable indicators to detect changes in water quality and the general ecological condition of a tidal-dominated estuary.

In this study, we start from the idea that transitional waters dominated by the macrotidal regime present their eutrophication state intensified more by the physical dynamics than by the

chemical and nutritional parameters. Therefore, we hypothesized that anthropogenic pressures and multiple stressors, when associated with the phenomenon of saline intrusion in a macrotidal estuary of the tropical coast, increase the general state of eutrophication and compromise water quality. To assess the marine environmental impact, we intend to examine this question through an integrated approach that includes multimetric analyses. This methodology is used to accomplish the following: i) define nutrient criteria that provide a basis for determining trophic conditions, ii) quantify the magnitude of multiple anthropogenic pressures, iii) estimate the effect of multiple stressors on the trophic state, and iv) rank the variables that act directly and indirectly in the explanation of trophic interactions in the tropical macrotidal systems.

2. Materials and methods

2.1 Study area, data collection and sample processing

The study area was located on the Amazon macrotidal mangrove coast within the coastal zone of Maranhão. This coastal sector has a highly indented shoreline consisting of bays, associated tidal creeks, and their tributaries, which form funnel-shaped estuaries (de Sousa et al., 2017). The Itapecuru River has an area of 53,216.84 km^2 and is the largest river in Maranhão, with an average annual rainfall of >2000 mm yr^{-1}. Its basin has a volume of 45.57 m^3 s^{-1}. It is a water supply for ∼1.6 million people and receives waste from 1,759,871 inhabitants (Masullo et al., 2019; Almeida et al., 2022) (Fig. 1; Table 1). The IRE is located in the Amazon–semiarid interface and has the characteristics of a humid regime that includes prevailing intense rains controlled by the Intertropical Convergence Zone (ITCZ), with average temperatures above 25 °C (Lefèvre et al., 2017).

The estuary is dominated by macrotides. The tidal excursion occurs approximately 40 km upstream of the river mouth. It has a large water catchment system 27 km from the limit of salt wedge penetration (Fig. 1). The maximum estuarine turbidity zone (ZMTE) is located downstream of the saline intrusion and moves according to the local seasonal period. The circulation pattern was of the well-mixed type, and the regional tides were semidiurnal, with measured daily amplitudes from 0 to 7 m and current speeds of 2. 5 m s^{-1}. Its influence is present up to 150 km off the coast of Maranhão. The IRE covers a surface area of 487.75 km^2, and the average depth of the estuary is 5.37 m (Sá et al., 2022). The estuarine volume during spring tide varies from 20×10^6 m^3 at low tide to 36×10^6 m^3 at high tide, while during the neap

tide it varies from 22 × 10^6 m^3 at low tide to 33 × 10^6 m^3 at high tide. The tidal prism during the spring tide was 15 × 10^6 m^3, and at the neap tide, it was 11 × 10^6 m^3.

Fig. 1. Map of the Itapecuru River estuary, showing the location of the sampling site, anthropogenic activities, and main urban centers.

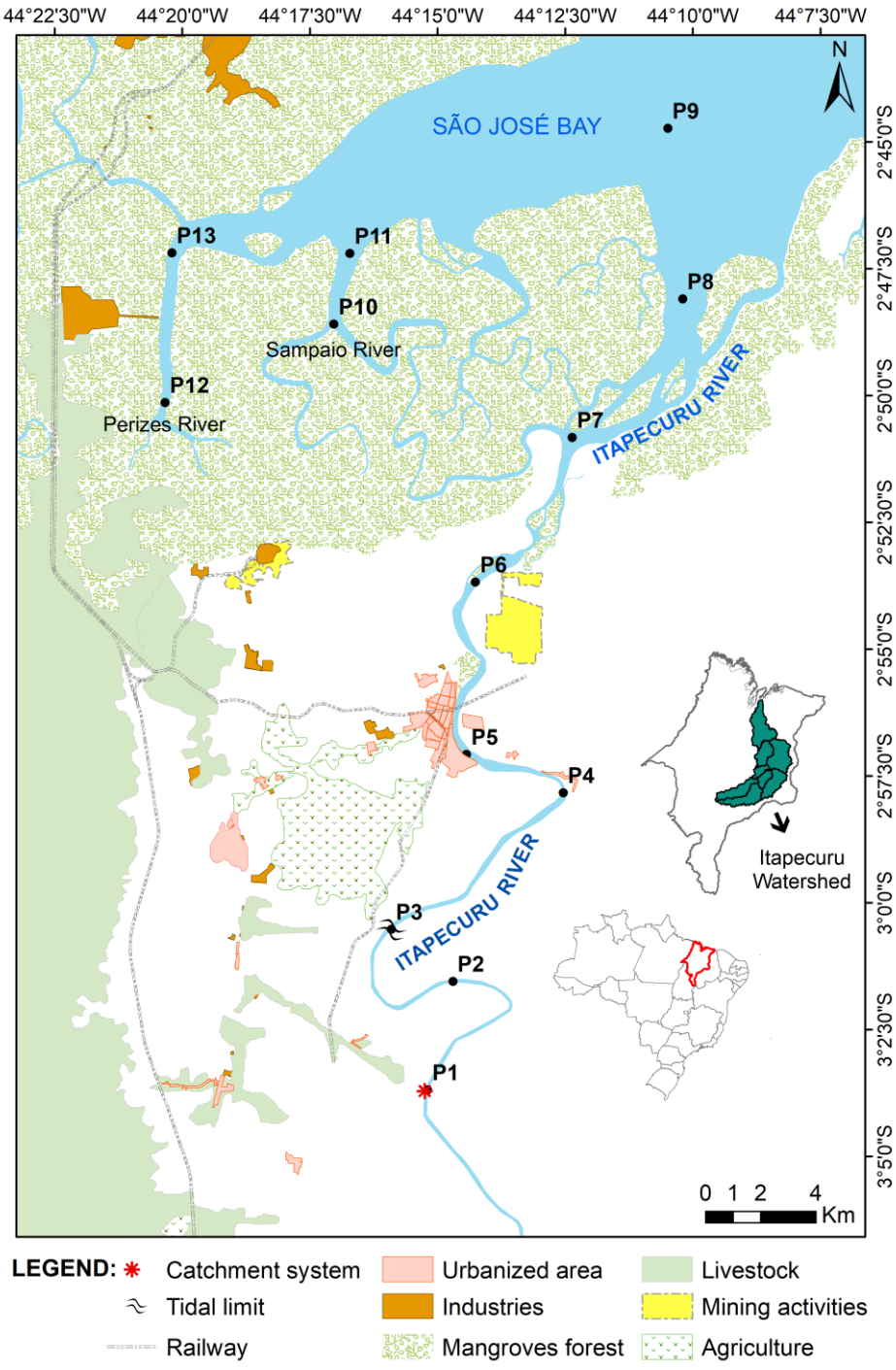

Source: The author (2022).

Table. 1 Summary of the physical characteristics of the Itapecuru River estuary.

Location		
Latitude S		2°35'
Longitude W		44°12.9'
Salinity zones		
Tidal freshwater (<0.5) km		31.8
Mixing (0.5–25) km		13.3
Seawater (>25) km		20.1
	At =	65.2
System Features		
Surface area (km^2)		487.75
Volume ($\times 10^6$ m^3)		36
Average depth (m)		5.4
Tidal range (m)		5.8
Stratification (upper layer as % of total volume)		0
Average freshwater discharge (m^3 s^{-1})		
	Rainy	121.2
	Dry	36.4
	Annual	78.47
Watershed population (hab.)		1,695,964
Surveying time		**N**
2012-2014		99
2019-2020		36
Total		135

Source: The author (2022).

The greatest population concentration in the state (1,695,964 inhabitants) occurs in the Itapecuru River basin, with a concentration of 5% (86,240 inhabitants) in the estuarine region. The main human uses of this system include urbanization, industrial development, agriculture, and fisheries (Instituto Brasileiro de Geografia e Estatística, IBGE, https://ibge.gov.br) (Fig. 1). In addition, the dilution capacity of domestic effluents is limited with high nitrogen load and releases in natura into the sea (2150,945 tn $year^{-1}$) (Water and Basic Sanitation – ANA, https://www.gov.br/ana/pt -br).

The data matrix analyzed utilized a time series (2012, 2013, and 2014) from the Environmental Impact Study of the Itapecuru River (commissioned by the Center for Studies and Tests in Risk and Environmental Modeling [CEERMA]) and bimonthly sampling performed during 2019 and 2020. The data matrix used 13 points along a salinity gradient. Three zones were defined by the salinity gradient: tidal freshwater (0–0.5), mixing (0.5–25) and seawater (>25) zones, which broadly correspond to the National Estuarine Inventory [NEI]. The NEI salinity characterization provides a consistent spatial framework for information collection. This model provides a consistent basis for comparisons among these highly variable systems (Bricker et al., 2003) (Table.1).

2.2. Water quality dataset

Salinity, water temperature (WT), and pressure were measured in situ in the middle channel of the estuary using a CTD probe (Castway, Sontek Instrument Company, USA). Total dissolved solids (TDS) and pH data were obtained using a multiparameter probe (HANNA 9878, Italy). Dissolved oxygen (DO) was determined using the chemical method of Winkler, as modified by Golterman et al. (1978). The dissolved oxygen saturation rate (DO%) followed the International Oceanographic Table standard for correlation between salinity and water temperature. Turbidity was measured using a turbidimeter (Lamotte 2020, USA). Water transparency was measured with a Secchi disk (SD), and suspended particulate matter (SPM), was measured by the gravimetric analysis described by Strickland and Parsons (1972). The concentrations of nitrite (NO_2^-) and nitrate (NO_3^-) were based on the method of Strickland and Parsons (1972), whereas that of orthophosphate (PO_4^{3-}) was determined using the methodology described by Grasshoff et al. (1983).

Chlorophyll-a (Chl-a) concentrations were determined by a spectrophotometric method (UNESCO, 1966) using a Spectronic 200 spectrophotometer (Thermo Fisher Scientific, USA; Strickland and Parsons, 1972). Phytoplankton quantification was performed using an inverted microscope (ZEISS Axiovert 100) at 400× magnification, based on Utermöhl's method (Utermöhl, 1958). Cell abundance was expressed as cells per liter (cells L^{-1}) according to the equation of Villafañe and Reid (1995). Phytoplankton were considered a bloom when a particular taxon reached or exceeded a density of 1×10^6 cells L^{-1} (Livingston, 2007).

2.3. Rainfall, river discharge and multivariate ENSO index

Historical precipitation and river discharge data (1972–2020) were obtained from the databases pertaining to the National Institute of Meteorology (INMET, https://portal.inmet.gov.br/) and the National Agency for Water and Basic Sanitation (ANA, https://www.snirh.gov.br/hidroweb). Data from the multivariate ENSO index (MEI), considered useful to identify the frequency and intensity of the El Niño Southern Oscillation (ENSO) in both phases (La Niña and El Niño) (Wolter and Timlin, 2011), were extracted from the website https://www.esrl.noaa.gov/psd/enso/mei/.

The index ranges from −3 to 3 and classifies ENSO events as weak (0.5–1), moderate (1–1.5), strong (1.5–2), and very strong (> 2). Negative values correspond to La Niña and positive values correspond to El Niño.

2.4. Numerical nutrient criteria

Nutrient criteria are defined as the maximum acceptable concentrations that could not threaten a particular designated beneficial use of the waterbody (Yang et al., 2019). According to Xie et al. (2021), if the coastal water is minimally impaired by eutrophication, the upper quartile, which is the 75th percentile of the accumulative frequency, of the sampled sites is used to develop nutrient criteria. If the coastal water is severely degraded by eutrophication, the lower quartile, which is the 25th percentile of the accumulative frequency, of the sampled sites is used to develop nutrient criteria.

Based on historical data from the IRE and adjacent waters, the frequency distribution approach was applied to develop nutrient criteria for a specific trophic state according to the method of Liu et al. (2018) and Yang et al. (2019). Based on the Nutrient Criteria Technical Guidance Manual: Estuarine and Coastal Marine Waters (2001), DIN, NO_3^-, NO_2^-, and DIP were selected as the causal variable, while Chl-a, DO, and SD were used as response variables. For classification purposes, inorganic nutrients were categorized as dissolved inorganic nitrogen (DIN = NO_3^- + NO_2^-) and dissolved inorganic phosphorus (DIP = PO_4^{3-}).

2.5. Trophic index (TRIX)

TRIX is a multivariate index that can synthesize environmental information and indicate spatiotemporal trends in the trophic conditions of coastal regions. As proposed by Vollenweider et al. (1998), TRIX uses Chl-a concentrations, absolute deviation of oxygen saturation (aD%O), concentration of dissolved inorganic nitrogen (DIN), and dissolved inorganic phosphorus (DIP) values. All variables were expressed in mg m^{-3} and saturation (DO %). The TRIX used in this work was adapted from Cotovicz Junior et al. (2012) for Brazilian estuaries, with the calculation based on formula (1) below:

$$\mathrm{TRIX} = \frac{\log[\mathrm{Chla.\,aD\%O.\,DIN.\,DIP}] - \mathrm{k}}{\mathrm{m}} \qquad (1)$$

where:

k = 1.5 e m = 1.2

Trophic scales are defined in the work of Giovanardi and Vollenweider (2004), Penna et al. (2004), Nasrollahzadeh et al. (2008), and Cotovicz Junior et al. (2012), with a numerical variation from 0 to 10 (Table 2).

Table. 2 Classification of trophic status for estuarine waters according to the trophic index (TRIX) model.

Trix value	Trophic status	Water quality	Conditions
0-4	Low (oligotrophic)	High	Water poorly productive
4-5	Medium (mesotrophic)	Good	Water moderately productive
5-6	High (mesotrophic to eutrophic)	Medium	Water moderate to highly productive
6-10	The highest (eutrophic)	Poor	Water highly productive

Source: The author (2022).

2.6. Assessment of estuarine trophic status

A detailed description of the ASSETS model is found in Bricker et al. (2003), Xiao et al. (2007), Ferreira et al. (2007), and Cotovicz Junior et al. (2013). The methodology is based on three diagnostic tools: a heuristic pressure index (overall human influence [OHI]), a symptom-based state assessment (overall eutrophic conditions [OEC]), and an indicator of management response (determination of future outlook [DFO]). The OHI, OEC, and DFO results were combined into a single estuary-eutrophication rating matrix. Thus, estuaries can be categorized into five eutrophication classes: bad (worsen), poor, moderate, good, and high (better). The completeness and reliability of the global assessment of eutrophication status were determined using NEEA software (National Estuarine Eutrophication Assessment, NOAA, http://www.eutro.org).

The calculations were based on the estuarine equation, considering the average estuarine and offshore salinities. Chlorophyll-a concentrations (Chl-a; coverage and periodicity) were considered as primary symptom. Nuisance and/or harmful algal blooms (NTB; coverage and periodicity) and dissolved oxygen (DO) are secondary symptoms. Chlorophyll-a status (90th percentile) and DO (10th percentile) were validated using annual mean values according to Ferreira et al. (2007).

The future IRE scenario for the next decade (2021–2031) was developed based on the system's natural susceptibility to eutrophication (e.g., discharge time and N loads) and predictable changes in land use and effluent treatment (Cabral et al., 2020). This simulation considered agriculture and urbanization, corresponding to the 10th and 90th IRE land uses. The projection of future perspectives for the next ten years considered a population growth trend of approximately 82%. This was based on data obtained by the IBGE and the expansion of agriculture, according to the planning of the municipalities. The simulation for urban effluents was based on the current situation of sewage treatment, with 91.7% of the urban population having no collection and treatment, and an effluent with a total biological oxygen demand (BOD) load equivalent to 1300.3 kg day^{-1}.

2.7. Statistical analysis

To select between the parametric and nonparametric tests, the normality and homoscedasticity of the variances were verified using the Shapiro-Wilk and Levene tests, respectively (IBM SPSS Statistics v.24). The Kruskal-Wallis (KW) test was used to verify significant ($p < 0.05$) univariate differences between the groups. When the KW was significant, Dunn's post-hoc test was used to obtain pairwise comparison results. Two-way permutational multivariate analysis of variance (PERMANOVA; Anderson, 2001) was applied to a Euclidean similarity matrix to evaluate the spatiotemporal differences of the environmental variables using a model of two fixed factors: i) zones (tidal freshwater, mixing, seawater) and ii) years (2012, 2013, 2014, 2019, and 2020).

Permutational analysis of multivariate dispersion (PERMDISP; Anderson, 2006) was used to test the dispersion homogeneity of these factors using the distance between centroids and Tukey's HSD pairwise test ($p < 0.05$). For the PERMANOVA and PERMDISP tests, a total of 9999 unrestricted permutations of transformed data to log scale ($x + 1$) were used, applying the ‘betadisper’ function in the ‘Vegan’ R package (Oksanen et al., 2020). Principal coordinate analysis (PCoA) ordination demonstrated the environmental heterogeneity of the IRE.

The evaluation of the effects of multiple stressors on the trophic state of the IRE was made from the construction of generalized additive models (GAM's). Model smoothing was evaluated using the estimated degrees of freedom (edf.) while model fit and significance were

assessed using R^2–adjusted and p-values ($p < 0.05$). GAM's were constructed using the R package 'mgcv' (Wood, 2011). GAM's formula (2) is:

$$\text{TRIX} = s(\text{salinity}) + s(\text{DO}) + s(\text{TW}) + s(\text{pH}) + S(\text{SD}) + s(\text{SPM}) + s(\text{Turbidity}) + s(\text{MEI}) + s(\text{river discharge}) \quad (2)$$

2.8. Random forest

Random forests are a combination of tree predictors such that each tree depends on the values of a random vector sampled independently and with the same distribution for all trees in the forest (Breiman, 2001). The random forest (RF) model was applied to explore the trophic changes in the IRE and rank the variables by influence upon the trophic state. The TRIX index was used as the response variable, and the entire dataset was randomly divided into two subsets: 80% of the data were used as training data to fit the model, and the remaining 20% were used to test the model's prediction.

The determination coefficient (R^2) was used to evaluate the RF model performance, and the importance of each predictor was characterized by an increased mean squared error (MSE). If the MSE is close to 0, it indicates a very close approximation to the actual values. Parameters such as mtry, ntree, and node size were adjusted to improve the accuracy of the RF model prediction. The RF model was implemented in the R package 'randomForest' (Liaw and Wiener, 2002) version 4.1.2.

3. Results

3.1. Long-term rainfall, river discharge and MEI index

The average annual precipitation over the last 49 years was 2192.29 mm $year^{-1}$, with 89.02% of the total accumulation recorded during the rainy season (January to June). This characterizes a symmetric and unimodal seasonal period. The minimum monthly precipitation rate occurs in October (5.91 ± 13.68 mm $month^{-1}$) and the maximum occurs in April (447.23 ± 167.77 mm $month^{-1}$). During the study period, 2012, 2013, and 2014 had an average annual rainfall of 1520.43 ± 745.07 mm $year^{-1}$. During 2019 and 2020, the observed annual average was 2730.70 ± 554.79 mm $year^{-1}$ (Fig. 2a).

The average annual Itapecuru River discharge was 1328.29 ± 812.80 m^3 s^{-1} (mean = 110.69 ± 67.73 m^3 s^{-1}) (Fig. 2b). The monthly average

values ranged from 244.44 ± 78.03 m^3 s^{-1} (mean = 48.88 ± 15.60 m^3 s^{-1}) during the dry season to 944.44 ± 134.95 m^3 s^{-1} (mean = 188.99 ± 134.95 m^3 s^{-1}) during the rainy season. The multivariate ENSO index (MEI) responsible for these fluctuations varied from −0.07 in 2012 to −1.16 in 2020, with lower values observed during the monitoring years (Fig. 2c). El Niño events were recorded in 2014 and 2019, whereas La Niña events were recorded in 2012 and 2013, both in the neutral phase (MEI between −0.5 and 0.5) (Fig. 2c). The period of increased rainfall during 2020 can be considered an atypical year, coinciding with the negative and strongest MEI of the entire sampled period which was characterized as a strong-intensity La Niña event.

Fig. 2. Variations annual of a) rainfall, b) river discharge an c) Multivariate ENSO Index (MEI) and (d-g) climate change correlations between river discharge and rainfall.

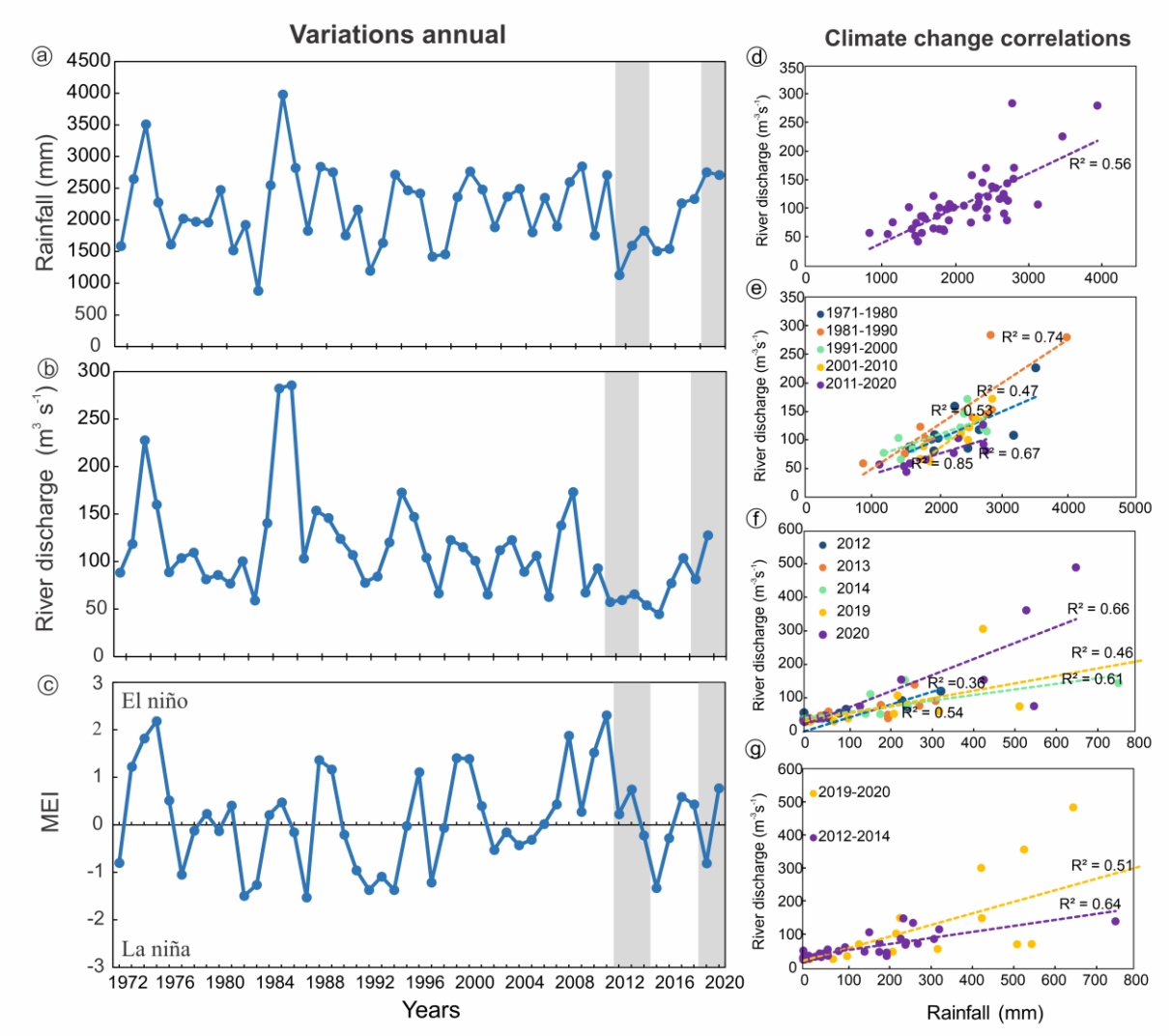

Source: The author (2022).

Based on this historical series, a direct relationship between rainfall and river discharge in the IRE (R = 0.56) (Fig. 2d) was observed, with moderate changes in freshwater discharge between 1972 and 2020. These fluctuations occurred every ten years, and the highest correlation between rainfall and river discharge occurred in the last decade of 2001–2010 (R = 0.85, $p < 0.05$) (Fig. 2e). During the years studied, the relationship between river discharge and rainfall correlation indicated a tendency of increasing flow in response to climate change in the last ten years (R = 0.67, $p < 0.05$). During 2019 and 2020, increased an average discharge values of 81.42 ± 83.83 m^3 s^{-1} and 127.78 ± 147.95 m^3 s^{-1}, respectively were observed (Fig. 2e–g).

3.2. Spatiotemporal heterogeneity of the environmental conditions

The PERMANOVA analysis indicated the main factors responsible for the significant variation ($p < 0.05$) in the multiple stressors observed in the zonal and temporal series. Differences were expressed in the interaction of these factors. The environmental heterogeneity tested by PERMDISP represents the effects of dispersion between zones ($p < 0.05$) and between years ($p < 0.05$). In terms of spatial variation, there was overlap between the mixing and seawater zones. Meanwhile, the temporal variation revealed dispersion between the years of monitoring (2012–2014) and sampled data (2019–2020) (Fig. 3; Table 3).

Table. 3 PERMANOVA results from the environmental data matrix among the factor zones (tidal freshwater, mixing, seawater) and years (2012–2014 and 2019–2020). Significant results (P = * < 0.05; ** < 0.01; *** < 0.001).

PERMANOVA						
	Df	**SumsOfSqs**	**MeanSqs**	**F.Model**	**R2**	**Pr(>F)**
Zones	2	22.739	113.695	137.731	**0.62**	0.001***
Years	1	2.101	21.014	25.456	0.05	0.001***
Zones *vs.* Years	2	1.310	0.6548	7.932	0.03	0.001***
Residual	129	10.649	0.0825	0.28938		
Total	134	36.799	100.000			
PERMDISP						
Zone	**Df**	**SumSq**	**MeanSq**	**F**	**Pr(>F)**	
Groups	2	43.143	215.716	11.459	0.03*	
Residuals	132	248.487	18.825			
Years	**Df**	**SumSq**	**MeanSq**	**F**	**Pr(>F)**	
Groups	4	17.426	43.564	25.757	0.04*	
Residuals	130	219875	16913			

Source: The author (2022).

Fig. 3. Principal coordinate analysis (PCoA) ordination of the environmental variables in the Itapecuru River estuary.

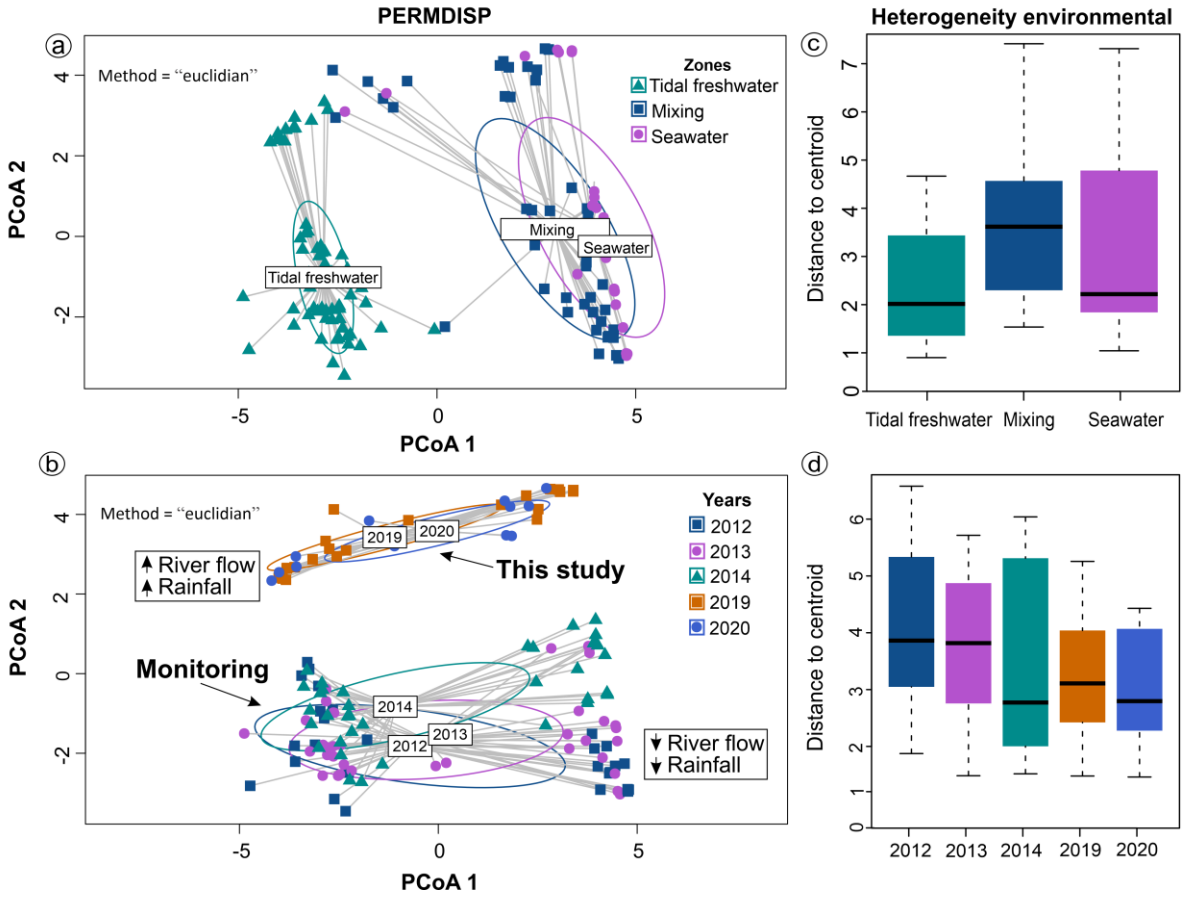

Source: The author (2022).

Tukey's HSD pairwise test indicated differences between estuarine zones as a function of annual variation. In 2012, there was a clear separation between the three estuarine zones, demonstrating a strong spatial heterogeneity in the IRE ($p < 0.001$). However, a high similarity was observed between the mixing and seawater zones. This indicated saline intrusion from 2013 onwards ($p > 0.05$).

3.3. Numerical nutrient criteria

The numerical nutrient criteria (NNC) of the IRE were calculated for different salinity ranges and compared with the CONAMA Resolution 357/05 data. The percentage values for each estuarine zone and the distribution of the environmental variables are presented in Table 4 and Supplementary Fig. 1.

In the tidal freshwater zone, the recommended criteria values for DIN and DIP were 0.12 mg L^{-1} and 0.04 mg L^{-1}, respectively. For DO, Chl-a, and SD, the threshold values were 5.30 mg L^{-1}, 19.20 µg $L^{-1}$and 0.25 cm, respectively. Likewise, the criteria values in the mixing zone were 0.10 mg L^{-1} and 0.04 mg L^{-1}, for DIN and DIP. The DO, Chl-a, and SD threshold values were 3.81 mg L^{-1}, 14.25 µg L^{-1} and 0.47 cm. The seawater zone presented nutrient criteria of 0.11 mg L^{-1} and 0.05 mg L^{-1} for DIN and DIP, respectively. The limiting values for DO, Chl-a, and SD in this area were 3.02 mg L^{-1}, 17 µg L^{-1}, and 0.38 cm, respectively (Supplementary Fig. 1).

Table. 4 Numerical nutrient criteria (NNC)-based frequency distribution results of variables in the transitional waters of the Itapecuru River estuary. The bold values show the recommended criteria values of the variables in each estuarine zone.

Zones	Index	DO	Chl-a	SD	Nitrite	Nitrate	DIN	DIP
Tidal freshwater Salinity - 0.5	5%	3.55	2.45	0.18	0.00	0.02	0.03	0.01
	25%	**5.30**	3.00	**0.25**	**0.01**	**0.10**	**0.12**	**0.04**
	50%	5.90	3.86	0.35	0.02	0.15	0.15	0.08
	75%	6.78	**19.20**	0.46	0.03	0.30	0.32	0.12
CONAMA 357/05	CLASSE I	6 mg L^{-1}	10 µg L^{-1}	-	1.0 mg L^{-1}	10 mg L^{-1}	-	-
Zones	**Index**	**DO**	**Chl-a**	**SD**	**Nitrite**	**Nitrate**	**DIN**	**DIP**
Mixing Salinity - 0.5-25	5%	1.79	3.00	0.1	0.00	0.04	0.05	0.02
	25%	**3.81**	6.00	**0.15**	**0.01**	**0.08**	**0.10**	**0.04**
	50%	4.62	10.69	0.23	0.02	0.18	0.18	0.08
	75%	5.40	**14.25**	0.47	0.10	0.30	0.32	0.57
CONAMA 357/05	CLASSE II	4 mg L^{-1}	-	-	0.20 mg L^{-1}	0.70 mg L^{-1}	-	-
Zones	Index	DO	Chl-a	SD	Nitrite	Nitrate	DIN	DIP
Seawater Salinity >25	5%	2.73	3.00	10.2	0.00	0.08	0.10	0.01
	25%	**3.02**	5.40	**0.20**	**0.01**	**0.12**	**0.11**	**0.05**
	50%	4.75	11.00	0.25	0.02	0.20	0.22	0.07
	75%	5.90	**17.00**	0.38	0.03	0.37	0.38	0.09
CONAMA 357/05	CLASSE II	5 mg L^{-1}	-	-	0.20 mg L^{-1}	0.70 mg L^{-1}	-	-
Total NNC		4.04	16.81	0.20	0.01	0.10	0.11	0.04

Source: The author (2022).

According to the Brazilian water quality standards, the reference value of Chl-a established for the freshwater zone in the study area was greater than allowed by CONAMA 357/05. The DO concentrations in the mixing and seawater zones were below this limit. The criteria values of DIN and DIP do not present reference values for classes I and II.

3.4. Influence of freshwater inputs and salinity gradient on the development of eutrophication condition

To understand the role of freshwater inputs in the development of IRE eutrophication, the mean values of Chl-a, DIN, DO, and DIP were evaluated considering the salinity gradient during two periods: low (37.55–41.87 $m^3 s^{-1}$) and high (146.46–298.07 $m^3 s^{-1}$) river discharge. This assessment indicated that river entry had a greater influence on the Chl-a and DIN concentrations (Fig. 4a–b). The spatial results for Chl-a (Fig. 4a) showed a decline in concentrations (7.33–7.48 μg L^{-1}) in the northern portion of the estuary as river flow increased. The highest values of Chl-a (13.74–33.19 μg L^{-1}) occurred during low river discharge along the estuary. The DO distribution showed a homogeneous pattern during the observational years, independent of river discharge (Fig. 4c). The input of river nutrients was evident in 2012–2014, with higher values of DIN (0.19 mg L^{-1}) and DIP (0.22 mg L^{-1}) observed during high flow. The greatest DIP values in 2019–2020 were restricted to the southern portion of the IRE (Fig. 4d).

Fig. 4. The a) chlorophyll-a (Chl-a), b) dissolved inorganic nitrogen (DIN), c) dissolved oxygen (DO) and d) dissolved inorganic phosphorus (DIP) results for changing river flows in the Itapecuru River estuary.

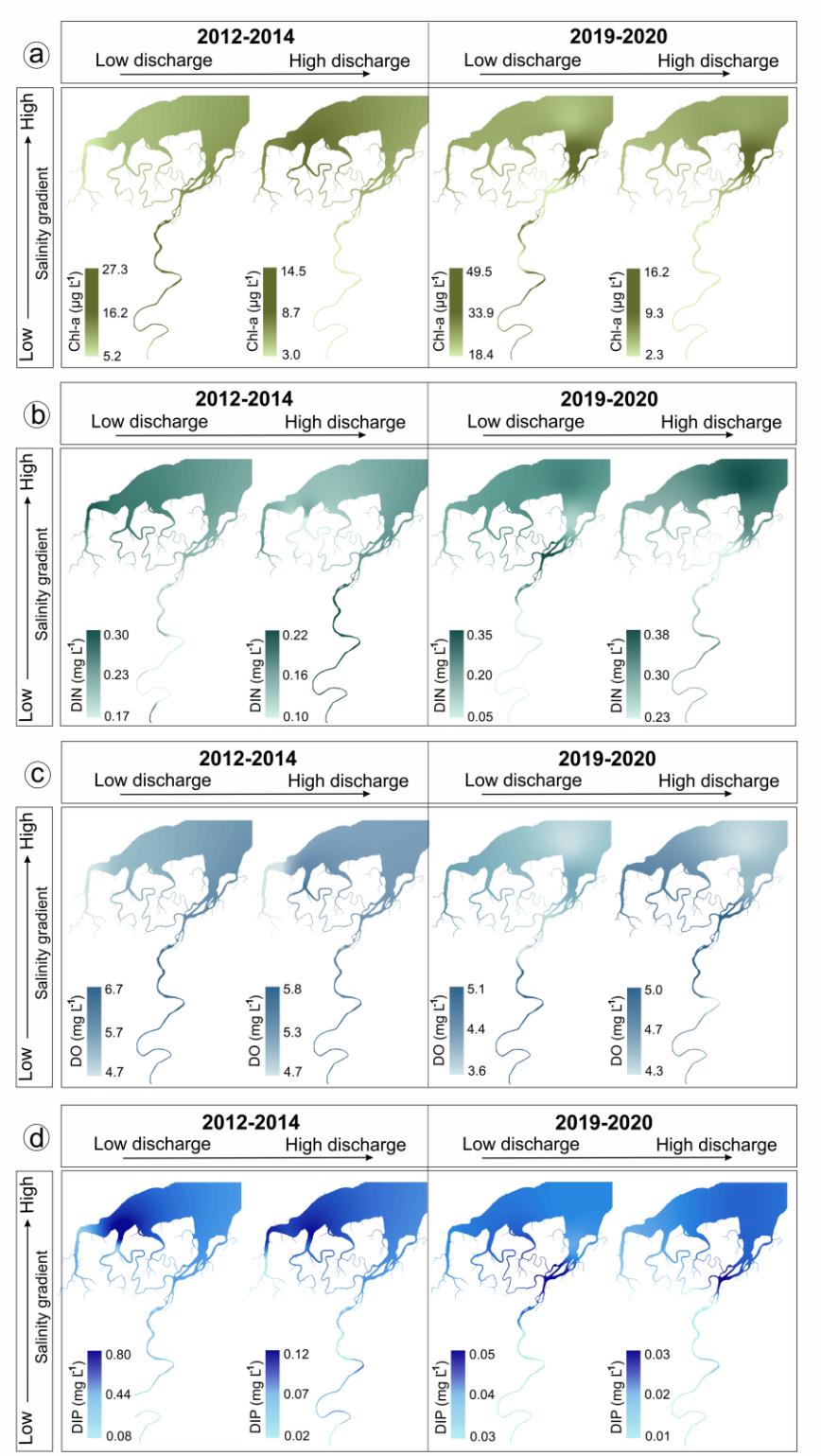

Source: The author (2022).

3.5. Spatiotemporal variability in salinity, turbidity, SPM and environmental predictors of trophic state

When assessing the salinity intrusion in the monitoring years from 2012 to 2014 and the newly sampled data from 2019 to 2020, salinity varied significantly between zones ($p < 0.001$) (Fig. 5a–c). However, a similarity between the mixing and seawater zones was observed during 2012–2014 ($p > 0.05$), indicating a saline intrusion. From 2019 to 2020, as a result of increased rainfall, the IRE presented well-delimited estuarine zones ($p < 0.001$). Only tidal freshwater and mixing zones were identified in response to high river discharge during 2020. Turbidity (Fig. 5d–f) and SPM (Fig. 5g–i) contained significant variations during 2012–2014 ($p < 0.05$), with a significant reduction in SPM during 2014 ($p < 0.0001$). SPM proved to be an important variable for the delimitation of saline intrusion by indicating that mixing and seawater zones were similar ($p > 0.05$).

Fig. 5. Boxplot (minimum, maximum, median, first quartile, third quartile, and outliers) of (a-c) salinity, (d-f) turbidity and (g-i) suspended particulate matter (SPM) results among the zones (tidal freshwater, mixing, seawater) and years (2012–2014 and 2019–2020) in the Itapecuru River estuary.

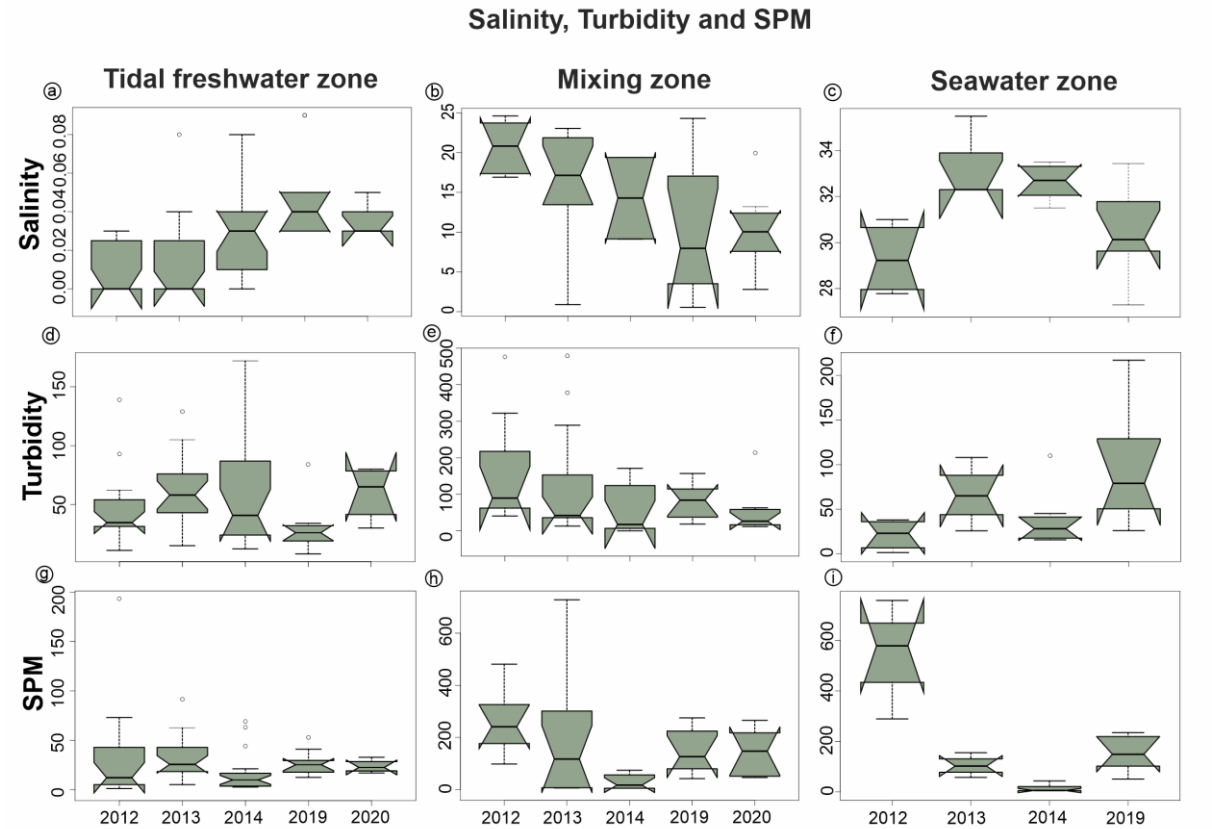

Source: The author (2022).

A multimetric index (TRIX) was calculated to determine the spatiotemporal variation for the trophic state in the IRE. The results indicate that over the five years analyzed, the IRE was in a high trophic state (TRIX = 6.64–7.44; $p > 0.05$). This indicated that the water was eutrophic and poor in quality. The spatial distribution results suggest that the trophic state of the zones varied significantly ($p < 0.0001$) from mesotrophic (TRIX = 5.17) to hypereutrophic (TRIX = 8.66). The tidal freshwater zone showed mesotrophic and hypereutrophic variations (TRIX = 4.00–7.79) (Fig. 6a). The mixing and seawater zones showed variations between eutrophic and hypereutrophic conditions (TRIX = 7.03–10.93). Eutrophication principally increased in the mixing zone (Fig. 6, b–c).

Fig. 6. Boxplot (minimum, maximum, median, first quartile, third quartile, and outliers) of (a-c) TRIX and (d-i) Generalized Additive Models (GAM's) describing the main factors that influenced the trophic state of the in Itapecuru River estuary. Solid lines represent smoothed response relationships from GAM's, and shaded areas are 95% confidence intervals. Points represent residuals. Significant results (*$p < 0.05$; **$p < 0.01$; *** $p < 0.001$).

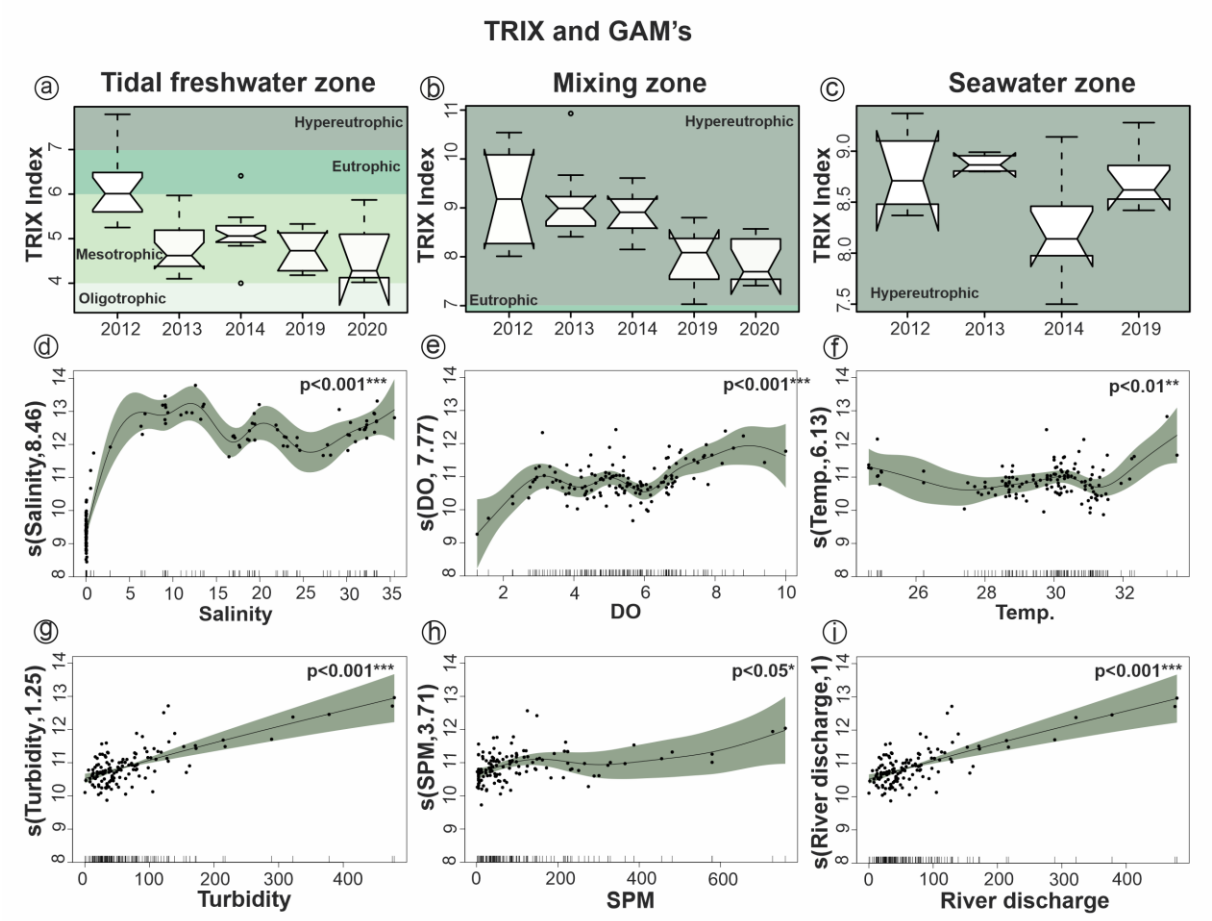

Source: The author (2022).

Regarding the trophic state response relationship (TRIX) as a function of spatiotemporal heterogeneity, the GAM model showed high predictability (95.3%; $R_{adj} = 0.93$) and significant partial correlations ($p < 0.001$). The GAM results showed a nonlinear TRIX response to salinity, DO, and water temperature. The model indicated that TRIX has a rapid response to increasing salinity (10−20) and DO (4–6 mg L^{-1}), while a water temperature between 30 and 32 °C initiates the inverse responses (Fig. 6, d–f). The results also suggest that turbidity, SPM, and river discharge are important causal factors for the IRE trophic state, but have limited explanatory usefulness as they have a linear relationship with the TRIX (Fig. 6, g–j). These relationships were direct with turbidity (>100 NTU) and SPM (>200 mg L^{-1}), and indirect with river discharge (>50 m^3 s^{-1}). These conditions characterize the mixing zone as being the most vulnerable to eutrophication in the IRE. Thus, these conditions modified the IRE eutrophication state.

3.6. Random forest model

To apply the local random forest (RF) model, a decision tree model was constructed that discriminates between two regions with salinities <0.31 and > 0.31. These regions were classified as mesotrophic and hypereutrophic by the TRIX (Fig. 7a). The RF model was trained on IRE data – containing 135 samples of 13 predictors (salinity, DO, nitrite, nitrate, DIP, WT, pH, SD, SPM, turbidity, MEI, river discharge, and Chl-a) and one target parameter (TRIX), as shown in Fig. 7b. The trained RF model had excellent performance with a R^2 value of 0.96, with a deviation of 94.5% (Fig. 7b).

The optimization of the hyperparameters was programmed with ten variables (mtry) in each node, using 1000 trees (ntree) as fixed. The model accuracy was tested with the lowest MSE of 0.38 and MAE of 0.29. The RF results (Fig. 7c) showed that salinity was the principal variable that significantly influenced the trophic state of the estuary, with a mean importance of 121.71, followed by DIP (38.42) and Chl-a (21.94), using the IncMSE metric. When quantifying the grade importance using IncNodePurity, salinity (279.44), pH (27.46), and DIP (16.77) were identified as the most influential variables. The quality of this result was confirmed by the OOB procedure.

Fig. 7. a) Decision tree model, b) prediction of TRIX index by the RF model and predicted and observed TRIX index are compared; c) predictors importance ranking for RF model. The importance of each predictor is measured by the increment in Mean Squared Error (MSE) (left) and Node Purity (right) of each predictor.

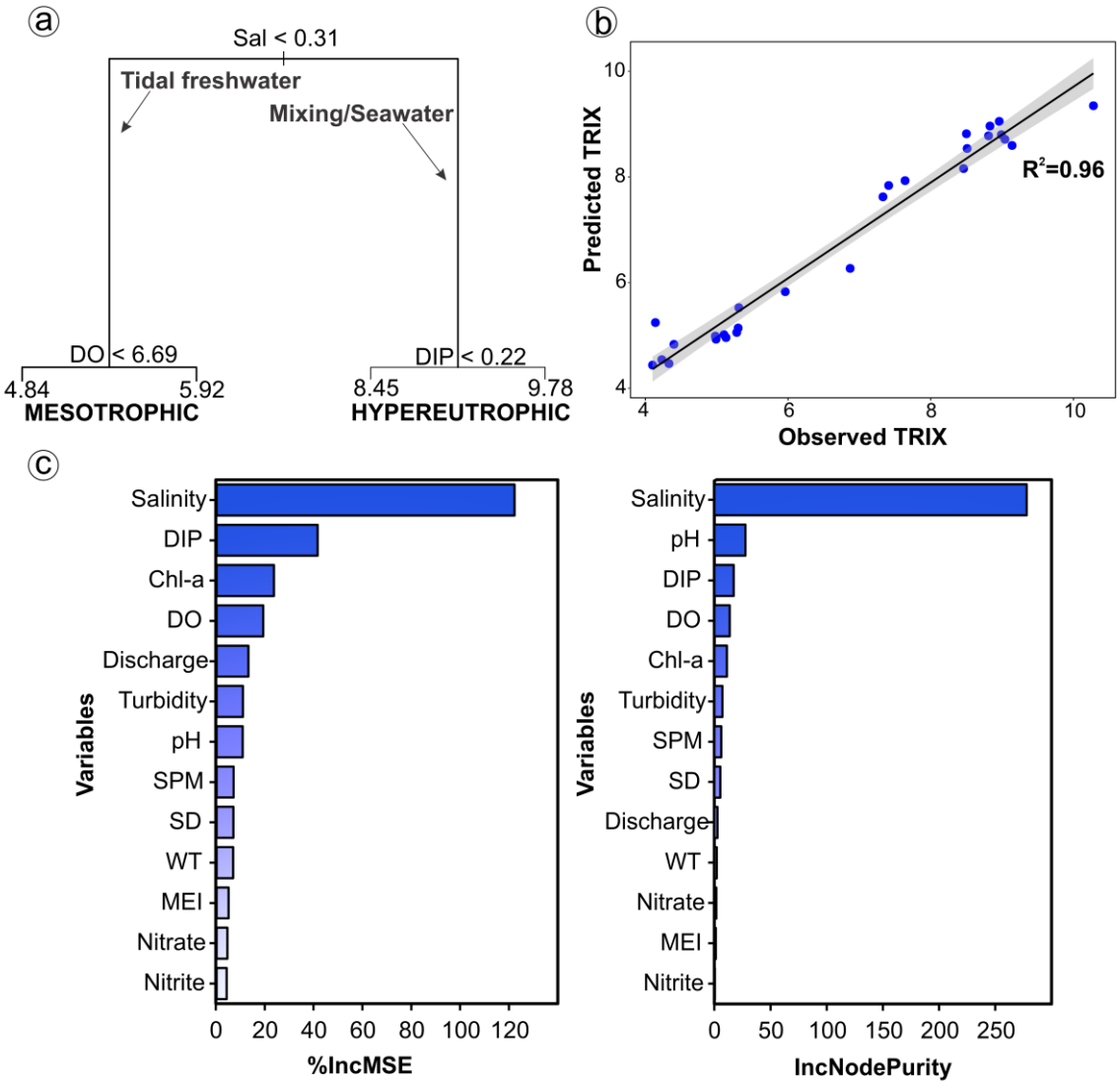

Source: The author (2022).

3.7. Assessment of estuarine trophic status of the Itapecuru River

3.7.1. Pressure - Overall Human Influence (OHI)

Based on the tidal range conditions (5.8 m) with the relationship between the inflow of freshwater (FI - 78.47 $m^3 s^{-1}$) and the volume of the estuary (EV - 36 × 10^6 m^3), the results show a low dilution of nutrients and a moderate flushing potential of urban effluent (2150.94 ton $year^{-1}$) into the system. The reference salinity in the estuary was 14.61 and that of the bay

was 31.5. The mean DIN concentrations of 3.90 μmol L^{-1} (estuary) and 4.06 μmol L^{-1} (bay), respectively were observed.

When compared, these concentrations infer contributions from both autochthonous and allochthonous sources into the IRE (Table 1). When considering only the conservative processes, the maximum concentration of DIN tends to occur during the dry season, with values of 20.48 μmol L^{-1} in tidal freshwater, 10.24 μmol L^{-1} in mixing and 8.80 μmol L^{-1} in seawater zones. The nutrient component of the OHI factor was 1.0, classifying the IRE as high susceptibility and subject to high estuarine pressure for the development of eutrophic symptoms.

3.7.2. State – Overall Eutrophic Condition (OEC)

According to the OEC, IRE showed a moderate-to-high state of eutrophication. This was mainly due to more critical primary indications, determined by elevated Chla concentrations at the 90th percentile (Chla≥40 μg L^{-1}). This highlighted seawater zones with high spatial coverage (>50%) and persistence (seasonal), with increased concentrations during the dry season. Secondary OEC indications were less critical, with greater expression in the mixing zone and a persistent frequency of occurrence.

The 10th percentile of DO values indicated biologically stressful conditions (DO<5 mg L^{-1}), with a decrease in DO in the mixing and seawater zone (DO<3 mg L^{-1}) (Supplementary Fig. 2). The occurrence of Harmful Algal Bloom (HABs) was restricted to tidal freshwater zone during 2012 and 2013 (cyanobacteria = 1.48–6.31 × 10^6 cells L^{-1}), with episodic frequency and seasonal duration being more frequent in the rainy season. The overall eutrophic conditions of IRE are shown in Table 5.

Table. 5 Overall eutrophic conditions (OEC) by the combination of primary and secondary symptoms for the Itapecuru River estuary. where: n.a = Not applicable.

Overall Eutrophic Condition - OEC						
			Tidal Freshwater	**Mixing**	**Seawater**	**Final**
Primary symptoms	Chlorophyll-a	Spatial coverage	Moderate	Moderate	High	
		Frequency	Periodic	Persistent	Persistent	
		Expression	High	High	High	
		Value	1	1	1	1
Secondary symptoms	Nuisance and Dissolved toxic blooms oxygen	Spatial coverage	High	High	High	
		Frequency	Periodic	Persistent	Periodic	
		Expression	Moderate	High	Moderate	
		Value	0.50	1	0.50	0.60
		Problem status	Observed	No problem	No problem	
		Duration	Seasonal	No problem	No problem	
		Frequency	Episodic	No problem	No problem	
		Expression	Moderate	Low	Low	
		Value	0.50	0	0	0.50

Density of Cyanobacteria					
	Period	**Season**	**Tidal freshwater**	**Mixing**	**Seawater**
(CyanoHABs) $\times 10^6$ cells L^{-1}	2012-2014	Rainy	**0.69±1.24**	0.09±0.19	n.a
		Dry	0.04±0.12	n.a	n.a
		Min.– Max.	**0.003–6.31**	0.003–0.675	n.a
	Period	**Season**	**Tidal freshwater**	**Mixing**	**Seawater**
	2019-2020	Rainy	0.04±0.06	0.01±0.02	0.01±0.01
		Dry	0.08±0.07	0.01±0.02	n.a
		Min.– Max.	0.00–0.160	0.00–0.046	0.022

Source: The author (2022).

The combination of DO and Chl-a allowed for a general assessment of the eutrophication status of the IRE (Fig. 8). The DO concentrations divide the estuary into two distinct regions. Of these two regions the tidal freshwater zone was considered the region with the best DO conditions (mean value; 4.7 < DO<6.5 mg L^{-1}) (Fig. 8a). The distribution of Chl-a along the river-estuary continuum is quite complex, segmenting it into three regions, alternating between low and very productive locations (mean value; 6.3 < Chl-a < 35.8 μg L^{-1}) (Fig. 7b).

The continuous concentration data, converted into a binary matrix, indicated that the seawater zone was a critical area. Low concentrations of DO (all values are <5 mg L^{-1}) and elevated concentrations of Chl-a (values>40 μg L^{-1}) presented a eutrophication problem

involving both parameters (Fig. 8c). Regarding adjacent tributaries, there was an eutrophication problem involving only one parameter (DO<5 mg L^{-1}).

Fig. 8. Division of the Itapecuru River estuary based on chlorophyll-a (Chl-a) and dissolved oxygen (DO) thresholds. Distribution of a) chlorophyll-a concentration; b) dissolved oxygen concentration and c) map algebra analysis results, where: Problem for both parameters (DO<5 mg L^{-1} and Chl-a > 40 µg L^{-1}), no problem for one parameter (DO<5 mg L^{-1} or Chl-a > 40 µg L^{-1}) and no problem for both parameters (DO >5 mg L^{-1} and Chl-a < 40 µg L^{-1}).

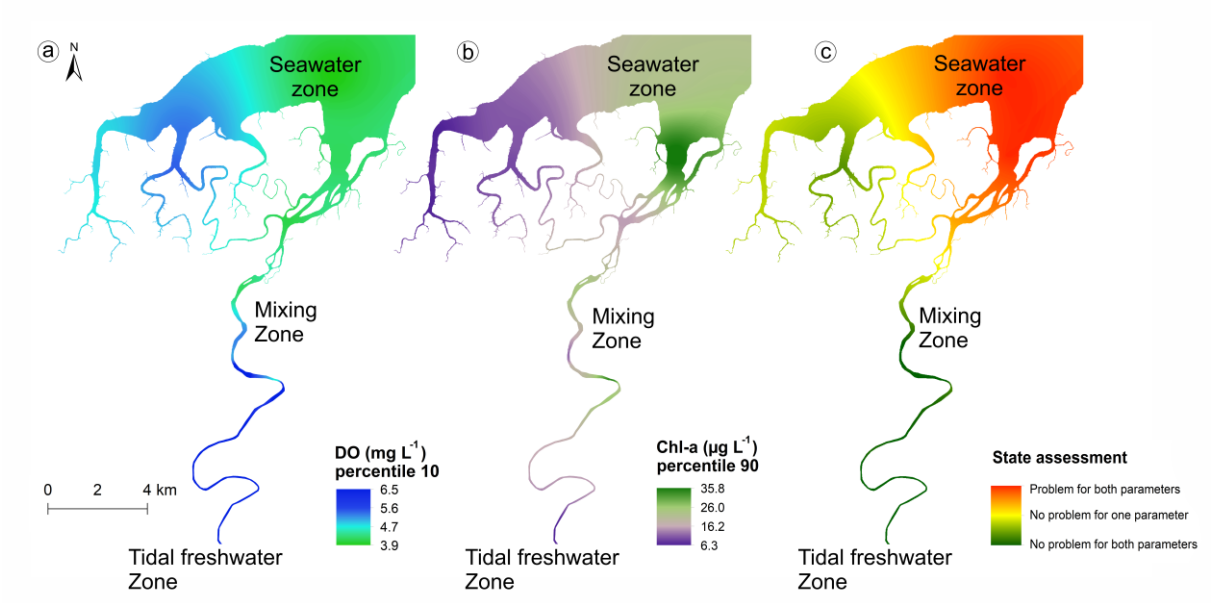

Source: The author (2022).

3.7.3. Response – Definition of Future Outlook (DFO)

According to the ASSETS model, the prospects for IRE showed a deterioration of the eutrophication state, modifying its classification to a more eutrophicated state. This condition reflects the future nutrient pressure increase in the estuary, indicating a high future susceptibility. The final results of the ASSETS are listed in Table 6.

Table. 6 Determination of future outlook by the combination of the susceptibility and future nutrient trend pressure or the Itapecuru River estuary. where high [red], moderate [yellow], moderate-high [orange], moderate-low [green] and low [blue].

Assessment of Estuarine Trophic Status - ASSETS					
Index and Grade	**Method**	**Parameter**	**Rating**	**Expression**	**Score**
Overall Human Influence (OHI)	Susceptibility	Dilution Potential Flushing Potential	Low Moderate	High	
ASSETS:1 High	Nutrient Inputs		High		
Overall Eutrophic Condition (OEC)	Primary Symptoms	Chlorophyll-a		High	
	Secondary Symptoms	Dissolved oxygen		Moderate	
		Nuisance and Toxic Algae		Moderate	
Definition of Future Outlook (DFO)	Future Nutrient Pressures		Increase		
ASSETS:1 Worsen-high					

Source: The author (2022).

By simulating the definition of the future outlook (DFO), including effluent treatment and changes in the use of the Itapecuru River watershed (e.g., agriculture), future nutrient pressures remained constant. A general state of eutrophication in the IRE with decreasing future nutrient pressure is unlikely, as decreasing future nutrients is directly associated with population reduction. Thus, management plans with mitigation measures and monitoring of its waters, including demographic trends and treatment plants, must be applied with the purpose of not allowing these IRE trophic conditions to evolve in the next ten years. Otherwise, nutrient-related indications are likely to worsen substantially in IRE.

4. Discussion

The pressure-state-response (PSR) framework, adopted by the Organization for Economic Co-operation and Development (OECD, 2003), contributed to the identification of pressures and changes in the IRE trophic state. This approach in estuarine systems is very efficient and can be extended to macrotidal estuaries with similar characteristics, as it facilitates the prioritization of the places where management and mitigation measures can be applied to reduce environmental risks (Bricker et al., 2003; Ferreira et al., 2007; Whitall et al., 2007; Lonsdale et al., 2015). Using this approach, we identified that the transitional waters of the IRE are under strong anthropogenic pressure, whose rapid economic development and population growth constitute one of the main threats to its water quality.

To better understand these conditions and their impacts, we discuss the influence of climate change on trophic conditions and the importance of multiple stressors in determining the general state of eutrophication. In this process, the relationships between natural and

anthropogenic drivers are considered. The ASSETS model addressed the interactions and predictions of these ecohydrological effects and parameterized a future scenario for a macrotidal estuary based on PSR indicators.

4.1. Climate change and multiple stressors on the trophic state of transitional waters

According to the historical series analyzed (1972–2020), the climatic regimes showed decadal variation in the ENSO-discharge relationship, increasing from 2010. However, the flow of the Itapecuru River decreased considerably between 2012 and 2016 (Fig. 2). This ENSO-discharge relationship is necessary for understanding changes in the trophic state of an estuary because climate influence is more pronounced in ENSO–hydrology relationships during the years of declining ENSO events (Räsänen and Kummu, 2013).

2019–2020 were considered atypical because of the La Niña event that caused an abnormal increase in rainfall levels, mainly during 2020 (MEI index; NOAA, https://psl.noaa.gov/data/climateindices/). PERMANOVA and PERMDISP indicated spatial changes in water quality during the study years. These spatial changes indicated a complex eutrophication process in the estuary caused by anthropogenic and hydroclimatic factors. The similarity between the mixing and seawater zones from 2013 may indicate an advance in saline intrusion and a decrease in spatial heterogeneity within the IRE. Cloern (2010) and Chaalali et al. (2013) stated that large-scale climate anomalies are positively and highly correlated with long-term spatial changes. For them, the cascading global climate system acts on the local scale of bays and estuaries and can restructure their biological communities.

The river flow component is one of the most relevant dynamic factors that determine the intrusion/export of saltwater in estuaries (Cavalcante et al., 2020). In addition, seasonal changes in water quality are common in tropical estuaries under the influence of unimodal regimes (Oliveira et al., 2022), similar to IRE. The intertropical convergence zone (ITCZ) influences the unimodal rainfall pattern (Santos Dos et al., 2020; Sá et al., 2022), acting directly on the trophic state of the estuary. During the dry season, the ITCZ moves to the Northern Hemisphere (>2°N latitude), resulting in lower rainfall (usually below 100 mm per month) (Pereira et al., 2013; Pereira et al., 2018; Lefèvre et al., 2017; Asp et al., 2018).

Therefore, understanding this climate pattern would explain the increased observed freshwater flow from 2019 to 2020, which was greater than that in 2012–2014 by a factor of

two. This significant increase in river flow in recent years has significantly influenced the concentrations of Chl-a and nutrients. The results showed that during periods of lower flow and predominance of El Niño (2012–2014) conditions, marine water entered the IRE, resulting in the entire estuary being rich in nitrogen and phosphorus. In recent years, the northern coast of Brazil has been increasingly impacted by atypical climatic conditions, causing fluctuations in environmental variables, including local hydrological characteristics and the advancement of saline intrusion (Pereira et al., 2013; Queiroz et al., 2022, Oliveira et al., 2022).

Conversely, during periods of higher river discharge and predominance of La Niña (2019–2020) conditions, saltwater was transported out of the estuary, where the chlorophyll-a and DIP concentrations were greater in the seawater zone, accumulating this productivity in the estuary region. Thus, the seawater zone was considered the region most affected by river discharge during the research period, corroborating the findings of Monteiro et al. (2016), Azhikodan and Yokoyama (2016), and Andricevic et al. (2021).

The most severe drought event during recent decades within the eastern Amazon and northeast Brazil occurred during 2012–2013. This was caused by an increase in the temperature of the surface waters of the tropical Atlantic, leading to decreased rainfall rates (Pereira et al., 2016; Brito et al., 2017; Marengo et al., 2018). This event generated numerous impacts in many areas of the northeastern semiarid region and Amazonian estuaries. This influences environmental variables, such as dissolved nutrient concentrations and phytoplankton biomass (Pereira et al., 2016; Queiroz et al., 2022). This influence would explain the behavior observed in IRE.

In regard to Brazilian water quality standards, the reference value of chlorophyll-a (>10 μg L^{-1}) established for the tidal freshwater zone in the IRE is greater than that allowed by CONAMA 357/05. Compared to other studies in tropical estuaries (Zhou et al., 2016; Carrasco Navas-Parejo et al., 2020; Karthik et al., 2020; Niveditha et al., 2022; Nguyen et al., 2022), the chlorophyll-a concentrations (7.33–33.19 μg L^{-1}) in the IRE were within the range. DO concentrations in mixing and seawater zones are below the standard, and the nutrient criteria for DIN and DIP do not have reference standards for resolution. This nutrient criteria approach can become relevant and consistent for future monitoring of IRE waters and reducing restrictions regarding the application of macrotidal estuary ecosystem principles. This approach is relevant and consistent with future IRE water monitoring.

The numerical nutrient criteria determine nutrient thresholds for coastal environments and provide a quantitative method for determining the baseline conditions and corresponding trophic status (Xie et al., 2021). This application is not only a measure to effectively prevent water eutrophication but also a scientific basis for the comprehensive monitoring, evaluation, and management of estuarine nutrients (Ke et al., 2022; Mazor et al., 2022). In addition, changes in the hydrological cycles affected the distribution of nutrient resources; these forces are the fundamental demand for phytoplankton growth (Tao et al., 2021). In this way, we believe that the numerical nutrient criteria for the estuary and adjacent coastal waters should be developed.

By considering nutrient variations and local hydrological conditions, we determined the recommended regional numerical nutrient criteria for DIN (0.11 mg L^{-1}) and DIP (0.04 mg L^{-1}) that contribute to coastal water quality management in tidal-dominated tropical regions similar to the IRE. According to Watanabe et al. (2014) and Acquavita et al. (2015), spatiotemporal changes in nutrient concentrations indicate that seasonal patterns are affected by both freshwater influx and seawater intrusion, corroborating the findings of Sulochanan et al. (2022). Sousa-Felix et al. (2017) and Paula-Filho et al. (2020) found it necessary to adapt the CONAMA criteria to the specific conditions of Amazonian transitional waters (high concentrations of dissolved nutrients and high turbidity) to avoid inadequate classification.

Compared to the monitoring years (2012–2014) and the newly sampled data (2019–2020), the concentration of DIN increased by 13.33%, whereas the concentration of DIP decreased by 82.05%. This input of DIN by the increased river flow is a consequence of anthropogenic emissions from wastewater discharge, application of fertilizers, soil loss in watersheds, and external sources of DIN in watersheds (Béjaoui et al., 2016; Pereira et al., 2021; Xie et al., 2021). Thus, nitrogen is the main input in the IRE, mainly in the form of NO_3^-, as reported by Acquavita et al. (2015) in a lagoon in the Mediterranean.

The effects of multiple stressors on coastal ecosystems are poorly understood (Deschutter et al., 2017), especially in the assessment of trophic status. Modeling approaches are limited to subsystems (reservoirs and lakes) (Hartnett et al., 2012, Hutchins and Hitt, 2019; Rankinen et al., 2019, Andersen et al., 2020). The current global trend is the implementation of legislative measures that assess the ecological integrity of marine systems (estuarine, coastal, and offshore) from this perspective (Bricker et al., 2003; Ferreira et al., 2006; Borja et al., 2008).

The TRIX multimetric index classifies the IRE as having a high trophic status, high eutrophication, and poor water quality. TRIX presented a classification similar to that observed in other assessments of estuaries on the north Brazilian coast. These estuaries also suffer continuous human pressure, such as the inflow of untreated domestic effluents (Cutrim et al., 2019; Sá et al., 2021; Cavalcanti et al., 2022). According to the GAM, brackish waters (salinity>10) with high temperatures (> 30 °C) and more oxygenated waters (>4 mg L^{-1}) have more intense trophic conditions, especially in the mixing zone. This region is considered more vulnerable to eutrophication in the IRE. The results also suggest that the reduction of the photic zone (increased turbidity and SPM) and lower river discharge result in IRE being in a state of hypereutrophy.

Consequently, the photic characteristics of IRE with high turbidity and low light penetration must be considered in the assessment of the typical trophic state conditions of tropical and macrotidal estuaries (Monteiro et al., 2016; Pereira et al., 2021). These conditions result from the broad drainage network and the high hydrodynamic energy of these environments. These factors act as synergistic factors for the suspension of particulate matter, contributing to the increase in turbidity levels (>100 NTU) and enrichment of the Amazonian coastal systems (de Sousa et al., 2017; Andrades et al., 2021).

4.2. Random forest model

Due to the complexity of identifying the main processes that govern eutrophication in macrotidal estuaries, the trophic indices used directly without testing their applicability to a macrotidal region can be a problem despite most methods of these traditional indexes assigning weights of metrics subjectively. Cordier et al. (2019) suggested that the weighting coefficient calculation of metrics based on objective methods is more critical in the unknown ecosystem. Random forest analysis uses multiple independent variables that have complex interactions or covariates in various research fields by robustly ranking variable importance (Lee et al., 2015).

This study used an RF model to define the appropriate predictor variables for determining the trophic state in a macrotidal estuary. Using the RF model, it was possible to evaluate the model performance for the transitional IRE waters using TRIX. In the RF model, salinity was the principal stressor that intensified eutrophication in the system. DIP and Chl-a were also included as the main predictors in the robust estimate of the trophic state, confirming good correlations with TRIX. Hadid et al. (2021) reported that Chl-a is one of the most relevant

markers of water body presence and the degree of eutrophication. Hadid et al. (2021) reported that Chl-a is one of the most relevant markers of water body presence and the degree of eutrophication. Recent studies on eutrophication indicate that inorganic nutrients (e.g., DIP) available in the water column support primary production and consequently stimulate eutrophication of estuarine systems (Li et al., 2017; Yang et al., 2018; Tao et al., 2021; Hadid et al., 2021; Ke et al., 2022).

Taillardat et al. (2020) and Tao et al. (2021) suggested that changes in nutrient concentrations are strongly associated with tide-river mixing processes and external P sources such as P cycling and regeneration, biodegradation, emissions of coastal cities, and adsorption of sediment. Thus, changes in nutrient concentrations were considerably modulated by biological uptake processes associated with physical mixing.

However, in mangrove-dominated macrotidal estuaries, such as the IRE, this relationship between salinity and nutrient concentrations should be taken into consideration. Tides are the main hydrological mechanism that leads to the lateral exchange of nutrients between mangroves and estuarine waters. Nutrient fluxes are positively correlated with water fluxes across the mangrove-estuary interface, suggesting that nutrient export was mainly driven by tidal exchange (Wang et al., 2021).

The excellent predictive power of the RF model supports our initial hypothesis that anthropogenic pressure and multiple stressors increase the general eutrophication state of the IRE. Consequently, we suggest the development of a simple index based on widely and routinely measured parameters, including salinity, chlorophyll-a, and DIP concentrations, or the inclusion of salinity in the TRIX formula. This index would be principally for tidal-dominated tropical estuaries.

Thus, we observed that the trophic state of the IRE was influenced by multiple stressors, which were affected by weather patterns (river runoff or ENSO events), mainly salinity. Its effects on seawater intrusion during periods of drought have contributed to the reduction in estuary water quality. In addition to being related to local anthropogenic effects (agricultural, hydrological, urban wastewater, port facilities), they are also influenced by hydrological modifications in response to climate change (Acquavita et al., 2015; Brugnoli et al., 2019). Therefore, climate change is a direct and indirect potentiator of multiple environmental

stressors and consequently of the trophic state (Rankinen et al., 2019; Espinosa-Díaz et al., 2021; Zhang et al., 2021).

4.3. Approach to PSR (Pressure–State–Response) indicators in a Brazilian macrotidal estuary

The PSR approach in transitional waters, such as the IRE, is regarded as a detailed survey for which different response scenarios potentially produce changes in pressure and state (Ferreira et al., 2007; Whitall et al., 2007; Hartnett et al., 2012; Ferreira et al., 2011). The methodology of the PSR model considers environmental pressures (driving forces–pressures), environmental conditions (state–impact), and societal responses (response), which are essential when prioritizing environmental planning actions and strategies (Gómez et al., 2019).

According to the assessment of estuarine trophic status (ASSETS) model, the IRE rating according to the overall human influence (OHI–pressure) factor was high, with a high input nutrient index, low dilution of nutrients, and moderate flushing potential of urban effluent. Thus, estuaries are highly susceptible and subject to high estuarine pressure for the development of eutrophic indications.

These conditions are secondary indications of toxic algal blooms, albeit episodic, in the tidal freshwater zone. This region deserves attention, as the risk of eutrophication is linked to the ability of the estuarine environment to confine the growing algae in the illuminated surface layer (Ferreira et al., 2007; Ferreira et al., 2011). Therefore, the ASSETS model indicates that eutrophication in the IRE is a seasonal process related to variations in climate and river flow.

It is important to mention that in tropical estuaries, seasonal changes in eutrophication are related to the natural susceptibility of the system. This includes the residence time of water and the entry of freshwater controlled by the unimodal precipitation pattern and associated nutrients. Multiple land use practices, especially in agriculture, are also considered (Cotovicz Junior et al., 2013; Taillardat et al., 2020).

Nevertheless, within the OEC assessment, the Itapecuru River basin provides nutrient flows from diffuse sources, including urban, agricultural, or mangrove sources. The low DO levels (DO<3 mg L^{-1}) and high chlorophyll-a concentrations in the seawater zone indicate that the lower portion of the estuary was the most critical. Therefore, this region functions as a sink for nutrients and the development of eutrophication. DO values <4 mg L^{-1} (10th percentile) were rarely recorded in the tidal freshwater zone, but high concentrations (90th percentile) of

chlorophyll-a were more frequent. This region deserves more attention regarding the eutrophication process because it includes the water catchment region, which is responsible for supplying the city of São Luís with over 1.109 million inhabitants.

The IRE estuarine zone showed a clear pattern for which the worst scenarios were found during the lower river flow and rainfall periods due to the higher intrusion of seawater, longer residence time, and concentration of nutrients. During periods of high flow, exceeding 200–300 m^3 s^{-1}, there was an abrupt reduction in residence time and chlorophyll-a, which is common in other Brazilian systems (Pamplona et al., 2013; Cavalcanti et al., 2021; Cavalcanti et al., 2022; Cabral et al., 2020; Sá et al., 2022) and in macrotidal estuaries worldwide (Glé et al., 2008; García et al., 2010; Garnier et al., 2010; Garnier et al., 2010; Bharathi and Sarma, 2019; Onabule et al., 2020; Taillardat et al., 2020).

According to the ASSETS final ranking (worsening–high) for the next decade (2021–2031), the planned strategies include the reduction of anthropogenic contributions and the improvement of trophic conditions in the IRE. Consequently, the ASSETS assessment method should be applied periodically to monitor trends in nutrient-related water quality over time to test management-related hypotheses and provide a basis for more successful management (Whitall et al., 2007). Some information gaps remain, notably with estimates of changes in submerged aquatic vegetation cover and macroalgae distribution. These data were not available, and their absence represented a limitation in this study. In addition, the quantification of harmful or potentially harmful algae (HABs = cyanobacteria) must be continuous. This is a consequence of the resulting data being fundamental for improving the applicability of the ASSETS model in the future, summarized in a conceptual model about the general eutrophication status of the Itapecuru River estuary shown in Fig. 9.

4.4. Future perspectives and management implications

Brazil has a significant population and hydrological diversity, with a deficient sewage collection or treatment system. Only 50.8% of homes received sewage treatment (www.tratabrasil.org.br›sanitation›no-brasil). In Maranhão, only 7.1% of the urban population (4283.4 per thousand inhabitants) has a collective sewage treatment system. The remaining homes discharge untreated sewage into estuaries, generating a load of 231.3 tBOD day^{-1}. Therefore, the Brazilian surface waters of rivers and coastal waters need attention to improve their trophic and ecological status.

Fig. 9. Conceptual model of multiple stressors that influence the general eutrophication status of the Itapecuru River estuary, using the Pressure, State, and Response (PSR) framework. The general eutrophication status is indicated in bold text.

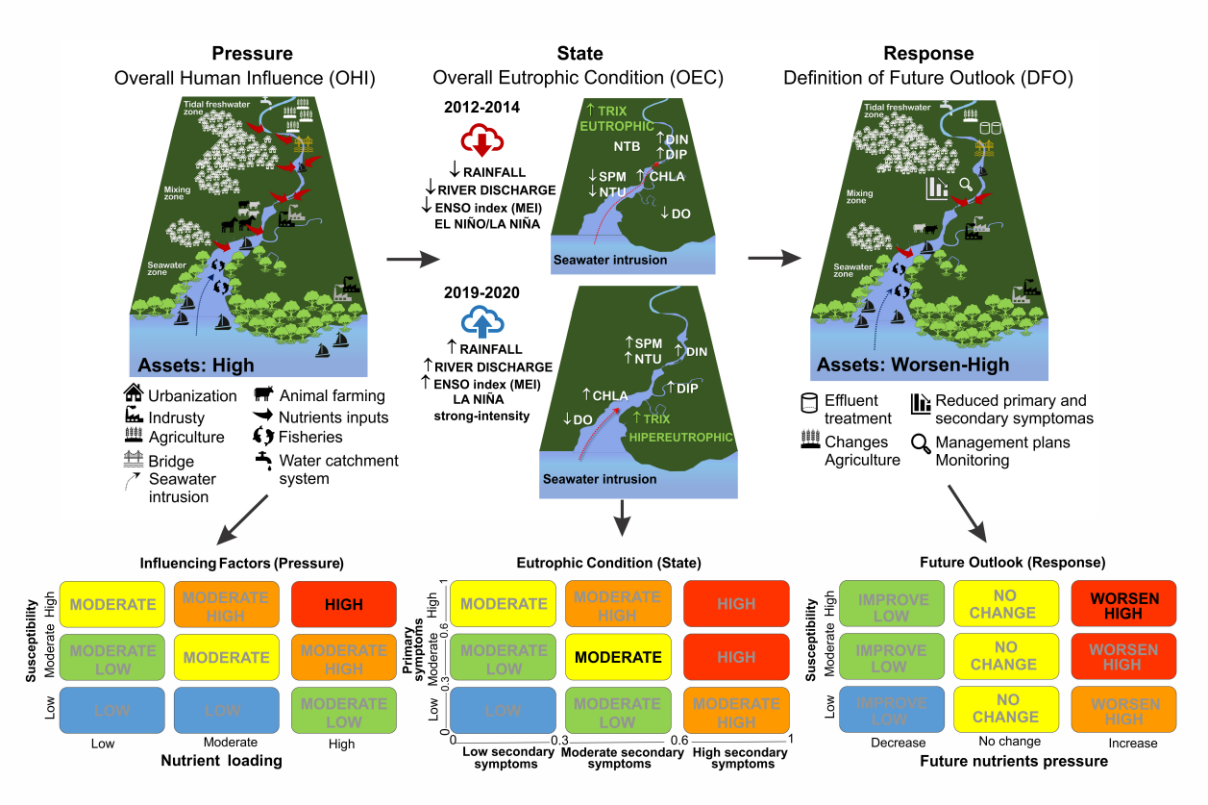

Source: The author (2022).

In the Itapecuru River estuarine region, the population has grown significantly and has a low sewage distribution efficiency. The possibility of direct sewage entering the sea is significant, requiring conventional sewage treatment to remove 60–80% of the BOD. Along with the estuarine sector, agriculture has a low influence on the water quality of the estuary, mainly because it is small-scale (subsistence agriculture). The principal modifying agent in the functioning of the IRE's natural ecosystems is the increase in occupied areas within the city of Rosário (Soares et al., 2017).

Finally, the predictive nature of models can determine potential impacts and assist in management decisions on estuarine water quality. This includes choices regarding the trophic state, which is a great advantage of the integrated approach (Hartnett et al., 2012). In addition, from the management units evaluated here and the zonal boundaries, it becomes possible to develop a sampling project that includes natural characteristics (morphology and salinity) and

human dimensions. In addition, the locations and sampling frequencies, as proposed by Ferreira et al. (2007) and Ferreira et al. (2011), may be implemented in such projects.

Consequently, this research can be used as a new perspective for the water quality management of transitional waters under the effect of macrotides. From this perspective, effective environmental planning strategies must be implemented in the Itapecuru River Basin to maintain its ecosystem services, principally water supply. Large-scale environmental monitoring programs and data surveys should be implemented, as they provide a robust foundation for environmental information that makes it possible to build an overview of transitional waters. Our findings show that this assessment of multiple stressors in the general state of eutrophication helps managers make broad decisions regarding eutrophication-susceptible estuaries in the saline intrusion domain.

5. Conclusions

This research constitutes a preliminary contribution to nutrient monitoring, evaluation, and management of the estuary of the Itapecuru River and its adjacent waters. Its trophic status and main environmental factors are associated with climate change and anthropogenic pressures. The results indicate that water quality decreases during periods of lower river discharge, precipitation, and the decline of ENSO events. Salinity was the most important predictor for determining the IRE trophic state while addressing multiple stressors, followed by DIP and chlorophyll-a. Consequently, we believe that these variables should always be included in the assessment of the IRE trophic state and can be expanded to other tropical and macrotidal estuaries. It is important to mention that the conditions of high temperature and the presence of oxygenated waters in the mixing zone infer an increase in the trophic state. The TRIX and ASSETS models classified the estuary as highly trophic and susceptible to the seasonal development of eutrophication indications, with the seawater zone being the most critical region. From these results, we observed that this study may facilitate the characterization of future risks and prioritize IRE monitoring needs. In addition, this study aimed to improve our understanding of the effects of multiple stressors in a complex macrotidal ecosystem. We propose that local management agencies implement a monitoring system for the trophic and ecological state of the Itapecuru River as the best way to maintain its trophic conditions in the future.

Acknowledgements

The authors would like to acknowledge the Laboratories of Phytoplankton (Federal University of Maranhão and Federal University of Pernambuco, Brazil) for the biological analyses support. We are incredibly grateful to Chemical Oceanography Laboratory (Federal University of Pernambuco, Brazil) for chemical analyses. Professor Moacyr Cunha de Araújo Filho and Marcus André Silva from the Center for Studies and Tests in Risk and Environmental Modeling (CEERMA) is gratefully acknowledged for his significant contribution to data analyses. We also thank the anonymous reviewers for their valuable comments and suggestions on our article. We would like to thank Editage (www.editage.com) for English language editing and the anonymous reviewers for the positive and insightful comments/suggestions in the manuscript.

References

ACQUAVITA, A., ALEFFI, I.F., BENCI, C., BETTOSO, N., CREVATIN, E., MILANI, L., TAMBERLICH, F., TONIATTI, L., BARBIERI, P., LICEN, S., MATTASSI, G., 2015. Annual characterization of the nutrients and trophic state in a Mediterranean coastal lagoon: The Marano and Grado Lagoon (northern Adriatic Sea). Reg. Stud. Mar. Sci. 2, 132–144. https://doi.org/10.1016/j.rsma.2015.08.017.

ALMEIDA, M.S., MORAES, P.S.S., NASCIMENTO, M.H.S., BIRINDELLI, J.L.O., ASSEGA, F.M., BARROS, M.C., FRAGA, E.C., 2022. New records of the occurrence of Megaleporinus macrocephalus (Garavello & Britski, 1988) (Characiformes, Anostomidae) from the basins of the Itapecuru and Mearim rivers in Maranhão, Northeastern Brazil. Braz. J. Biol. 82, e232868. https://doi.org/10.1590/1519-6984.232868.

ANDERSEN, J.H., AL-HAMDANI, Z., HARVEY, E.T., KALLENBACH, E., MURRAY, C., STOCK, A., 2020. Relative impacts of multiple human stressors in estuaries and coastal waters in the North Sea–Baltic Sea transition zone. Sci. Total Environ. 704, 135316. https://doi.org/10.1016/j.scitotenv.2019.135316.

ANDERSON, M.J., 2001. A new method for non-parametric multivariate analysis of variance. Austral Ecol. 26, 32–46. https://doi.org/10.1111/j.1442-9993.2001.01070.pp.x.

ANDRADES, R., MARTINS, R.F., GUABIROBA, H.C., RODRIGUES, V.L.A., SZABLAK, F.T., BASTOS, K.V., BASTOS, P.G.P., LIMA, L.R.S., VILAR, C.C., JOYEUX, J.-C., 2021. Effects of seasonal contaminant remobilization on the community trophic dynamics in a Brazilian tropical estuary. Sci. Total Environ. 801, 149670. https://doi.org/10.1016/j.scitotenv.2021.149670.

ANDRICEVIC, R., KEKEZ, T., VOJKOVIC, M., 2021. Trophic status assessment of Central Eastern Adriatic Sea using water quality variables and loading capacity concept for estuaries. Mar. Pollut. Bull. 173, 113126. https://doi.org/10.1016/j.marpolbul.2021.113126.

ASP, N.E., GOMES, V.J.C., SCHETTINI, C.A.F., SOUZA-FILHO, P.W.M., SIEGLE, E., OGSTON, A.S., NITTROUER, C.A., SILVA, J.N.S., NASCIMENTO, W.R., SOUZA, S.R., PEREIRA, L.C.C., QUEIROZ, M.C., 2018. Sediment dynamics of a tropical tide-dominated estuary: Turbidity maximum, mangroves and the role of the Amazon River sediment load. Estuar. Coast. Shelf Sci. 214, 10–24. https://doi.org/10.1016/j.ecss.2018.09.004.

BÉJAOUI, B., ARMI, Z., OTTAVIANI, E., BARELLI, E., GARGOURI-ELLOUZ, E., CHÉRIF, R., TURKI, S., SOLIDORO, C., ALEYA, L., 2016. Random Forest model and TRIX used in combination to assess and diagnose the trophic status of Bizerte Lagoon, southern Mediterranean. Ecol. Indic. 71, 293–301. https://doi.org/10.1016/j.ecolind.2016.07.010.

BHARATHI, M.D., SARMA, V.V.S.S., 2019. Impact of monsoon-induced discharge on phytoplankton community structure in the tropical Indian estuaries. Reg. Stud. Mar. Sci. 31, 100795. https://doi.org/10.1016/j.rsma.2019.100795.

BORJA, A., BRICKER, S.B., DAUER, D.M., DEMETRIADES, N.T., FERREIRA, J.G., FORBES, A.T., HUTCHINGS, P., JIA, X., KENCHINGTON, R., MARQUES, J.C., ZHU, C., 2008. Overview of integrative tools and methods in assessing ecological integrity in estuarine and coastal systems worldwide. Mar. Pollut. Bull. 56, 1519–1537. https://doi.org/10.1016/j.marpolbul.2008.07.005.

BREIMAN, L. 2001. Random Forests. Mach. Learn. 45, 5–32. https://doi.org/10.1023/A:1010933404324.

BRICKER, S.B., FERREIRA, J.G., SIMAS, T., 2003. An integrated methodology for assessment of estuarine trophic status. Ecol Modell. 169, 39–60. https://doi.org/10.1016/s0304-3800(03)00199-6.

BRICKER, S.B., RICE, K.C., BRICKER, O.P., 2014. From Headwaters to Coast: Influence of Human Activities on Water Quality of the Potomac River Estuary. Aquat. Geochem. 20, 291–323. https://doi.org/10.1007/s10498-014-9226-y.

BRITO, S.S.B., CUNHA, A.P.M.A., CUNNINGHAM, C.C., ALVALÁ, R.C., MARENGO, J.A., CARVALHO, M.A., 2017. Frequency, duration and severity of drought in the Semiarid Northeast Brazil region. Int. J. Climatol. 38, 517–529. https://doi.org/10.1002/joc.5225.

BRUGNOLI, E., MUNIZ, P., VENTURINI, N., BRENA, B., RODRÍGUEZ, A., GARCÍA-RODRÍGUEZ, F., 2019. Assessing multimetric trophic state variability during an ENSO event in a large estuary (Río de la Plata, South America). Reg. Stud. Mar. Sci. 28, 100565. https://doi.org/10.1016/j.rsma.2019.100565.

CABRAL, A., BONETTI, C.H.C., GARBOSSA, L.H.P., PEREIRA-FILHO, J., BESEN, K., FONSECA, A.L., 2020. Water masses seasonality and meteorological patterns drive the biogeochemical processes of a subtropical and urbanized watershed-bay-shelf continuum. Sci. Total Environ. 749, 141553. https://doi.org/10.1016/j.scitotenv.2020.141553.

CARRASCO NAVAS-PAREJO, J.C., CORZO, A., PAPASPYROU, S., 2020. Seasonal cycles of phytoplankton biomass and primary production in a tropical temporarily open-

closed estuarine lagoon — The effect of an extreme climatic event. Sci. Total Environ. 723, 138014. https://doi.org/10.1016/j.scitotenv.2020.138014.

CAVALCANTE, G., VIEIRA, F., CAMPOS, E., BRANDINI, N., MEDEIROS, P.R.P., 2020. Temporal streamflow reduction and impact on the salt dynamics of the São Francisco River Estuary and adjacent coastal zone (NE/Brazil). Reg. Stud. Mar. Sci. 38, 101363. https://doi.org/10.1016/j.rsma.2020.101363.

CAVALCANTI, L.F., CUTRIM, M.V.J. MACIEL, C.C.S. DUARTE DOS SANTOS, A.K., DE AZEVEDO-CUTRIM, A.C.G., SANTOS, T.P., DA CRUZ, Q.S., 2021. Application of multiple indices to the evaluation of trophic and ecological status in a tropical macrotidal estuary (Equatorial Margin, Brazil). Chem Ecol. 38, 122-144. https://doi.org/10.1080/02757540.2021.2023509.

CAVALCANTI, L.F., DO N FEITOSA, F. A., CUTRIM, M.V.J., MONTES, M.J.F., LOURENÇO, C.B., FURTADO, J.A., DOS S SÁ, A.K.D., 2022. Drivers of phytoplankton biomass and diversity in a macrotidal bay of the Amazon Mangrove Coast, a Ramsar site. Ecohydrol. Hydrobiol. https://doi.org/10.1016/j.ecohyd.2022.02.002.

CHAALALI, A., BEAUGRAND, G., BOËT, P., SAUTOUR, B., 2013. Climate-Caused Abrupt Shifts in a European Macrotidal Estuary. Estuaries Coast. 36, 1193–1205. https://doi.org/10.1007/s12237-013-9628-x.

CLOERN, J.E., 2010. How does climate variability influence estuarine-coastal ecosystems? In ClimECO2 International Summer School-Oceans, Marine Ecosystems, and Society facing Climate Change. Brest, France.

CORDIER, T., LANZ´EN, A., APOTH´ELOZ-PERRET-GENTIL, L., STOECK, T., PAWLOWSKI, J., 2019. Embracing environmental genomics and machine learning for routine biomonitoring. Trends Microbiol. 27, 387–397. https://doi.org/10.1016/j.tim.2018.10.012.

COTOVICZ JUNIOR, L.C., BRANDINI, N., KNOPPERS, B.A., MIZERKOWSKI, B.D., STERZA, J.M., OVALLE, A.R.C., MEDEIROS, P.R.P., 2012. Assessment of the trophic status of four coastal lagoons and one estuarine delta, eastern Brazil. Environ. Monit. Assess. 185, 3297–3311. https://doi.org/10.1007/s10661-012-2791-x.

COTOVICZ JUNIOR, L.C., BRANDINI, N., KNOPPERS, B.A., MIZERKOWSKI, B.D., STERZA, J.M., OVALLE, A.R.C., MEDEIROS, P.R.P., 2013. Assessment of the trophic status of four coastal lagoons and one estuarine delta, eastern Brazil. Environ. Monit. Assess. 185, 3297–3311. https://doi.org/10.1007/s10661-012-2791-x.

CUTRIM, M.V.J., FERREIRA, F.S., DUARTE DOS SANTOS, A.K., CAVALCANTI, L.F., ARAÚJO, B.DE O., DE AZEVEDO-CUTRIM, A.C.G., FURTADO, J.A., OLIVEIRA, A.L.L., 2019. Trophic state of an urban coastal lagoon (northern Brazil), seasonal variation of the phytoplankton community and environmental variables. Estuar. Coast. Shelf Sci. 216, 98–109. https://doi.org/10.1016/j.ecss.2018.08.013.

DESCHUTTER, Y., EVERAERT, G., DE SCHAMPHELAERE, K., DE TROCH, M., 2017. Relative contribution of multiple stressors on copepod density and diversity dynamics in the

Belgian part of the North Sea. Mar. Pollut. Bull. 125, 350–359. https://doi.org/10.1016/j.marpolbul.2017.09.038.

ESPINOSA-DÍAZ, L.F., ZAPATA-REY, Y.-T., IBARRA-GUTIERREZ, K., BERNAL, C.A., 2021. Spatial and temporal changes of dissolved oxygen in waters of the Pajarales complex, Ciénaga Grande de Santa Marta: Two decades of monitoring. Sci. Total Environ. 785, 147203. https://doi.org/10.1016/j.scitotenv.2021.147203.

FELD, C.K., SEGURADO, P., GUTIÉRREZ-CÁNOVAS, C., 2016. Analysing the impact of multiple stressors in aquatic biomonitoring data: A 'cookbook' with applications in R. Sci. Total Environ. 573, 1320–1339. https://doi.org/10.1016/j.scitotenv.2016.06.243.

FERREIRA, J.G., ANDERSEN, J.H., BORJA, A., BRICKER, S.B., CAMP, J., CARDOSO DA SILVA, M., GARCÉS, E., HEISKANEN, A.-S., HUMBORG, C., IGNATIADES, L., LANCELOT, C., MENESGUEN, A., TETT, P., HOEPFFNER, N., CLAUSSEN, U., 2011. Overview of eutrophication indicators to assess environmental status within the European Marine Strategy Framework Directive. Estuar. Coast. Shelf Sci. 93, 117–131. https://doi.org/10.1016/j.ecss.2011.03.014.

FERREIRA, J.G., BRICKER, S.B., SIMAS, T.C., 2007. Application and sensitivity testing of a eutrophication assessment method on coastal systems in the United States and European Union. J. Environ. Manage, 82, 433–445. https://doi.org/10.1016/j.jenvman.2006.01.003.

GARCÍA, A., JUANES, J.A., ÁLVAREZ, C., REVILLA, J.A., MEDINA, R., 2010. Assesment of the response of a shallow macrotidal estuary to changes in hydrological and wastewater inputs through numerical modelling. Ecol Modell, 221, 1194–1208. https://doi.org/10.1016/j.ecolmodel.2009.12.027.

GARMENDIA, M., BRICKER, S., REVILLA, M., BORJA, Á., FRANCO, J., BALD, J., VALENCIA, V., 2012. Eutrophication Assessment in Basque Estuaries: Comparing a North American and a European Method. Estuaries Coast. 35, 991–1006. https://doi.org/10.1007/s12237-012-9489-8.

GARNIER, J., BILLEN, G., NÉMERY, J., SEBILO, M., 2010. Transformations of nutrients (N, P, Si) in the turbidity maximum zone of the Seine estuary and export to the sea. Estuar. Coast. Shelf Sci. 90, 129–141. https://doi.org/10.1016/j.ecss.2010.07.012.

GIOVANARDI, F., VOLLENWEIDER, R.A., 2004. Trophic conditions of marine coastal waters: experience in applying the Trophic Index TRIX to two areas of the Adriatic and Tyrrhenian seas. J. Limnol. 63, 199. https://doi.org/10.4081/jlimnol.2004.199.

GLÉ, C., DEL AMO, Y., SAUTOUR, B., LABORDE, P., CHARDY, P., 2008. Variability of nutrients and phytoplankton primary production in a shallow macrotidal coastal ecosystem (Arcachon Bay, France). Estuar. Coast. Shelf Sci. 76, 642–656. https://doi.org/10.1016/j.ecss.2007.07.043.

GOLTERMAN, H.L., CLYMO, R.S., OHNSTAD, M.A.M., 1978. Methods for physical and chemical analysis of freshwater, second ed. IPB Handbook No. 8. Blackwell, Oxford.

GÓMEZ, A.G., VALDOR, P.F., ONDIVIELA, B., DÍAZ, J.L., JUANES, J.A., 2019. Mapping the environmental risk assessment of marinas on water quality: The Atlas of the Spanish coast. Mar. Pollut. Bull. 139, 355–365. https://doi.org/10.1016/j.marpolbul.2019.01.008.

GRASSHOFF, K., EHRHARDT, M., KREMLING, K., 1983. Methods of Seawater Analysis, second ed. Verlag Chemie, New York.

HADID, N.B., GOYET, C., CHAAR, H., MAIZ, N.B., GUGLIELMI, V., SHILI, A., 2021. Machine Learning Modeling Techniques for Forecasting the Trophic Level in a Restored South Mediterranean Lagoon Using Chlorophyll-a. Wetlands, 41, 111. https://doi.org/10.1007/s13157-021-01479-6.

HAGY, J.D., KREAKIE, B.J., PELLETIER, M.C., NOJAVAN, F., KIDDON, J.A., OCZKOWSKI, A.J., 2022. Quantifying coastal ecosystem trophic state at a macroscale using a Bayesian analytical framework. Ecol. Indic. 142, 109267. https://doi.org/10.1016/j.ecolind.2022.109267.

HARTNETT, M., NASH, S., OLBERT, I., 2012. An integrated approach to trophic assessment of coastal waters incorporating measurement, modelling and water quality classification. Estuar. Coast. Shelf Sci. 112, 126–138. https://doi.org/10.1016/j.ecss.2011.08.012.

HUTCHINS, M.G., HITT, O.E., 2019. Sensitivity of river eutrophication to multiple stressors illustrated using graphical summaries of physics-based river water quality model simulations. J. Hydrol. 577, 123917. https://doi.org/10.1016/j.jhydrol.2019.123917.

ITO, T., 1959. The Venice system for the classification of marine waters according to salinity: Symposium on the classification of brackish waters, Venice, 8-14 April 1958. Japanese J. Limnology. 20, 119-120. https://doi.org/10.3739/rikusui.20.119.

KARTHIK, R., ROBIN, R.S., ANANDAVELU, I., PURVAJA, R., SINGH, G., MUGILARASAN, M., JAYALAKSHMI, T., DEEPAK SAMUEL, V., RAMESH, R. (2020). Diatom bloom in the Amba River, west coast of India: A nutrient-enriched tropical river-fed estuary. Reg. Stud. Mar. Sci. 35, 101244. https://doi.org/10.1016/j.rsma.2020.101244.

KE, S., ZHANG, P., OU, S., ZHANG, J., CHEN, J., ZHANG, J., 2022. Spatiotemporal nutrient patterns, composition, and implications for eutrophication mitigation in the Pearl River Estuary, China. Estuar. Coast. Shelf Sci. 266, 107749. https://doi.org/10.1016/j.ecss.2022.107749.

KONG, X., CHE, X., SU, R., ZHANG, C., YAO, Q., SHI, X., 2017. A new technique for rapid assessment of eutrophication status of coastal waters using a support vector machine. J. Oceanol. Limnol. 36, 249–262. https://doi.org/10.1007/s00343-017-6224-0.

LATIF, S.D., BIRIMA, A.H., AHMED, A.N., HATEM, D.M., AL-ANSARI, N., FAI, C.M., EL-SHAFIE, A., 2022. Development of prediction model for phosphate in reservoir water system based machine learning algorithms. Ain Shams Eng. J. 13, 101523. https://doi.org/10.1016/j.asej.2021.06.009.

LEE, T.M., MARKOWITZ, E.M., HOWE, P.D., KO, C.-Y., LEISEROWITZ, A.A., 2015. Predictors of public climate change awareness and risk perception around the world. Nat. Clim. Change. 5, 1014–1020. https://doi.org/10.1038/nclimate2728.

LEFÈVRE, N., DA SILVA DIAS, F.J., DE TORRES, A.R., NORIEGA, C., ARAUJO, M., DE CASTRO, A.C.L., ROCHA, C., JIANG, S., IBÁNHEZ, J.S.P., 2017. A source of CO2 to the atmosphere throughout the year in the Maranhense continental shelf (2°30'S, Brazil). Cont. Shelf Res. 141, 38–50. https://doi.org/10.1016/j.csr.2017.05.004.

LEMLEY, D.A., ADAMS, J.B., STRYDOM, N.A., 2017. Testing the efficacy of an estuarine eutrophic condition index: Does it account for shifts in flow conditions? Ecol. Indic. 74, 357–370. https://doi.org/10.1016/j.ecolind.2016.11.034.

LEMLEY, D.A., ADAMS, J.B., TALJAARD, S., STRYDOM, N.A., 2015. Towards the classification of eutrophic condition in estuaries. Estuar. Coast. Shelf Sci. 164, 221–232. https://doi.org/10.1016/j.ecss.2015.07.033.

LI, R., XU, J., LI, X., SHI, Z., HARRISON, P.J., 2017. Spatiotemporal Variability in Phosphorus Species in the Pearl River Estuary: Influence of the River Discharge. Sci. Rep. 7 , 13649. https://doi.org/10.1038/s41598-017-13924-w.

LIAW, A., WIENER, M., 2002. Classification and regression by randomForest. R news. 23, 18-22.

LIU, B., CAO, W., HUANG, Z., CHEN, W., CHEN, H., LIU, L., 2018. Developing nutrient criteria for the Jiulong River Estuary, Southeast China. Acta Oceanol. Sin. 37, 1–13. https://doi.org/10.1007/s13131-017-1121-0.

LIVINGSTON, R.J., 2007. Phytoplankton Bloom Effects On A Gulf Estuary: Water Quality Changes And Biological Response. Ecol Appl. 17, S110–S128. https://doi.org/10.1890/05-0769.1.

LONSDALE, J.-A., WESTON, K., BARNARD, S., BOYES, S.J., ELLIOTT, M., 2015. Integrating management tools and concepts to develop an estuarine planning support system: A case study of the Humber Estuary, Eastern England. Mar. Pollut. Bull. 100, 393–405. https://doi.org/10.1016/j.marpolbul.2015.08.017.

MARENGO, J.A., ALVES, L.M., ALVALA, R.C.S., CUNHA, A.P., BRITO, S., MORAES, O.L.L., 2018. Climatic characteristics of the 2010-2016 drought in the semiarid Northeast Brazil region. Anais Da Academia Brasileira de Ciências. 90, 1973–1985. https://doi.org/10.1590/0001-3765201720170206.

MASULLO, Y.A.G., SOARES, L.S., DE CASTRO, C.E., PINHEIRO, E.A.L., 2019. Dinâmica da paisagem da bacia hidrográfica do rio Itapecuru - MA. Rev. Bras. Geogr. Fís. 12, 1054. https://doi.org/10.26848/rbgf.v12.3.p1054-1073.

MAZOR, R.D, SUTULA, M., THEROUX, S., BECK, M, ODE, P.R., 2022. Eutrophication thresholds associated with protection of biological integrity in California wadeable streams. Ecol. Indic., 142, 109180. https://doi.org/10.1016/j.ecolind.2022.109180.

MONTEIRO, M.C., JIMÉNEZ, J.A., PEREIRA, L.C.C., 2016. Natural and human controls of water quality of an Amazon estuary (Caeté-PA, Brazil). Ocean Coast. Manag. 124, 42–52. https://doi.org/10.1016/j.ocecoaman.2016.01.014.

NASROLLAHZADEH, H.S., DIN, Z.B., FOONG, S.Y., MAKHLOUGH, A., 2008. TROPHIC status of the Iranian Caspian Sea based on water quality parameters and phytoplankton diversity. Cont. Shelf Res. 28, 1153–1165. https://doi.org/10.1016/j.csr.2008.02.015.

NGUYEN, A.T., NÉMERY, J., GRATIOT, N., DAO, T.-S., LE, T.T.M., BADUEL, C., GARNIER, J., 2022. Does eutrophication enhance greenhouse gas emissions in urbanized tropical estuaries? Environ. Pollut. 303, 119105. https://doi.org/10.1016/j.envpol.2022.119105.

NIVEDITHA, S.K., HARIDEVI, C.K., HARDIKAR, R., RAM, A., 2022. Phytoplankton assemblage and chlorophyll a along the salinity gradient in a hypoxic eutrophic tropical estuary-Ulhas Estuary, West Coast of India. Mar. Pollut. Bull. 180, 113719. https://doi.org/10.1016/j.marpolbul.2022.113719.

NOBRE, A.M., BRICKER, S.B., FERREIRA, J.G., YAN, X., DE WIT, M., NUNES, J.P., 2011. Integrated Environmental Modeling and Assessment of Coastal Ecosystems: Application for Aquaculture Management. Coast Manage. 39, 536–555. https://doi.org/10.1080/08920753.2011.600238.

OKSANEN, J., BLANCHET, F.G., FRIENDLY, M., KINDT, R., LEGENDRE, P., MCGLINN, D., MINCHIN, P.R., O'HARA, R.B., SIMPSON, G.L., SOLYMOS, P., STEVENS, M.H.H., SZOECS, E., WAGNER, H., 2020. Vegan: Community ecology package (manual).

OLIVEIRA, A.R.G., ODEBRECHT, C., PEREIRA, L.C.C., COSTA, R.M., 2022. Phytoplankton variation in an Amazon estuary with emphasis on the diatoms of the Order Eupodiscales. Ecohydrol. Hydrobiol. 22, 55-74. https://doi.org/10.1016/j.ecohyd.2021.12.001.

ONABULE, O. A., MITCHELL, S.B., COUCEIRO, F., 2020. The effects of freshwater flow and salinity on turbidity and dissolved oxygen in a shallow Macrotidal estuary: a case study of Portsmouth Harbour. Ocean Coast. Manag. 191, 105179. https://doi.org/10.1016/j.ocecoaman.2020.105179.

PAMPLONA, F.C., PAES, E.T., NEPOMUCENO, A., 2013. Nutrient fluctuations in the Quatipuru river: A macrotidal estuarine mangrove system in the Brazilian Amazonian basin. Estuar. Coast. Shelf Sci. 133, 273–284. https://doi.org/10.1016/j.ecss.2013.09.010.

PAULA-FILHO, F.J., MARINS, R.V., CHICHARO, L., SOUZA, R.B., SANTOS, G.V., BRAZ, E.M.A., 2020. Evaluation of water quality and trophic state in the Parnaíba River Delta, northeast Brazil. Reg. Stud. Mar. Sci. 34, 101025. https://doi.org/10.1016/j.rsma.2019.101025.

PENNA, N., CAPELLACCI, S., RICCI, F., 2004. The influence of the Po River discharge on phytoplankton bloom dynamics along the coastline of Pesaro (Italy) in the Adriatic Sea. Mar. Pollut. Bull. 48, 321–326. https://doi.org/10.1016/j.marpolbul.2003.08.007.

PEREIRA, L.C.C., NASCIMENTO TRINDADE, W., DA SILVA, I.R., VILA-CONCEJO, A., SHORT, A.D., 2016. Maranhão Beach Systems, Including the Human Impact on São Luís Beaches. Brazilian Beach Systems. 5, 125–152. https://doi.org/10.1007/978-3-319-30394-9_5.

PEREIRA, L.C.C., OLIVEIRA, S.M.O. DE, COSTA, R.M.DA, COSTA, K.G.DA, VILA-CONCEJO, A., 2013. What happens on an equatorial beach on the Amazon coast when La Niña occurs during the rainy season? Estuar. Coast. Shelf Sci. 135, 116–127. https://doi.org/10.1016/j.ecss.2013.07.017.

PEREIRA, L.C.C., SOUSA, N.DO S. DA S., RODRIGUES, L.M. DOS S., MONTEIRO, M.C., SILVA, S.R.S. DA, OLIVEIRA, A.R.G. DE, DIAS, A.B.B., COSTA, R. M. DA, 2021. Effects of the lack of basic public sanitation on the water quality of the Caeté River estuary in northern Brazil. Ecohydrol. Hydrobiol. 21, 299–314. https://doi.org/10.1016/j.ecohyd.2020.12.003.

PEREIRA, L.C.C., SOUSA-FELIX, R.C. DE, COSTA, R.M. DA, JIMENEZ, J.A., 2018. Challenges of the recreational use of Amazon beaches. Ocean Coast. Manag. 165, 52–62. https://doi.org/10.1016/j.ocecoaman.2018.08.012.

RANKINEN, K., CANO BERNAL, J.E., HOLMBERG, M., VUORIO, K., GRANLUND, K., 2019. Identifying multiple stressors that influence eutrophication in a Finnish agricultural river. Sci. Total Environ. 658, 1278–1292. https://doi.org/10.1016/j.scitotenv.2018.12.294.

RÄSÄNEN, T.A., KUMMU, M., 2013. Spatiotemporal influences of ENSO on precipitation and flood pulse in the Mekong River Basin. J. Hydrol. 476, 154–168. https://doi.org/10.1016/j.jhydrol.2012.10.028.

SÁ, A. K.D.S., FEITOSA, F.A.N., CUTRIM, M.V.J., FLORES-MONTES, M.J., DOS S. COSTA, D., CAVALCANTI, L.F., 2022. Phytoplankton community dynamics in response to seawater intrusion in a tropical macrotidal river-estuary continuum. Hydrobiologia. https://doi.org/10.1007/s10750-022-04851-7.

SÁ, A.K.D.S., CUTRIM, M.V.J., COSTA, D.S., CAVALCANTI, L.F., FERREIRA, F.S., OLIVEIRA, A.L.L., SEREJO, J.H.F., 2021. Algal blooms and trophic state in a tropical estuary blocked by a dam (Northeastern Brazil). Ocean Coast. Res. 69, e21009. https://doi.org/10.1590/2675-2824069.20-006akddss.

SANTOS DOS, V.H.M., DA SILVA DIAS, F.J., TORRES, A.R., SOARES, R.A., TERTO, L.C., DE CASTRO, A.C.L., SANTOS, R.L., CUTRIM, M.V.J., 2020. Hydrodynamics and suspended particulate matter retention in macrotidal estuaries located in Amazonia-semiarid interface (Northeastern-Brazil). Int. J. Sediment Res. 35, 417–429. https://doi:10.1016/j.ijsrc.2020.03.004.

SOARES, L.S., LOPES, W.G.R., DE CASTRO, A.C.L., SILVA, E.V. DA, ARAÚJO, G.C. DE, MOREIRA, M.D.S., FRANÇA, V.L. DE, MENDES, K.C., 2017. Analysis of Spatiotemporal Changes in Land Use and Land Cover in Sub-Watersheds of the Lower Itapecuru River in the State of Maranhão, Brazil. Geography Department University of Sao Paulo, 34, 55-67. https://doi.org/10.11606/rdg.v34i0.133551.

SOUSA, R.C. DE, PEREIRA, L.C.C., COSTA, R.M. DA, JIMÉNEZ, J.A., 2017. Management of estuarine beaches on the Amazon coast though the application of recreational carrying capacity indices. Tour. Manag. 59, 216–225. https://doi.org/10.1016/j.tourman.2016.07.006.

SOUSA-FELIX, R.C., PEREIRA, L.C.C., TRINDADE, W.N., DE SOUZA, I.P., DA COSTA, R.M., JIMENEZ, J.A., 2017. Application of the DPSIR framework to the evaluation of the recreational and environmental conditions on estuarine beaches of the Amazon coast. Ocean Coast. Manag. 149, 96–106. https://doi.org/10.1016/j.ocecoaman.2017.09.011.

STRICKLAND, J.D.H., PARSONS, T.R., 1972. A practical handbook of seawater analysis, second ed. Bulletin Fisheries Research Board of Canada, Ottawa.

TAILLARDAT, P., MARCHAND, C., FRIESS, D.A., WIDORY, D., DAVID, F., OHTE, N., NAKAMURA, T., VAN VINH, T., THANH-NHO, N., ZIEGLER, A.D., 2020. Respective contribution of urban wastewater and mangroves on nutrient dynamics in a tropical estuary during the monsoon season. Mar. Pollut. Bull. 160, 111652. https://doi.org/10.1016/j.marpolbul.2020.111652.

TAO, W., NIU, L., DONG, Y., FU, T., LOU, Q., 2021. Nutrient Pollution and Its Dynamic Source-Sink Pattern in the Pearl River Estuary (South China). Front. Mar. Sci. 8, 713907. https://doi.org/10.3389/fmars.2021.713907.

UNITED NATIONS EDUCATIONAL, SCIENTIFIC AND CULTURAL ORGANIZATION – UNESCO, 1966. Determination of photosynthetic pigments in sea-water, first ed. (Monographs on Oceanographic Methodology), Paris.

UTERMÖHL, H., 1958. Zur vervollkommung der quantitativen phytoplankton - methodik. Mitteilungen Internationale Vereinigung fuer Theoretische und Angewandte Limnologie. 9, 1-38.

VILAFAÑE, V.E., REID, F.M.H., 1995. Métodos de microscopia para la cuantificación del fitoplancton, in: Alvear, K., Ferrario, M.E., Oliveira Filho, E.C., Sars, E. (Eds.), Manual de métodos ficológicos. Universidad de Concepción, Chile, pp.169-185.

VOLLENWEIDER, R.A., GIOVANARDI, F., MONTANARI, G., RINALDI, A., 1998. Characterization of the trophic conditions of marine coastal waters with special reference to the NW Adriatic Sea: proposal for a trophic scale, turbidity and generalized water quality index. Environmetrics. 9, 329–357. https://doi.org/10.1002/(sici)1099-095x(199805/06)9:3<329::aid-env308>3.0.co;2-9.

WANG B., SUN X., WEI Q., XIE L., 2012. A new method for assessment of eutrophication status in estuarine and coastal waters off China and its application. Acta Oceanol. Sin. 34, 61-66.

WANG, F., CHENG, P., CHEN, N., KUO, Y.-M., 2021. Tidal driven nutrient exchange between mangroves and estuary reveals a dynamic source-sink pattern. Chemosphere. 270, 128665. https://doi.org/10.1016/j.chemosphere.2020.128665.

WATANABE, K., KASAI, A., ANTONIO, E.S., SUZUKI, K., UENO, M., YAMASHITA, Y., 2014. Influence of salt-wedge intrusion on ecological processes at lower trophic levels in the Yura Estuary, Japan. Estuar. Coast. Shelf Sci. 139, 67–77. https://doi.org/10.1016/j.ecss.2013.12.018.

WHITALL, D., BRICKER, S., FERREIRA, J., NOBRE, A.M., SIMAS, T., SILVA, M., 2007. Assessment of Eutrophication in Estuaries: Pressure–State–Response and Nitrogen Source Apportionment. Environ. Manag. 40, 678–690. https://doi.org/10.1007/s00267-005-0344-6.

WOLTER, K., TIMLIN, M.S., 2011. El Niño/Southern Oscillation behaviour since 1871 as diagnosed in an extended multivariate ENSO index (MEI.ext). Int. J. Climatol. 31, 1074–1087. https://doi.org/10.1002/joc.2336.

WU, M.-L., WANG, Y.-S., WANG, Y.-T., SUN, F.-L., SUN, C.-C., CHENG, H., DONG, J.-D., 2016. Seasonal and spatial variations of water quality and trophic status in Daya Bay, South China Sea. Mar. Pollut. Bull. 112, 341–348. https://doi.org/10.1016/j.marpolbul.2016.07.042.

XIAO, Y., FERREIRA, J.G., BRICKER, S.B., NUNES, J.P., ZHU, M., ZHANG, X., 2007. Trophic Assessment in Chinese coastal systems-review of methods and application to the Changjiang (Yangtze) Estuary and Jiaozhou Bay. Estuaries Coast. 30, 901–918. https://doi.org/10.1007/bf02841384.

XIE, L., XU, H., XIN, M., WANG, B., TU, J., WEI, Q., SUN, X., 2021. Regime shifts in trophic status and regional nutrient criteria for the Bohai Bay, China. Mar. Pollut. Bull. 170, 112674. https://doi.org/10.1016/j.marpolbul.2021.112674.

YANG, B., KANG, Z.-J., LU, D.-L., DAN, S., NING, Z.-M., LAN, W.-L., ZHONG, Q.-P., 2018. Spatial Variations in the Abundance and Chemical Speciation of Phosphorus across the River–Sea Interface in the Northern Beibu Gulf. Water. 10, 1103. https://doi.org/10.3390/w10081103.

YANG, F., MI, T., CHEN, H., YAO, Q., 2019. Developing numeric nutrient criteria for the Yangtze River Estuary and adjacent waters in China. J. Hydrol. 579, 124188. https://doi.org/10.1016/j.jhydrol.2019.124188.

8 CONSIDERAÇÕES FINAIS

Nesta seção, as conclusões gerais referentes aos capítulos publicados destacam os principais aspectos da pesquisa, tais como: indicadores fitoplanctônicos de intrusão salina, níveis de eutrofização de um estuário tropical sob influência de macromarés e múltiplos estressores estuarinos, bem como, sugestões para futuras pesquisas na região.

8.1 Conclusões Gerais

Um dos passos mais importantes para avançar nosso conhecimento sobre intrusão salina no estuário do rio Itapecuru (ERI) foi ampliar o entendimento do seu funcionamento, enquadrando-o como um estuário tropical e de macromarés, que está sob influência dos fatores climáticos globais e regionais. Um dos grandes desafios foi compreender as respostas ecológicas da comunidade fitoplanctônica ao fenômeno da intrusão salina em escala espacial e temporal, até então não estudado. Assim, levantamos as seguintes questões: a intrusão salina ao alterar os gradientes ambientais promove mudanças abruptas ou graduais na comunidade fitoplanctônica? De que forma essas mudanças ocorrem? Como a comunidade responde a essas mudanças espaço-temporais?

Então, a partir da metodologia utilizada foi possível conhecer a dinâmica dos gradientes ambientais que caracterizaram o ERI como um ambiente bastante heterogêneo regido pelos padrões de chuva local. Além disso, observamos que a magnitude da intrusão salina foi mais expressiva no período de estiagem e isso contribuiu para o aumento da concentração de nutrientes e dispersão de espécies ao longo do continuum rio-estuário.

Em nossas observações, também ficou evidente que a zona máxima de turbidez estuarina, marcador do limite da intrusão salina, é deslocada sazonalmente, funcionando como um centro de dispersão de espécies entre o setor superior e inferior do estuário. Esse ambiente turvo, formado por mudanças graduais das condições ambientais, caracteriza-se como um ecótono estuarino, onde as alterações de salinidade, MPS e nutrientes, tornam-se desfavoráveis para as espécies de água doce que migram para essa região. Por outro lado, espécies marinhas são favorecidas.

Neste estudo foi possível selecionar 76 indicadores do fitoplâncton que respondem por meio dos seus traços funcionais às mudanças nos gradientes ambientais e determinam seu padrão de distribuição conforme as escalas temporais. Por exemplo, as diatomáceas cêntricas,

marinhas, com maior dimensão linear máxima (DLM > 20 μm), como: *Craticula ambigua*, *Nitzschia palea*, *Polymyxus coronalis* e *Skeletonema costatum* constituem o grupo de indicadores mais expressivo e resiliente ao aumento da intrusão salina. Não menos importante, a fração de cianobactérias foi favorecida pela intrusão salina no período de estiagem, com ocorrência de CyanoHab no setor superior do ERI.

Dentre esses indicadores, a densidade de *P. coronalis*, constituindo-se primeira citação para o Maranhão, varia inversamente a salinidade, com aumento da densidade celular em condições de baixa salinidade, turbidez e temperatura da água (Figura 3 – Apêndice 1). Sendo assim, selecionamos o *P. coronalis* como um bom indicador do limite de intrusão de água do mar no ERI.

Desta forma, nossos resultados indicam que a comunidade fitoplanctônica do ERI é constituída por espécies indicadoras que apresentam uma capacidade adaptativa e tolerante aos estressores que afetam seus padrões de sucessão. Isto promove uma vantagem competitiva, aumentando a dispersão de espécies e a diversidade da comunidade que ultrapassam a barreira física da zona máxima de turbidez estuarina (setor médio do estuário). Assim, informações adicionais sobre a comunidade fitoplanctônica encontram-se no apêndice 1 deste documento.

Outro desafio para este estudo foi definir o estado geral de eutrofização do ERI utilizando ferramentas numéricas a fim de inferir respostas que auxiliem no gerenciamento de suas águas. Partindo do pressuposto que estuários de macromarés apresentam seu estado de eutrofização intensificado mais pela dinâmica física que química, nós respondemos os seguintes questionamentos: pressões antropogênicas e múltiplos estressores, quando associados ao fenômeno de intrusão salina em um estuário de macromaré, intensificam o seu estado geral de eutrofização? Qual variável atua diretamente e em que nível de importância sobre as condições tróficas do ERI? Como as mudanças climáticas inferem sobre as condições tróficas do estuário?

Portanto, a partir da aplicação dos modelos de eutrofização (TRIX e ASSETS), enquadramos o ERI como um estuário hipereutrófico e suscetível ao desenvolvimento dos sintomas de eutrofização sazonal, classificando a zona costeira como a região mais crítica. A salinidade foi selecionada como o principal estressor que em conjunto com as concentrações de nutrientes (DIP) e clorofila *a* intensificam o processo de eutrofização no sistema. Os padrões climáticos globais atuam de forma direta no estado geral de eutrofização do ERI, onde períodos de menor descarga (2012-2014), resultantes da predominância de condições de El Niño,

contribuíram para maior retenção de nutrientes no estuário e consequentemente intensificação do estado trófico. Os efeitos antropogênicos locais (ex.: agrícolas, esgotos urbanos e instalações portuárias) associados ao crescimento populacional classificaram o ERI como de forte influência humana, onde o sistema não suportará o aumento das cargas de nutrientes, devido sua baixa capacidade de diluição de efluentes urbanos, principalmente na estiagem, período de maior tempo de residência e vulnerabilidade a florações nocivas ou potencialmente tóxicas na zona de rio.

A partir do modelo ASSETS, nós projetamos para a próxima década (2021-2031) que a eutrofização irá aumentar consideravelmente, e estratégias de redução das contribuições antrópicas, bem como, melhoria das condições tróficas deve ser inseridas em planos de gestão governamentais. Com base nesses resultados, nós sugerimos que para a manutenção das condições tróficas atuais e continuação do fornecimento dos serviços ecossistêmicos do estuário, torna-se necessário a implementação de programas de monitoramento e gerenciamento da qualidade da água do ERI. Sendo assim, o uso de modelo preditivos e de estado trófico podem ser aplicados, como ferramentas eficientes, uma vez que, estes suportaram nossa hipótese inicial de que a pressão antropogênica e múltiplos estressores aumentam o estado geral de eutrofização do ERI.

8.2. Perspectivas Futuras

Espera-se que os efeitos sinergéticos das futuras mudanças climáticas e crescimento populacional no ERI promova um avanço da intrusão salina, mudanças ecológicas drásticas e intensificação dos sintomas que definem o seu estado geral de eutrofização. As futuras respostas do ERI à ação antrópica e climática dependerá da aplicação de estratégias efetivas de planejamento na Bacia do Rio Itapecuru. Aqui, destacamos o uso de técnicas de modelagem e seleção de indicadores como ferramentas essenciais para prever mudanças futuras no estuário, tornando-se importante o monitoramento contínuo de suas águas para identificar as pressões e o estado, bem como, para informar as respostas que serão utilizadas no gerenciamento deste ecossistema.

Algumas lacunas precisam ser preenchidas, considerando séries espaço-temporais ao longo do gradiente estuarino do ERI. Desta forma, sugerimos que pesquisas futuras utilizem a avaliação da produtividade primária, identificação do fitoplâncton <5µm, estudo das relações fito/zooplâncton, quantificação de coliformes termotolerantes e da vegetação aquática

submersa. Sendo assim, torna-se necessário o desenvolvimento de mais estudos para colmatar essas lacunas entre a água doce do rio e a água costeira nos critérios e fontes de nutrientes associados ao ERI, a fim de mitigar eficazmente a eutrofização e conter a proliferação de algas nocivas.

REFERÊNCIAS

ABREU, J. M. S.; SARAIVA, A. C. S.; ALBERT, J. S.; PIORSKI, N. M. Paleogeographic influences on freshwater fish distributions in northeastern Brazil. **Journal of South American Earth Sciences,** v.102, 2020.

ALCÂNTARA, E. H.; MOCHEL, F. R.; AMORIM, A. J. E. Modelagem da Profundidade Secchi e da Concentração de Clorofila *a* no Estuário do Rio Anil, São Luís - MA. **Caminhos da Geografia**. São Luís, v. 13, n. 5, p. 19 – 40, 2004.

ALLABY, A.; ALLABY, M. **Dictionary of earth sciences**. 2. ed. Oxford: Oxford University Press, 1999. 661p.

ALVES, G.; FLORES-MONTES, M.; GASPAR, F.; GOMES, J.; FEITOSA, F. Eutrophication and water quality in a tropical Brazilian estuary. Journal of Coastal Research, v.1, n. 65, p. 7-12, 2013. DOI: 10.2112/SI65-002.1.

AZEVEDO, A. C. G DE; FEITOSA, F. A. N.; KOENING, M. L. Distribuição espacial e temporal da biomassa fitoplanctônica e variáveis ambientais no Golfão Maranhense, Brasil. **Acta Botanica Brasilica**, v. 22, n. 3, p. 870-877, 2008. DOI: https://doi.org/10.1590/s0102-33062008000300022.

AZHIKODAN, G.; YOKOYAMA, K. Spatio-temporal variability of phytoplankton (Chlorophyll-a) in relation to salinity, suspended sediment concentration, and light intensity in a macrotidal estuary. **Continental Shelf Research**, v. 126, p. 15–26, 2016. DOI: https://doi.org/10.1016/j.csr.2016.07.006.

BATISTA, D. L.; CARVALHO, I. DE S.; DE LA FUENTE, M. S. A new Cretaceous Pleurodira Pelomedusoides from the Lower Cretaceous of Parnaíba Basin, Brazil. **Journal of South American Earth Sciences**, v. 105, 2021. DOI: https://doi.org/10.1016/j.jsames.2020.102872.

BATISTA, T. N. F.; FLORES-MONTES, M. D. J. Estado trófico dos estuários dos rios Ipojuca e Merepe – PE. **Tropical Oceanography**, v. 42, n. 3, 2014. DOI: https://doi.org/10.5914/tropocean.v42i3.5767.

BHARATHI, M. D.; VENKATARAMANA, V.; SARMA, V. V. S. S. Phytoplankton community structure is governed by salinity gradient and nutrient composition in the tropical estuarine system. **Continental Shelf Research**, v. 234, 2022. DOI: https://doi.org/10.1016/j.csr.2021.104643.

BORGES, G. C. P.; AQUINO, E. P. DE; ESKINAZI-LEÇA, E.; SANTOS-JUNIOR, A. DE C.; SANTIAGO, M. F.; FERREIRA, L. C.; NORIEGA, C.; ARAÚJO, M.; GREGO, C. K. DA S.; SILVA-CUNHA, M. DA G. G. DA. Cell biovolume and carbon biomass of phytoplankton in degraded tropical estuaries in Northeastern Brazil. **Regional Studies in Marine Science**, v. 40, 2020. DOI: https://doi.org/10.1016/j.rsma.2020.101522.

BRICKER, S. B.; FERREIRA, J. G.; SIMAS, T. An integrated methodology for assessment of estuarine trophic status. **Ecological Modelling**, v. 169, n. 1, p. 39–60, 2003. DOI: https://doi.org/10.1016/s0304-3800(03)00199-6.

BRICKER, S.; LONGSTAFF, B.; DENNISON, W.; JONES, A.; BOICOURT, K.; WICKS, C.; WOERNER, J. Effects of nutrients enrichment in the nations estuaries: a decade of changes. **Harmful Algae**, v. 8, n. 1, p. 21-32, 2008.

BRUGNOLI, E.; MUNIZ, P.; VENTURINI, N.; BRENA, B.; RODRÍGUEZ, A.; GARCÍA-RODRÍGUEZ, F. Assessing multimetric trophic state variability during an ENSO event in a large estuary (Río de la Plata, South America). **Regional Studies in Marine Science**, v. 28, n. 100565, 2019. DOI: https://doi.org/10.1016/j.rsma.2019.100565.

CARLSON, R. E. A trophic state index for lakes. **Limnology and Oceanography**, v. 22, n. 2, p. 361-369, 1977. DOI: http://dx.doi.org/10.4319/lo.1977.22.2.0361.

CAVALCANTI, L. F.; CUTRIM, M. V. J.; LOURENÇO, C. B.; SÁ, A. K. D. S.; OLIVEIRA, A. L. L.; AZEVEDO-CUTRIM, A. C. G. Patterns of phytoplankton structure in response to environmental gradients in a macrotidal estuary of the Equatorial Margin (Atlantic coast, Brazil). **Estuarine, Coastal and Shelf Science**, v. 245, 2020. DOI: https://doi.org/10.1016/j.ecss.2020.106969.

CAVALCANTI, L. F.; CUTRIM, M. V. J.; MACIEL, C. C. S.; SÁ, A. K. D. DOS S.; AZEVEDO-CUTRIM, A. C. G.; SANTOS, T. P.; CRUZ, Q. S. Application of multiple indices to the evaluation of trophic and ecological status in a tropical macrotidal estuary (Equatorial Margin, Brazil). **Chemistry and Ecology**, v. 38, n. 2, p. 122–144, 2022. DOI: https://doi.org/10.1080/02757540.2021.2023509.

CHANDER, S.; GUJRATI, A.; KRISHNA, A. V.; SAHAY, A.; SINGH, R. P. Remote sensing of inland water quality: a hyperspectral perspective. **Hyperspectral Remote Sensing**, [s.l.], p. 197–219, 2020. DOI: https://doi.org/10.1016/b978-0-08-102894-0.00017-6.

CLOERN, J. E.; FOSTER, S. Q.; KLECKNER, A. E. Phytoplankton primary production in the world's estuarine-coastal ecosystems. **Biogeosciences**, v. 11, n. 9, p. 2477–2501, 2014. DOI: https://doi.org/10.5194/bg-11-2477-2014.

CONCEIÇÃO, L. P.; DE JESUS AFFE, H. M.; DA SILVA, D. M. L.; DE CASTRO NUNES, J. M. Spatio-temporal variation of the phytoplankton community in a tropical estuarine gradient, under the influence of river damming. **Regional Studies in Marine Science**, v. 43, 2021. DOI: https://doi.org/10.1016/j.rsma.2021.101642

COSTA, D. DOS S.; CUTRIM, M. V. J. Spatial and seasonal variation in physicochemical characteristics and phytoplankton in an estuary of a tropical delta system. Regional Studies in Marine Science, 44, 2021. DOI: https://doi.org/10.1016/j.rsma.2021.101746.

COTOVICZ JUNIOR L.C.; BRANDINI N.; KNOPPERS B.A.; SOUZA W.F.L.; MEDEIROS P.R.P. Comparação de Modelos e Índices para Avaliação do Estado Trófico do Complexo Estuarino-Lagunar Mundaú-Manguaba, (AL). **Geochemica Brasiliensis**, v. 26, n. 1, p. 2-12, 2013. DOI: 10.21715/gb.v26i1.353.

COTOVICZ JUNIOR, L. C.; BRANDINI, N.; KNOPPERS, B. A.; MIZERKOWSKI, B. D.; STERZA, J. M.; OVALLE, A. R. C.; MEDEIROS, P. R. P. Assessment of the trophic status of four coastal lagoons and one estuarine delta, eastern Brazil. **Environmental Monitoring and Assessment**, v. 185, n. 4, p. 3297–3311, 2012. DOI: https://doi.org/10.1007/s10661-012-2791-x.

COTOVICZ JUNIOR, L.C.; RIBEIRO, R.P.; RÉGIS, C.R.; BERNARDES, M.; SOBRINHO, R.; VIDAL, L. O.; TREMMEL, D.; KNOPPERS, B. A.; ABRIL, G. Emissões de gases de efeito estufa (CO_2 e CH_4) e comportamento de carbono inorgânico em uma lagoa costeira tropical urbana altamente poluída (SE, Brasil). **Environmental Science and Pollution Research**, v. 28, p. 38173-38192, 2021. DOI: https://doi.org/10.1007/s11356-021-13362-2.

COUTINHO, P. N.; MORAIS, J. O. DE. Distribuição de sedimentos na Baía de São José, no Estado do Maranhão (Brasil). **Arquivos De Ciências Do Mar**. v.16, p. 123–127, 1976.

CUNILLERA-MONTCUSÍ, D.; BEKLIOĞLU, M.; CAÑEDO-ARGÜELLES, M.; JEPPESEN, E.; PTACNIK, R.; AMORIM, C. A.; ARNOTT, S. E.; BERGER, S. A.; BRUCET, S.; DUGAN, H. A.; GERHARD, M.; HORVÁTH, Z.; LANGENHEDER, S.; NEJSTGAARD, J. C.; REINIKAINEN, M.; STRIEBEL, M.; URRUTIA-CORDERO, P.; VAD, C. F.; ZADEREEV, E.; MATIAS, M. Freshwater salinisation: a research agenda for a saltier world. **Trends in Ecology & Evolution**, v. 37, n. 5, p. 440–453, 2022. DOI: https://doi.org/10.1016/j.tree.2021.12.005.

CUTRIM, M. V. J.; FERREIRA, F. S.; DUARTE DOS SANTOS; A. K, CAVALCANTI, L. F.; OLIVEIRA ARAÚJO B.; AZEVEDO- CUTRIM, A. C. G.; OLEIVEIRA, A. L. L. Trophic state of an urban coastal lagoon (northern Brazil), seasonal variation of the phytoplankton community and environmental variables. **Estuarine, Coastal and Shelf Science,** v. 216, p. 98–109, 2019. DOI: https://doi.org/10.1016/j.ecss.2018.08.013.

CZIZEWESKI, A.; PIMENTA, F. M.; SAAVEDRA, O. R. Numerical modeling of Maranhão Gulf tidal circulation and power density distribution. **Ocean Dynamics**, v. 70, n. 5, p. 667–682, 2020. DOI: https://doi.org/10.1007/s10236-020-01354-8.

DALRYMPLE, R. W.; ZAITLIN, B. A.; BOYD, R. Estuarine facies models, conceptual basis and stratigraphic implications. **Journal of Sedimentary Petrology**, v. 62, n. 6, p.1130–1146, 1992.

DAME, R. F. **Estuaries**. 2. ed. [s. l.]: Encyclopedia of Ecology, p. 484-490, 2008. ISBN 9780444641304. DOI: https://doi.org/10.1016/B978-0-444-63768-0.00329-2.

DAUVIN, J. C.; RUELLET, T. The estuarine quality paradox: Is it possible to define an ecological quality status for specific modified and naturally stressed estuarine ecosystems? **Marine Pollution Bulletin**, v. 59, n.1–3, p. 38–47, 2009. DOI: https://doi.org/10.1016/j.marpolbul.2008.11.008.

DEVLIN, A. T.; PAN, J. **Dynamical Estuaries: Comprehensive Remote Sensing**, v. 8, p. 121–144, 2018. DOI: https://doi.org/10.1016/b978-0-12-409548-9.10406-3**.**

DHAL, L.; SWAIN, S. **Understanding and modeling the process of seawater intrusion: a review**. Advances in Remediation Techniques for Polluted Soils and Groundwater, Elsevier, p. 269-290, 2022. DOI: https://doi.org/10.1016/B978-0-12-823830-1.00009-2.

DOMINGUEZ, J. M. L. The Coastal Zone of Brazil. In: **Geology and Geomorphology of Holocene Coastal Barriers of Brazil**. Lecture Notes in Earth Sciences, v. 107. Springer, Berlin, Heidelberg, 2009. DOI: https://doi.org/10.1007/978-3-540-44771-9_2.

DYER, K. R. **Estuaries, A Physical Introduction**. 2. ed. Londres, John Wiley, 1997. 195 p.

EEA - **European Environmental Agency.** Europe's Environment: the Dobris Assessment. Copenhagen, 1995, p. 8.

ELLIOTT, M.; DAY, J. W.; RAMACHANDRAN, R.; WOLANSKI, E. A Synthesis: What Is the Future for Coasts, Estuaries, Deltas and Other Transitional Habitats in 2050 and Beyond? **Coasts and Estuaries**, [s.I.], p. 1–28, 2019. DOI: https://doi.org/10.1016/b978-0-12-814003-1.00001-0.

ELLIOTT, M.; MCLUSKY, D. S. The Need for Definitions in Understanding Estuaries. **Estuarine, Coastal and Shelf Science**, [s. l.], v. 55, n. 6, p. 815–827, 2002. DOI: https://doi.org/10.1006/ecss.2002.1031.

EL-ROBRINI, M.; MARQUES JÚNIOR, V.; SILVA, M. A. M. A.; EL-ROBRINI, M. H. S.; FEITOSA, A. C.; TAROUCO, J. E. F.; SANTOS, J. H. S.; VIANA, J. R. Maranhão. In: MUEHE, D. (eds). **Erosão e progradação no litoral brasileiro**. Brasília: MMA, p. 87-130, 1992.

FAIRBRIDGE, R. W. The estuary: its definition and geodynamic cycle. In: OLAUSSON E, C. (Ed). **Chemistry and Biochemistry of Estuaries**. New York: John Wiley and Sons, p. 1-35, 1980.

FEITOSA, A. C. **O Maranhão primitivo: uma tentativa de constituição**. Ed. Augusta, São Luís. 1983. 142 p.

FERREIRA, J. G.; BRICKER, S. B.; SIMAS, T. C. Application and sensitivity testing of a eutrophication assessment method on coastal systems in the United States and European Union. **Journal of Environmental Managment**, v. 82, n. 4, p. 433–445, 2007. DOI: https://doi.org/10.1016/j.jenvman.2006.01.003.

FERREIRA, N. N.; FERREIRA, E. P.; RAMOS, R. R. C.; CARVALHO, I. DE S. Terrestrial and marine palynomorphs from deposits of the pull-apart rift of West Gondwana (Parnaíba Basin, northern Brazil): Biostratigraphy and relation to tectonic events. **Journal of South American Earth Sciences**, v. 101, 2020. DOI: https://doi.org/10.1016/j.jsames.2020.102612.

FERREIRA, N. N.; FERREIRA, E. P.; RAMOS, R. R. C.; CARVALHO, I. S. Palynological and sedimentary analysis of the Igarapé Ipiranga and Querru 1 outcrops of the Itapecuru Formation (Lower Cretaceous, Parnaíba Basin), Brazil. **Journal of South American Earth Sciences**, v. 66, p. 15–31, 2016. DOI: https://doi.org/10.1016/j.jsames.2015.12.005.

FERREIRA, N. N.; RAMOS, R. R. C.; FERREIRA, E. P.; CARVALHO, I. DE S. Lithofaciological analysis of the exposed rocks of the Itapecuru Formation, northeastern Parnaíba Basin, Brazil: paleoenvironmental implications. **Journal of South American Earth Sciences,** v. 107, 2021. DOI: https://doi.org/10.1016/j.jsames.2020.103114.

FORTUNE, J.; BUTLER, E. C. V.; GIBB, K. A decade of nitrogen inputs to a tropical macrotidal estuary of Northern Australia, Darwin Harbour. **Regional Studies in Marine Science**, v. 36, n. 101275, 2020. DOI: https://doi.org/10.1016/j.rsma.2020.101275.

GIOVANARDI, F.; VOLLENWEIDER, R.A. Trophic conditions of marine coastal waters: experience in applying the Trophic Index TRIX to two areas of the Adriatic and Tyrrhenian seas. **Journal of Limnology**, v. 63, n. 2, p. 199-218, 2009. DOI: https://doi.org/10.4081/jlimnol.2004.199.

GLASPIE, C. N.; JENKINSON, S. R.; SEITZ, R. D. Effects of Estuarine Acidification on an Oyster-Associated Community in New South Wales, Australia. **Journal of Shellfish Research**, v. 37, n. 1, p. 63–72, 2018. DOI: https://doi.org/10.2983/035.037.0105.

GÖLTENBOTH, F.; SCHOPPE, S. Estuaries and soft bottom shores. **Ecology of Insular.** Southeast Asia, p. 215–228. 2006. DOI: https://doi.org/10.1016/b978-044452739-4/50012-7.

GOMES, R. K. S.; PEREIRA, L. C. C.; RIBEIRO, C. M. M.; COSTA, R. M. DA. Dinâmica Socioambiental em uma Comunidade Pesqueira Amazônica, PA-Brasil. **Revista de Gestão Costeira Integrada**, v. 9, n. 2, p. 101–111, 2009. DOI: https://doi.org/10.5894/rgci121.

GONG, W.; LIN, Z.; ZHANG, H.; LIN, H. The response of salt intrusion to changes in river discharge, tidal range, and winds, based on wavelet analysis in the Modaomen estuary, China. **Ocean & Coastal Management**, v. 2019, n.106060, 2022. DOI: https://doi.org/10.1016/j.ocecoaman.2022.106060.

GONZÁLEZ-GORBEÑA, E.; ROSMAN, P. C. C.; QASSIM, R. Y. Assessment of the tidal current energy resource in São Marcos Bay, Brazil. **Journal of Ocean Engineering and Marine Energy**, v. 1, n. 4, p. 421–433, 2015. DOI: https://doi.org/10.1007/s40722-015-0031-5.

GUENTHER, M.; ARAÚJO, M.; FLORES-MONTES, M.; GONZALEZ-RODRIGUEZ, E.; NEUMANN-LEITÃO, S. Eutrophication effects on phytoplankton size-fractioned biomass and production at a tropical estuary. **Marine Pollution Bulletin**, v. 91, n. 2, p. 537–547, 2015. DOI: https://doi.org/10.1016/j.marpolbul.2014.09.048.

GUO, J.; KILDOW, J. The gap between science and policy: Assessing the use of nonmarket valuation in estuarine management based on a case study of US federally managed estuaries. **Ocean & Coastal Management**, v.108, p. 20–26, 2015. DOI: https://doi.org/10.1016/j.ocecoaman.2014.09.017.

KARYDIS, M. Eutrophication assessment of coastal waters based on indicators: a literature review. **Global Nest Journal**, v. 11, n. 4, p. 373-390, 2009. DOI: https://doi.org/10.30955/gnj.000626.

KASAI, A.; KURIKAWA, Y.; UENO, M.; ROBERT, D.; YAMASHITA, Y. Salt-wedge intrusion of seawater and its implication for phytoplankton dynamics in the Yura Estuary, Japan. Estuarine, **Coastal and Shelf Science**, v. 86, n. 3, p. 408–414, 2010. DOI: https://doi.org/10.1016/j.ecss.2009.06.001.

KJERFVE, B.; PERILLO, G.; GARDNER, L.; RINE, J.; DIAS, G.; MOCHEL, F. Morphodynamics of muddy environments along the Atlantic coasts of North and South America. In: HEALY, T.; WANG, Y.; HEALY, J. (eds) **Muddy coasts of the world: processes, deposits and functions**. Elsevier Science, Amsterdam, p. 479–532, 2002.

KJERFVE, B; LACERDA, L. D. Mangroves of Brazil. In: LACERDA, L. D. (eds) **Mangrove ecosystem studies in Latin America and Africa**. International Society for Mangrove Ecosystem, Technical reports, v. 2, 1993, p. 245-272.

KRVAVICA, N.; RUŽIĆ, I. Assessment of sea-level rise impacts on salt-wedge intrusion in idealized and Neretva River Estuary. **Estuarine, Coastal and Shelf Science**, v. 234, n. 106638, 2020. DOI: https://doi.org/10.1016/j.ecss.2020.106638.

LANCELOT, C.; MUYLAERT, K. Trends in estuarine phytoplankton ecology. In: Treatise on estuarine and coastal science, **Academic Press Waltham**, p. 5-15, 2011.

LARA, R. J. Amazonian mangroves–a multidisciplinary case study in Pará State, North Brazil: Introduction. **Wetlands ecology and management**, v. 11, n. 4, p. 217-221, 2003.

LE MOAL, M.; GASCUEL-ODOUX, C.; MÉNESGUEN, A.; SOUCHON, Y.; ÉTRILLARD, C.; LEVAIN, A.; MOATAR, F.; PANNARD, A.; SOUCHU, P.; LEFEBVRE, A.; PINAY, G. Eutrophication: A new wine in an old bottle? **Science of The Total Environment**, v. 651, p. 1–11, 2019. DOI: https://doi.org/10.1016/j.scitotenv.2018.09.139.

LEFÈVRE, N.; DA SILVA DIAS, F. J.; DE TORRES, A. R.; NORIEGA, C.; ARAUJO, M.; DE CASTRO, A. C. L.; ROCHA, C.; JIANG, S.; IBÁNHEZ, J. S. P. A source of CO2 to the atmosphere throughout the year in the Maranhense continental shelf (2°30'S, Brazil). **Continental Shelf Research**, v. 141, p. 38–50, 2017. https://doi.org/10.1016/j.csr.2017.05.004.

LELES, S. G.; SOUZA, C. A.; FARIA, C. O.; RAMOS, A. B.; FERNANDES, A. M.; MOSER, G. A. O. Short-term phytoplankton dynamics in response to tidal stirring in a tropical estuary (Southeastern Brazil). **Brazilian Journal of Oceanography**, v. 62, n. 4, p. 341–349, 2014. DOI: https://doi.org/10.1590/s1679-87592014070506204.

LEMLEY, D. A.; ADAMS, J. B. Eutrophication. **Encyclopedia of Ecology**, [s.I.], p. 86–90, 2019. DOI: https://doi.org/10.1016/b978-0-12-409548-9.10957-1.

LEMLEY, D. A.; ADAMS, J. B.; TALJAARD, S.; STRYDOM, N. A. Towards the classification of eutrophic condition in estuaries. **Estuarine, Coastal and Shelf Science**, v.164, p. 221–232, 2015. DOI: https://doi.org/10.1016/j.ecss.2015.07.033.

LERUSTE, A.; VILLÉGER, S.; MALET, N.; DE WIT, R.; BEC, B. Complementarity of the multidimensional functional and the taxonomic approaches to study phytoplankton communities in three Mediterranean coastal lagoons of different trophic status.

Hydrobiologia, v. 815, n. 1, p. 207–227, 2018. DOI: https://doi.org/10.1007/s10750-018-3565-4.

LIMA, H. P.; DIAS, F. J. S.; TEIXEIRA, C. E. P.; GODOI, V. A.; TORRES, A. R.; ARAÚJO, R. S. Implications of turbulence in a macrotidal estuary in northeastern Brazil - The São Marcos Estuarine Complex. **Regional Studies in Marine Science**, 47, 2021. DOI: https://doi.org/10.1016/j.rsma.2021.101947.

LINCOLN, R. J.; BOXSHALL G. A.; CLARK P. F. **A dictionary of ecology, evolution and systematics**. Cambridge: Cambridge University Press, 1982. 371p.

LØNBORG, C.; MÜLLER, M.; BUTLER, E. C. V.; JIANG, S.; OOI, S. K.; TRINH, D. H.; WONG, P. Y.; ALI, S. M.; CUI, C.; SIONG, W. B.; YANDO, E. S.; FRIESS, D. A.; ROSENTRETER, J. A.; EYRE, B. D.; MARTIN, P. Nutrient cycling in tropical and temperate coastal waters: Is latitude making a difference? **Estuarine, Coastal and Shelf Science**, v. 262, n. 107571, 2021. DOI: https://doi.org/10.1016/j.ecss.2021.107571.

MACEDO, L. A. A. Controle ambiental do Golfão Maranhense. **DAE**, v. 49, n.155, 1989.

MASULLO, Y. A. G.; SOARES, L. S.; DE CASTRO, C. E.; PINHEIRO, E. A. L. Dinâmica da paisagem da bacia hidrográfica do rio Itapecuru - MA. **Revista Braileira de Geografia Física,** v.12, 2019. DOI: https://doi.org/10.26848/rbgf.v12.3.p1054-1073.

MCLUSKY, D. S.; ELLIOTT, M. Life in estuaries. **The Estuarine Ecosystem**, [s.l.], p. 19–33. DOI: https://doi.org/10.1093/acprof:oso/9780198525080.003.0002.

MEERSSCHE, V. E.; PINCKNEY, J. L. Nutrient Loading Impacts on Estuarine Phytoplankton Size and Community Composition: Community-Based Indicators of Eutrophication. **Estuaries and Coasts**, v. 42, n. 2, p. 504–512, 2018. DOI: https://doi.org/10.1007/s12237-018-0470-z.

MENEZES, M. N.; ARAÚJO-JÚNIOR, H. I.; DAL' BÓ, P. F.; MEDEIROS, M. A. A. Integrating ichnology and paleopedology in the analysis of Albian alluvial plains of the Parnaíba Basin, Brazil. **Cretaceous Research**, v. 96, p. 210–226, 2019. DOI: https://doi.org/10.1016/j.cretres.2018.12.013.

MOURÃO, F. V.; SANTOS, M. L. S.; SOUSA, P. H. C.; RIBEIRO, D. C. S.; GADELHA, E. S. Dinâmica sazonal de nutrientes em estuário amazônico. **Revista Brasileira de Geografia Física**, v. 14, n. 1, p. 372-381, 2020. DOI: 10.26848/rbgf.v14.1.p372-381.

MUYLAERT, K.; SABBE, K.; VYVERMAN, W. Changes in phytoplankton diversity and community composition along the salinity gradient of the Schelde estuary (Belgium/The Netherlands). **Estuarine, Coastal and Shelf Science**, [s.l.], v.82, n. 2, p. 355-340, 2009. DOI: https://doi.org/10.1016/j.ecss.2009.01.024.

NCHE-FAMBO, F. A.; SCHARLER, U. M.; TIROK, K. Resilience of estuarine phytoplankton and their temporal variability along salinity gradients during drought and hypersalinity. **Estuarine, Coastal and Shelf Science**, v. 158, p. 40–52, 2015. https://doi.org/10.1016/j.ecss.2015.03.011.

NEEA/ASSETS. Assessment of Estuarine Trophic Status: Methods. Disponível em: http://www.eutro.org/methods.aspx. Acesso em: 03 jan. 2021.

NEUBAUER, S. C. Ecosystem Responses of a Tidal Freshwater Marsh Experiencing Saltwater Intrusion and Altered Hydrology. **Estuaries and Coasts**, v. 36, n. 3, p. 491–507, 2011. https://doi.org/10.1007/s12237-011-9455-x.

NGUYEN, A. T.; GRATIOT, J. N. N.; DAO, T. S.; LE, T. T. M.; GARNIER, C. B. J. Does eutrophication enhance greenhouse gas emissions in urbanized tropical estuaries? **Environmental Pollution**, v. 303, n. 119105, 2022. DOI: https://doi.org/10.1016/j.envpol.2022.119105.

NICOLODI, J. L.; ZAMBONI, A.; BARROSO, G. F. Gestão Integrada de Bacias Hidrográficas e Zonas Costeiras no Brasil: Implicações para a Região Hidrográfica Amazônica. **Revista de Gestão Costeira Integrada**, v. 9, n. 2, p. 9–32, 2009. DOI: https://doi.org/10.5894/rgci115.

NIVEDITHA, S. K.; HARIDEVI, C. K.; HARDIKAR, R.; RAM, A. Phytoplankton assemblage and chlorophyll a along the salinity gradient in a hypoxic eutrophic tropical estuary-Ulhas Estuary, West Coast of India. **Marine Pollution Bulletin**, v. 180, 2022. DOI: https://doi.org/10.1016/j.marpolbul.2022.113719.

NORIEGA, C.; ARAUJO, M.; FLORES-MONTES, M.; ARAUJO, J. Trophic dynamics (Dissolved Inorganic Nitrogen-DIN and Dissolved Inorganic Phosphorus-DIP) in tropical urban estuarine systems during periods of high and low river discharge rates. **Anais Da Academia Brasileira de Ciências**, v. 9, n.2, 2019. DOI: https://doi.org/10.1590/0001-3765201920180244

NWE, L.W.; YOKOYAMA, K.; AZHIKODAN G. Phytoplankton habitats and size distribution during a neap-spring transition in the highly turbid macrotidal Chikugo River estuary. **Science of The Total Environment**, v. 850, 2022. DOI: https://doi.org/10.1016/j.scitotenv.2022.157810.

OECD. **Organization for Economic Cooperation and Development**. Core Set of Indicators for Environmental Performance Reviews. Paris, 1993, p. 93.

OLIVEIRA, A. R. G.; ODEBRECHT, C.; PEREIRA, L. C. C.; COSTA, R. M. Phytoplankton variation in an Amazon estuary with emphasis on the diatoms of the Order Eupodiscales. **Ecohydrology & Hydrobiology**, v. 22, n. 1, p. 55–74, 2022. DOI: https://doi.org/10.1016/j.ecohyd.2021.12.001.

OLLI, K.; PTACNIK, R.; KLAIS, R.; TAMMINEN, T. Phytoplankton Species Richness along Coastal and Estuarine Salinity Continua. **The American Naturalist**, v. 194, n. 2, p. 41–51, 2019. DOI: https://doi.org/10.1086/703657.

OLOFSSON, M.; HAGAN, J. G.; KARLSON, B.; GAMFELDT, L. Large seasonal and spatial variation in nano- and microphytoplankton diversity along a Baltic Sea—North Sea salinity gradient. **Scientific Reports**, v. 10, n. 1, 2020. https://doi.org/10.1038/s41598-020-74428-8.

PAERL, H. W. Structure and function of anthropogenically altered microbial communities in coastal waters. **Current Opinion in Microbiology**, v. 1, n.3, p. 296–302. 2018. DOI: https://doi.org/10.1016/s1369-5274(98)80033-7

PAERL, H. W., HALL, N. S., PEIERLS, B. L., ROSSIGNOL, K. L. (2014). Evolving Paradigms and Challenges in Estuarine and Coastal Eutrophication Dynamics in a Culturally and Climatically Stressed World. **Estuaries and Coasts**, v. 37, n. 2, p. 243–258. DOI: https://doi.org/10.1007/s12237-014-9773-x

PAERL, H. W.; JUSTIĆ, D. Primary Producers. **Treatise on Estuarine and Coastal** Science, [s.l.], p. 23–42, 2011. DOI: https://doi.org/10.1016/b978-0-12-374711-2.00603-3.

PAULA-FILHO, F. J.; MARINS, R. V.; CHICHARO, L.; SOUZA, R. B.; SANTOS, G. V.; BRAZ, E. M. A. Evaluation of water quality and trophic state in the Parnaíba River Delta, northeast Brazil. **Regional Studies in Marine Science**, v. 34, n. 101025. DOI: https://doi.org/10.1016/j.rsma.2019.101025.

PAULA-FILHO, F. J.; MARINS, R. V.; DE LACERDA, L. D. Natural and anthropogenic emissions of N and P to the Parnaíba River Delta in NE Brazil. **Estuarine, Coastal and Shelf Science**, v. 166, p. 34–44, 2015. DOI: https://doi.org/10.1016/j.ecss.2015.03.020.

PEREIRA, L. C. C.; DA COSTA, Á. K. R.; DA COSTA, R. M.; MAGALHÃES, A.; DE JESUS FLORES-MONTES, M., JIMÉNEZ, J. A. Influence of a Drought Event on Hydrological Characteristics of a Small Estuary on the Amazon Mangrove Coast. **Estuaries and Coasts**, v. 41, n. 3, p. 676–689, 2018. DOI: https://doi.org/10.1007/s12237-017-0310-6.

PEREIRA, L. C. C.; DIAS, J. A.; DO CARMO, J. A.; POLETTE, M. A Zona costeira amazônica brasileira. **Revista de Gestão Costeira Integrada**, v. 9, n. 2, p. 3-7, 2009.

PERILLO, G. M. E. Definitions and geomorphologic classifications of estuaries. In: PERILLO, G. M. E. (Ed). Geomorphology and sedimentology of estuaries, developments in sedimentology. **Elsevier Science**, Berlin, v. 53, p. 12-47, 1995.

POTTER, I. C.; CHUWEN, B. M.; HOEKSEMA, S. D.; ELLIOTT, M. The concept of an estuary: A definition that incorporates systems which can become closed to the ocean and hypersaline. **Estuarine, Coastal and Shelf Science**, [s.l.], v. 87, n. 3, p. 497-500, 2010.

PRITCHARD, D. W. What is an estuary? Physical viewpoint. In: LAUFF, G. H. (Ed). **Estuaries: American Association for the Advancement of Science**, Publication 83, p. 3-5, 1967.

RÊGO, J. C. L.; SOARES-GOMES, A.; DA SILVA, F. S. Loss of vegetation cover in a tropical island of the Amazon coastal zone (Maranhão Island, Brazil). Land Use Policy, v. 71, p. 593–601, 2018. DOI: https://doi.org/10.1016/j.landusepol.2017.10.055.

REIS, F. N.; BELÚCIO, L. F.; PAMPLONA, F. C.; REIS, L. T. L.; VEIGA, G. D.; MELO, N. F. A. C. Microphytoplankton dynamics in Curuperé estuary at the amazonian mangrove ecosystem. **Boletim Do Instituto de Pesca**, v. 46, n.1, 2019. DOI: https://doi.org/10.20950/1678-2305.2020.46.1.513.

RIBEIRO, D. C. DE S.; PALHETA, G. D. A.; PAMPLONA, F. C.; HAMOY, I. G.; SANTOS, M. DE L. S.; MELO, N. F. A. C. DE. Effects of environmental factors on succession of micro-phytoplankton community in a marine shrimp pond and adjacent amazon estuary. **Boletim Do Instituto de Pesca**, v. 45, n. 4, 2019. DOI: https://doi.org/10.20950/1678-2305.2019.45.4.508.

ROSHITH, C. M.; MEENA, D. K.; MANNA, R. K.; SAHOO, A. K.; SWAIN, H. S.; RAMAN, R. K.; SENGUPTA, A.; DAS, B. K. Phytoplankton community structure of the Gangetic (Hooghly-Matla) estuary: Status and ecological implications in relation to eco-climatic variability. **Flora**, v. 240, p. 133–143, 2018. DOI: https://doi.org/10.1016/j.flora.2018.01.001.

SÁ, A. K. D. DOS S.; CUTRIM, M. V. J.; COSTA, D. S.; CAVALCANTI, L. F.; FERREIRA, F. S.; OLIVEIRA, A. L. L.; SEREJO, J. H. F. Algal blooms and trophic state in a tropical estuary blocked by a dam (northeastern Brazil). **Ocean and Coastal Research**, v. 69, [s.I.], 2021. DOI: https://doi.org/10.1590/2675-2824069.20-006akddss.

SANTIAGO, M. F.; SILVA-CUNHA, M. DA G. G. DA; NEUMANN-LEITÃO, S.; COSTA, K. M. P. DA; PALMEIRA, G. C. B.; PORTO NETO, F. DE F.; NUNES, F. S. Phytoplankton dynamics in a highly eutrophic estuary in tropical Brazil. **Brazilian Journal of Oceanography**, v. 58, n. 3, p. 189–205, 2010. DOI: https://doi.org/10.1590/s1679-87592010000300002.

SANTOS, A. K. D. DOS; OLIVEIRA, A. L. L.; FURTADO, J. A.; FERREIRA, F. S.; ARAÚJO, B. DE O.; CORRÊA, J. J. M.; CAVALCANTI, L. F.; CUTRIM, A. C. G. DE A.; CUTRIM, M. V. J. Spatial and seasonal variation of microphytoplankton community and the correlation with environmental parameters in a hypereutrophic tropical estuary - Maranhão - Brazil. **Brazilian Journal of Oceanography**, v. 65, n.3, p. 356–372, 2017. DOI: https://doi.org/10.1590/s1679-87592017134406503.

SCHAEFFER-NOVELLI, Y.; CINTRÓN MOLERO, G.; ROTHLEDER ADAIME, R.; CAMARGO, T. M. D. Variability of mangrove ecosystems along the Brazilian coast. **Estuaries,** v. 13, n. 2, p. 204–218, 1990.

SENA, B. A.; COSTA, V. B.; NAKAYAMA, L.; ROCHA, R. M. Composition of Microphytoplankton of an Estuarine Amazon River, Pará, Brazil. **Biota Amazônia**, v. 5, n. 2, p. 1–9, 2015. DOI: https://doi.org/10.18561/2179-5746/biotaamazonia.v5n2p1-9.

SEREJO, J. H. F.; SANTOS, T. T. L.; LIMA, H. P.; AZEVEDO, I. H. R.; DOS SANTOS, V. H. M.; ESCHRIQUE, S. A. Fortnightly variability of total suspended solids and bottom sediments in a macrotidal estuarine complex on the Brazilian northern coast. **Journal of Sedimentary Environments**, v. 5, n. 1, p. 101–115, 2020. DOI: https://doi.org/10.1007/s43217-020-00005-8.

SILVA, A. S. X.; NORIEGA, C.; KOENING, M. L.; MONTES, M. F.; ARAUJO, M. Distribution of Nutrients and Changes in Phytoplankton Composition in a Tropical Mesotidal Estuary, Northeastern Brazil. **Open Journal of Ecology**, v. 7, n. 7, p. 460–494, 2017. DOI: https://doi.org/10.4236/oje.2017.77032.

SILVA, B. J.; IBÁNHEZ, J. S. P.; PINHEIRO, B. R.; LADLE, R. J.; MALHADO, A. C.; PINTO, T. K.; FLORES-MONTES, M. J. Seasonal influence of surface and underground continental runoff over a reef system in a tropical marine protected area. **Journal of Marine Systems**, v.226, 2022. DOI: https://doi.org/10.1016/j.jmarsys.2021.103660.

SILVA, N. B. A.; FLORES-MONTES, M.; GUENNES, M.; BORGES, G.; NORIEGA, C.; ARAUJO, M.; SILVA-CUNHA, M. DA G. G. Phytoplankton cell size in an urban tropical estuarine system in Northeast Brazil. **Regional Studies in Marine Science**, v. 43, 2021. DOI: https://doi.org/10.1016/j.rsma.2021.101659.

SOUSA-FELIX, R. C.; PEREIRA, L. C. C.; TRINDADE, W. N.; DE SOUZA, I. P.; DA COSTA, R. M.; JIMENEZ, J. A. Application of the DPSIR framework to the evaluation of the recreational and environmental conditions on estuarine beaches of the Amazon coast. **Ocean & Coastal Management**, v. 149, p. 96–106, 2017. DOI: https://doi.org/10.1016/j.ocecoaman.2017.09.011.

SOUZA-FILHO, P. W. M.; GONÇALVES, F. D.; BEISL, C. H.; MIRANDA, F. P.; ALMEIDA, E. F.; CUNHA, E.R.S.P. Coastal observing system and the role of the remote sensors in the Northern Brazilian coast monitoring, Amazon. **Revista Brasileira de Cartografia**, v. 57, p. 79-86, 2005.

STRAMMA, L.; FISCHER, J.; BRANDT, P.; SCHOTT, F. Circulation, variability and near-equatorial meridional flow in the central tropical Atlantic. **Elsevier Oceanography Series**, v. 68, p. 1–22, 2003.

SZLAFSZTEIN, C. F. The Brazilian Amazon coastal zone management: implementation and development obstacles. **Journal of Coastal Conservation**, v. 16, n. 3, p. 335–343, 2012. DOI: https://doi.org/10.1007/s11852-012-0184-5.

TARAFDAR, L.; KIM, J. Y.; SRICHANDAN, S.; MOHAPATRA, M.; MUDULI, P. R.; KUMAR, A.; MISHRA, D. R.; RASTOGI, G. Responses of phytoplankton community structure and association to variability in environmental drivers in a tropical coastal lagoon. **Science of The Total Environment**, v. 783, 2021. DOI: https://doi.org/10.1016/j.scitotenv.2021.146873.

TAS, S.; YILMAZ, I. N.; OKUS, E. Phytoplankton as an Indicator of Improving Water Quality in the Golden Horn Estuary. **Estuaries and Coasts**, v. 32, n. 6, p. 1205–1224, 2009. DOI: https://doi.org/10.1007/s12237-009-9207-3.

TAVARES, J. L.; CALADO, A. L. A.; FONTES, R. F. C. Initial studies to use the index TRIX for analysis of eutrophication in estuary Potengi river - Natal – RN – Brazil. **Revista AIDIS de Ingeniería y Ciencias Ambientales: Investigación Desarrollo Práct**., v. 7, n. 3, p. 297-308, 2014.

TEIXEIRA, S. G.; SOUZA-FILHO, P. W. M. E. Mapeamento de ambientes costeiros tropicais (Golfão Maranhense, Brasil) utilizando imagens de sensores remotos orbitais. **Revista Brasileira de Geofísica**, v. 27, p. 69–82, 2009. DOI: https://doi.org/10.1590/s0102-261x2009000500006.

TWEEDLEY, J. R.; DITTMANN, S. R.; WHITFIELD, A. K.; WITHERS, K.; HOEKSEMA, S. D.; POTTER, I. C. Hypersalinity: Global Distribution, Causes, and Present and Future Effects on the Biota of Estuaries and Lagoons. **Coasts and Estuaries**, [s.l.], p. 523–546, 2019. https://doi.org/10.1016/b978-0-12-814003-1.00030-7.

VANNUCCI, M. **Os manguezais e nós: Uma síntese de percepcões**. ESDUP, São Paulo, 1999. 233 p.

VEERAPAGA, N.; AZHIKODAN, G.; SHINTANI, T.; IWAMOTO, N.; YOKOYAMA, K. A three-dimensional environmental hydrodynamic model, Fantom-Refined: Validation and application for saltwater intrusion in a meso-macrotidal estuary. **Ocean Modelling**, v. 141, n.101425, 2019. DOI: https://doi.org/10.1016/j.ocemod.2019.101425.

VILHENA, M. P. S. P.; COSTA, M. L.; BERRÊDO, J. F.; PAIVA, R. S.; MOREIRA, M. Z. Trace elements and C and N isotopes in sediments, phytoplankton and oysters as indicators of anthropogenic activities in estuaries in the Brazilian Amazon. **Regional Studies in Marine Science**, v. 41, 2021. DOI: https://doi.org/10.1016/j.rsma.2021.101618.

VISSCHERS, L. L. B.; SANTOS, C. D.; FRANCO, A. M. A. Accelerated migration of mangroves indicate large-scale saltwater intrusion in Amazon coastal wetlands. **Science of The Total Environment**, v. 836, n. 155679, 2022. DOI: https://doi.org/10.1016/j.scitotenv.2022.155679.

VOLLENWEIDER, R.A.; GIOVANARDI, F.; MONTANARI, G.; RINALDI, A. Characterization of the trophic conditions of marine coastal waters with special reference to the NW Adriatic Sea: proposal for a trophic scale, turbidity and generalized water quality index. **Environmetrics**, v. 9, p. 329-357, 1998. DOI: https://doi.org/10.1002/(SICI)1099-095X(199805/06)9:3<329::AID-ENV308>3.0.CO;2-9.

WERNER, A. D.; BAKKER, M.; POST, V. E. A.; VANDENBOHEDE, A.; LU, C.; ATAIE-ASHTIANI, B.; SIMMONS, C. T.; BARRY, D. A. Seawater intrusion processes, investigation and management: Recent advances and future challenges. **Advances in Water Resources**, v. 51, p. 3–26, 2013. DOI: https://doi.org/10.1016/j.advwatres.2012.03.004.

WETZ, M. S.; YOSKOWITZ, D. W. An 'extreme' future for estuaries? Effects of extreme climatic events on estuarine water quality and ecology. **Marine Pollution Bulletin**, v. 69, n. 1–2, p. 7–18, 2013. DOI: https://doi.org/10.1016/j.marpolbul.2013.01.020.

WHITFIELD, A.; ELLIOTT, M. Ecosystem and Biotic Classifications of Estuaries and Coasts. **Treatise on Estuarine and Coastal Science**, [s.l.], p. 99–124. DOI: https://doi.org/10.1016/b978-0-12-374711-2.00108-x.

WINDER, M.; CARSTENSEN, J.; GALLOWAY, A. W. E.; JAKOBSEN, H. H.; CLOERN, J. E. The land-sea interface: A source of high-quality phytoplankton to support secondary production. **Limnology and Oceanography**, v. 62, n. 1, p. 258–271, 2017. DOI: https://doi.org/10.1002/lno.10650.

ZHANG, P.; OU S.; ZHANG, J.; ZHAO, L.; ZHANG, J. Categorizing numeric nutrients criteria and implications for water quality assessment in the Pearl River Estuary, China.

Frontiers Marine Science, v. 9, n.1004235, p. 1-17. 2022. DOI: https://doi.org/10.3389/fmars.2022.1004235

APÊNDICE A – ARTIGO 1

PHYTOPLANKTON COMMUNITY DYNAMICS IN RESPONSE TO SEAWATER INTRUSION IN A TROPICAL MACROTIDAL RIVER-ESTUARY CONTINUUM

Figura 1 - Distribuição taxonômica geral da comunidade fitoplanctônica ao longo do estuário do rio Itapecuru (Golfão Maranhense).

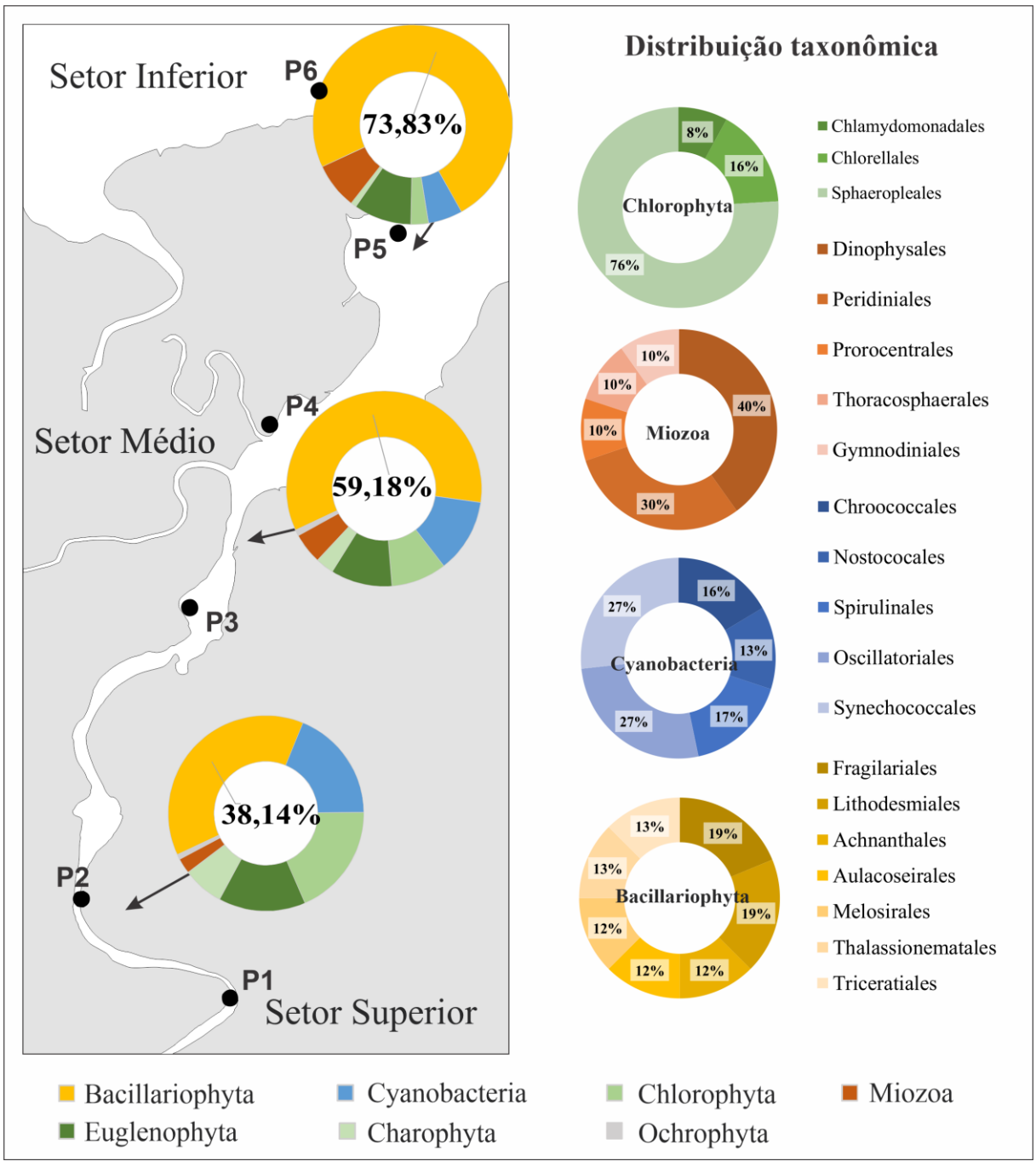

Fonte: O Autor (2022)

Figura 2 - Diagramas de classificação dos táxons identificados nos setores superior (SS), médio (SM) e inferior (SI) do Estuário do Rio Itapecuru (ERI). Onde: a representação de Olmstead-Tukey (OT) relacionou a frequência de ocorrência e a densidade média do fitoplâncton. Os códigos das espécies identificadas foram descritos na tabela 4 do artigo 1.

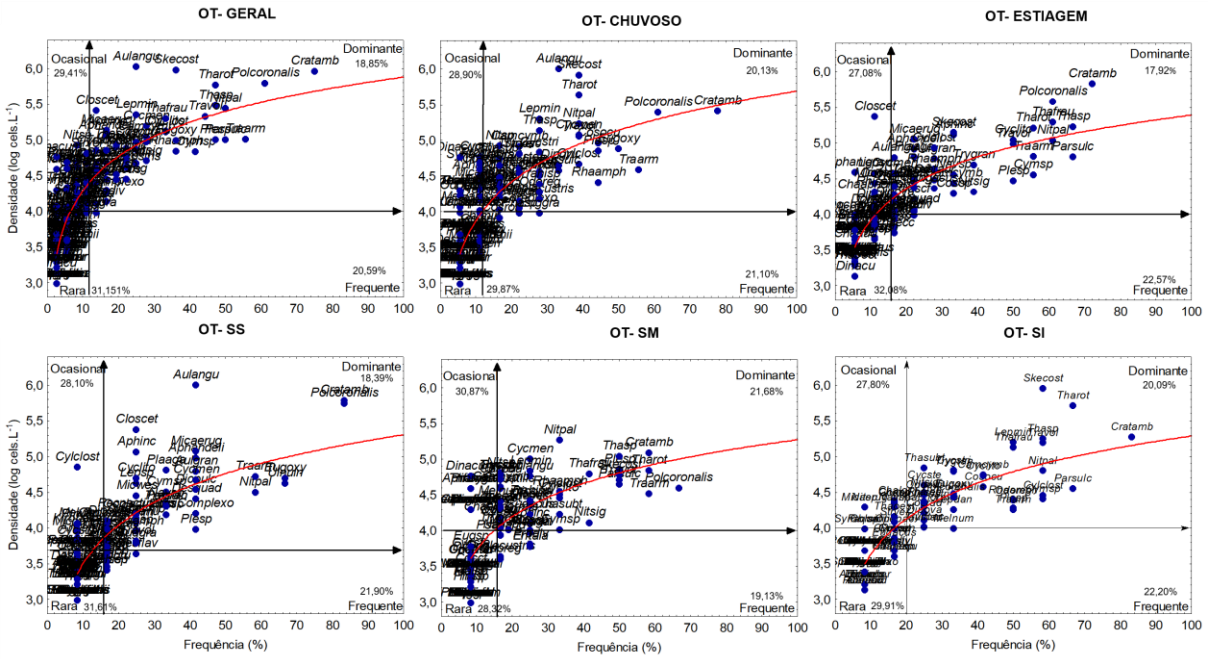

Fonte: O Autor (2022)

Figura 3 - Correlação entre os principais indicadores do fitoplâncton e variáveis ambientais ao longo do estuário do Rio Itapecuru (ERI).

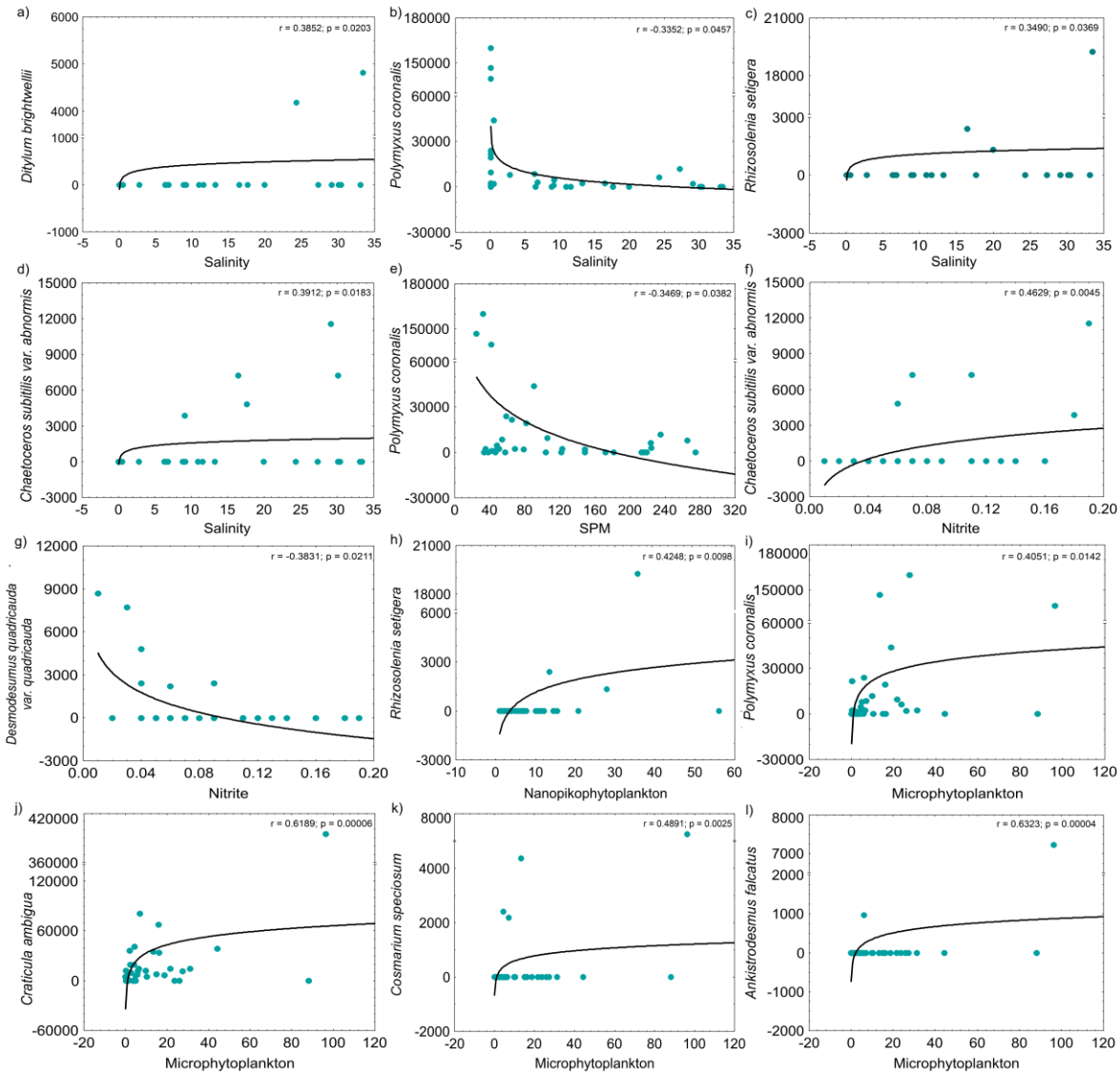

Fonte: O Autor (2022)

Tabela 1- Distribuição das cianobactérias nos setores do estuário do rio Itapecuru (Golfão Maranhense).

CYANOBACTERIA	Abundância (x 10^3 céls L^{-1})	Superior	Médio	Inferior	Classe	Ordem	Família	Ecologia
Aphanizomenon gracile Lemmermann, 1907	39	-	+	-	Cyanophyceae	Nostococales	Aphanizomenonaceae	Dulcícola
Aphanocapsa incerta (Lemmermann) G.Cronberg & Komárek, 1994	129	+	+	-	Cyanophyceae	Synechococcales	Merismopediaceae	Dulcícola
Aphanocapsa delicatissima West & G.S.West, 1912	114	+	+	-	Cyanophyceae	Synechococcales	Merismopediaceae	Dulcícola
Arthrospira platensis Gomont, 1892	2	+	-	-	Cyanophyceae	Oscillatoriales	Microcoleaceae	Dulcícola
Chroococcus minutus (Kützing) Nägeli, 1849	9	+	-	+	Cyanophyceae	Chroococcales	Chroococcaceae	Dulcícola
Cuspidothrix issatschenkoi (Usachev) P.Rajaniemi, Komárek, R.Willame, P. Hrouzek, K.Kastovská, L.Hoffmann & K.Sivonen, 2005	7	+	-	-	Cyanophyceae	Nostococales	Aphanizomenonaceae	Dulcícola
Dolichospermum planctonicum (Brunnthaler) Wacklin, L.Hoffmann & Komárek, 2009	12	+	-	-	Cyanophyceae	Nostococales	Aphanizomenonaceae	Dulcícola
Dolichospermum crassum (Lemmermann) P.Wacklin, L.Hoffmann & J.Komárek, 2009	2	+	-	-	Cyanophyceae	Nostococales	Aphanizomenonaceae	Dulcícola
Geitlerinema sp.	6	+	+	-	Cyanophyceae	Oscillatoriales	Coleofasciculaceae	Dulcícola
Komvophoron crassum (Vozzhennikova) Anagnostidis & Komárek, 1988	2	-	+	-	Cyanophyceae	Oscillatoriales	Gomontiellaceae	Dulcícola
Leptolyngbya sp.	42	+	-	-	Cyanophyceae	Synechococcales	Leptolyngbyaceae	Dulcícola
Limnothrix borgertii (Lemmermann) Anagnostidis, 2001	2	+	-	-	Cyanophyceae	Synechococcales	Pseudanabaenaceae	Dulcícola
Lyngbya sp.	9	+	-	-	Cyanophyceae	Oscillatoriales	Oscillatoriaceae	Dulcícola
Merismopedia tenuissima Lemmermann, 1898	13	+	+	-	Cyanophyceae	synechococcales	Merismopediaceae	Dulcícola
Microcystis aeruginosa (Kützing) Kützing, 1846	136	+	-	+	Cyanophyceae	Chroococcales	Microcystaceae	Estuarina
Microcystis panniformis Komárek, Komárková-Legnerová, Sant'Anna, M.T.P.Azevedo, & P.A.C.Senna, 2002	9	+	-	-	Cyanophyceae	Chroococcales	Microcystaceae	Dulcícola
Microcystis wesenbergii (Komárek) Komárek ex Komárek, 2006	47	+	+	-	Cyanophyceae	Chroococcales	Microcystaceae	Dulcícola
Oscillatoria sp_1	2	-	+	-	Cyanophyceae	Oscillatoriales	Oscillatoriaceae	Dulcícola
Oscillatoria sp_2	5	+	+	-	Cyanophyceae	Oscillatoriales	Oscillatoriaceae	Dulcícola
Oscillatoria limosa C.Agardh ex Gomont, 1892	2	-	-	+	Cyanophyceae	Oscillatoriales	Oscillatoriaceae	Dulcícola
Planktolyngbya limnetica (Lemmermann) Komárková-Legnerová & Cronberg, 1992	14	+	+	-	Cyanophyceae	Synechococcales	Leptolyngbyaceae	Dulcícola
Planktothrix agardhii (Gomont) Anagnostidis & Komárek, 1988	76	+	+	+	Cyanophyceae	Oscillatoriales	Microcystaceae	Dulcícola
Pseudanabaena acicularis (Nygaard) Anagnostidis & Komárek ,1988	9	+	-	-	Cyanophyceae	Synechococcales	Pseudanabaenaceae	Dulcícola
Radiocystis elongata Hindák, 1996	2	+	-	-	Cyanophyceae	Chroococcales	Micocystaceae	Dulcícola
Spirulina sp. (Complexo)	18	+	-	+	Cyanophyceae	Spirulinales	Spirulinaceae	Dulcícola
Spirulina laxissima G.S.West, 1907	5	+	-	-	Cyanophyceae	Spirulinales	Spirulinaceae	Dulcícola
Synechocystis aquatilis Sauvageau, 1892	48	-	+	+	Cyanophyceae	Synechococcales	Merismopediaceae	Dulcícola

Fonte: O Autor (2022)

Tabela 2 - Distribuição das clorofíceas nos setores do estuário do rio Itapecuru (Golfão Maranhense).

CHLOROPHYTA	Abundância (x 10^3 céls L^{-1})	Superior	Médio	Inferior	Classe	Ordem	Família	Ecologia
Ankistrodesmus falcatus (Corda) Ralfs, 1848	15	+	-	-	Chlorophyceae	Sphaeropleales	Selenastraceae	Dulcícola
Chlamydomonas sp.	16	+	+	+	Chlorophyceae	Chlamydomonadales	Chlamydomonadaceae	Dulcícola
Coelastrum microporum Nägeli, 1855	19	-	+	-	Chlorophyceae	Sphaeropleales	Scenedesmaceae	Dulcícola
Desmodesmus armatus var. bicaudatus (Guglielmetti) E.H.Hegewald, 2000	3	+	-	-	Chlorophyceae	Sphaeropleales	Scenedesmaceae	Dulcícola
Desmodesmus communis (E.Hegewald) E.Hegewald, 2000	2	+	-	-	Chlorophyceae	Sphaeropleales	Scenedesmaceae	Dulcícola
Desmodesmus denticulatus (Lagerheim) S.S.An, T.Friedl & E.Hegewald, 1999	1	+	-	-	Chlorophyceae	Sphaeropleales	Scenedesmaceae	Dulcícola
Desmodesmus flavescens (Chodat) E.Hegewald, 2000	24	+	+	-	Chlorophyceae	Sphaeropleales	Scenedesmaceae	Dulcícola
Desmodesmus lunatus (West & G.S.West) E.Hegewald, 2000	3	+	-	-	Chlorophyceae	Sphaeropleales	Scenedesmaceae	Dulcícola
Desmodesmus protuberans (F.E.Fritsch & M.F.Rich) E.Hegewald, 2000	4	+	-	-	Chlorophyceae	Sphaeropleales	Scenedesmaceae	Dulcícola
Desmodesmus serratus (Corda) S.S.An, Friedl & E.Hegewald, 1999	3	+	-	-	Chlorophyceae	Sphaeropleales	Scenedesmaceae	Dulcícola
Desmodesmus spinulatus (Biswas) E.Hegewald, 2000	2	+	-	-	Chlorophyceae	Sphaeropleales	Scenedesmaceae	Dulcícola
Dictyosphaerium pulchellum H.C.Wood, 1873	58	+	+	-	Trebouxiophyceae	Chlorellales	Chlorellaceae	Dulcícola
Eudorina elegans Ehrenberg, 1832	1	+	-	-	Chlorophyceae	Chlamydomonadales	Volvocaceae	Dulcícola
Eutetramorus fottii (Hindák) Komárek, 1979	2	+	-	-	Chlorophyceae	Sphaeropleales	Radiococcaceae	Dulcícola
Kirchneriella obesa (West) West & G.S.West, 1894	10	+	-	-	Chlorophyceae	Sphaeropleales	Scenedesmaceae	Dulcícola
Monoraphidium griffithii (Berkeley) Komárková-Legnerová, 1969	3	+	+	-	Chlorophyceae	Sphaeropleales	Selenastraceae	Dulcícola
Oocystis borgei J.W.Snow, 1903	12	+	-	-	Trebouxiophyceae	Chlorellales	Oocystaceae	Dulcícola
Oocystis lacustris Chodat, 1897	41	+	+	+	Trebouxiophyceae	Chlorellales	Oocystaceae	Dulcícola
Pectinodesmus pectinatus (Meyen) E.Hegewald, M.Wolf, Al.Keller, Friedl & Krienitz, 2010	40	+	+	+	Chlorophyceae	Sphaeropleales	Scenedesmaceae	Dulcícola
Pediastrum duplex Meyen, 1829	5	+	-	-	Chlorophyceae	Sphaeropleales	Hydrodictyaceae	Dulcícola
Pediastrum privum (Printz) Hegewald, 1979	1	-	+	-	Chlorophyceae	Sphaeropleales	Hydrodictyaceae	Dulcícola
Scenedesmus ecornis (Ehrenberg) Chodat, 1926	1	+	-	-	Chlorophyceae	Sphaeropleales	Scenedesmaceae	Dulcícola
Scenedesmus javanensis Chodat, 1926	5	+	-	-	Chlorophyceae	Sphaeropleales	Scenedesmaceae	Dulcícola
Scenedesmus obtusus Meyen, 1829	3	+	-	-	Chlorophyceae	Sphaeropleales	Scenedesmaceae	Dulcícola
Scenedesmus quadricauda (Turpin) Brébisson, 1835	28	+	+	-	Chlorophyceae	Sphaeropleales	Scenedesmaceae	Dulcícola

Fonte: O Autor (2022)

Tabela 3 - Distribuição das clorofíceas nos setores do estuário do rio Itapecuru (Golfão Maranhense).

CHAROPHYTA	Abundância (x 10^3 céls L^{-1})	Superior	Médio	Inferior	Classe	Ordem	Família	Ecologia
Actinotaenium globosum (Bulnheim) Kurt Förster ex Compère, 1976	4	+	-	-	Zygnematophyceae	Desmidiales	Desmidiaceae	Dulcícola
Closterium kuetzingii Brébisson, 1856	1	+	-	-	Zygnematophyceae	Desmidiales	Closteriaceae	Dulcícola
Closterium setaceum Ehrenberg ex Ralfs, 1848	257	+	+	-	Zygnematophyceae	Desmidiales	Closteriaceae	Dulcícola
Cosmarium speciosum P.Lundell, 1871	16	+	+	-	Zygnematophyceae	Desmidiales	Desmidiaceae	Dulcícola
Gonatozygon aculeatum W.N.Hastings, 1892	27	+	-	+	Zygnematophyceae	Desmidiales	Gonatozygaceae	Dulcícola
Micrasterias furcata C.Agardh ex Ralfs, 1848	2	-	+	-	Zygnematophyceae	Desmidiales	Desmidiaceae	Dulcícola
Staurastrum elongatum J.Barker, 1869	3	+	-	-	Zygnematophyceae	Desmidiales	Desmidiaceae	Dulcícola
Staurastrum rotula Nordstedt, 1869	1	+	-	-	Zygnematophyceae	Desmidiales	Desmidiaceae	Dulcícola
Staurastrum senarium Ralfs, 1848	2	+	-	-	Zygnematophyceae	Desmidiales	Desmidiaceae	Dulcícola

Fonte: O Autor (2022)

Tabela 4 - Distribuição de dinoflagelados nos setores do estuário do rio Itapecuru (Golfão Maranhense).

MIOZOA	Abundância (x 10^3 céls L^{-1})	Superior	Médio	Inferior	Classe	Ordem	Família	Ecologia
Dinophysis acuminata Claparède & Lachmann, 1859	58	-	+	-	Dinophyceae	Dinophysales	Dinophysaceae	Marinha
Dinophysis acuta Ehrenberg, 1839	1	-	-	+	Dinophyceae	Dinophysales	Dinophysaceae	Marinha
Dinophysis caudata Kent, 1881	3	-	+	+	Dinophyceae	Dinophysales	Dinophysaceae	Marinha
Gymnodinium wulffii J.Schiller, 1932	5	-	-	+	Dinophyceae	Gymnodiniales	Gymnodiniaceae	Marinha
Heterocapsa rotundata (Lohmann) Gert Hansen, 1995	7	+	-	+	Dinophyceae	Peridiniales	Heterocapsaceae	Marinha
Oxyphysis oxytoxoides Kofoid, 1926	2	-	-	+	Dinophyceae	Dinophysales	Oxyphysaceae	Marinha
Prorocentrum micans Ehrenberg, 1834	48	-	+	+	Dinophyceae	Prorocentrales	Prorocentraceae	Marinha
Protoperidinium brevipes (Paulsen) Balech, 1974	1	-	+	-	Dinophyceae	Peridiniales	Protoperidiniaceae	Marinha
Protoperidinium divergens (Ehrenberg) Balech, 1974	14	+	+	+	Dinophyceae	Peridiniales	Protoperidiniaceae	Marinha
Scrippsiella trochoidea (F.Stein) A.R.Loeblich III, 1976	14	+	-	+	Dinophyceae	Thoracosphaerales	Thoracosphaeraceae	Marinha

Fonte: O Autor (2022)

Tabela 5 - Distribuição de euglenofíceas nos setores do estuário do rio Itapecuru (Golfão Maranhense).

EUGLENOPHYTA	Abundância (x 10^3 céls L^{-1})	Superior	Médio	Inferior	Classe	Ordem	Família	Ecologia
Euglena sp.	8	+	+	-	Euglenophyceae	Euglenida	Euglenidae	Dulcícola
Euglena deses Ehrenberg, 1834	2	-	-	+	Euglenophyceae	Euglenida	Euglenidae	Dulcícola
Euglena gracilis G.A.Klebs, 1883	9	+	+	+	Euglenophyceae	Euglenida	Euglenidae	Dulcícola
Euglena proxima P.A.Dangeard, 1902	1	+	-	-	Euglenophyceae	Euglenida	Euglenidae	Dulcícola
Euglena viridis (O.F.Müller) Ehrenberg, 1830	1	+	-	-	Euglenophyceae	Euglenida	Euglenidae	Marinha
Lepocinclis acus (O.F.Müller) B.Marin & Melkonian 2003 (O.F.Müller) Ehrenberg, 1830	28	+	+	+	Euglenophyceae	Euglenida	Phacaceae	Dulcícola/Salobra
Lepocinclis conica (P.Allorge & M.Lefèvre) Zakryś & Lukomska, 2019	2	+	-	-	Euglenophyceae	Euglenida	Phacaceae	Dulcícola
Lepocinclis ovum (Ehrenberg) Lemmermann, 1901	2	+	-	-	Euglenophyceae	Euglenida	Phacaceae	Dulcícola
Lepocinclis oxyuris (Schmarda) B.Marin & Melkonian, 2003	99	+	+	+	Euglenophyceae	Euglenida	Euglenidae	Dulcícola
Lepocinclis pyriformis A.M.Cunha, 1913	2	+	-	-	Euglenophyceae	Euglenida	Phacaceae	Dulcícola
Phacus sp.	9	+	+	+	Euglenophyceae	Euglenida	Euglenidae	Dulcícola
Phacus acuminatus A.Stokes, 1885	1	+	-	-	Euglenophyceae	Euglenida	Phacaceae	Dulcícola
Phacus longicauda (Ehrenberg) Dujardin, 1841	4	+	+	-	Euglenophyceae	Euglenida	Phacaceae	Dulcícola
Strombomonas gibberosa M.T.Philipose, 1988	2	+	-	-	Euglenophyceae	Euglenida	Euglenidae	Outros
Strombomonas verrucosa (E.Daday) Deflandre, 1930	65	-	+	+	Euglenophyceae	Euglenida	Euglenidae	Dulcícola
Trachelomonas armata (Ehrenberg) F.Stein, 1878	103	+	+	+	Euglenophyceae	Euglenida	Euglenidae	Dulcícola
Trachelomonas armata var. longispina Playfair, 1915	5	-	-	+	Euglenophyceae	Euglenida	Euglenidae	Dulcícola
Trachelomonas armata var. rangpurensis A.K.Islam, 1981	2	+	-	-	Euglenophyceae	Euglenida	Euglenidae	Dulcícola
Trachelomonas hispida (Perty) F.Stein, 1878	33	+	+	+	Euglenophyceae	Euglenida	Euglenidae	Dulcícola
Trachelomonas volvocina (Ehrenberg) Ehrenberg, 1834	212	+	+	+	Euglenophyceae	Euglenida	Euglenidae	Dulcícola

Fonte: O Autor (2022)

Tabela 6 - Distribuição de ocrófitas nos setores do estuário do rio Itapecuru (Golfão Maranhense).

OCHROPHYTA	Abundância (x 10^3 céls L^{-1})	Superior	Médio	Inferior	Classe	Ordem	Família	Ecologia
Mallomonas acaroides Perty, 1852	4	+	+	-	Chrysophyceae	Synurales	Mallomonadaceae	Dulcícola

Fonte: O Autor (2022)

Tabela 7 - Distribuição de diatomáceas nos setores do estuário do rio Itapecuru (Golfão Maranhense).

BACILLARIOPHYTA	Abundância (x 10^3 céls L^{-1})	Superior	Médio	Inferior	Classe	Ordem	Família	Ecologia
Actinoptychus campanulifer Schmidt, 1875	2	+	-	-	Coscinodiscophyceae	Coscinodiscales	Heliopeltaceae	Marinha
Amphora richardiana Cholnoky, 1968	2	-	-	+	Bacillariophyceae	Thalassiophysales	Catenulaceae	Marinha
Aulacoseira granulata (Ehrenberg) Simonsen, 1979	73	+	+	+	Coscinodiscophyceae	Aulacoseirales	Aulacoseiraceae	Dulcícola
Aulacoseira granulata var. *angustissima* (O.Müller) Simonsen, 1979	1058	+	+	+	Coscinodiscophyceae	Aulacoseirales	Aulacoseiraceae	Dulcícola
Bellerochea malleus (Brightwell) Van Heurck, 1885	2	-	-	+	Mediophyceae	Mediophyceae	Bellerocheaceae	Marinha
Caloneis permagna (Bailey) Cleve, 1894	6	-	+	+	Bacillariophyceae	Naviculales	Naviculaceae	Estuarina
Campylosira cymbelliformis (A.W.F.Schmidt) Grunow ex Van Heurck, 1885	109	+	+	+	Mediophyceae	Cymatosirales	Cymatosiraceae	Marinha
Chaetoceros sp_1	28	+	+	+	Mediophyceae	Chaetocerotales	Chaetocerotaceae	Marinha
Chaetoceros sp_2	5	-	-	+	Mediophyceae	Chaetocerotales	Chaetocerotaceae	Marinha
Chaetoceros aequatorialis Cleve, 1901	4	-	-	+	Mediophyceae	Chaetocerotales	Chaetocerotaceae	Marinha
Chaetoceros affinis Lauder, 1864	2	-	-	+	Mediophyceae	Chaetocerotales	Chaetocerotaceae	Marinha
Chaetoceros atlanticus f. audax (F.Schütt) Gran, 1904	4	-	+	-	Mediophyceae	Chaetocerotales	Chaetocerotaceae	Marinha
Chaetoceros lorenzianus Grunow, 1863	26	-	+	+	Mediophyceae	Chaetocerotales	Chaetocerotaceae	Marinha
Chaetoceros peruvianus Brightwell, 1856	2	-	-	+	Mediophyceae	Chaetocerotales	Chaetocerotaceae	Marinha
Chaetoceros subtilis Cleve, 1896	2	-	-	+	Mediophyceae	Chaetocerotales	Chaetocerotaceae	Marinha
Chaetoceros subtilis f. *simplex* Proshkina-Lavrenko, 1961	5	-	-	+	Mediophyceae	Chaetocerotales	Chaetocerotaceae	Marinha
Chaetoceros subtilis var. *abnormis* Prosckina-Lavrenko, 1961	35	-	+	+	Mediophyceae	Chaetocerotales	Chaetocerotaceae	Marinha
Cocconeis sp.	39	-	+	+	Bacillariophyceae	Achnanthales	Cocconeidaceae	Dulcícola
Cocconeis placentula Ehrenberg, 1838	5	-	-	+	Bacillariophyceae	Achnanthales	Cocconeidaceae	Dulcícola
Corethron hystrix Hensen, 1887	5	+	+	+	Bacillariophyceae	Corethrales	Corethraceae	Marinha
Coscinodiscus sp.	19	-	-	+	Coscinodiscophyceae	Coscinodiscales	Coscinodiscaceae	Marinha
Coscinodiscus concinnus W.Smith, 1856	5	+	+	+	Bacillariophyceae	Coscinodiscales	Coscinodiscaceae	Marinha
Coscinodiscus oculus-iridis (Ehrenberg) Ehrenberg, 1840	94	-	-	+	Coscinodiscophyceae	Coscinodiscales	Coscinodiscaceae	Marinha
Coscinodiscus radiatus Ehrenberg, 1840	16	+	+	+	Coscinodiscophyceae	Coscinodiscales	Coscinodiscaceae	Marinha
Coscinodiscus rothii (Ehrenberg) Grunow, 1878	10	+	+	+	Coscinodiscophyceae	Coscinodiscales	Coscinodiscaceae	Marinha
Craticula ambigua (Ehrenberg) D.G.Mann, 1990	920	+	+	+	Bacillariophyceae	Naviculales	Stauroneidaceae	Dulcícola
Cyclotella litoralis Lange & Syvertsen, 1989	132	+	+	+	Mediophyceae	Stephanodiscales	Stephanodiscales	Estuarina
Cyclotella meneghiniana Kützing, 1844	155	+	+	+	Mediophyceae	Stephanodiscales	Stephanodiscales	Estuarina
Cyclotella stelligera (Cleve & Grunow) Van Heurck, 1882	46	+	+	+	Mediophyceae	Stephanodiscales	Stephanodiscales	Dulcícola
Cyclotella striata (Kützing) Grunow, 1880	79	+	+	+	Mediophyceae	Stephanodiscales	Stephanodiscales	Dulcícola
Cyclotella stylorum Brightwell, 1860	70	+	+	+	Mediophyceae	Stephanodiscales	Stephanodiscales	Estuarina
Cylindrotheca closterium (Ehrenberg) Reimann & J.C.Lewin, 1964	131	+	+	+	Bacillariophyceae	Bacillariales	Bacillariaceae	Marinha
Cymbela sp.	67	-	-	+	Bacillariophyceae	Cymbellales	Cymbellaceae	Outras
Diploneis bombus (Ehrenberg) Ehrenberg, 1853	2	+	+	+	Bacillariophyceae	Naviculales	Diploneidaceae	Marinha
Diploneis gruendleri (A.W.F.Schmidt) Cleve, 1894	59	+	-	+	Bacillariophyceae	Naviculales	Diploneidaceae	Marinha
Diploneis ovalis (Hilse) Cleve, 1891	25	-	+	+	Bacillariophyceae	Naviculales	Diploneidaceae	Dulcícola
Ditylum brightwellii (T.West) Grunow, 1885	9	+	+	+	Mediophyceae	Lithodesmiales	Lithodesmiaceae	Marinha
Entomoneis alata (Ehrenberg) Ehrenberg, 1845	13	-	+	-	Bacillariophyceae	Surirellales	Entomoneidaceae	Marinha
Epithemia pelagica Schvarcz, Stancheva & Steward, 2022	1	-	-	+	Bacillariophyceae	Rhopalodiales	Rhopalodiaceae	Marinha
Eunotia exigua (Brébisson ex Kützing) Rabenhorst, 1864	2	+	+	+	Bacillariophyceae	Eunotiales	Eunotiaceae	Dulcícola
Fragilaria sp.	20	-	-	+	Bacillariophyceae	Fragilariales	Fragilariaceae	Outras

Conitinua...

BACILLARIOPHYTA	Abundância (x 10^3 céls L^{-1})	Superior	Médio	Inferior	Classe	Ordem	Família	Ecologia
Frustulia interposita (Lewis) De Toni, 1891	20	-	+	-	Bacillariophyceae	Naviculales	Amphipleuraceae	Dulcícola
Guinardia flaccida (Castracane) H.Peragallo, 1892	13	-	+	+	Coscinodiscophyceae	Rhizosoleniales	Rhizosoleniaceae	Marinha
Gyrosigma balticum (Ehrenberg) Rabenhorst, 1853	2	-	-	+	Bacillariophyceae	Naviculales	Naviculaceae	Marinha
Hantzschia amphioxys (Ehrenberg) Grunow, 1880	2	-	-	+	Bacillariophyceae	Bacillariales	Bacillariaceae	Dulcícola
Helicotheca tamesis (Shrubsole) M.Ricard, 1987	1	-	+	-	Mediophyceae	Lithodesmiales	Lithodesmiaceae	Marinha
Hemiaulus indicus Karsten, 1907	2	-	-	+	Mediophyceae	Hemiaulales	Hemiaulaceae	Marinha
Hobaniella longicruris (Greville) P.A.Sims & D.M.Williams, 2018	5	-	-	+	Mediophyceae	Eupodiscales	Odontellaceae	Marinha
Leptocylindrus danicus Cleve, 1889	18	-	-	+	Mediophyceae	Chaetocerotales	Leptocylindraceae	Marinha
Leptocylindrus minimus Gran, 1915	226	-	+	+	Mediophyceae	Chaetocerotales	Leptocylindraceae	Marinha
Lithodesmium undulatum Ehrenberg, 1839	6	-	+	+	Mediophyceae	Lithodesmiales	Lithodesmiaceae	Marinha
Melosira nummuloides C.Agardh, 1824	35	-	+	+	Coscinodiscophyceae	Melosirales	Melosiraceae	Marinha
Melosira varians C.Agardh, 1827	12	+	-	-	Coscinodiscophyceae	Melosirales	Melosiraceae	Dulcícola
Navicula sp.	50	+	+	+	Bacillariophyceae	Naviculales	Naviculaceae	Outras
Nitzschia sp.	83	-	+	+	Bacillariophyceae	Bacillariales	Bacillariaceae	Outras
Nitzschia linearis W.Smith, 1853	1	-	+	-	Bacillariophyceae	Bacillariales	Bacillariaceae	Estuarina
Nitzschia palea (Kützing) W.Smith, 1856	277	+	+	+	Bacillariophyceae	Bacillariales	Bacillariaceae	Dulcícola
Nitzschia sigma (Kützing) W.Smith, 1853	51	+	+	+	Bacillariophyceae	Bacillariales	Bacillariaceae	Estuarina
Odontella aurita (Lyngbye) C.Agardh, 1832	47	+	+	+	Mediophyceae	Eupodiscales	Odontellaceae	Marinha
Opephora marina (W.Gregory) Petit, 1888	6	-	+	+	Bacillariophyceae	Fragilariales	Staurosiraceae	Marinha
Opephora pacifica (Grunow) Petit, 1888	12	+	-	+	Bacillariophyceae	Fragilariales	Staurosiraceae	Marinha
Paralia sulcata (Ehrenberg) Cleve, 1873	100	+	+	+	Coscinodiscophyceae	Paraliales	Paraliaceae	Marinha
Pinnularia interrupta W.Smith, 1853	1	-	+	-	Bacillariophyceae	Naviculales	Pinnulariaceae	Dulcícola
Pinnularia subcapitata W.Gregory, 1856	4	+	-	-	Bacillariophyceae	Naviculales	Pinnulariaceae	Dulcícola
Pinnularia viridis (Nitzsch) Ehrenberg, 1843	18	+	-	+	Bacillariophyceae	Naviculales	Pinnulariaceae	Dulcícola
Pleurosigma angulatum (J.T.Quekett) W.Smith, 1852	3	+	-	+	Bacillariophyceae	Naviculales	Pleurosigmataceae	Marinha
Pleurosigma elongatum W.Smith, 1852	100	+	+	+	Bacillariophyceae	Naviculales	Pleurosigmataceae	Marinha
Polymyxus coronalis L.W.Bailey, 1862	624	+	+	+	Coscinodiscophyceae	Coscinodiscales	Heliopeltaceae	Marinha
Psammodictyon panduriforme (W.Gregory) D.G.Mann, 1990	11	+	+	+	Bacillariophyceae	Bacillariales	Bacillariaceae	Marinha
Pseudo-nitzschia pungens (Grunow ex Cleve) Hasle, 1993	5	-	-	+	Bacillariophyceae	Bacillariales	Bacillariaceae	Marinha
Pseudosolenia calcar-avis (Schultze) B.G.Sundström, 1986	2	-	-	+	Coscinodiscophyceae	Rhizosoleniales	Rhizosoleniaceae	Marinha
Rhaphoneis amphiceros (Ehrenberg) Ehrenberg, 1844	69	+	+	+	Bacillariophyceae	Rhaphoneidales	Rhaphoneidaceae	Marinha
Rhizosolenia hebetata J.W.Bailey, 1856	2	-	-	+	Coscinodiscophyceae	Rhizosoleniales	Rhizosoleniaceae	Marinha
Shionodiscus oestrupii (Ostenfeld) A.J.Alverson, S.-H.Kang & E.C.Theriot, 2006	37	-	+	+	Mediophyceae	Thalassiosirales	Thalassiosiraceae	Marinha
Skeletonema costatum (Greville) Cleve, 1873	954	-	+	+	Mediophyceae	Thalassiophysales	Skeletonemataceae	Marinha
Sundstroemia setigera (Brightwell) Medlin, 2021	23	-	-	+	Coscinodiscophyceae	Rhizosoleniales	Rhizosoleniaceae	Marinha
Surirella angusta Kützing, 1844	5	+	-	-	Bacillariophyceae	Surirellales	Surirellaceae	Dulcícola
Surirella litoralis Hustedt, 1955	2	+	-	-	Bacillariophyceae	Surirellales	Surirellaceae	Marinha
Thalassionema frauenfeldii (Grunow) Tempère & Peragallo, 1910	199	+	+	+	Bacillariophyceae	Thalassionematales	Thalassionemataceae	Marinha
Thalassionema nitzschioides (Grunow) Mereschkowsky, 1902	2	-	-	+	Bacillariophyceae	Thalassionematales	Thalassionemataceae	Marinha
Thalassiosira sp.	303	+	+	+	Mediophyceae	Thalassiosirales	Thalassiosiraceae	Outras
Thalassiosira eccentrica (Ehrenberg) Cleve, 1904	25	+	+	+	Mediophyceae	Thalassiosirales	Thalassiosiraceae	Marinha
Thalassiosira gravida Cleve, 1896	592	+	+	+	Mediophyceae	Thalassiosirales	Thalassiosiraceae	Marinha

Continua...

BACILLARIOPHYTA	Abundância (x 10^3 céls L^{-1})	Superior	Médio	Inferior	Classe	Ordem	Família	Ecologia
Thalassiosira leptopus (Grunow) Hasle & G.Fryxell, 1977	26	+	-	+	Mediophyceae	Thalassiosirales	Thalassiosiraceae	Marinha
Thalassiosira nanolineata (A.Mann) Fryxell & Hasle, 1977	21	+	+	-	Mediophyceae	Thalassiosirales	Thalassiosiraceae	Marinha
Thalassiosira subtilis (Ostenfeld) Gran, 1900	87	-	+	+	Mediophyceae	Thalassiosirales	Thalassiosiraceae	Marinha
Triceratium sp.	2	-	+	-	Coscinodiscophyceae	Triceratiales	Triceratiaceae	Outras
Triceratium favus Ehrenberg, 1839	40	-	+	+	Coscinodiscophyceae	Triceratiales	Triceratiaceae	Marinha
Trieres mobiliensis (Bailey) Ashworth & ECTheriot, 2013	5	-	-	+	Mediophyceae	Eupodiscales	Parodontellaceae	Marinha
Trieres regia (M.Schultze) Ashworth & E.C.Theriot, 2013	28	-	+	+	Mediophyceae	Eupodiscales	Parodontellaceae	Marinha
Tryblionella granulata (Grunow) D.G.Mann, 1990	93	+	+	+	Bacillariophyceae	Bacillariales	Bacillariaceae	Marinha
Trybliоptychus cocconeiformis (Grunow) Hendey, 1958	71	+	+	+	Bacillariophyceae	Surirellales	Surirellaceae	Marinha
Ulnaria ulna (Nitzsch) Compère, 2001	47	+	-	+	Bacillariophyceae	Licmophorales	Ulnariaceae	Dulcícola

Fonte: O Autor (2022)

Tabela 8 - Lista de espécies potencialmente nocivas e tóxicas que ocorrem no estuário do rio Itapecuru (Golfão Maranhense).

	Abundância (x 10^3 céls L^{-1})			
Cyanobacteria	**Superior**	**Médio**	**Inferior**	**Nocividade/Toxicidade**
Aphanizomenon gracile Lemmermann, 1907	0	39	0	Produção de saxitoxinas
Synechocystis aquatilis Sauvageau, 1892	0	38	10	Biodegradação de hidrocarbonetos (n-octadecano e pristano)
Miozoa				
Dinophysis acuta Ehrenberg, 1839	0	0	1	Espécie tóxica que produz ácido ocadáico e Dinophysistoxin-1.
Dinophysis acuminata Claparède & Lachmann, 1859	0	58	0	Espécie produz ácido ocadáico, causando intoxicação diarreica por mariscos (DSP)
Dinophysis caudata Kent, 1881	0	1	2	Espécie é conhecida por produzir marés vermelhas resultando em mortalidade de peixes
Prorocentrum micans Ehrenberg, 1834	0	39	10	Esta espécie é capaz de formar flores, geralmente é considerada inofensiva.
Scrippsiella trochoidea (F.Stein) A.R.Loeblich III, 1976	10	0	5	
Bacillariophyta				Injúrias mecânicas
Chaetoceros aequatorialis Cleve, 1901	0	0	4	Injúrias mecânicas
Chaetoceros lorenzianus Grunow, 1863	0	0	2	Injúrias mecânicas
Chaetoceros peruvianus Brightwell, 1856	0	0	3	Injúrias mecânicas
Chaetoceros subtilis Cleve, 1896	0	0	3	Injúrias mecânicas
Cylindrotheca closterium (Ehrenberg) Reimann & J.C.Lewin, 1964	70	32	28	Injúrias mecânicas/Produz mucilagem
Leptocylindrus minimus Gran, 1915	0	67	**159**	Não tóxica/ Potencialmente danosa
Thalassiosira eccentrica (Ehrenberg) Cleve, 1904	2	21	1	Injúrias mecânicas
Thalassiosira gravida Cleve, 1896	7	69	**516**	Injúrias mecânicas
Thalassiosira leptopus (Grunow) Hasle & G.Fryxell, 1977	2	0	23	Injúrias mecânicas
Thalassiosira subtilis (Ostenfeld) Gran, 1900	0	17	70	Injúrias mecânicas
Skeletonema costatum (Greville) Cleve, 1873	0	0	1	Não tóxica/ Potencialmente danosa

Fonte: O Autor (2022)

APÊNDICE B – ARTIGO 2

MULTIPLE STRESSORS INFLUENCING THE GENERAL EUTROPHICATION STATUS OF TRANSITIONAL WATERS OF THE BRAZILIAN TROPICAL COAST: AN APPROACH UTILIZING THE PRESSURE, STATE, AND RESPONSE (PSR) FRAMEWORK

Supplementary Fig. 1. Frequency distribution of environmental variables in the Itapecuru River estuary.

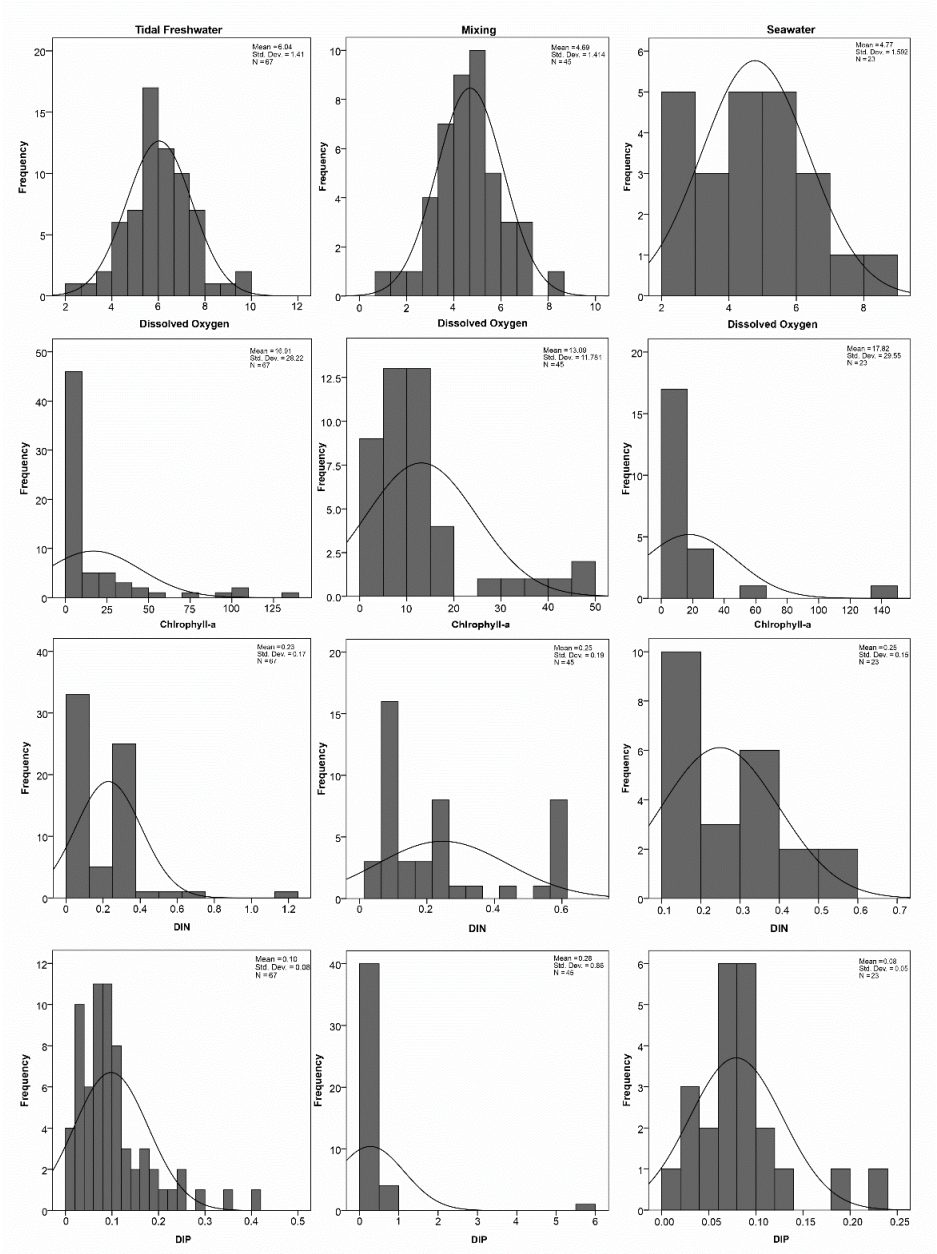

Source: The author (2022).

Supplementary Fig. 2. Percentile 90 value for chlorophyll-a and 10 value for dissolved oxygen (dashed lines intersection) in the estuarine zones of the Itapecuru River estuary (IRE).

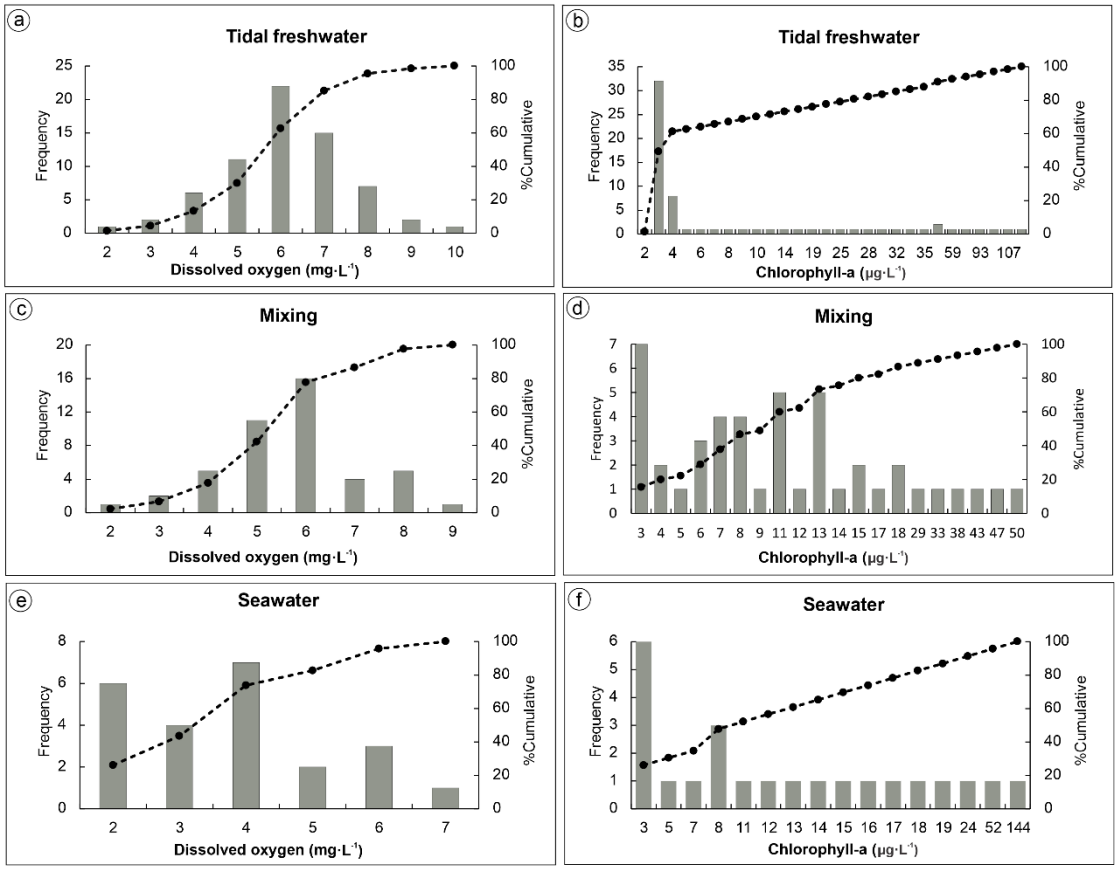

Source: The author (2022).

ANEXO A – PESQUISAS DESENVOLVIDAS DURANTE O DOUTORADO

(i) Artigos publicados durante o curso de doutorado

1. CAVALCANTI, L. F.; AZEVEDO-CUTRIM, A. C. G.; OLIVEIRA, A. L. L.; FURTADO, J. A.; ARAÚJO, B. DE O.; **SÁ, A. K. D. S.**; FERREIRA, F. S.; SANTOS, N. G. R.; DIAS, F. J. S.; CUTRIM, M. V. J. Structure of microphytoplankton community and environmental variables in a macrotidal estuarine complex, São Marcos Bay, Maranhão - Brazil. Brazilian Journal of Oceanography, v. 66, n. 3, p. 283–300, 2018. DOI: https://doi.org/10.1590/s1679-87592018021906603

2. CAVALCANTI, L. F.; CUTRIM, M. V. J.; LOURENÇO, C. B.; **SÁ, A. K. D. S**.; OLIVEIRA, A. L. L.; AZEVEDO-CUTRIM, A. C. G. Patterns of phytoplankton structure in response to environmental gradients in a macrotidal estuary of the Equatorial Margin (Atlantic coast, Brazil). Estuarine, Coastal and Shelf Science, 245, e106969, 2020. DOI: https://doi.org/10.1016/j.ecss.2020.106969

3. CAVALCANTI, L. F.; CUTRIM, M. V. J.; MACIEL, C. C. S.; **SÁ, A. K. D. S.**; AZEVEDO-CUTRIM, A. C. G.; SANTOS, T. P.; CRUZ, Q. S. Application of multiple indices to the evaluation of trophic and ecological status in a tropical macrotidal estuary (Equatorial Margin, Brazil). Chemistry and Ecology, v. 38, n. 2, p. 122–144, 2022. DOI: https://doi.org/10.1080/02757540.2021.2023509

4. CUTRIM, M. V. J.; FERREIRA, F. S.; **DUARTE-DOS-SANTOS, A. K.**; CAVALCANTI, L. F.; ARAÚJO, B. O.; AZEVEDO-CUTRIM, A. C. G.; FURTADO, J. A.; OLIVEIRA, A. L. L. Trophic state of an urban coastal lagoon (northern Brazil), seasonal variation of the phytoplankton community and environmental variables. Estuarine, Coastal and Shelf Science, v. 216, p. 98– 109, 2019. DOI: https://doi.org/10.1016/j.ecss.2018.08.013

5. **SÁ, A. K. D. S.**; CUTRIM, M. V. J.; COSTA, D. S.; CAVALCANTI, L. F.; FERREIRA, F. S.; OLIVEIRA, A. L. L.; SEREJO, J. H. F. Algal blooms and trophic state in a tropical estuary blocked by a dam (northeastern Brazil). Ocean and Coastal Research, v. 69, p. 1-16, 2021. DOI: https://doi.org/10.1590/2675-2824069.20-006akddss

6. **SÁ, A. K. D. S.;** FEITOSA, F. A. N.; CUTRIM, M. V. J.; FLORES-MONTES, M. J.; COSTA, D.S.; CAVALCANTI, L. F. Phytoplankton community dynamics in response to seawater intrusion in a tropical macrotidal river-estuary continuum. Hydrobiologia, [S.I.], 2022a. DOI: https://doi.org/10.1007/s10750- 022-04851-7

7. **SÁ, A. K. D. S.;** CUTRIM, M. V. J.; FEITOSA, F. A. N.: FLORES-MONTES, M. J.; CAVALCANTI, L. F.; COSTA, D. S.; CRUZ, Q. S. Multiple stressors influencing the general eutrophication status of transitional waters of the Brazilian tropical coast: An approach utilizing the pressure, state, and response (PSR) framework. Journal of Sea Research, v. 189, 102282, 2022b. DOI: https://doi.org/10.1016/j.seares.2022.102282

(ii) Capítulo de livro

1. CAVALCANTI, L. F.; OLIVEIRA, A. L. L.; ARAUJO, B. O.; FURTADO, J. A.; **DUARTE-DOS-SANTOS, A. K.;** FERREIRA, F. S.; CUTRIM, M. V. J. Divisão Bacillariophyta (diatomáceas) e gradiente de salinidade em um estuário tropical (Estuário do Rio Paciência, Maranhão). In: SANTOS, M. E. M. (Org.). Tópicos multidisciplinares em ciências biológicas: trabalhando ensino, pesquisa e extensão. 1ed. SÃO LUÍS: Universidade Estadual do Maranhão - UEMA, v. 1, p. 13-24, 2018.

2. CUTRIM, M. V. J.; FERREIRA, F. S.; CAVALCANTI, L. F.; **SÁ, A. K. D. S.**; AZEVEDO-CUTRIM, A. C. G.; SANTOS, R. L. Phytoplankton Biomass and Environmental Descriptors of Water Quality of an Urban Lagoon. In: PAN, J.; DEVLIN, A. (Eds.) Estuaries and Coastal Zones - Dynamics and Response to Environmental Changes, p. 1-18, IntechOpen, 2019.

3. CAVALCANTI, L. F.; **SÁ, A. K. D. S.**; CRUZ, Q. S.; SANTOS, T. P.; OLIVEIRA, A. L. L.; COSTA, D. S.; BRITO, M. V.; FERREIRA, F. S.; AZEVEDO-CUTRIM, A. C.G.; CUTRIM, M. V. J. Fitoplâncton da área portuária da Baía de São Marcos (Costa Norte do Brasil). In: SOUSA, D. B. P.; CASTRO, J. S.; JESUS, W. B. (Org.). Monitoramento Ambiental: metodologias e estudos de casos. 1ed.São Luís: i-EDUCAM, p. 1-183, 2022.